

Test Report:
Cyclic Performance of Steel Sheet Connections
for CFS Steel Sheet Shear Walls

Z. Zhang, B.W. Schafer

July 2020

COLD-FORMED STEEL RESEARCH CONSORTIUM
REPORT SERIES
CFSRC R-2020-06

CFSRC Information

The Cold-Formed Steel Research Consortium (CFSRC) is a multi-institute consortium of university researchers dedicated to providing world-leading research that enables structural engineers and manufacturers to realize the full potential of structures utilizing cold-formed steel. More information can be found at www.cfsrc.org. All CFSRC reports are hosted permanently by the Johns Hopkins University library in the DSpace collection: <https://jscholarship.library.jhu.edu/handle/1774.2/40427>.

Financial Acknowledgment

This work is part of the research project Seismic Resiliency of Repetitively Framed Mid-Rise Cold-Formed Steel Building (CFS-NHERI) which is supported by the National Science Foundation under Grant No. 1663348. Some of the test materials are provided by ClarkDietrich. Any opinions, findings, and conclusions or recommendations expressed in this publication are those of the authors and do not necessarily reflect the views of the sponsors.

Research Acknowledgment

The tests conducted herein were assisted by Gbenga Olaolorun and Joel John, the authors would like to express gratitude to their great help. Moreover, the testing would not have been possible without the support from lab staff Nick Logvinovsky and test facilities adjustment and advice from Dr. Shahab Torabian, we greatly appreciate their assistance.

Table of Contents

| | |
|---|----|
| Abstract..... | 4 |
| 1 Introduction | 5 |
| 2 Test Setup and Specimen..... | 7 |
| 3 Test Matrix and Loading Protocol..... | 11 |
| 4 Material Testing..... | 15 |
| 5 Failure Modes | 17 |
| 6 Test Results | 19 |
| 6.1 Phase I monotonic test “32-54-8-13-M” | 20 |
| 6.2 Phase I asymmetric cyclic test “29-54-8-13-T” | 22 |
| 6.3 Phase I monotonic test “47-54-8-30-M” | 23 |
| 6.4 Phase I asymmetric cyclic test “42-54-8-30-A” | 24 |
| 6.5 Phase I asymmetric cyclic test “44-54-8-30-T” | 25 |
| 6.6 Phase I tension only cyclic test “72-97-10-30-Ten”..... | 27 |
| 6.7 Phase II asymmetric cyclic test “116-97-12-30-97-A” | 28 |
| 6.8 Phase III asymmetric cyclic test “143-188-24-30-A” | 29 |
| 7 Backbone Response Test Data Characterization | 31 |
| 8 Discussion..... | 34 |
| 8.1 Phase I Test Strength | 34 |
| 8.2 Phase II & III Test Strength..... | 37 |
| 8.3 Test Ductility | 40 |
| 8.4 Backbone Fitting and Averaging..... | 42 |
| 9 Conclusions | 45 |
| References | 46 |
| Appendix 1: Test Result Summary..... | 48 |
| Appendix 2: Test Data Characterization Summary | 52 |
| Appendix 3: Test Detail Report..... | 64 |

List of Tables

| | |
|--|----|
| Table 1a. Steel framing-to-steel sheet fastener test matrix (in.; ksi) | 13 |
| Table 2a. Material test result (in.; ksi)..... | 16 |
| Table 3a. Average test results for each test series (in.; kip) | 19 |
| Table 4. 32-54-8-13-M test limit states and deformation development summary | 21 |
| Table 5. 29-54-8-13-T test limit states and deformation development summary | 22 |
| Table 6. 47-54-8-30-M test limit states and deformation development summary | 23 |
| Table 7. 42-54-8-30-A test limit states and deformation development summary | 25 |
| Table 8. 44-54-8-30-T test limit states and deformation development summary | 26 |
| Table 9. 72-97-10-30-Ten test limit states and deformation development summary..... | 27 |
| Table 10. 116-97-12-30-97-A test limit states and deformation development summary..... | 29 |
| Table 11. 143-188-24-30-A test limit states and deformation development summary | 30 |
| Table 12. Test data characterization deformation values before and after adjustment | 32 |
| Table 13a. Test ductility index values of cyclic tests for each test series (in.)..... | 42 |
| Table 14a. Test data characterization average values for all cyclic tests (in.; kip) | 44 |
| Table 15. Test result summary | 48 |
| Table 16. Test data characterization summary | 52 |
| Table 17. Test data characterization average values for monotonic tests | 55 |

| | |
|---|----|
| Table 18. Test data characterization average values for buckling away cyclic tests..... | 56 |
| Table 19. Test data characterization average values for buckling towards cyclic tests | 56 |
| Table 20. Test data characterization average values for tension only cyclic tests | 57 |
| Table 21. Test ductility index summary | 58 |
| Table 22. Test ductility index values for monotonic tests..... | 61 |
| Table 23. Test ductility index values for buckling away cyclic tests | 62 |
| Table 24. Test ductility index values for buckling towards cyclic tests..... | 62 |
| Table 25. Test ductility index values for tension only cyclic tests..... | 63 |

List of Figures

| | |
|--|----|
| Figure 1. Recent CFS-framed steel sheet sheathed shear wall tests..... | 5 |
| Figure 2. Shear buckling and Pull-through failure modes of CFS-framed steel sheet shear wall...8 | |
| Figure 3. Test specimen and test rig | 9 |
| Figure 4. Axial compression and buckling deformation | 11 |
| Figure 5. Asymmetric cyclic loading protocol | 12 |
| Figure 6. Test nomenclature | 14 |
| Figure 7. Material test..... | 16 |
| Figure 8. Fastener failure modes | 18 |
| Figure 9. Force-displacement curve for test “32-54-8-13-M”..... | 21 |
| Figure 10. Deformation and failure of test “32-54-8-13-M”..... | 22 |
| Figure 11. Force-displacement curves for test “29-54-8-13-T” | 22 |
| Figure 12. Deformation and failure of test “29-54-8-13-T” | 23 |
| Figure 13. Force-displacement curve for test “47-54-8-30-M”..... | 24 |
| Figure 14. Deformation and failure of test “47-54-8-30-M”..... | 24 |
| Figure 15. Force-displacement curves for test “42-54-8-30-A”..... | 25 |
| Figure 16. Deformation and failure of test “42-54-8-30-A” | 25 |
| Figure 17. Force-displacement curves for test “44-54-8-30-T” | 26 |
| Figure 18. Deformation and failure of test “44-54-8-30-T” | 27 |
| Figure 19. Force-displacement curve for test “72-97-10-30-Ten” | 28 |
| Figure 20. Deformation and failure of test “72-97-10-30-Ten” | 28 |
| Figure 21. Force-displacement curves for test “116-97-12-30-97-A” | 29 |
| Figure 22. Deformation and failure of test “116-97-12-30-97-A” | 29 |
| Figure 23. Force-displacement curves for test “143-188-24-30-A”..... | 30 |
| Figure 24. Deformation and failure of test “143-188-24-30-A” | 30 |
| Figure 25. Experimental data characterization..... | 33 |
| Figure 26. Force-displacement curves of four Phase I test types | 35 |
| Figure 27. Force-displacement curves of six Phase I test types | 36 |
| Figure 28. Force-displacement curves for test type “97-10-30” | 37 |
| Figure 29. Force-displacement curves of six Phase II test types..... | 38 |
| Figure 30. Force-displacement curves of two Phase III test types | 39 |
| Figure 31. Force-displacement curves for test type “188-12-30” | 40 |
| Figure 32. Test ductility index..... | 41 |
| Figure 33. Test data characterization average values for test type “54-8-30”..... | 43 |

Abstract

The objective of this report is to provide fastener-level force-deformation response appropriate for cold-formed steel (CFS) framed steel sheet sheathed shear walls under cyclic loads. A key feature of the fastened connection is the impact of the steel sheet shear buckling on the local fastener-level response. Recent CFS shear wall tests employing thin steel sheets screw fastened to cold-formed steel framing have examined the impact of thicker and stiffer boundary framing, double steel sheet sheathing, and sandwiching the steel sheet between boundary members - all demonstrating the potential for higher capacity and ductility for steel sheet sheathed CFS-framed shear walls. For the seismic performance of screw fastened, steel sheet sheathed shear walls, the cyclic nonlinear response of the fastener connection is particularly important and should incorporate the impact of the steel sheet local buckling on the strength and ductility of the connection. Minimal cyclic fastener-level shear test data exists, especially for combinations of screw fastened thin steel sheet and thick framing steel. A lap shear testing configuration, featuring either one thin steel sheet ply and one thick framing ply or one thin steel sheet ply and two thick framing plies connected by a single fastener with appropriate sensors is designed. The lap shear tests follow the AISI S905 test standard and are augmented for this particular configuration including adding asymmetric loading cycles following a modified FEMA 461 loading protocol. The asymmetric cyclic loading protocol is selected with a small displacement applied in the direction which buckles the thin steel sheet followed by progressively larger displacements in the opposite direction. A total of 156 tests, covering a wide range of framing thickness, sheet thickness, fastener type and size, and loading types are conducted. Key statistics from each test, including characterization with a multilinear backbone curve are provided. The testing is intended to provide critical missing information for the design and simulation of CFS-framed steel sheet sheathed shear walls.

1 Introduction

Cold-formed steel (CFS)-framed structures potentially feature low installation and maintenance costs, are lightweight and recyclable, and properly designed are durable, and ductile. Furthermore, the high strength-to-weight ratio, stiffness, dimensional consistency, and non-combustibility of CFS affords the system potential benefits over certain aspects of competing solutions.

CFS-framed mid-rise structures have the potential to fulfill the need for low cost, multi-hazard resilient, sustainable building structures. The cyclic fastener test efforts reported here are part of an ongoing research project: CFS-NHERI¹, aiming to advance the state of the art for seismic performance and design of mid-rise CFS-framed buildings.

Recent steel sheet sheathed CFS-framed shear wall tests employing thin steel sheets screw fastened to cold-formed steel framing have examined the impact of thicker and stiffer boundary framing, double steel sheet sheathing, and sandwiching the steel sheet between boundary members (i.e. a mid-ply steel sheet shear wall) (Rizk et. al. 2018, Santos et. al. 2018, Briere et. al. 2018), as presented in Figure 1a & 1b. It has been found that all the aforementioned configurations demonstrate the potential for higher shear capacity and ductility necessary in mid-rise CFS construction. Further, recent CFS-framed shear wall line test efforts within the CFS-NHERI project (Singh et. al. 2020) also adopt thin steel sheets with thick boundary framing in pursuit of higher capacity and ductility, as shown in Figure 1c.



(a) Double sheathed shear wall test by Briere et. al. (2018) (b) Mid-ply sheathed shear wall test by Santos et. al. (2018) (c) CFS-NHERI wall line test by Singh (2020)

Figure 1. Recent CFS-framed steel sheet sheathed shear wall tests

For seismic performance of screw fastened, steel sheet sheathed shear walls, the cyclic nonlinear response of the fastener connection is especially significant and should incorporate the impact of the steel sheet local buckling on the strength and ductility of the connection. Some monotonic and cyclic fastener-level shear test data (Rogers et. al. 2000, Tao et. al. 2016, Torabian et. al. 2017, Shi et. al. 2018) exists, but minimal data is available for thin steel sheet - thick framing combinations.

This report summarizes experimental efforts on fastener-level force-deformation response under cyclic loads incorporating steel sheet local buckling consistent with the demands on perimeter fasteners in screw fastened CFS-framed steel sheet sheathed shear walls. A lap shear testing configuration featuring either one thin steel sheet ply and one thick framing ply (consistent with a

¹ CFS-NHERI is the shortened name for the collaborative research project: Seismic Resiliency of Repetitively Framed Mid-Rise Cold-Formed Steel Buildings with principal funding from the National Science Foundation (NSF) under the award ID: #1663348. NHERI stands for NSF-supported Natural Hazards Engineering Research Infrastructure.

steel sheet shear wall fastened to the outside face of the wall) or one thin steel sheet ply and two thick framing plies (consistent with a steel sheet shear wall where the sheet is sandwiched mid-distance between two chord studs) connected by a single fastener with proper sensors is designed. The cyclic loading protocol investigated is asymmetric with a small displacement applied in the direction which buckles the thin steel sheet, followed by progressively larger displacements in the opposite direction. A total of 156 tests including monotonic and cyclic tests are completed in this test program. The test data are idealized with a multi-segment linear backbone phenomenological model intended to support the development of high fidelity numerical models adopting nonlinear hysteretic fastener response with steel sheet local buckling incorporated.

2 Test Setup and Specimen

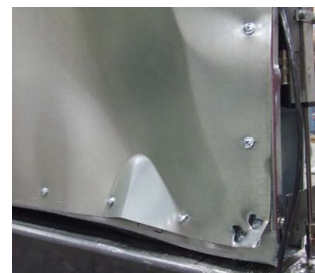
Under cyclic demands CFS-framed shear walls with screw fastened steel sheet sheathing exhibit a number of fastener connection failure modes including bearing, tilting and bearing, pull-through, pull-over, pull-out and shear rupture, as shown from existing tests in Figure 2a and 2b. In cyclic or dynamic tests, as the lateral demand switches direction, within the steel sheet the tension field direction (red lines in Figure 2c & 2d) switches and the sheet buckles as it becomes the compression direction.

Behavior of the fastener connection for steel sheet sheathed CFS-framed shear walls is unique because in addition to resisting the primary shear forces transferred between the sheet and framing, the connection must also resist out-of-plane forces that work on the fastener head due to extensive buckling of the thin steel sheet under cyclic loading. The force generated by buckling itself is not a large demand on the fastener, but can potentially lead to premature pull-through behavior in a damaged fastener connection. This “shear-tension” interaction is of interest both for the fastener connection behavior as well as the overall shear wall behavior.

Screw-fastened connections between cold-formed steel members tested in cyclic shear provide a symmetric response dominated by bearing and influenced by tilting and shear rupture for some geometries (Rogers et. al. 2000, Tao et. al. 2016, Torabian et. al. 2017, Shi et. al. 2018). Therefore, the fundamental shear response for screw-fastened connections can be captured by one-sided cyclic shear testing. Screw-fastened steel sheet connections, unlike full members, buckle significantly when under compression. To capture this phenomenon, which introduces a potential “shear-tension” interaction in the connection, the cyclic testing protocol for a lap shear test can include a small compression displacement which buckles the thin steel sheet each cycle. The resulting asymmetric cyclic lap shear testing protocol then would switch between progressively larger tension cycles, which place the connection in shear, and small compression cycles, which buckle the thin steel sheet and maximizes the opportunity that the fastener tilts and the fastener head slips/pulls-through the thin steel sheet. The result is that the potential for the pull-through limit state is incorporated into the shear behavior (detailed descriptions can be found in test result section).



(a) Pull-through failure development incorporating steel sheet shear buckling wave and in Briere et. al. (2018)



(b) Steel sheet shear buckling and Pull-through in Yu et. al. (2007)



(c) Shear wall test in Briere et. al. (2018)



(d) Shear wall test in Yu et. al. (2007)

Figure 2. Shear buckling and Pull-through failure modes of CFS-framed steel sheet shear wall

The developed lap shear test configuration is based on small modifications to the AISI S905 test standard. A typical test specimen consists of one thin steel sheet ply and one thick framing ply connected by a single fastener (either self-drilling screw or powder-actuated fastener in this test program), as presented in Figure 3a. The upper and bottom shaded parts in Figure 3a, with 2 in. length, are clamping areas for the grips, and 2 in. x 2 in. spacers are placed inside the grips to avoid eccentric loading. The thin steel sheet ply length in the lap shear test corresponds to the observed buckling half-wave length of the steel sheet close to the boundary of a steel sheet sheathed shear wall. After reviewing typical shear wall tests (M11 test by Yu et. al. 2007, W2 test by Rizk et. al. 2018, W21 test by Santos et. al. 2018), an estimate for the buckling half-wave length close to the framing boundary, as indicated with red lines in Figure 2a and 2b, is approximately 4 in., Thus, the length between the top grip and fastener head of all specimens in this test program is selected as 4 in.. The edge distance for the thick framing ply is chosen to be 0.81 in. which corresponds to half of the flange width of a typical chord stud section (362S162-97), and the edge distance for the thin sheet ply is set to $\frac{3}{4}$ in. which meets the 1.5d minimum edge distance requirement (J4.2 in AISI S100-16) for all tests. The length between the fastener and bottom grip is minimized to 1 in. to minimize tilting of the steel ply in a standard lap-joint shear test per AISI S905. A typical test specimen, placed in the test rig, is shown in Figure 3b.

Note, there is a second category of lap shear specimens consisting of one thin steel sheet ply sandwiched by two thick framing plies with one single fastener designed to investigate the CFS-framed mid-ply steel sheet sheathed shear wall fastener behavior (see Santos et. al. 2018, Briere et. al. 2018 for the shear wall performance of this configuration). Tests in this configuration are designated as part of Phase II as detailed later in Section 3.

All of the test specimens are assembled in the Thin-walled Structures Laboratory at Johns Hopkins University. The thin steel sheet plies and thick framing steel plies are cut using a horizontal metal cut band saw. The self-drilling fasteners are driven by HILTI ST 1800 Screwdriver with appropriate torque settings. A pilot hole is utilized if the self-drilling screw point number is not enough to drill through all the steel sheet materials (all the double shear configuration test specimens and single shear configuration specimens featuring 97 mil thick framing ply with #8 screw or 188 mil thick framing ply with #12 screw). The stand-up HILTI DX 860-HSN fully automatic powder-actuated tool is used to install the HILTI X-HSN-24 PAF while the HILTI DX 76 fully automatic powder-actuated tool is used to install the HILTI X-ENP-19 PAF with the appropriate caliber cartridges and tool settings to obtain the manufacturers' recommended nail head standoff distances.

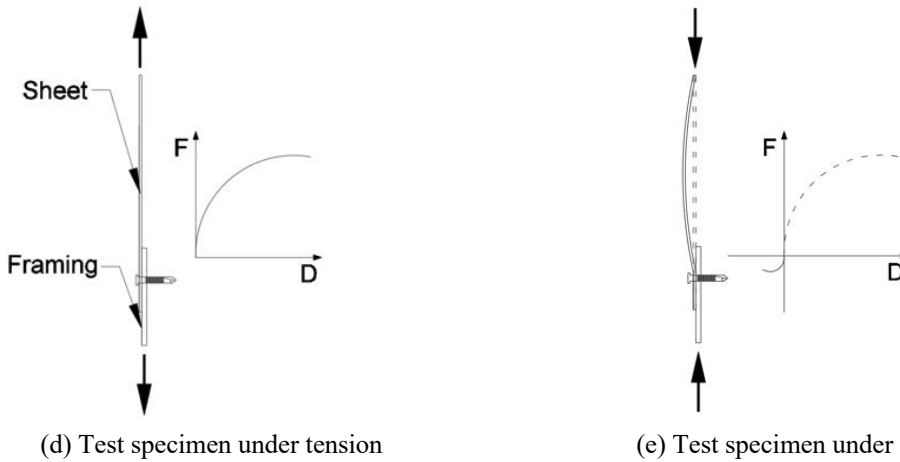
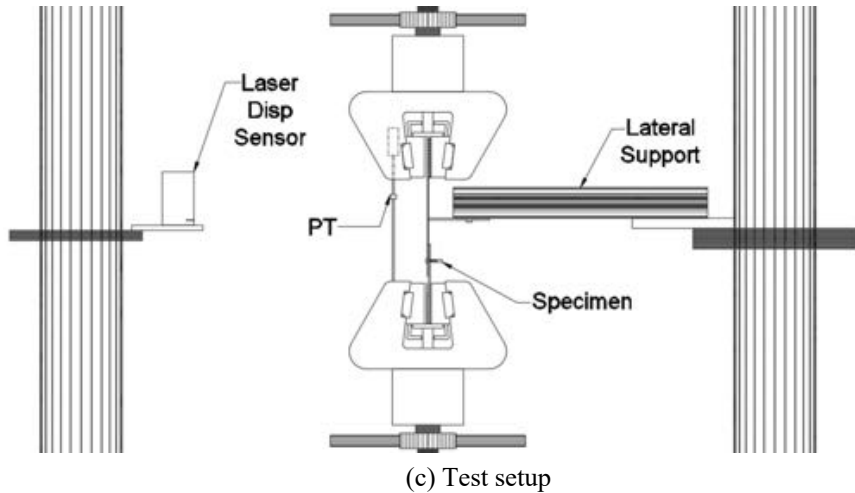
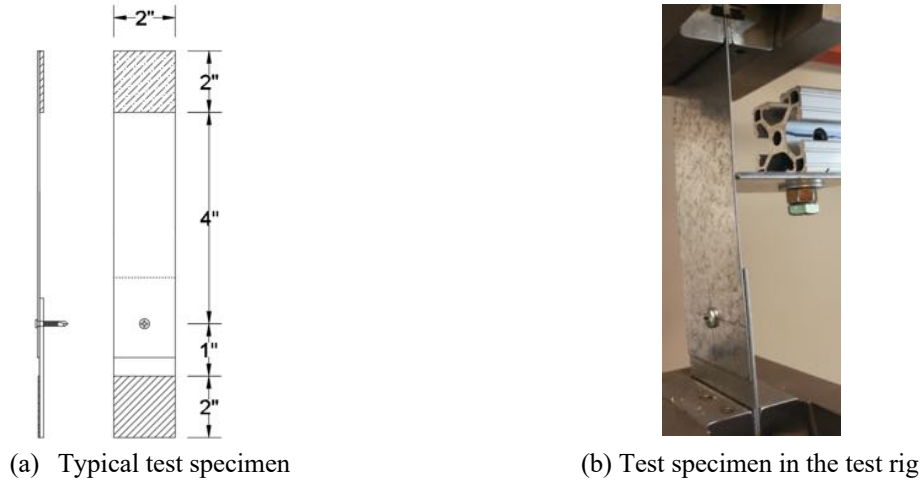


Figure 3. Test specimen and test rig

All of the tests were conducted in the 100 kip capacity MTS servohydraulic test system in the Thin-walled Structures Laboratory at Johns Hopkins University. The test setup is shown in Figure 3c. The test specimen is placed inside the grips and a position transducer with 1 in. measurement range is installed using a magnet between the two grips to provide accurate displacement data of the fastener connection. A 5 kip load cell is installed to accurately measure the force level. The

force and displacement data from the 5 kip load cell and 1 in. range position transducer are adopted as the main test data source. In addition, one KEYENCE IL-600 laser displacement sensor is fixed at the left column of the MTS machine to monitor the out-of-plane thin steel sheet buckling displacement in compression. Moreover, a mechanical lateral support is placed at either the left or right side of the specimen to guide the thin sheet to buckle away or towards the fastener head, because strength differences were found between different thin steel sheet ply buckling directions in initial shakedown tests. The lateral support is released once a plastic hinge in the thin sheet ply (caused by buckling) is observed. Note, when the lateral support is placed at the left side of the specimen, it is minimally offset from the thin sheet center point to accommodate the laser displacement sensor light beam.

Figure 3d and Figure 3e present a typical specimen's response in tension and compression loading correspondingly. Under tension demand, the force-displacement curve provides the bearing stiffness and fastener strength in shear. When the specimen is in compression, the force-displacement curve reflects the thin steel sheet buckling.

3 Test Matrix and Loading Protocol

Recently completed CFS fastener-level cyclic shear tests (Tao et. al. 2016, Torabian et. al. 2017, Shi et. al. 2018) implement the FEMA 461 Quasi-Static loading protocol (FEMA 2007). The FEMA 461 loading protocol is adopted and modified in this test program.

The FEMA 461 Quasi-Static cyclic loading protocol may be adopted to derive constituent force-deformation relationship and obtain corresponding hysteretic response characteristics for structural components. The protocol has a displacement amplitude increasing at a ratio of 1.4 after each step (i.e. two cycles). The protocol is designed to take 20 cycles (10 steps) for the deformation to develop from the lowest damage state (Δ_0) to the initiation of the most severe damage state (Δ_m). The protocol suggests that there should be at least six cycles prior to the lowest damage state (Δ_0). The protocol is relatively generic, not linked to any specific earthquake motion, and can be implemented easily.

In the testing, a small magnitude of compression displacement leads to large out-of-plane buckling of the thin steel sheet ply - adequate to exercise the fastener head and trigger the “shear-tension” interaction of interest. Therefore, the compression side of the FEMA 461 Quasi-Static loading protocol needs to be modified to fulfill the asymmetric cyclic displacement demand.

The axial compression and buckling deformation of the specimen thin steel sheet ply is shown in Figure 4. The original length of the thin steel sheet is S and a compression deformation u_1 will generate a corresponding out-of-plane buckling deformation u_2 . To estimate the out-of-plane buckling deformation of thin steel sheet buckling waves close to the framing boundary, a simplified ABAQUS shear wall model (Zhang et. al. 2019) is adopted. From this model, 0.2 in. - 0.4 in. is determined as a reasonable range of the out-of-plane buckling deformation u_2 . Furthermore, a sine wave in Eq. 1 is introduced to approximate the buckling wave. The arc length of the buckling wave can be calculated using the integral in Eq. 2 and the integral can be simplified with the first two terms of binomial series (Taylor series), as presented in Eq. 3. Then the compression deformation u_1 can be represented by Eq. 4. Based on Eq. 1 and Eq. 4, the relationship between the compression deformation u_1 and the out-of-plane buckling deformation u_2 can be derived, as shown in Eq. 5. When the out-of-plane buckling deformation u_2 reaches 0.4 in. and the original steel sheet length S equals to 4 in., then the maximum compression deformation u_1 is determined as 0.1 in.. Therefore, 0.1 in. is selected as a reasonable target for the compression cycles in the testing.

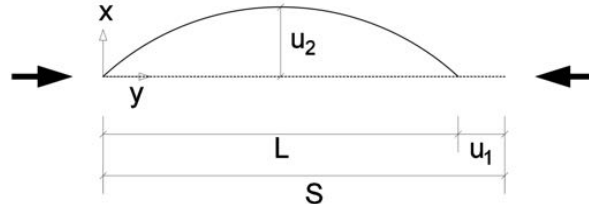


Figure 4. Axial compression and buckling deformation

$$y = u_2 \sin\left(\frac{\pi x}{L}\right), \quad 0 < x < L \quad (1)$$

$$S = \int_0^L \sqrt{1 + \left(\frac{dy}{dx}\right)^2} dx \quad (2)$$

$$S = \int_0^L \left[1 + \frac{1}{2} \left(\frac{dy}{dx}\right)^2\right] dx \quad (3)$$

$$u_1 = S - L = \frac{1}{2} \int_0^L \left(\frac{dy}{dx}\right)^2 dx \quad (4)$$

$$u_2 = \sqrt{\frac{4u_1(S-u_1)}{\pi^2}} \quad (5)$$

As shown in Figure 5, the modified FEMA 461 loading protocol is asymmetric with 0.1 in. constant displacement applied in the compression direction after initial three steps which buckles the thin steel sheet ply followed by larger displacements in the opposite direction with the increasing ratio of 1.4. The first three steps are symmetric and adopt a loading rate of 0.0011 in./sec to augment the displacement resolution for small deformation amplitudes at the test beginning while later steps employ 0.0033 in./sec loading rate. With these protocols total test time to complete an asymmetric cyclic test is about one hour. To reduce the total test time, which is significantly affected by large displacement cycles, after the tension displacement reaches 0.81 in., the displacement increases monotonically on tension side with a constant rate 0.0033 in./sec until the end of the test.

For the monotonic tests, following AISI S905 standard, the loading rate of 0.00083 in./sec is implemented to realize reasonable strain rates and results in around 15 minutes of total test time.

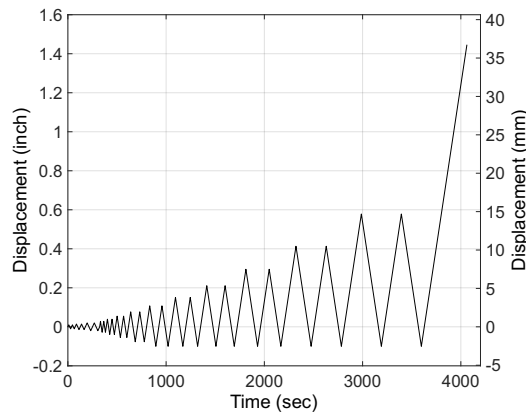


Figure 5. Asymmetric cyclic loading protocol

The test program was designed considering both existing fastener and shear wall test data and covering a wide range of steel sheet thickness, fastener size, fastener type, and loading type. Existing fastener level test data and shear wall test data related to CFS-framed steel sheet sheathed shear walls were first collected. Existing monotonic and cyclic steel sheet fastener tests in shear completed by Rogers et. al. 2000, Tao et. al. 2016, Torabian et. al. 2017, or Shi et. al. 2018 are marked as light yellow in the test matrix presented in Table 1. Existing steel sheet sheathed shear wall tests including monotonic, cyclic, and dynamic tests with specific fastener and steel sheet thickness combination scenarios completed by Singh et. al. 2020, Rizk et. al. 2018, Santos et. al. 2018, Briere et. al. 2018, DaBreo et. al. 2012, or Yu et. al. 2009 are marked as yellow in Table 1. Note that some CFS-framed steel sheet shear wall tests do not adopt the fastener and steel sheet thickness combination scenarios in Table 1 since the framing thickness is less than 54 mil (Balh et. al. 2010, Ong-Tone et. al. 2009, Yu et. al. 2007, Serrette et. al. 2002&1997). If both fastener testing (Tao et. al. 2016) and shear wall testing (DaBreo et. al. 2012) are available this is marked as blue in Table 1. Note, in only one case in Table 1 (marked in blue) is fastener-level data available that aligns with tested shear walls – this lack of data was a primary motivation for this work.

Some combinations in Table 1 are not applicable based on selecting an appropriate fastener based on thickness (CFSEI 2012), the corresponding cells in the test matrix of Table 1 are shadowed. Note, 0.019 in. steel sheet thickness are assumed applicable to 0.018 in. sheet; and 0.03 in. steel sheet thickness are assumed applicable to 0.027 in. or 0.033 in. sheet (only) when referring to existing fastener or shear wall test configurations in the test matrix.

The full test matrix consists of three phases (I-III) as summarized in Table 1. In Phase I the test specimen consists of one thick cold-formed steel framing ply and one thin steel sheet ply (in contact with fastener head) fastened by one single fastener. In Phase II the test specimen consists of one thin steel sheet ply sandwiched by two cold-formed steel framing plies (in contact with fastener head) which represents steel sheet sheathed shear walls sandwiching the steel sheet between boundary members (i.e. a mid-ply steel sheet shear wall configuration). Phase III testing investigates the strength and ductility contribution of a stronger framing system using steel plates that have the same thickness as common HSS sections, i.e. with larger thickness than cold-formed steel (of course the thin steel sheet is still in contact with the fastener head). The basic geometry of all three phases of testing are the same, as shown in Figure 3a (in detail) for Phase I.

During initial cyclic testing it was found that the direction in which the thin steel sheet ply buckles (i.e. away from or toward the fastener head) for some combinations of geometry can have a significant effect on the fastener connection strength. As a result, in the standard test scenario there are 7 tests for one basic specimen type: one monotonic test, three asymmetric cyclic tests with the thin sheet buckling away from the fastener head, and three asymmetric cyclic tests with thin sheet buckling towards the fastener head. In the 97-10-30 test series (See Figure 6 for test nomenclature), an additional 3 tension only cyclic tests are completed in addition to the standard scenario for comparison. Note, due to repeating a specific test to verify the result or other repetitions, the number of conducted tests in each test series may be slightly larger than the initial minimum number detailed in the Table 1 test matrix. A total of 143 tests are presented in the proposed test matrix and 156 tests were finally completed in this test program including 93 phase I tests, 42 phase II tests, and 21 phase III tests.

Table 1a. Steel framing-to-steel sheet fastener test matrix (in.; ksi)

| Phase | Framing Thickness (in.) ($f_{yn} \sim 50$ ksi) | Steel Sheet Thickness (in.) | | | | | | | | | |
|-------|--|-------------------------------|-----|-----|-------------------------------|-----|-----|------------------------------|-----|-----|-----|
| | | 0.013 ($f_{yn} \sim 50$ ksi) | | | 0.019 ($f_{yn} \sim 33$ ksi) | | | 0.03 ($f_{yn} \sim 33$ ksi) | | | PAF |
| | | #8 | #10 | #12 | #8 | #10 | #12 | #8 | #10 | #12 | |
| I | CFS | 0.054 | 7 | 7 | | 7 | 7 | | 7 | 7 | |
| | | 0.068 | | | | | | | | | |
| | | 0.097 | | 7 | | | 7 | | 7 | 10 | 7 |
| | | 0.118 | | | | | | | | | |
| II | 2 Ply CFS | 2 x 0.097 | | 7 | | | 7 | | | 7 | 7 |
| | | 2 x 0.118 | | | | | | | | | |
| III | HSS | 0.188 | | | | | | | | | 7 |
| | | 0.375 | | | | | | | | | 7 |

-  Fastener testing existing (monotonic and cyclic)
 -  Steel sheet sheathed shear wall testing existing (monotonic, cyclic, and/or dynamic)
 -  Both Fastener and shear wall testing existing
 -  Combination of fastener and steel thickness which is not applicable based on TN of CFSEI
- 7 test series: 1 Monotonic ; 3 Asymmetric Cyclic Buckling Away ; 3 Asymmetric Cyclic Buckling
10 test series: 3 Tension Only Cyclic + 7 test series

Table 1b. Steel framing-to-steel sheet fastener test matrix (mm; Mpa)

| Phase | Framing Thickness (mm) ($f_{yn} \sim 345$ Mpa) | Steel Sheet Thickness (mm) | | | | | | | | | |
|-------|--|-------------------------------|-----|-----|-------------------------------|-----|-----|-------------------------------|-----|-----|-----|
| | | 0.33 ($f_{yn} \sim 345$ Mpa) | | | 0.48 ($f_{yn} \sim 227$ Mpa) | | | 0.76 ($f_{yn} \sim 227$ Mpa) | | | PAF |
| | | #8 | #10 | #12 | #8 | #10 | #12 | #8 | #10 | #12 | |
| I | CFS | 1.37 | 7 | 7 | | 7 | 7 | 7 | 7 | | |
| | | 1.73 | | | | | | | | | |
| | | 2.46 | | 7 | | | 7 | | 7 | 10 | 7 |
| | | 3.00 | | | | | | | | | |
| II | 2 Ply CFS | 2 x 2.46 | | 7 | | | 7 | | 7 | 7 | 7 |
| | | 2 x 3.00 | | | | | | | | | 7 |
| III | HSS | 4.76 | | | | | | | | 7 | 7 |
| | | 9.53 | | | | | | | | | 7 |

Fastener testing existing (monotonic and cyclic)
 Steel sheet sheathed shear wall testing existing (monotonic, cyclic, and/or dynamic)
 Both Fastener and shear wall testing existing
 Combination of fastener and steel thickness which is not applicable based on TN of CFSEI
 7 test series: 1 Monotonic ; 3 Asymmetric Cyclic Buckling Away ; 3 Asymmetric Cyclic Buckling
 10 test series: 3 Tension Only Cyclic + 7 test series

The Phase I test nomenclature in this test program, for example, “47-54-8-30-M”, as shown in Figure 6a, consists of three parts “47”, “54-8-30”, and “M”. The first part “47” refers to the test ID. The second part “54-8-30” is the specimen type, which stands for 30 mil thin steel sheet ply (in contact with fastener head) and 54 mil thick framing steel ply fastened by one single ¾” long #8 self-drilling Phillips Rounded Head screw with 18 thread number and No. 2 point type (1” long #10 self-drilling Phillips Rounded Head screw with 16 thread number and No. 3 point type and 7/8” long #12 self-drilling Flat Pan Head screw with 18 thread number and No. 3 point type are also adopted) in Phase I tests. The third part “M” represents test type, and stands for monotonic. Other test types include “A”, for asymmetric cyclic tests with thin steel sheet buckling **away** from the fastener head, “T” for asymmetric cyclic tests with the thin steel sheet buckling **towards** the fastener head, and “Ten” for tension-only cyclic tests. The Phase II test nomenclature is similar, for example “121-97-12-30-97-M” is presented in Figure 6b, and the first number “121” is the test ID, the second part “97-12-30-97” refers to double 97 mil thick framing steel plies sandwiching the 30 mil thin steel sheet ply connected by one single #12 self-drilling screw in (thick ply in contact with fastener head), and the final “M” refers to a monotonic test type. The Phase III test nomenclature is similar to Phase I, for example in “149-188-24-30-M” the first number “149” is the test ID, the second part “188-24-30” represents 30 mil thin steel sheet ply (in contact with fastener head) and 188 mil thick framing HSS steel plate ply fastened by one single Hilti Powder-Actuated Fastening X-HSN 24 fastener (“19” referring to Hilti Powder-Actuated Fastening X-ENP-19 is also adopted in other test series), and the final part “M” refers to a monotonic test type.

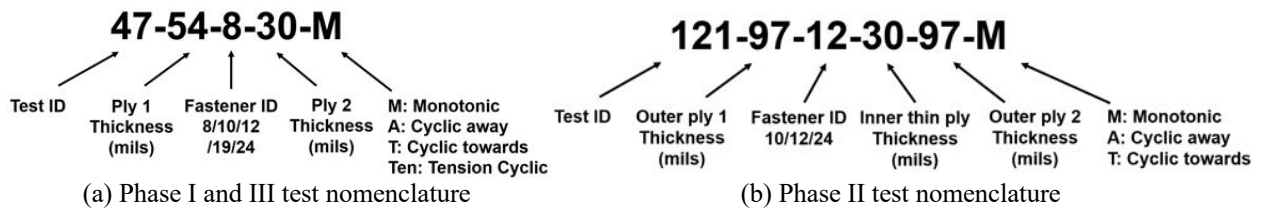
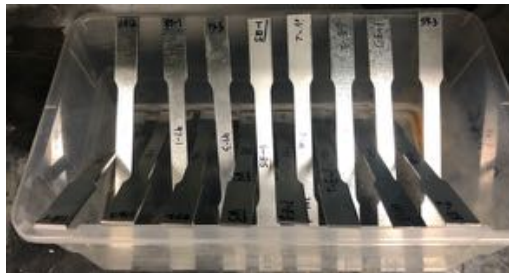


Figure 6. Test nomenclature

4 Material Testing

To determine the material properties of the steel sheet and framing plies in the test program, 18 coupon specimens were tested. For the sheet plies, raw galvanized steel materials were provided as 2 in. wide strips and shipped in the same batch. Three tension samples were milled for each thickness level per dimensions from ASTM E8-11. The coupons were tested with coating; however, the zinc coating at the two ends of the coupon were stripped for measuring accurate base metal thickness by putting the specimen into Hydrochloride acid (HCL-1N) for about 30 min, as shown in Figure 7a. Note the yield stress, etc. needs to be determined based on the accurate base metal thickness (e.g., Torabian et. al. 2016, Fratamico et. al. 2017).

The material testing was performed on a 10 kip MTS Criterion 43 Electromechanical Universal Test System, as shown in Figure 7b. Specimens were installed in the loading grips and a level was utilized to ensure the specimen axially aligned with the actuator. An extensometer was installed on the specimens within the gauge length to measure the engineering strain more precisely. The test setup is shown in Figure 7c. The specimen was loaded at a rate of 0.00083 in./sec constantly throughout the test, and the specimen status before and after the material testing are presented in Figure 7d and Figure 7e. Five width measurements with a caliper and five thickness measurements with a micrometer within the gauge length were conducted to guarantee accurate measurement of the initial cross-sectional area properties. Moreover, the marked gauge length before and after test were also measured to determine the total elongation.



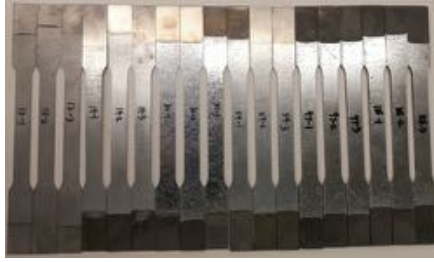
(a) Stripping the zinc coating using hydrochloride acid



(b) MTS Electromechanical Universal Test System



(c) Specimen in the test rig



(d) Specimens before test



(e) Specimens after test

Figure 7. Material test

The coupon test result summary for each thickness is provided in Table 2. Note that the HSS steel plate material properties were not tested and the nominal yield strength, 50 ksi, and nominal tensile strength, 65 ksi, will be adopted if the strength value is needed. Table 2 includes yield strength (based on 0.2% offset method), strain at yield, tensile strength, strain at tensile strength, and percent elongation at rupture.

Most of the tested thin sheet materials have low yield stress and high ultimate elongation, which aligns with the CFS-framed steel sheet sheathed shear wall design philosophy that the steel sheet sheathing should work as a fuse to generate the majority of the energy dissipation in the shear walls.

Table 2a. Material test result (in.; ksi)

| Nominal Thickness (in) | True Thickness (in.) | f_{yn} (ksi) | $f_{0.2}$ (ksi) | ϵ_y (%) | f_u (ksi) | ϵ_u (%) | ϵ_r (%)* |
|------------------------|----------------------|----------------|-----------------|------------------|-------------|------------------|-------------------|
| 0.013 | 0.012 | 50 | 48.213 | 0.36 | 60.313 | 17.64 | 26.36 |
| 0.019 | 0.019 | 33 | 30.312 | 0.30 | 49.853 | 21.79 | 40.95 |
| 0.030 | 0.030 | 33 | 21.810 | 0.27 | 45.268 | 22.32 | 46.04 |
| 0.054 | 0.058 | 50 | 51.435 | 0.37 | 67.622 | 20.15 | 36.57 |
| 0.097 | 0.100 | 50 | 61.269 | 0.41 | 77.480 | 10.75 | 16.18 |
| 0.118 | 0.122 | 50 | 65.187 | 0.42 | 81.873 | 12.92 | 21.64 |

Note: ϵ_r * implies the total elongation after rupture based on a 2 inch gauge length.

Table 2b. Material test result (mm; Mpa)

| Nominal Thickness (mm) | True Thickness (mm) | f_{yn} (Mpa) | $f_{0.2}$ (Mpa) | ϵ_y (%) | f_u (Mpa) | ϵ_u (%) | ϵ_r (%)* |
|------------------------|---------------------|----------------|-----------------|------------------|-------------|------------------|-------------------|
| 0.33 | 0.31 | 345 | 332.42 | 0.36 | 415.84 | 17.64 | 26.36 |
| 0.48 | 0.48 | 227 | 208.99 | 0.30 | 343.72 | 21.79 | 40.95 |
| 0.76 | 0.78 | 227 | 150.37 | 0.27 | 312.11 | 22.32 | 46.04 |
| 1.37 | 1.47 | 345 | 354.63 | 0.37 | 466.24 | 20.15 | 36.57 |
| 2.46 | 2.54 | 345 | 422.43 | 0.41 | 534.21 | 10.75 | 16.18 |
| 3.00 | 3.11 | 345 | 449.45 | 0.42 | 564.49 | 12.92 | 21.64 |

Note: ϵ_r * implies the total elongation after rupture based on a 50 mm gauge length.

5 Failure Modes

Although the primary purpose of the cyclic shear testing conducted herein is to provide nonlinear fastener-level force-deformation response for use in models of steel sheet shear walls the manner in which these connections fail, and the strength that they develop is also of interest. Since the connections are not in pure shear, but rather a combination of shear and shear + tension the failure modes from design (AISI S100-16) and the literature currently associated with shear and tension failure in screw connections are summarized herein. This terminology is used to describe the observed response in the tests and is intended to be useful when comparing to design specifications.

Pull-over and pull-out are common screw failure modes under tension demand defined in AISI S100-16. These two failure modes both refer to the case that tension load is applied on the thin steel sheet ply (in contact with the fastener head) such as occurs in wind suction on sheeting. Pull-over, as presented in Figure 8a, implies that the thin steel sheet ply is damaged and pulled over the fastener head, while pull-out implies that the thin steel sheet ply together with the fastener itself are undamaged and instead the damage is at the screw to thicker ply as it is pulled out from the damaged fastener hole as presented in Figure 8b.

Pull-through is not a failure mode defined in AISI S100-16, but is closely associated with the pull-over failure mode. The pull-through failure mode is recognized in the related technical literature (e.g., Peterman 2014). Different from pull-over, or pull-out failure modes under tension demand as presented in Figure 8a & 8b, pull-through is a failure mode under shear demand where the thick framing steel ply (e.g., corresponding to the stud or track flange in a CFS-framed shear wall) deforms and pulls the fastener with it resulting in the fastener head pulling-through and damaging the thin steel sheet ply. For example, consider a fastener connecting a thin sheet to a thicker stud which is failing in buckling. If the stud develops major axis flexure the thick framing steel ply generates predominantly tension demand on fastener and may trigger a pull-through failure mode as shown in Figure 8c, but if the stud develops flexural-torsional buckling then there will be a shear-tension interaction demand on the fastener which leads to bearing or tilting and fastener slipping through the thin steel sheathing sheet ply (i.e., pull-through with tilting/bearing failure mode) as presented Figure 8d.

Bearing, tilting and bearing, and shear rupture are three normal fastener failure modes under shear demand (besides screw shear failure). Tilting and bearing, and shear rupture are defined in AISI S100-16. Bearing implies that the thin steel sheet ply material in front of the fastener contour develops damage in bearing or piling up and/or minor tearing as shown in Figure 8e. Tilting and bearing refers to the failure mode where the fastener tilts resulting from the eccentric shear forces acting on the fastener and localized bearing of the thin steel sheet ply can be observed around the tilted fastener, accompanied by the fastener head prying on the thin steel sheet edge, as presented in Figure 8f. Moreover, if the fastener continues bearing in the thin steel sheet ply and pull-through with tilting/bearing failure mode is not initiated, another failure mode: shear rupture, as shown in Figure 8g which is the end shearing failure demonstrating longitudinal shearing of the thin steel sheet along two approximately parallel lines can be triggered.

Tests on screw fastened steel sheet sheathed CFS-framed shear walls have exhibited, bearing, shear rupture, tilting and bearing, and pull-through with tilting/bearing failure modes (Singh et. al. 2020, Rizk et. al. 2018, Santos et. al. 2018, Briere et. al. 2018, DaBreo et. al. 2012, Yu et. al. 2009).

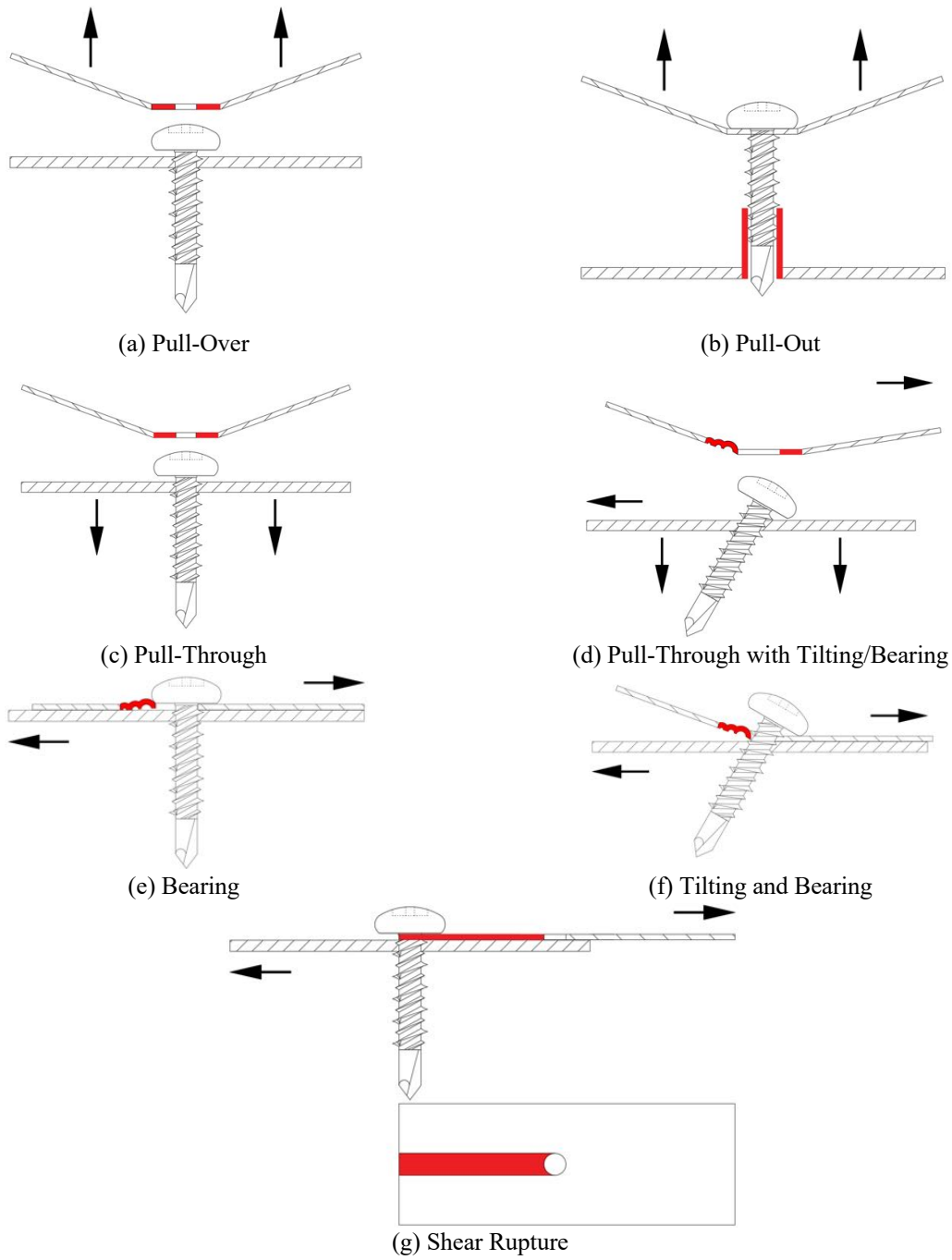


Figure 8. Fastener failure modes

6 Test Results

Test series information including specimen type, nominal thickness of the sheet plies, fastener size, the number of conducted tests and average cyclic test values including initial stiffness (based on the 40% peak strength point), peak strength and corresponding deformation, post-peak deformation at 80% peak strength are presented in Table 3. Detailed test information and results including peak strength, deformation at peak strength, and failure modes for each conducted test are summarized in Appendix 1. Displacement-force curves and deformation development pictures for each test are provided in Appendix 3.

Table 3a. Average test results for each test series (in.; kip)

| Specimen Type | Phase | Fastener (#) | Thin sheet ply (mil) | Thick framing ply (mil) | Total test # | Initial stiffness (kip/in.) | Deformation @ Pmax (in.) | Pmax (kip) | D _{postpeak80%} (in.) |
|---------------|-------|--------------|----------------------|-------------------------|--------------|-----------------------------|--------------------------|------------|--------------------------------|
| 54-10-13 | I | 10 | 13 | 54 | 7 | 55.819 | 0.042 | 0.301 | 0.152 |
| 54-10-19 | I | 10 | 19 | 54 | 7 | 95.742 | 0.132 | 0.423 | 0.204 |
| 54-10-30 | I | 10 | 30 | 54 | 11 | 113.693 | 0.403 | 0.918 | 0.478 |
| 54-8-13 | I | 8 | 13 | 54 | 7 | 65.639 | 0.041 | 0.255 | 0.147 |
| 54-8-19 | I | 8 | 19 | 54 | 7 | 101.961 | 0.134 | 0.376 | 0.204 |
| 54-8-30 | I | 8 | 30 | 54 | 8 | 57.259 | 0.494 | 0.931 | 0.556 |
| 97-10-13 | I | 10 | 13 | 97 | 7 | 100.425 | 0.004 | 0.340 | 0.109 |
| 97-10-19 | I | 10 | 19 | 97 | 7 | 113.839 | 0.113 | 0.394 | 0.216 |
| 97-10-30 | I | 10 | 30 | 97 | 14 | 146.184 | 0.225 | 0.766 | 0.296 |
| 97-12-30 | I | 12 | 30 | 97 | 9 | 203.632 | 0.215 | 0.789 | 0.290 |
| 97-8-30 | I | 8 | 30 | 97 | 9 | 215.883 | 0.209 | 0.800 | 0.283 |
| 97-10-13-97 | II* | 10 | 13 | 97 | 7 | 103.633 | 0.150 | 0.580 | 0.271 |
| 97-10-19-97 | II* | 10 | 19 | 97 | 7 | 43.100 | 0.336 | 0.778 | 0.428 |
| 97-10-30-97 | II* | 10 | 30 | 97 | 7 | 36.283 | 0.369 | 1.128 | 0.490 |
| 97-12-30-97 | II* | 12 | 30 | 97 | 7 | 36.981 | 0.394 | 1.199 | 0.534 |
| 97-24-30-97 | II* | X-HSN-24 | 30 | 97 | 7 | 201.572 | 0.376 | 1.091 | 0.532 |
| 118-24-30-118 | II* | X-HSN-24 | 30 | 118 | 7 | 191.821 | 0.390 | 1.140 | 0.542 |
| 188-12-30 | III | 12 | 30 | 188 | 7 | 126.134 | 0.165 | 0.766 | 0.261 |
| 188-24-30 | III | X-HSN-24 | 30 | 188 | 7 | 266.026 | 0.227 | 1.098 | 0.352 |
| 375-19-30 | III | X-ENP-19 | 30 | 375 | 7 | 73.139 | 0.208 | 1.051 | 0.306 |

Note: II* refers to test series with two outer thick steel framing plies sandwiching one inner thin steel sheet ply.

Table 3b. Average test results for each test series (mm; kN)

| Specimen Type | Phase | Fastener (#) | Thin sheet ply (mm) | Thick framing ply (mm) | Total test # | Initial stiffness (kN/mm) | Deformation @ Pmax (mm) | Pmax (kN) | D _{postpeak80%} (mm) |
|---------------|-------|--------------|---------------------|------------------------|--------------|---------------------------|-------------------------|-----------|-------------------------------|
| 54-10-13 | I | 10 | 0.33 | 1.37 | 7 | 6.55 | 1.07 | 1.34 | 3.87 |
| 54-10-19 | I | 10 | 0.48 | 1.37 | 7 | 10.13 | 3.36 | 1.88 | 5.18 |
| 54-10-30 | I | 10 | 0.76 | 1.37 | 11 | 11.65 | 10.23 | 4.08 | 12.14 |
| 54-8-13 | I | 8 | 0.33 | 1.37 | 7 | 8.11 | 1.04 | 1.14 | 3.73 |
| 54-8-19 | I | 8 | 0.48 | 1.37 | 7 | 9.75 | 3.39 | 1.67 | 5.19 |
| 54-8-30 | I | 8 | 0.76 | 1.37 | 8 | 5.33 | 12.55 | 4.14 | 14.13 |
| 97-10-13 | I | 10 | 0.33 | 2.46 | 7 | 14.68 | 0.10 | 1.51 | 2.77 |
| 97-10-19 | I | 10 | 0.48 | 2.46 | 7 | 12.80 | 2.88 | 1.75 | 5.49 |
| 97-10-30 | I | 10 | 0.76 | 2.46 | 14 | 16.80 | 5.70 | 3.41 | 7.52 |
| 97-12-30 | I | 12 | 0.76 | 2.46 | 9 | 27.51 | 5.45 | 3.51 | 7.36 |
| 97-8-30 | I | 8 | 0.76 | 2.46 | 9 | 21.75 | 5.32 | 3.56 | 7.18 |

| | | | | | | | | | |
|---------------|-----|----------|------|------|---|-------|-------|------|-------|
| 97-10-13-97 | II* | 10 | 0.33 | 2.46 | 7 | 8.66 | 3.80 | 2.58 | 6.89 |
| 97-10-19-97 | II* | 10 | 0.48 | 2.46 | 7 | 4.59 | 8.53 | 3.46 | 10.87 |
| 97-10-30-97 | II* | 10 | 0.76 | 2.46 | 7 | 5.89 | 9.38 | 5.02 | 12.45 |
| 97-12-30-97 | II* | 12 | 0.76 | 2.46 | 7 | 6.12 | 10.01 | 5.33 | 13.58 |
| 97-24-30-97 | II* | X-HSN-24 | 0.76 | 2.46 | 7 | 34.21 | 9.56 | 4.85 | 13.50 |
| 118-24-30-118 | II* | X-HSN-24 | 0.76 | 3.00 | 7 | 31.51 | 9.89 | 5.07 | 13.78 |
| 188-12-30 | III | 12 | 0.76 | 4.76 | 7 | 13.91 | 4.19 | 3.41 | 6.62 |
| 188-24-30 | III | X-HSN-24 | 0.76 | 4.76 | 7 | 40.53 | 5.77 | 4.89 | 8.95 |
| 375-19-30 | III | X-ENP-19 | 0.76 | 9.53 | 7 | 12.11 | 5.29 | 4.67 | 7.77 |

Note: II* refers to test series with two outer thick steel framing plies sandwiching one inner thin steel sheet ply.

Dominant failure modes observed in this testing program are bearing, tilting and bearing, pull-through with tilting/bearing, and shear rupture (similar failure modes were observed in tests of screw-fastened CFS-framed steel sheet sheathed shear walls). When the thin steel sheet ply fails in bearing, even modest tilting of the fastener, or just piling up of the material in front of the fastener head with tilting and bearing can lead to disengagement of the fastener from the thin steel sheet ply (in contact with the fastener head). This failure mode, where disengagement of the fastener head from the steel sheet ply in contact with the head occurs, is termed pull-through with tilting/bearing in this report, aligning with the failure mode shown in Figure 8d. This pull-through failure mode occurs only after bearing or tilting and bearing failure modes have been initiated and may be accompanied by the tearing of the thin steel sheet ply area in contact with the fastener head. The pull-through with tilting/bearing failure mode is abbreviated as “pull-through” in later discussions in this test report. Note, it is common to observe coupling between different failure modes in this testing program. For example, bearing or tilting and bearing failure modes are developed at small deformations, then followed by either pull-through or shear rupture at larger deformation cycles, resulting in quite different response in the specimen as discussed fully in the following.

Fundamental test results, including the observed force-displacement relationship and deformation development and failure modes for eight representative tests are presented below. For the Phase I series, six tests are summarized:

- monotonic tests with #8 fasteners: “32-54-8-13-M” and “47-54-8-30-M”;
- an asymmetric cyclic test with #8 fastener and the thin steel sheet ply buckling away from the fastener head “42-54-8-30-A”;
- two asymmetric cyclic tests with #8 fastener and the thin steel sheet ply buckling towards the fastener head: “44-54-8-30-T” and “29-54-8-13-T”;
- a tension only cyclic test with #10 fastener: “72-97-10-30-Ten”.

In addition, for the Phase II tests an asymmetric cyclic test with the mid-ply configuration “116-97-12-30-97-A” is selected and for the Phase III tests an asymmetric cyclic test connected with a PAF and oriented so the thin sheet ply buckles away from the fastener head “143-188-PAF24-30-A” are also discussed in this section.

6.1 Phase I monotonic test “32-54-8-13-M”

“32-54-8-13-M” which includes a 54 mil ply and a 13 mil ply connected by a #8 fastener is representative of a number of monotonic tests, so its deformation and failure are discussed in detail herein. For the “32-54-8-13-M” monotonic test, the force-displacement curve is shown in Figure 9. The deformation development and limit states at the peak force level and post peak force levels

corresponding to approximately 80% and 10% peak load are presented in Figure 10. The bearing limit state develops throughout the test and minimal tilting is observed since the 54 mil thick framing ply is much stiffer than the 13mil thin steel sheet ply. The pull-through limit state gradually develops after the peak force level and finally the fastener disengages from the thin steel sheet ply. The demand on the fastener is primarily shear with minimal tension at deformations prior to peak load and then incorporates a growing amount of tension on the connection, especially in the post-peak force response. Observed bending deformation at the edge of the thin steel sheet ply is initiated by the fastener prying prior to reaching peak force and progresses rapidly as the fastener head tears the thin steel sheet ply in the post-peak deformation regime. There is no obvious deformation in the thicker, 54 mil, framing ply throughout the test.

Table 4. 32-54-8-13-M test limit states and deformation development summary

| Force level | Before Peak | Peak | Post peak (~80%) | Post peak (~10%) |
|-----------------------|-----------------------|-----------------------|------------------------|------------------|
| Limit State | bearing | bearing | bearing / pull-through | disengagement |
| Fastener Demand | shear + small tension | shear + small tension | shear + tension | — |
| Thin Ply Deformation | minor bending | bending | bending / tearing | permanent damage |
| Thick Ply Deformation | — | — | — | — |

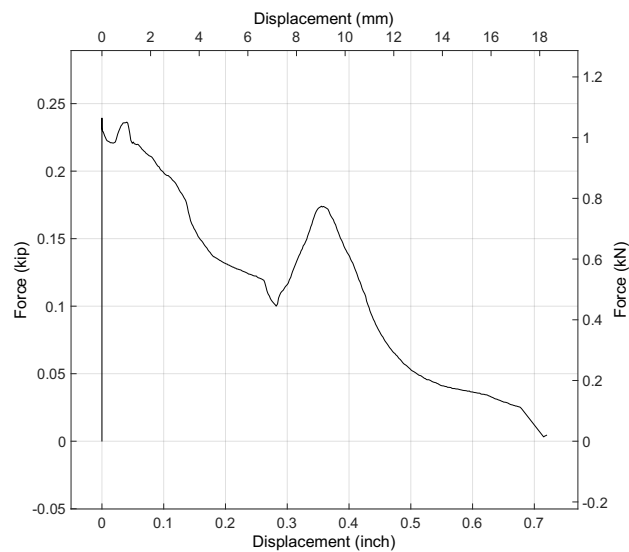


Figure 9. Force-displacement curve for test “32-54-8-13-M”



(a) @Peak strength-front view (b) @Peak strength-side view (c) @ 80% post peak (d) After test

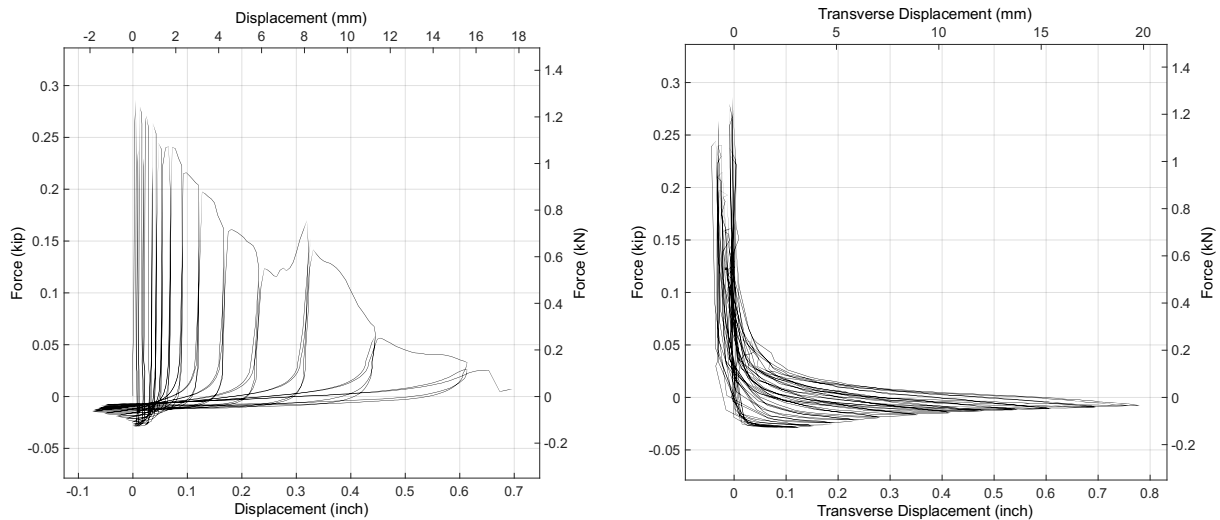
Figure 10. Deformation and failure of test “32-54-8-13-M”

6.2 Phase I asymmetric cyclic test “29-54-8-13-T”

The force-displacement curve, description of deformation development, and observed limit states for test “29-54-8-13-T” which includes 54 mil and 13 mil plies connected with a #8 screw and tested cyclically are provided in Figure 11 and Figure 12. The thin steel sheet ply in contact with fastener head is constrained to buckle towards the fastener head (“T” test type in the nomenclature) when the test specimen is in compression. The force-displacement relationship using the transverse displacement of the thin steel sheet ply at the middle point of the thin ply is presented in Figure 11b. A plastic hinge develops in the middle of the thin steel sheet after a few compression cycles. Bearing is observed in the 13 mil thin steel sheet ply and bearing and pull-through are observed after the peak force level. Failure is ultimately accompanied by tearing out of the thin steel sheet ply edge (disengagement of the fastener from the thin ply). No tilting is observed in the 54 mil thick framing ply. The demand on the fastener is primarily shear, but in the post-peak response shear-tension interaction is observed. Bending of the thin steel sheet ply edge is initialized by the fastener prying and develops as the test progresses. There is no obvious deformation in the 54 mil thick framing ply. In general, the cyclic response is similar to the monotonic response for this configuration.

Table 5. 29-54-8-13-T test limit states and deformation development summary

| Force level | Before Peak | Peak | Post peak (~80%) | Post peak (~10%) |
|-----------------------|-----------------------|-----------------------|-----------------------|------------------|
| Limit State | bearing | bearing | bearing /pull-through | disengagement |
| Fastener Demand | shear + small tension | shear + small tension | shear + tension | — |
| Thin Ply Deformation | minor bending | bending | bending / tearing | permanent damage |
| Thick Ply Deformation | — | — | — | — |



(a) Force-PT displacement curve

(b) Force-Laser sensor displacement

Figure 11. Force-displacement curves for test “29-54-8-13-T”

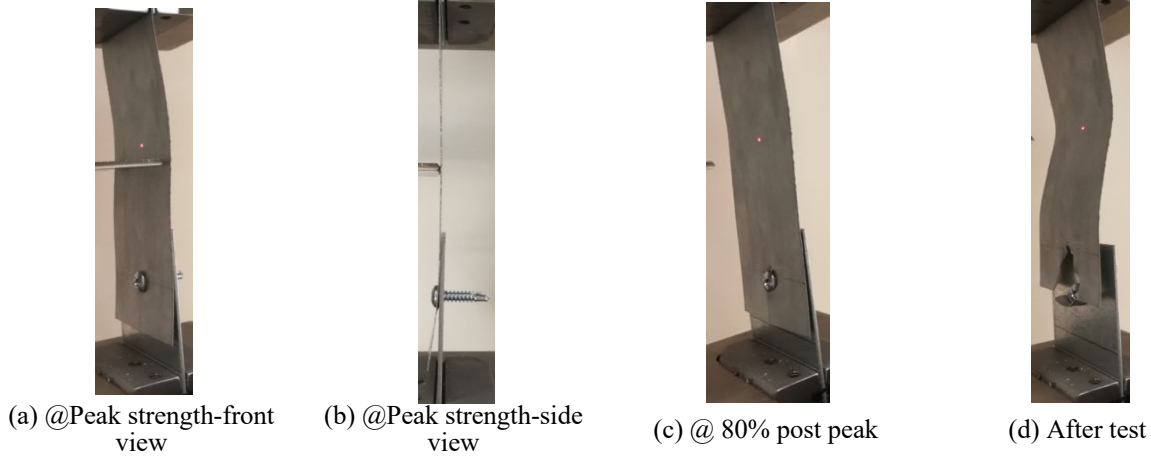


Figure 12. Deformation and failure of test “29-54-8-13-T”

6.3 Phase I monotonic test “47-54-8-30-M”

Test “47-54-8-30-M” which includes 54 and 30 mil plies connected by a #8 screw responds differently than the 54-8-13 specimens and is representative of the response when the two plies are more similar in thickness. The force-displacement curve of the “47-54-8-30-M” monotonic test is shown in Figure 13. The description of the deformation development and observed limit states are presented in Figure 14. The limit states include bearing and shear rupture of the thin steel sheet ply and fastener tilting throughout the test. The demand on the fastener is predominately shear. The shear rupture failure in the 30 mil thin steel sheet ply is initialized before peak force and develops together with bearing failure as the test progresses. Minor bending is observed in the thick framing steel ply prior to peak load, and remains relatively small, though observable, throughout the test.

Table 6. 47-54-8-30-M test limit states and deformation development summary

| Force level | Before Peak | Peak | Post peak (~80%) | Post peak (~10%) |
|-----------------------|----------------------------------|----------------------------------|----------------------------------|------------------|
| Limit State | tilting & bearing /shear rupture | tilting & bearing /shear rupture | tilting & bearing /shear rupture | disengagement |
| Fastener Demand | shear | shear | shear | — |
| Thin Ply Deformation | end shearing out | end shearing out | end shearing out | permanent damage |
| Thick Ply Deformation | minor bending | minor bending | minor bending | — |

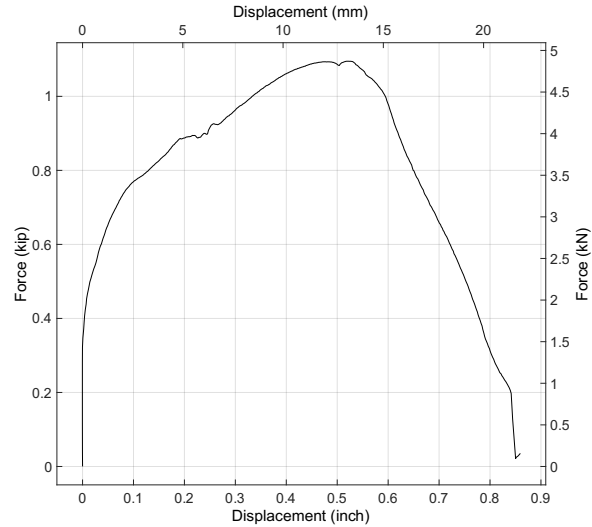


Figure 13. Force-displacement curve for test “47-54-8-30-M”

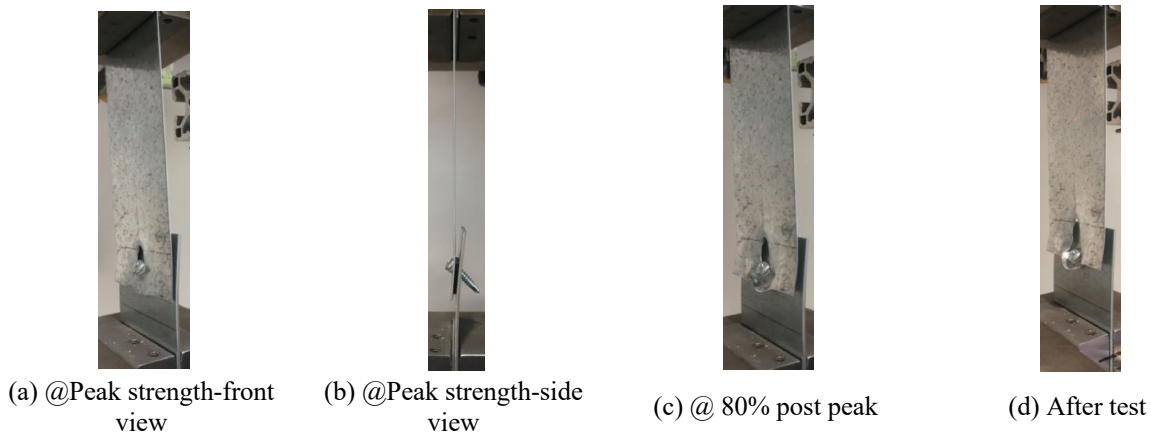


Figure 14. Deformation and failure of test “47-54-8-30-M”

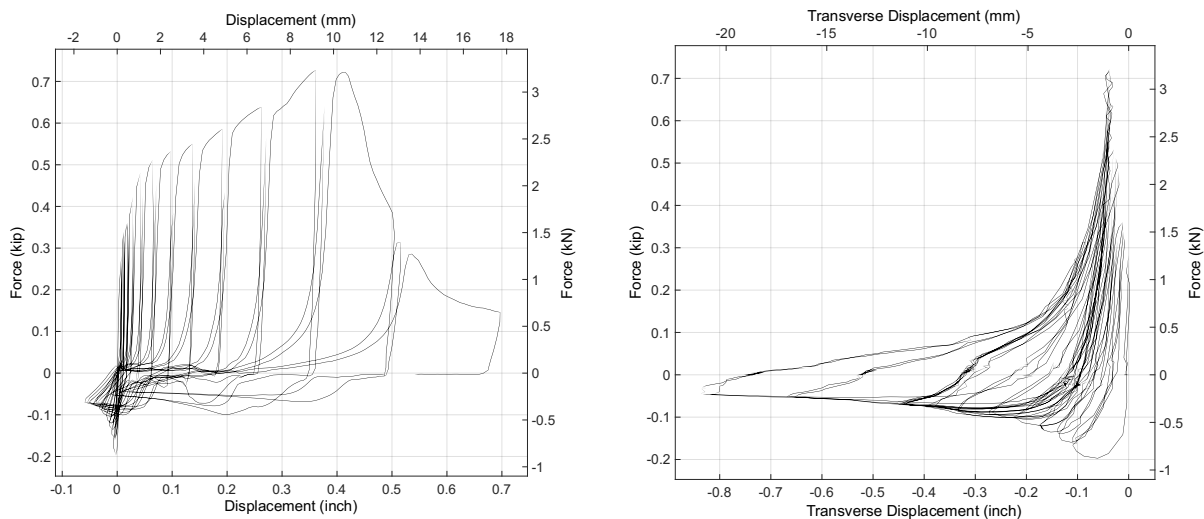
6.4 Phase I asymmetric cyclic test “42-54-8-30-A”

Test “42-54-8-30-A” which is the same configuration (54 and 30 mil plies with #8 fastener) as the monotonic test detailed in the previous section is here tested cyclically with the thin 30 mil steel sheet ply buckling away from the fastener head. The force-displacement curve for “42-54-8-30-A” is presented in Figure 15 and the description of the deformation development and limit states are provided in Figure 16. When the test specimen is in compression, the thin steel sheet ply in contact with the fastener head is restrained to buckle away from the fastener head. The force-displacement relationship based on the transverse displacement of the thin steel sheet ply at the middle point of the thin ply as detected by a laser displacement sensor is provided in Figure 15b. After a few cycles, a plastic hinge develops at the middle section of the thin steel sheet ply. Bearing in the thin steel sheet ply, and fastener tilting limit states are observed throughout the test and the pull-through limit state gradually develops after peak load. Pull-through ultimately triggers disengagement of the fastener from the thin steel sheet ply (it is not obvious in Figure 16d, but when the specimen is in compression the disengagement is readily observed). The demand on the fastener in the test is primarily shear with a small amount of tension in the pre-peak load regime and clear shear-tension interaction (demand) at and after the peak load. Bending of the thin 30 mil

steel sheet ply edge is initialized by fastener prying and continues throughout the test. Also, past peak load the pull-through limit state is also accompanied by the fastener head tearing the thin steel sheet ply area in contact with the fastener head. Minor bending deformation of the thicker 54 mil framing steel ply is also identified, but remains relatively small throughout the test.

Table 7. 42-54-8-30-A test limit states and deformation development summary

| Force level | Before Peak | Peak | Post peak (~80%) | Post peak (~10%) |
|-----------------------|-----------------------|---------------------------------|---------------------------------|------------------|
| Limit State | tilting & bearing | tilting & bearing /pull-through | tilting & bearing /pull-through | disengagement |
| Fastener Demand | shear + small tension | shear + tension | shear + tension | — |
| Thin Ply Deformation | minor bending | bending | bending / tearing | permanent damage |
| Thick Ply Deformation | — | minor bending | minor bending | — |



(a) Force-PT displacement curve (b) Force-Laser sensor displacement

Figure 15. Force-displacement curves for test “42-54-8-30-A”

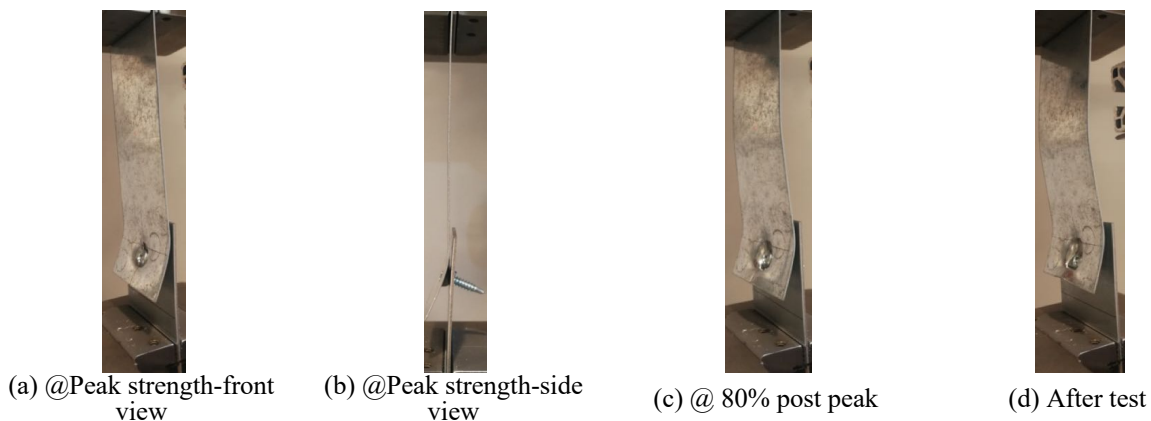


Figure 16. Deformation and failure of test “42-54-8-30-A”

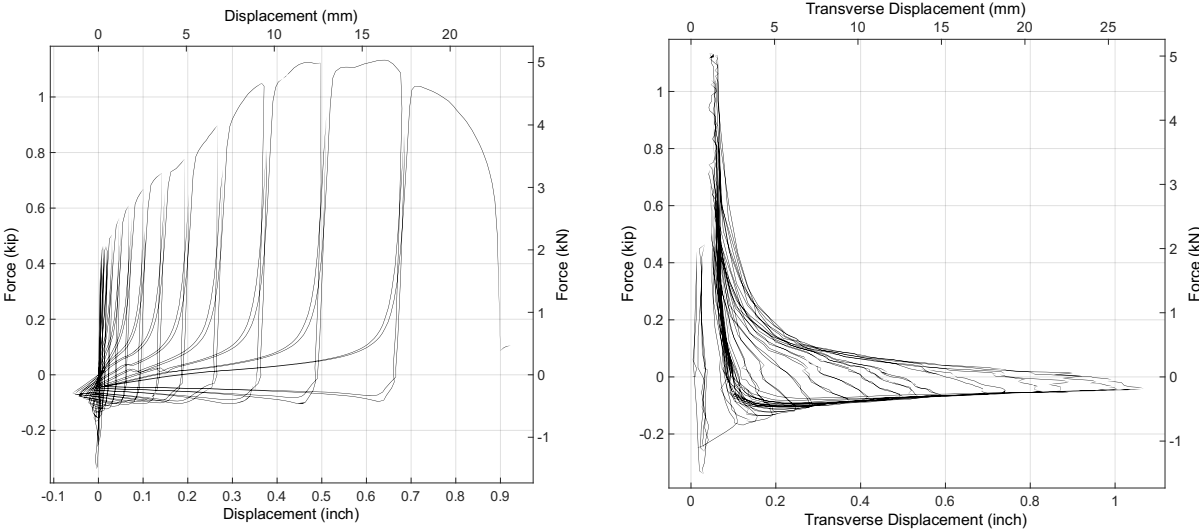
6.5 Phase I asymmetric cyclic test “44-54-8-30-T”

Test “44-54-8-30-T” is a direct companion to “42-54-8-30-A” described in the previous section. The only difference is that in “44-54-8-30-T” the 30 mil thin steel sheet is constrained to buckle

towards the fastener head (instead of away/“A”). For this configuration of sheet plies: 54 mil and 30 mil the buckling direction (away or towards) influences the observed behavior in many cases (e.g., compare Figure 17a to Figure 15a). For the “44-54-8-30-T” test the force-displacement curves and description of the deformation development and limit states are presented in Figure 17 and Figure 18. When the test specimen is in compression, the thin steel sheet ply in contact with the fastener head will buckle towards the fastener head under the guidance of the lateral support, and the force-displacement relationship based on the transverse displacement of the thin steel sheet ply at the middle point at the thin ply is plotted in Figure 17b. A plastic hinge develops at the middle section of the thin steel sheet after a few compression cycles. Bearing, fastener tilting, and shear rupture limit states are all observed in the thinner 30mil sheet ply throughout the test and demand for the fastener is predominately shear. The tearing deformation (shear rupture) of the thin steel sheet ply demonstrating longitudinal shearing of the thin steel sheet along two approximately parallel planes is initialized prior to peak load and develops as the test progresses until disengagement. Minor bending in the 54 mil thick framing is observed throughout the test.

Table 8. 44-54-8-30-T test limit states and deformation development summary

| Force level | Before Peak | Peak | Post peak (~80%) | Post peak (~10%) |
|-----------------------|-----------------------------------|-----------------------------------|-----------------------------------|------------------|
| Limit State | tilting & bearing / shear rupture | tilting & bearing / shear rupture | tilting & bearing / shear rupture | disengagement |
| Fastener Demand | shear | shear | shear | — |
| Thin Ply Deformation | end tearing | end tearing | end tearing | permanent damage |
| Thick Ply Deformation | minor bending | minor bending | minor bending | — |



(a) Force-PT displacement curve (b) Force-Laser sensor displacement
 Figure 17. Force-displacement curves for test “44-54-8-30-T”

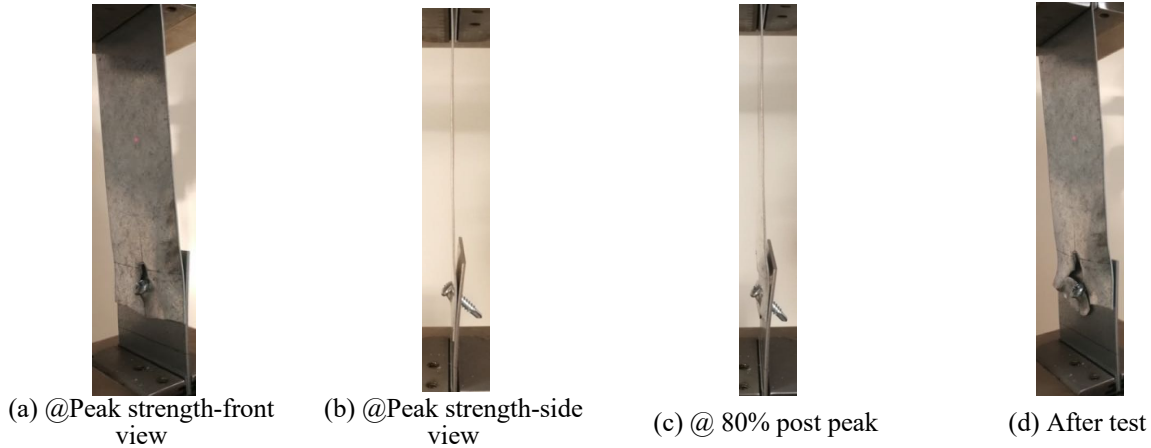


Figure 18. Deformation and failure of test “44-54-8-30-T”

6.6 Phase I tension only cyclic test “72-97-10-30-Ten”

Test “72-97-10-30-Ten” provides a test with tension-only cyclic response, in this case with 97 and 30 mil plies connected by a #10 screw. The force-displacement curve is presented in Figure 19 and description of the deformation development and limit states are shown in Figure 20. Since there are no compression cycles in the loading protocol, no buckling deformation or plastic hinge of the thin steel sheet ply are observed in this test. The thin steel sheet ply bearing develops throughout the test and pull-through limit state occurs after the peak force level, ultimately accompanied by tearing out of the thin steel sheet ply edge (disengagement of the fastener head from the thin ply). The demand on the fastener is primarily shear prior to peak load and shear-tension interaction after peak load. Bending of the thin 30 mil steel sheet ply is initialized and driven by the prying of fastener head. There is no obvious deformation in the thick 97 mil framing ply.

Table 9. 72-97-10-30-Ten test limit states and deformation development summary

| Force level | Before Peak | Peak | Post peak (~80%) | Post peak (~10%) |
|-----------------------|--------------------------|--------------------------|--------------------------|------------------|
| Limit State | bearing | bearing /pull-through | bearing /pull-through | disengagement |
| Fastener Demand | shear + small tension | shear + tension | shear + tension | — |
| Thin Ply Deformation | minor bending | bending | bending / tearing | permanent damage |
| Thick Ply Deformation | — | — | — | — |

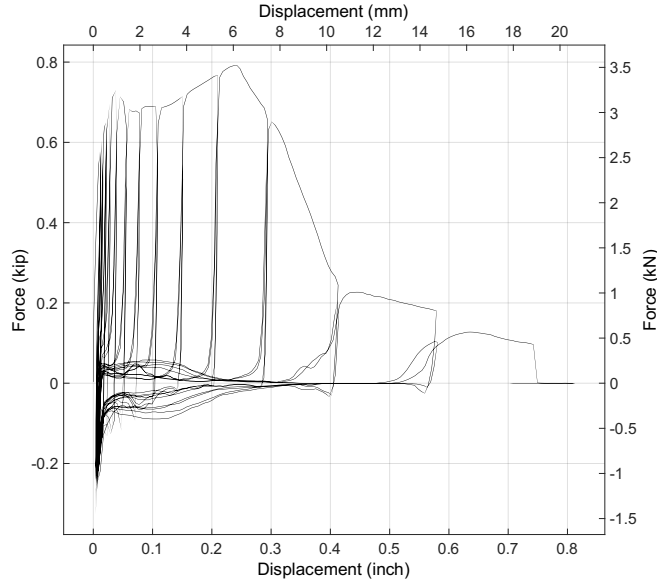


Figure 19. Force-displacement curve for test “72-97-10-30-Ten”

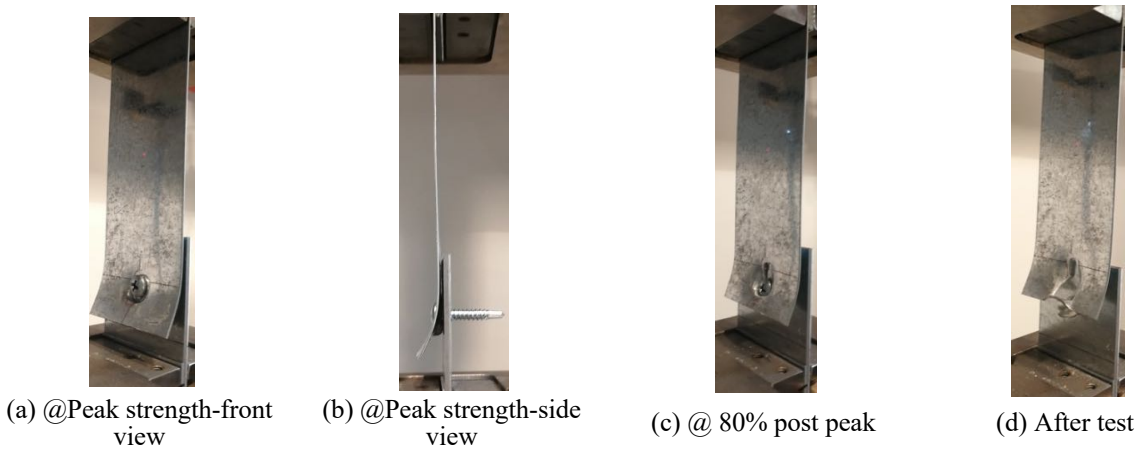


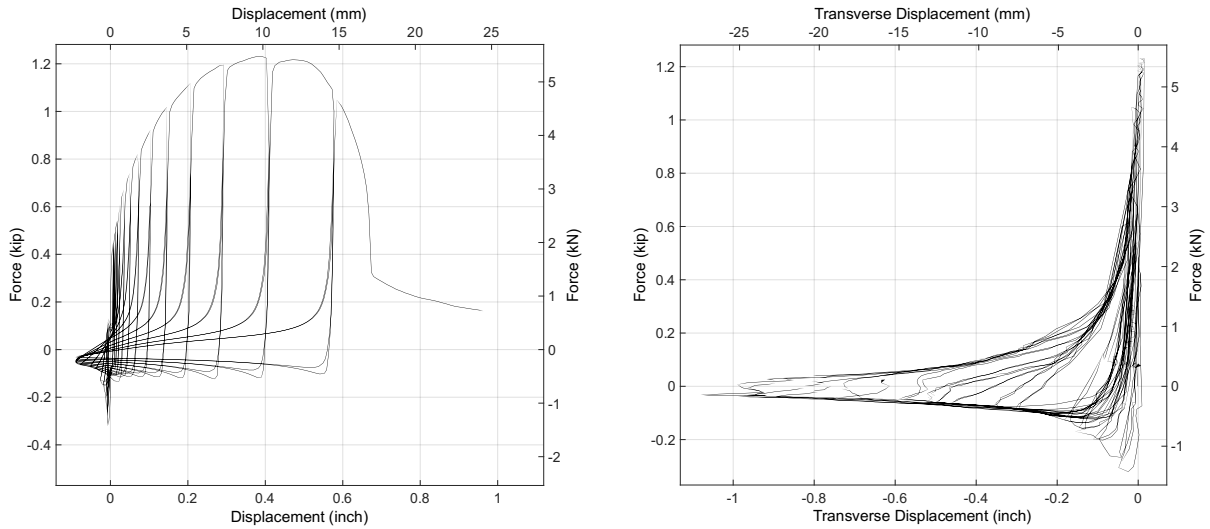
Figure 20. Deformation and failure of test “72-97-10-30-Ten”

6.7 Phase II asymmetric cyclic test “116-97-12-30-97-A”

For the Phase II tests, which are a mid-ply configuration, test “116-97-12-30-97-A” is selected as representative, and consists of two 97 mil plies sandwiching a 30 mil ply and fastened with a #12 screw. The force-displacement relationship and description of the deformation development and limit states are shown in Figure 21 and Figure 22. The inner thin 30 mil steel sheet ply is constrained to buckle away from the fastener head when the specimen is in compression, and the force-displacement relationship based on the transverse displacement of the inner thin steel sheet ply at the middle point of the inner ply is provided in Figure 21b. A plastic hinge at the middle section of the inner ply develops after a few compression cycles. Bearing and shear rupture limit states are observed in the thin steel sheet ply. No tilting was observed since the double shear connection does not generate eccentric forces. No obvious deformation is observed in the two thick 97 mil framing plies.

Table 10. 116-97-12-30-97-A test limit states and deformation development summary

| Force level | Before Peak | Peak | Post peak (~80%) | Post peak (~10%) |
|-----------------------|-------------------------|-------------------------|-------------------------|------------------|
| Limit State | bearing / shear rupture | bearing / shear rupture | bearing / shear rupture | disengagement |
| Fastener Demand | shear | shear | shear | — |
| Thin Ply Deformation | end tearing | end tearing | end tearing | permanent damage |
| Thick Ply Deformation | — | — | — | — |



(a) Force-PT displacement curve (b) Force-Laser sensor displacement
 Figure 21. Force-displacement curves for test “116-97-12-30-97-A”

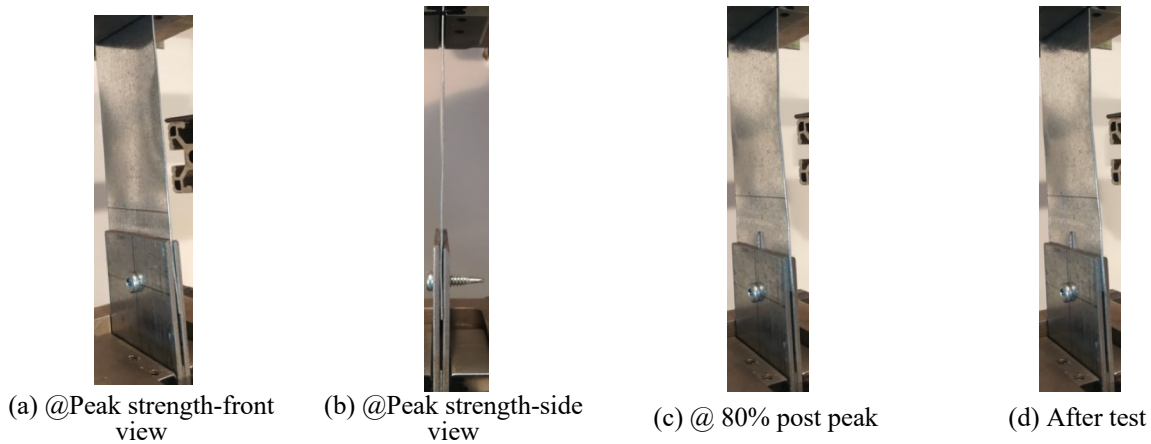


Figure 22. Deformation and failure of test “116-97-12-30-97-A”

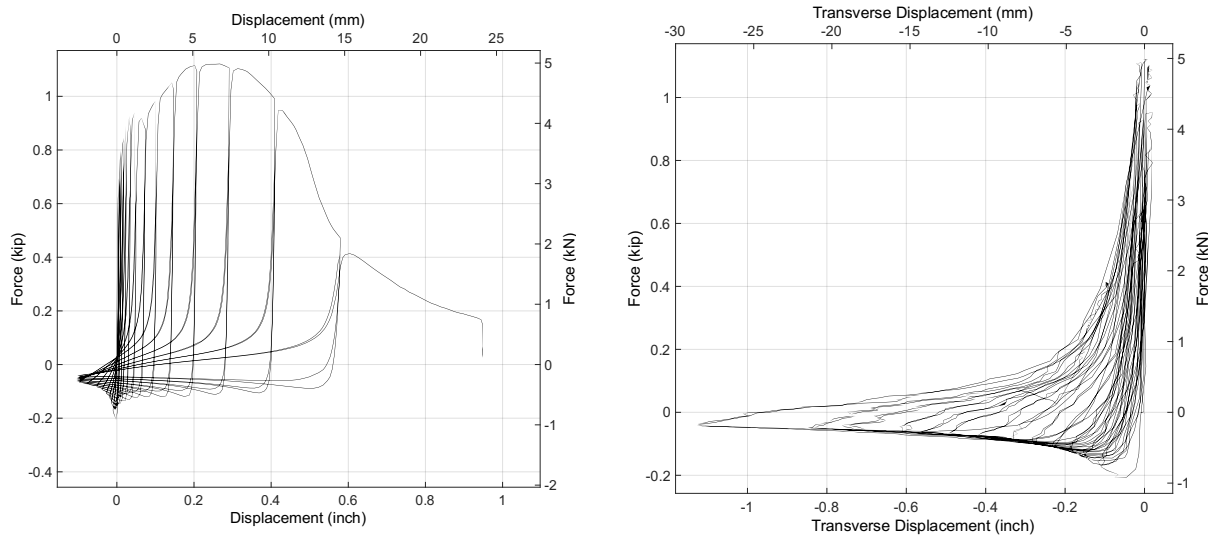
6.8 Phase III asymmetric cyclic test “143-188-24-30-A”

Test “143-188-24-30-A” is selected to represent the Phase III tests which features much thicker framing plies (188 mil) attached by a X-HSN-24 PAF to a thin 30 mil sheet ply. The force-displacement relationship is presented in Figure 23 and description of the deformation development and limit states are shown in Figure 24. The force-displacement relationship based on the transverse displacement of the thin steel sheet ply at the middle point of the thinner ply is presented in Figure 23b. A plastic hinge develops in the middle section of the thinner ply after a

few compression cycles. Since the thick steel plate is stiff and the PAF fastener head moment-resisting arm is larger than for typical screws, tilting is constrained. Bearing and shear rupture in the thin ply are the dominant limit states and the demand on the fastener is predominantly shear with minimal tension. Bending of the thin steel sheet ply is initialized by the PAF fastener and progresses throughout the test. No obvious steel plate deformation is observed in the thicker 188 mil steel plate.

Table 11. 143-188-24-30-A test limit states and deformation development summary

| Force level | Before Peak | Peak | Post peak (~80%) | Post peak (~10%) |
|-----------------------|-----------------------------|-------------------------|-------------------------|------------------|
| Limit State | bearing / shear rupture | bearing / shear rupture | bearing / shear rupture | disengagement |
| Fastener Demand | shear | shear | shear | — |
| Thin Ply Deformation | minor bending / end tearing | bending / end tearing | bending / end tearing | permanent damage |
| Thick Ply Deformation | — | — | — | — |



(a) Force-PT displacement curve (b) Force-Laser sensor displacement
Figure 23. Force-displacement curves for test “143-188-24-30-A”

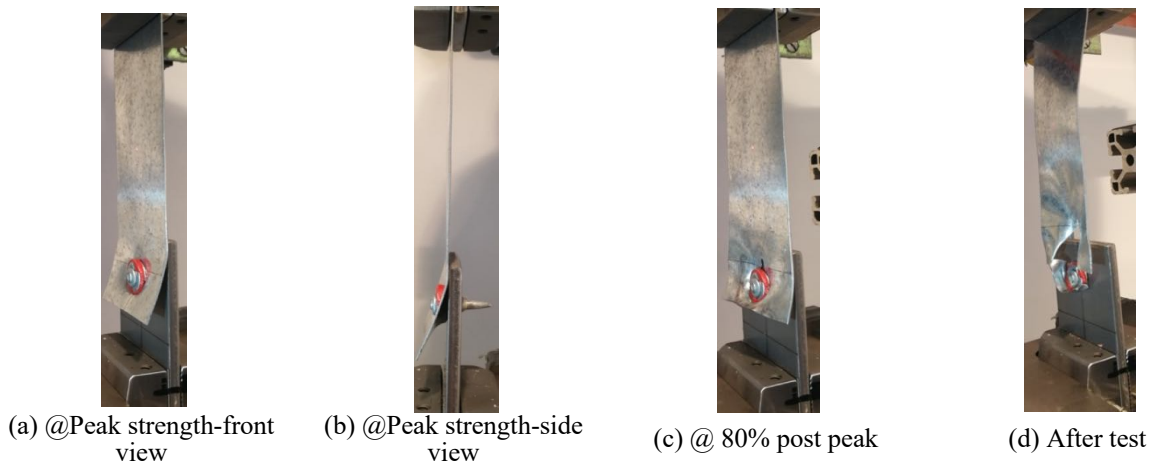


Figure 24. Deformation and failure of test “143-188-24-30-A”

7 Backbone Response Test Data Characterization

To provide a convenient means to implement the tested connections in models a procedure is developed for idealizing the test results with a multi-segment linear backbone phenomenological model. A four segment model, consistent with the Pinching4 material model in OpenSees, is selected for the backbone. The model is fit by balancing energy between the linear segment model and the nonlinear test results. Only the tension side test result is adopted for the data characterization herein. The developed modeling parameters (D_1, P_1 ; D_2, P_2 ; D_3, P_3 ; D_4, P_4) are intended to support numerical models which need to simulate the nonlinear (hysteretic) fastener response, e.g. in a shear wall simulation. Appendix 2 provides the four point backbone fit to every test. Test data characterization results plotted together with displacement-force curve for each conducted test are provided in Appendix 3.

The Phase I monotonic test “47-54-8-30-M” and asymmetric cyclic test “44-54-8-30-T”, which are both for the 54 mil - 30 mil configuration with #8 screws, are adopted herein to explain the characterization procedure. For the cyclic test “44-54-8-30-T” as shown in Figure 25b, the procedure first generates an “idealized backbone” based on the test data, composed of the peak load point of each loading step before the last loading cycle and the peak displacement point of the last loading cycle. Then a multi-segment linear backbone model is developed based on energy dissipation balance (i.e., the accumulative absolute value of the product between force and displacement) between the tested backbone response and the multi-segment linear backbone model. The multi-segment linear backbone model consists of four points, as shown in Figure 25a, the third point is the peak strength point in the test curve while the strength value of the first, second and fourth point are set as 40%, 80%, and 10% (post-peak) of the peak strength respectively. The first point displacement is determined based on the force level and the initial stiffness of the test curve, and the second point displacement is used for adjusting the linear backbone model’s energy dissipation (area underneath the backbone curve) to be the same with the “idealized backbone” from the test results before the peak strength. Similarly, the fourth point displacement is adopted to balance the energy dissipation after the peak strength. For the monotonic test curve presented in Figure 25c, the test curve itself is an “idealized backbone” and the same multi-segment linear backbone phenomenological model is applied.

Note that some tests demonstrate “two” peak strengths where the displacement magnitude at the first peak is quite small (essentially linear response) and the second peak strength is only a few percent lower than the first peak, but occurs at larger deformation and is observed to have actual damage - test “10-54-10-19-A” shown in Figure 25d is an example. In these cases, for the backbone fitting the force of the third point in the backbone model is set as the actual peak strength, but the displacement is set as the same as the second peak. This characterization adjustment is adopted in “6-54-10-13-T”, “27-54-8-13-A”, “38-54-8-19-T”, “56-97-10-19-A”, “57-97-10-19-A”, “60-97-10-19-T”, and “136-188-12-30-A”. The results of the fitting may be observed in Appendix 2.

Additionally, note that in some test data characterization results the backbone first segment stiffness is unreasonably high since the first point displacement value is quite small implying that the fastener connector might undergo pre-compression before testing. The deformation parameter D_1 needs to be adjusted based on a reasonable estimate of the first linear segment stiffness P_1/D_1 , and D_2 , D_3 , D_4 will be adjusted with the offset same as D_1 . As an upperbound, the thin steel sheet ply stiffness and the thick framing steel ply stiffness in tension can be evaluated by Eq. 6, where E , A , and L are the Young's modulus, net section area excluding the fastener hole diameter, and sheet length respectively. The total stiffness of the specimen in tension k can be calculated using

Eq. 7 assuming a series model based on the thin and thick ply stiffness k_1 and k_2 . If the experimental initial stiffness is larger than k then the results are adjusted to be no greater than k . The deformation values before and after adjustment are provided in Table 12. Note that the test data characterization results provided in the later section and appendix are all adjusted values.

Overall, this linear backbone phenomenological model can capture the initial stiffness, peak strength and displacement, post-peak behavior, and also the energy dissipation of the experimental data. Additional data characterization to provide the unloading, reloading, pinching, and energy degradation parameters for a complete Pinching 4 material model are not completed at this time.

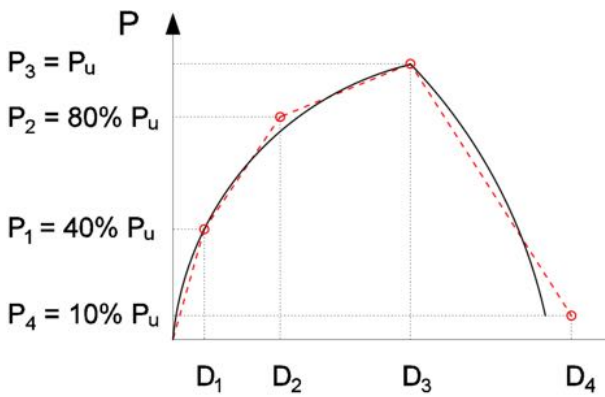
$$k = \frac{EA}{L} \quad (6)$$

$$\frac{1}{k} = \frac{1}{k_1} + \frac{1}{k_2} \quad (7)$$

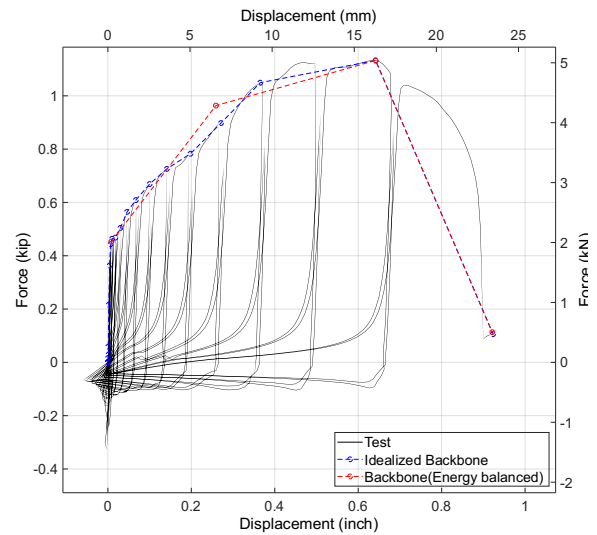
Table 12. Test data characterization deformation values before and after adjustment

| Test | D ₁ (in.) | D ₂ (in.) | D ₃ (in.) | D ₄ (in.) | D ₁ * (in.) | D ₂ * (in.) | D ₃ * (in.) | D ₄ * (in.) |
|-------------------|----------------------|----------------------|----------------------|----------------------|------------------------|------------------------|------------------------|------------------------|
| 7-54-10-13-M | 0.0000 | 0.0000 | 0.0324 | 0.4445 | 0.0006 | 0.0006 | 0.0329 | 0.4450 |
| 19-54-10-30-T | 0.0006 | 0.0484 | 0.3481 | 0.6322 | 0.0008 | 0.0487 | 0.3484 | 0.6325 |
| 23-54-10-30-M | 0.0006 | 0.1041 | 0.2594 | 0.6879 | 0.0008 | 0.1043 | 0.2596 | 0.6881 |
| 31-54-8-13-T | 0.0002 | 0.0026 | 0.0158 | 0.5921 | 0.0005 | 0.0030 | 0.0161 | 0.5924 |
| 32-54-8-13-M | 0.0000 | 0.0000 | 0.0403 | 0.5944 | 0.0005 | 0.0005 | 0.0408 | 0.5949 |
| 38-54-8-19-T | 0.0002 | 0.0014 | 0.0893 | 0.6919 | 0.0006 | 0.0017 | 0.0896 | 0.6922 |
| 46-54-8-30-M | 0.0000 | 0.1579 | 0.4359 | 0.9307 | 0.0011 | 0.1590 | 0.4370 | 0.9317 |
| 51-97-10-13-T | 0.0001 | 0.0002 | 0.0003 | 0.4569 | 0.0007 | 0.0009 | 0.0009 | 0.4576 |
| 54-97-10-13-M | 0.0000 | 0.0000 | 0.0000 | 0.3434 | 0.0008 | 0.0008 | 0.0008 | 0.3442 |
| 55-97-10-19-A | 0.0003 | 0.0005 | 0.0950 | 0.5396 | 0.0005 | 0.0008 | 0.0953 | 0.5399 |
| 76-97-12-30-A | 0.0004 | 0.0067 | 0.1863 | 0.5324 | 0.0007 | 0.0069 | 0.1865 | 0.5326 |
| 84-97-12-30-M | 0.0000 | 0.0000 | 0.1772 | 0.6298 | 0.0007 | 0.0007 | 0.1779 | 0.6304 |
| 87-97-8-30-A | 0.0004 | 0.0499 | 0.2089 | 0.4689 | 0.0006 | 0.0501 | 0.2092 | 0.4692 |
| 93-97-8-30-M | 0.0000 | 0.0000 | 0.1793 | 0.6070 | 0.0007 | 0.0007 | 0.1800 | 0.6077 |
| 100-97-10-13-97-M | 0.0000 | 0.0452 | 0.1330 | 0.6462 | 0.0013 | 0.0465 | 0.1344 | 0.6476 |

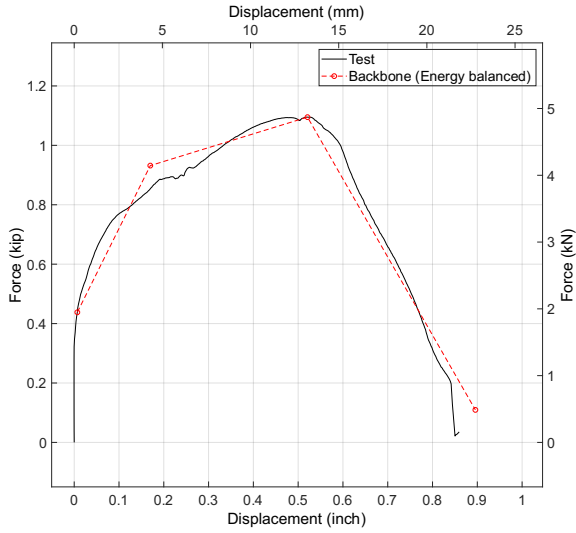
Note: D₁*, D₂*, D₃*, D₄* are the adjusted deformation values.



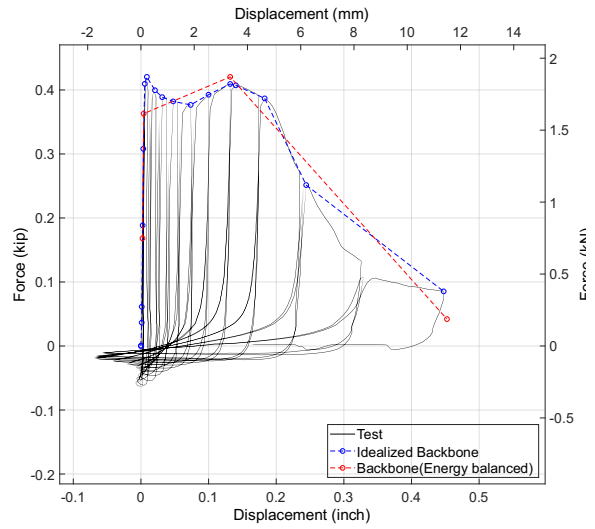
(a) Test data characterization diagram



(b) Characterization of test "44-54-8-30-T"



(c) Characterization of test “47-54-8-30-M”



(d) Characterization of test “10-54-10-19-A”

Figure 25. Experimental data characterization

Note, additional fitting to characterize loading and unloading stiffness, pinching parameters, and energy or deformation-based criteria as available in the Pinching04 material model in OpenSees have not been completed at this time. As the results indicate, elastic unloading/reloading dominates the response and as the connections are bearing controlled the response is nearly fully pinched.

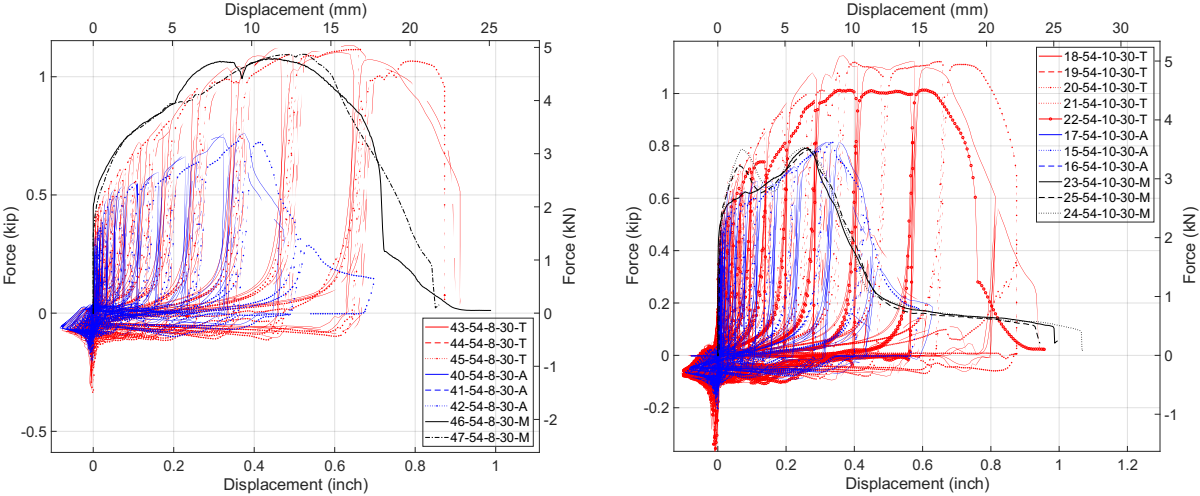
8 Discussion

8.1 Phase I Test Strength

For the case when the framing and steel sheet are similar in thickness, such as the 54 mil - 30 mil configuration with #8 screws, as presented in Figure 26a, the response is sensitive to whether the thin steel sheet ply (in contact with the fastener head) is buckling away from or towards the fastener head in the compression cycles. Based on visual observation in the experiments and the test force-displacement curves, the asymmetric cyclic tests with buckling away from the fastener head creates additional tension demand on the fastener connection which triggers the pull-through limit state and degrades the strength and post-peak shear behavior. The limit states of the buckling away from the fastener head cases tend to be dominated by bearing, tilting, and pull-through.

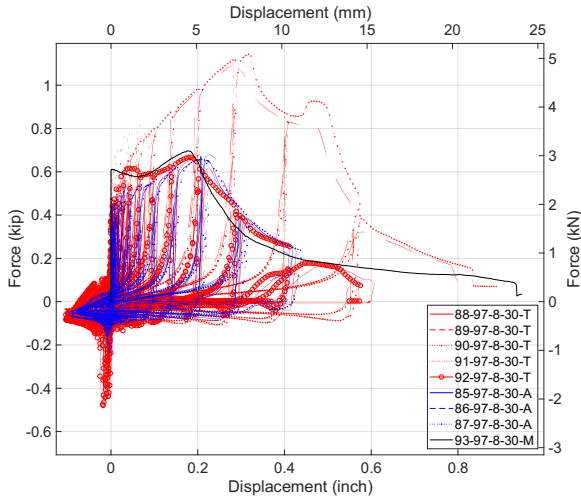
In the asymmetric cyclic tests with thin steel sheet buckling towards the fastener head, the thin steel sheet ply tends to flatly align with the shear load path and the fastener head does not create additional tension demand on the connection, resulting in only bearing and no pull-through limit state being triggered. The dominant limit states are bearing and shear rupture, which can result in higher strength.

Moreover, buckling towards (i.e., “T”) cases demonstrating higher test strength than the buckling away (i.e., “A”) cases can also be observed in other configurations including: “54-10-30”, “97-8-30”, and “97-12-30” test series, as shown in Figure 26. Only the monotonic tests in the “54-8-30” test series demonstrate similar higher strength and failure modes between buckling towards or away cases. Monotonic tests in other test series tend to be similar to the cyclic tests with thin steel sheet buckling away (i.e., “A” case) from the fastener head.

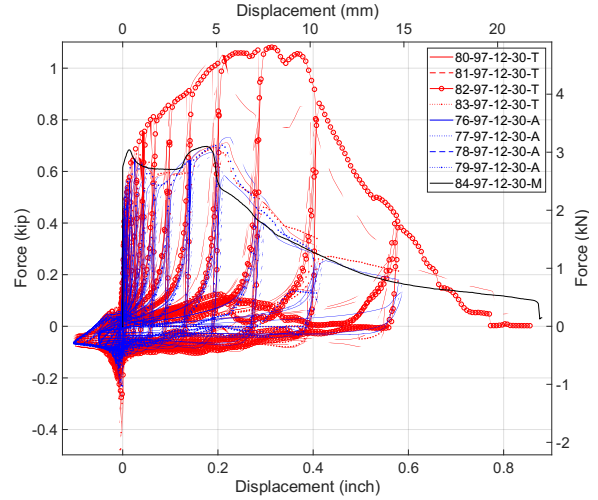


(a) Force-Disp curves of test type “54-8-30”

(b) Force-Disp curves of test type “54-10-30”



(c) Force-Disp curves of test type "97-8-30"

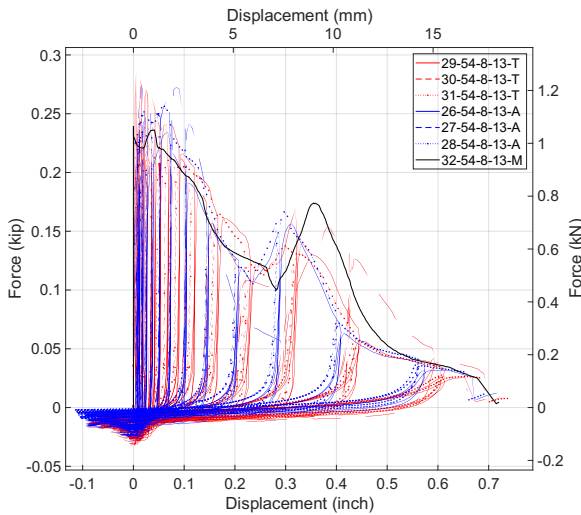


(d) Force-Disp curves of test type "97-12-30"

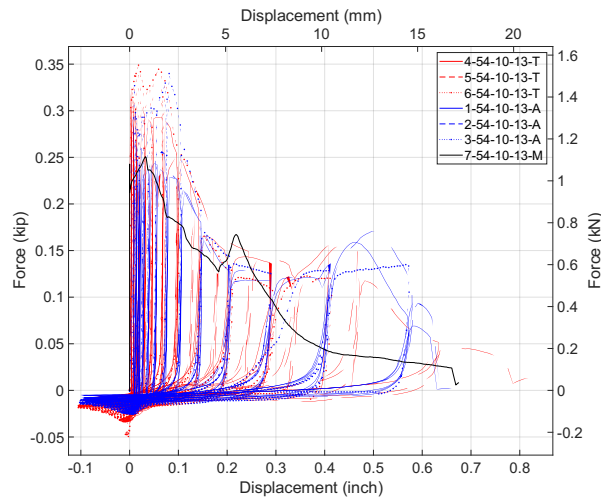
Figure 26. Force-displacement curves of four Phase I test types

The test strength is not always sensitive to whether the thin steel sheet ply is buckling away from or towards the fastener head. As presented in Figure 27a, for all the "54-8-13" specimens, great consistency in strength and post-peak behavior for the monotonic tests and cyclic tests with thin steel sheet buckling away from or towards the fastener head is observed. Different from the former "54-8-30" case, the thin 13 mil steel sheet ply is thin and flexible under compression demand and it cannot significantly influence the connector behavior. The shear-tension interaction demand on the fastener connection triggers the pull-through limit state after the peak strength level and the limit state tends to be dominated by bearing.

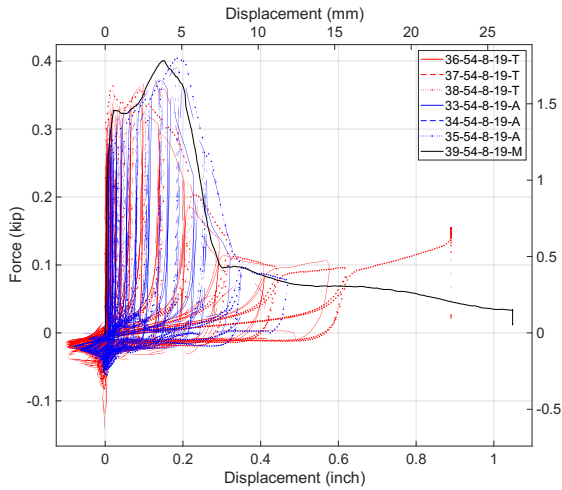
In Phase I tests, the same insensitivity to whether the thin steel sheet ply is buckling away or towards the fastener head can also be observed in the "54-10-13", "54-8-19", "54-10-19", "97-10-13", and "97-10-19" test series, as presented in in Figure 27. In all of these cases the difference between the thick and thin plies is significant.



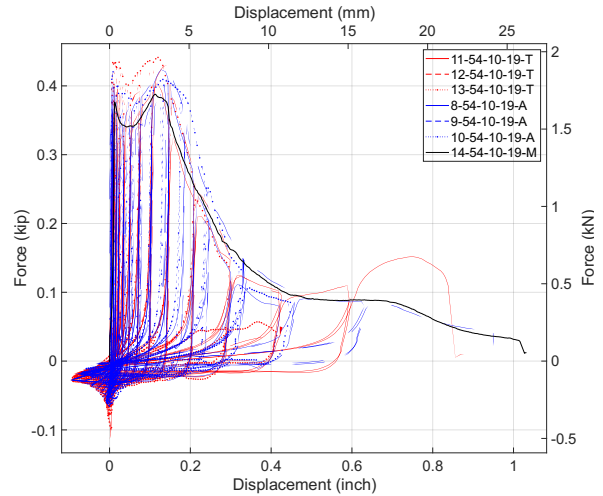
(a) Force-Disp curves of test type "54-8-13"



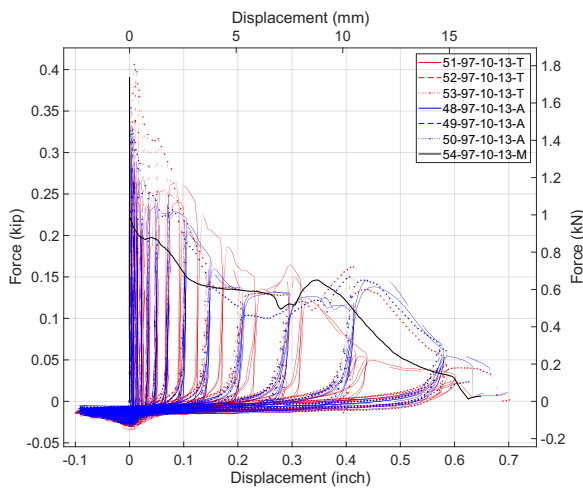
(b) Force-Disp curves of test type "54-10-13"



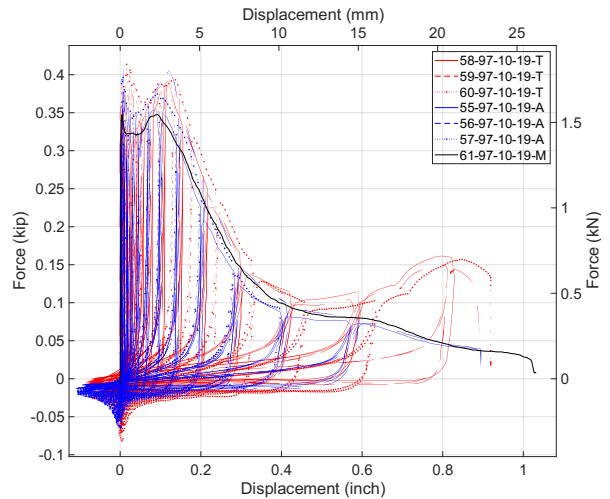
(c) Force-Disp curves of test type “54-8-19”



(d) Force-Disp curves of test type “54-10-19”



(e) Force-Disp curves of test type “97-10-13”



(f) Force-Disp curves of test type “97-10-19”

Figure 27. Force-displacement curves of six Phase I test types

For the “97-10-30” test series (i.e. 97 mil - 30 mil with a #10 screw), monotonic, asymmetric cyclic tests with thin steel sheet buckling away from or towards the fastener head, were conducted and also three tension-only asymmetric cyclic tests were conducted. As presented in Figure 28, the displacement-force curves of monotonic, asymmetric cyclic tests with thin steel sheet buckling away from or towards the fastener head lie in the same range except one of the asymmetric cyclic tests with thin steel sheet buckling towards the fastener head. This aligns with the finding that the test strength is not always sensitive to whether the thin steel sheet ply is buckling away from or towards the fastener head.

The tension-only cyclic tests have higher strength than the monotonic tests and the cyclic test with the thin steel sheet buckling away from the fastener head (an average of 0.744 kip for the tension only tests, 0.722 kip for the “M” test, 0.730 kip for the “A” tests), but the post-peak shear behavior, and limit states are the same. This implies that the compression displacement does create additional demand on the fastener connection that degrades the strength even in the early stages of the test, as shown in Figure 28. Therefore, asymmetric cyclic lap shear testing with a small compression

displacement is adequate and potentially necessary to study the impact of cyclic sheet buckling on the performance of connections in steel sheet shear walls.

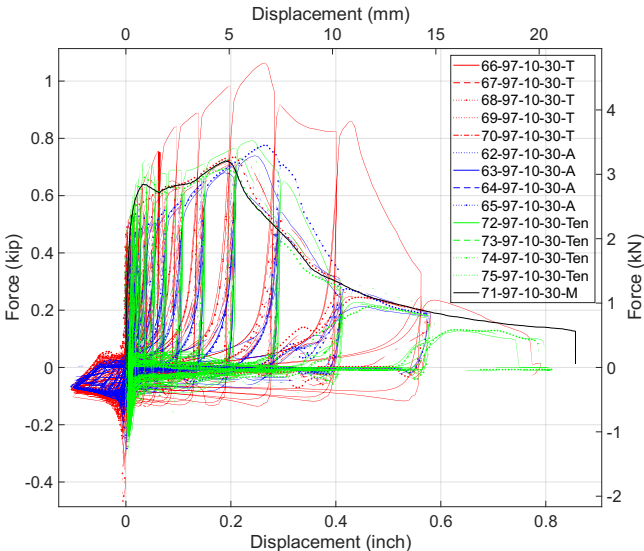
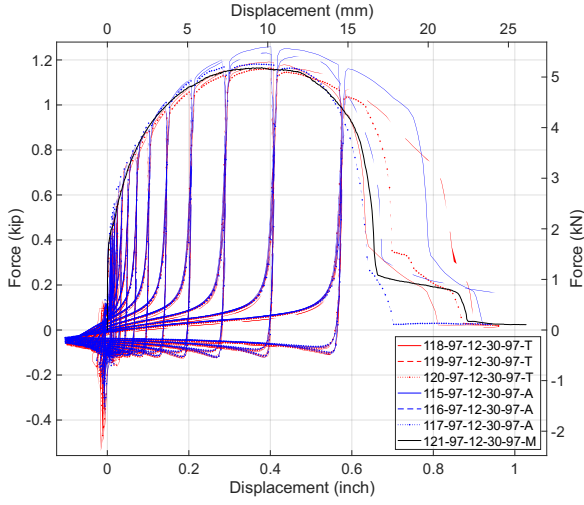


Figure 28. Force-displacement curves for test type “97-10-30”

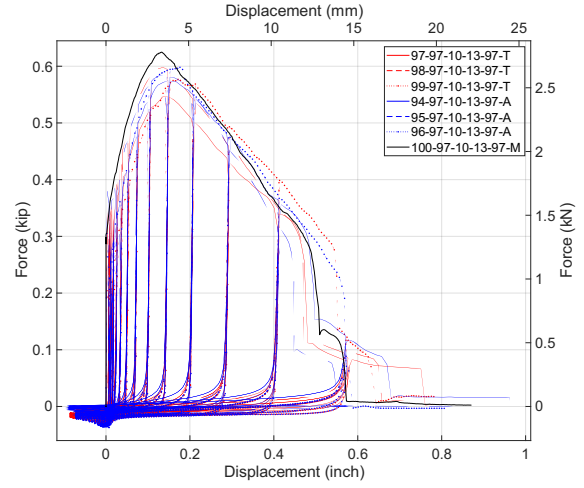
8.2 Phase II & III Test Strength

The Phase II & III tests are intended to investigate higher strength connection configurations through different paths, corresponding to recent steel sheet sheathed CFS-framed shear wall configurations demonstrating higher strength and ductility. The Phase II tests chase the fastener pure shear strength path by adopting two outer thick steel framing plies sandwiching one inner thin steel sheet ply, aligning with the mid-ply sheathing shear wall concept (Santos et. al. 2018, Briere et. al. 2018). The Phase III tests make the thick framing plies even thicker, utilizing steel plates of the same thickness as common HSS sections, and add PAFs as an additional fastener type corresponding to the stronger framing component.

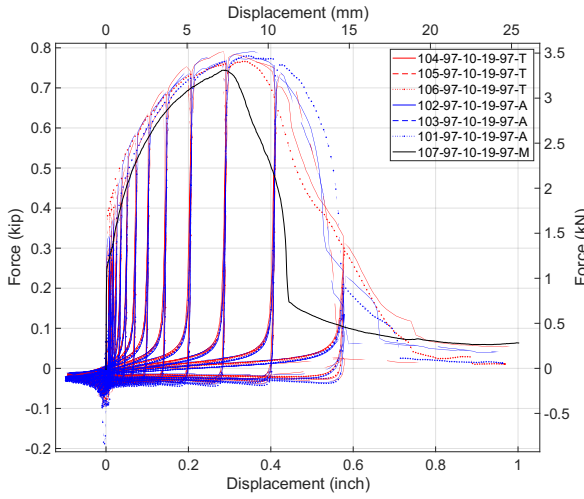
Compared with the strongest Phase I test series: “97-12-30” as presented in Figure 26d, the Phase II “97-12-30-97” test series, as shown in shown in Figure 29a, generates consistently higher strength (an average of 1.199 kips for the cyclic tests in “97-12-30-97” test series and 0.789 kip for the cyclic tests in “97-12-30” test series) since the dominant limit states are bearing and shear rupture and no tilting is developed in the double shear connection. Consistency in strength and post-peak behavior are observed in all monotonic tests and cyclic tests in double shear. The same limit states and consistency are also observed in Phase II tests: “97-10-13-97”, “97-10-19-97”, “97-10-30-97”, “97-24-30-97”, “118-24-30-118” test series, as presented in Figure 29. These results underpin the mid-ply shear wall tests and demonstrate specifically why the mid-ply configuration is highly favorable and, if it can be utilized in CFS-framed steel sheet shear walls, provides a significantly improved strength and ductility for steel sheet systems.



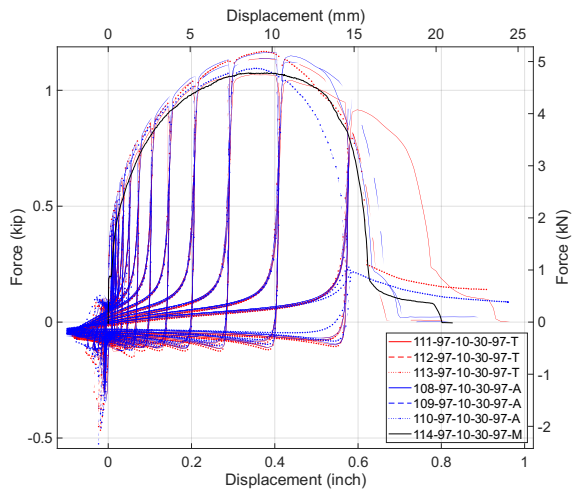
(a) Force-Disp curves of test type “97-12-30-97”



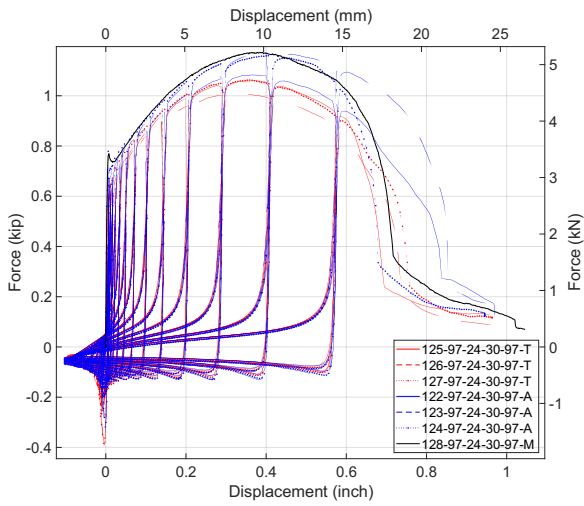
(b) Force-Disp curves of test type “97-10-13-97”



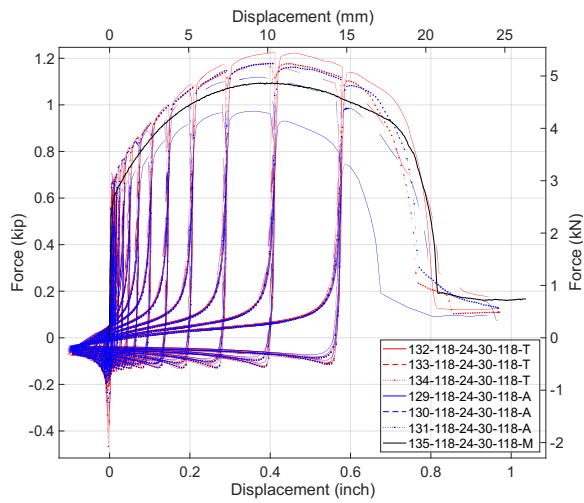
(c) Force-Disp curves of test type “97-10-19-97”



(d) Force-Disp curves of test type “97-10-30-97”



(e) Force-Disp curves of test type “97-24-30-97”

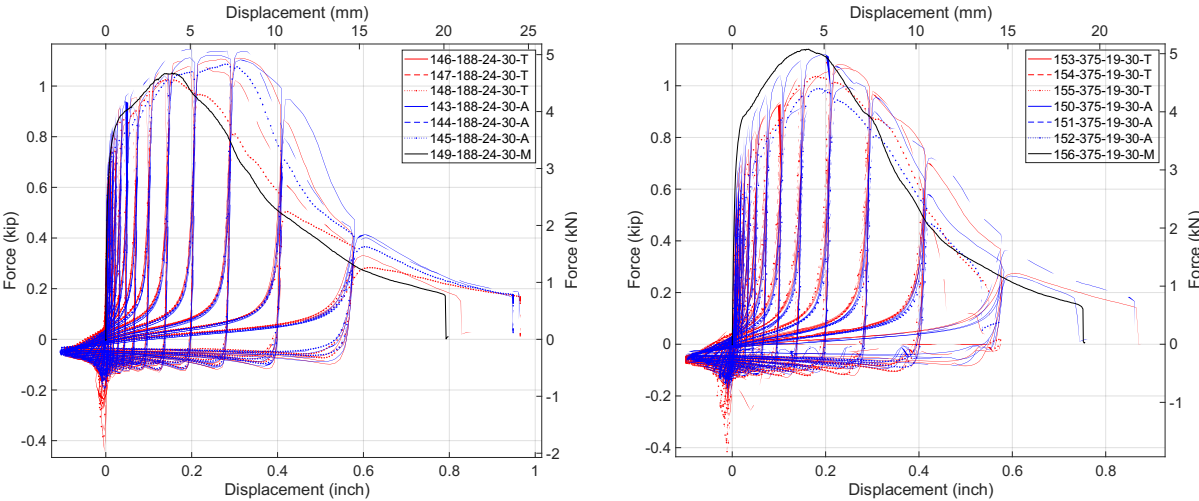


(f) Force-Disp curves of test type “118-24-30-118”

Figure 29. Force-displacement curves of six Phase II test types

Compared with the strongest Phase I test series “97-12-30”, as presented in Figure 26d, the Phase III “188-24-30” test series, as shown in Figure 30a, generates consistently higher strength (an average of 1.098 kips for the cyclic tests in “188-24-30” test series and 0.789 kip for the cyclic tests in “97-12-30” test series) since the dominant limit states are bearing and shear rupture without tilting because of the quite thick steel plate. Consistency in strength and post-peak behavior are observed in all the monotonic tests and cyclic tests. The same limit states and consistency are also observed in the Phase III “375-19-30” test series, as presented in Figure 30b. However, when the PAF is replaced by a #12 screw as in the Phase III “188-12-30” test series shown in Figure 31, the strength is similar to the Phase I “97-12-30” test series. Thus, the efficient installation and superior performance of the PAF connections may be worth pursuing for thicker framing members – this has also been observed in cyclic tests on deck attached to thicker framing with PAF vs. screws (Torabian et. al. 2017).

So, adopting two outer thick steel framing plies sandwiching one inner thin steel sheet ply to chase the higher fastener pure shear strength does generate higher strength than the normal Phase I connection configuration, which aligns with the higher shear wall strength reported in the related literature (Santos et. al. 2018, Briere et. al. 2018). However, thicker framing itself, as tested in Phase III, does not result in higher fastener strength. This is within expectation since the stronger framing design concept aims to increase the stud axial capacity rather than increase the shear wall lateral resistance. However, adopting thicker framing steel with appropriate fasteners such as PAFs (or perhaps even screws with washers) can contribute to the fastener strength, as observed in the comparison between Phase III “188-24-30” test series and Phase I “97-12-30” test series (39% increase in the average cyclic test strength). This is because the enlarged PAF fastener head design increases the moment-resisting arm of the connection and limits the tilting, resulting in in-plane shear slot deformation, which is similar to the Phase II double shear fastener connection configuration’s effect.



(a) Force-Disp curves of test type “188-24-30” (b) Force-Disp curves of test type “375-19-30”
 Figure 30. Force-displacement curves of two Phase III test types

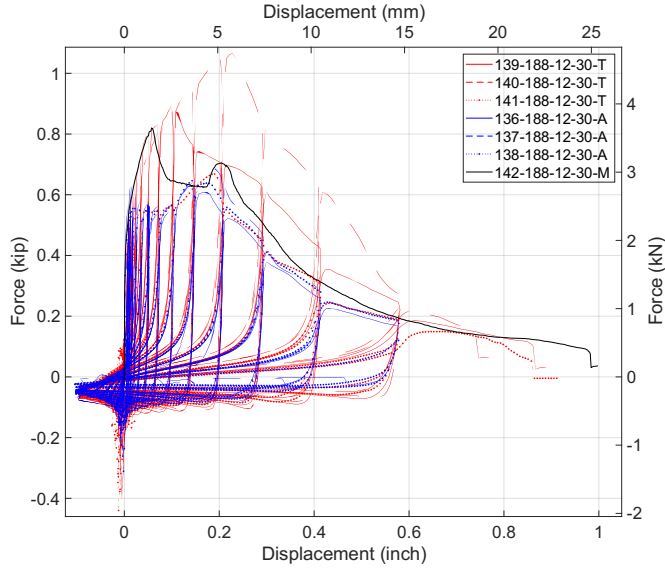
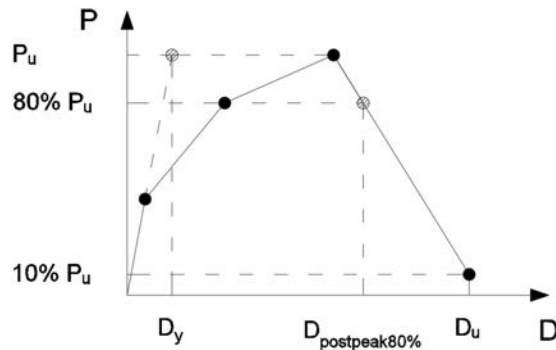


Figure 31. Force-displacement curves for test type “188-12-30”

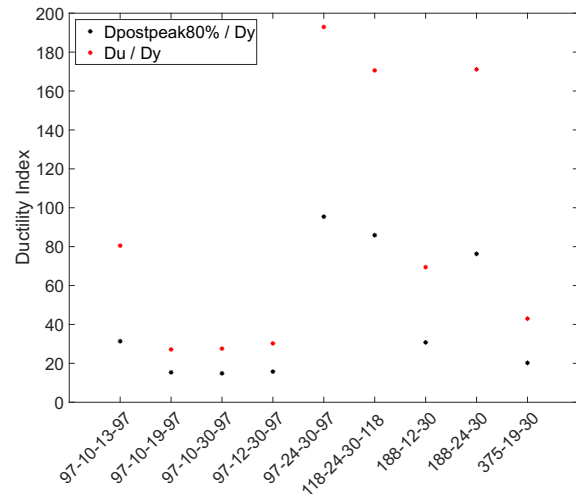
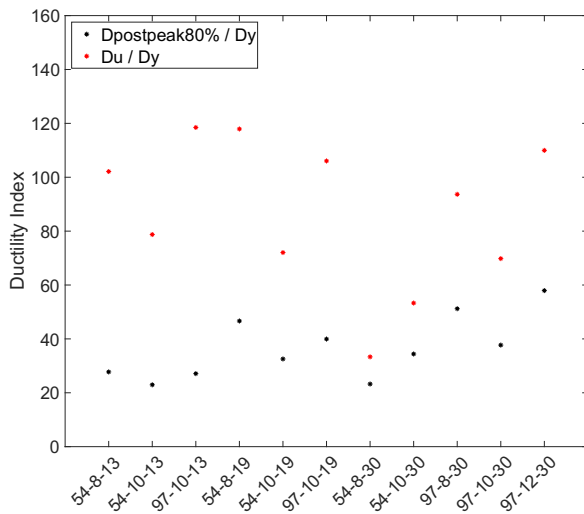
8.3 Test Ductility

Two ductility indices $D_{\text{postpeak80\%}}/D_y$ and D_u/D_y are introduced herein to assess the ductility of different fastener connection configurations. Three displacement levels: D_y , $D_{\text{postpeak80\%}}$, and D_u are generated based on the average value of cyclic test data characterization results. As presented in Figure 32a, D_y corresponds to the displacement level where the force level equals to the peak force but the stiffness is the initial stiffness. $D_{\text{postpeak80\%}}$ and D_u refers to the displacement level corresponding to the 80% post peak strength and 10% post peak strength force level in the fourth segment in the multi-segment linear backbone fit to the test data.

The average ductility index values of cyclic tests for each test series are tabulated in Table 13. The test ductility index comparison is presented in Figure 32b & 32c. Summaries of ductility index value of each test and the average ductility index values for different test types are provided in Appendix 2. The $D_{\text{postpeak80\%}}/D_y$ index is obviously more consistent than D_u/D_y since D_u relies greatly on the test ending deformation where D_u can be quite large if a complete disengagement develops. All the fastener connector configurations in this test program feature good ductility since $D_{\text{postpeak80\%}}/D_y$ index is generally high with a minimum of 15 and a Phase I average of 36, Phase II average of 43, and Phase III average of 42.



(a) Test displacement level diagram



(b) Phase I test ductility index comparison

(c) Phase II&III test ductility index comparison

Figure 32. Test ductility index

The $D_{\text{postpeak80\%}}/D_y$ index is adopted herein to quantify and discuss the ductility of different test series. The Phase II (double shear/mid-ply) test series with self-drilling screws, except “97-10-13-97”, demonstrates lower ductility than most Phase I tests (the average index value of “97-10-19-97”, “97-10-30-97”, and “97-12-30-97” is 15.335). Even though the average Phase II test series has higher post-peak displacement the initial displacement (D_y) increases even more for comparable configurations between Phase I and II resulting in lower ductility..

Through the comparison between “97-8-30” and “97-10-30”, it can be found that #10 screw case demonstrates lower ductility than #8 screw case (from 51 down to 38). This can be attributed to the fact that smaller screw sizes result in more extensive deformation and failure at the same force stage. The effect of larger screws can also be observed in the comparison between “54-8-13” and “54-10-13”, and “54-8-19” and “54-10-19”; however, this decreased ductility effect is not observed in the “54-8-30” and “54-10-30” series.

Phase II and Phase III tests with the X-HSN-24 PAF fastener generate systematically high ductility (average of 86), this may be in part because the shank nominal diameter of the X-HSN-24 PAF is even smaller than a #8 self-drilling screw.

In the Phase I test series, the 97 mil thick framing ply test series commonly feature higher ductility (43 on average) than the 54 mil thick framing ply test series (31 on average) under the same condition. This can be observed in the comparisons between the “54-10-19” and “97-10-19”, “54-8-30” and “97-8-30”, “54-10-30” and “97-10-30” series, but is not observed in the comparison between the “54-10-13” and “97-10-13” series. Presumably this is mainly because the 97 mil thick framing ply is relatively thicker than the thin steel sheet ply resulting in constraining the fastener tilting and more energy can be dissipated through the thin steel sheet ply deformation in pure bearing and shear rupture. Additionally, no clear relationship between thin steel sheet ply thickness and fastener connector ductility is observed.

Table 13a. Test ductility index values of cyclic tests for each test series (in.)

| Specimen Type | Phase | D_y (in.) | $D_{\text{postpeak80\%}}$ (in.) | D_u (in.) | $D_{\text{postpeak80\%}}/D_y$ | D_u/D_y |
|---------------|-------|-------------|---------------------------------|-------------|-------------------------------|-----------|
| 54-10-13 | I | 0.008 | 0.152 | 0.537 | 22.959 | 78.737 |
| 54-10-19 | I | 0.007 | 0.204 | 0.454 | 32.550 | 72.051 |
| 54-10-30 | I | 0.014 | 0.478 | 0.742 | 34.398 | 53.308 |
| 54-8-13 | I | 0.006 | 0.147 | 0.517 | 27.740 | 102.128 |
| 54-8-19 | I | 0.007 | 0.204 | 0.453 | 46.643 | 117.918 |
| 54-8-30 | I | 0.031 | 0.556 | 0.774 | 23.251 | 33.331 |
| 97-10-13 | I | 0.004 | 0.109 | 0.477 | 27.104 | 118.483 |
| 97-10-19 | I | 0.005 | 0.216 | 0.575 | 39.941 | 106.049 |
| 97-10-30 | I | 0.008 | 0.296 | 0.547 | 37.703 | 69.799 |
| 97-12-30 | I | 0.005 | 0.290 | 0.552 | 57.929 | 109.974 |
| 97-8-30 | I | 0.006 | 0.283 | 0.539 | 51.198 | 93.668 |
| 97-10-13-97 | II | 0.012 | 0.271 | 0.697 | 31.385 | 80.493 |
| 97-10-19-97 | II | 0.030 | 0.428 | 0.750 | 15.372 | 27.156 |
| 97-10-30-97 | II | 0.034 | 0.490 | 0.914 | 14.880 | 27.571 |
| 97-12-30-97 | II | 0.034 | 0.534 | 1.025 | 15.752 | 30.268 |
| 97-24-30-97 | II | 0.006 | 0.532 | 1.076 | 95.399 | 192.918 |
| 118-24-30-118 | II | 0.006 | 0.542 | 1.077 | 85.904 | 170.606 |
| 188-12-30 | III | 0.010 | 0.261 | 0.594 | 30.780 | 69.457 |
| 188-24-30 | III | 0.005 | 0.352 | 0.790 | 76.290 | 171.147 |
| 375-19-30 | III | 0.015 | 0.306 | 0.648 | 20.248 | 42.992 |

Table 13b. Test ductility index values of cyclic tests for each test series (mm)

| Specimen Type | Phase | D_y (mm) | $D_{\text{postpeak80\%}}$ (mm) | D_u (mm) | $D_{\text{postpeak80\%}}/D_y$ | D_u/D_y |
|---------------|-------|------------|--------------------------------|------------|-------------------------------|-----------|
| 54-10-13 | I | 0.20 | 3.87 | 13.65 | 22.96 | 78.74 |
| 54-10-19 | I | 0.19 | 5.18 | 11.53 | 32.55 | 72.05 |
| 54-10-30 | I | 0.35 | 12.14 | 18.85 | 34.40 | 53.31 |
| 54-8-13 | I | 0.14 | 3.73 | 13.13 | 27.74 | 102.13 |
| 54-8-19 | I | 0.17 | 5.19 | 11.50 | 46.64 | 117.92 |
| 54-8-30 | I | 0.78 | 14.13 | 19.66 | 23.25 | 33.33 |
| 97-10-13 | I | 0.10 | 2.77 | 12.11 | 27.10 | 118.48 |
| 97-10-19 | I | 0.14 | 5.49 | 14.61 | 39.94 | 106.05 |
| 97-10-30 | I | 0.20 | 7.52 | 13.88 | 37.70 | 69.80 |
| 97-12-30 | I | 0.13 | 7.36 | 14.02 | 57.93 | 109.97 |
| 97-8-30 | I | 0.16 | 7.18 | 13.68 | 51.20 | 93.67 |
| 97-10-13-97 | II | 0.30 | 6.89 | 17.69 | 31.39 | 80.49 |
| 97-10-19-97 | II | 0.75 | 10.87 | 19.04 | 15.37 | 27.16 |
| 97-10-30-97 | II | 0.85 | 12.45 | 23.21 | 14.88 | 27.57 |
| 97-12-30-97 | II | 0.87 | 13.58 | 26.04 | 15.75 | 30.27 |
| 97-24-30-97 | II | 0.14 | 13.50 | 27.32 | 95.40 | 192.92 |
| 118-24-30-118 | II | 0.16 | 13.78 | 27.36 | 85.90 | 170.61 |
| 188-12-30 | III | 0.24 | 6.62 | 15.10 | 30.78 | 69.46 |
| 188-24-30 | III | 0.12 | 8.95 | 20.08 | 76.29 | 171.15 |
| 375-19-30 | III | 0.39 | 7.77 | 16.47 | 20.25 | 42.99 |

8.4 Backbone Fitting and Averaging

For modeling, average backbone curves are expected to be used. Averaged values for the Phase I “54-8-30” test series, which is sensitive to buckling direction of the thin ply, are provided in Figure 33 as an example. The red dashed backbone curve is the average data characterization of the two

monotonic tests. The magenta dashed curve is the average data characterization of three asymmetric cyclic tests with the thin steel sheet buckling towards the fastener head. The blue dashed curve is the average data characterization of three asymmetric cyclic tests with the thin steel sheet buckling away from the fastener head. The black linear backbone curve is the average values across all cyclic tests.

The average value of all cyclic data for each test series is summarized in Table 14, which is a reasonable cyclic force-deformation behavior characterization of the fastener connection for modeling purpose. Note that the average value of all cyclic data is not consistent with any real test since it is a mixture of the results of cyclic tests with the thin steel sheet buckling away from or towards the fastener head. For some test series such as “54-8-30”, as presented in Figure 33, there exists obvious difference among the tests with different thin ply buckling directions. While the specimens with a thicker framing ply (greater difference between the thick and thin ply) are not sensitive to buckling direction of the thin ply, averaging the data of cyclic tests with thin steel sheet buckling away from and towards the fastener head still leads to little difference from the tests themselves. The average values of tests with the same test type for each test series are also provided in Appendix 2.

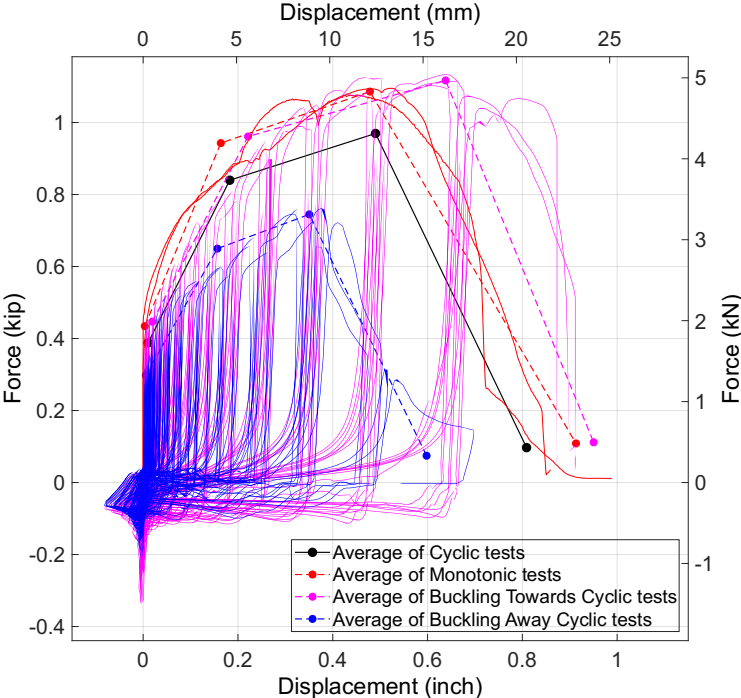


Figure 33. Test data characterization average values for test type “54-8-30”

Table 14a. Test data characterization average values for all cyclic tests (in.; kip)

| Specimen Type | D ₁ (in.) | D ₂ (in.) | D ₃ (in.) | D ₄ (in.) | P ₁ (kip) | P ₂ (kip) | P ₃ (kip) | P ₄ (kip) |
|---------------|----------------------|----------------------|----------------------|----------------------|----------------------|----------------------|----------------------|----------------------|
| 54-10-13 | 0.003 | 0.005 | 0.042 | 0.537 | 0.120 | 0.254 | 0.301 | 0.030 |
| 54-10-19 | 0.003 | 0.005 | 0.132 | 0.454 | 0.169 | 0.353 | 0.423 | 0.042 |
| 54-10-30 | 0.006 | 0.118 | 0.403 | 0.742 | 0.367 | 0.792 | 0.918 | 0.092 |
| 54-8-13 | 0.002 | 0.004 | 0.041 | 0.517 | 0.102 | 0.219 | 0.255 | 0.026 |
| 54-8-19 | 0.003 | 0.021 | 0.134 | 0.453 | 0.150 | 0.325 | 0.376 | 0.038 |
| 54-8-30 | 0.012 | 0.189 | 0.494 | 0.774 | 0.372 | 0.805 | 0.931 | 0.093 |
| 97-10-13 | 0.002 | 0.003 | 0.004 | 0.477 | 0.136 | 0.270 | 0.340 | 0.034 |
| 97-10-19 | 0.002 | 0.004 | 0.113 | 0.575 | 0.158 | 0.331 | 0.394 | 0.039 |
| 97-10-30 | 0.003 | 0.066 | 0.225 | 0.547 | 0.307 | 0.660 | 0.766 | 0.077 |
| 97-12-30 | 0.002 | 0.030 | 0.215 | 0.552 | 0.316 | 0.648 | 0.789 | 0.079 |
| 97-8-30 | 0.003 | 0.062 | 0.209 | 0.539 | 0.320 | 0.676 | 0.800 | 0.080 |
| 97-10-13-97 | 0.005 | 0.058 | 0.150 | 0.697 | 0.234 | 0.488 | 0.580 | 0.058 |
| 97-10-19-97 | 0.012 | 0.099 | 0.336 | 0.750 | 0.311 | 0.680 | 0.778 | 0.078 |
| 97-10-30-97 | 0.013 | 0.118 | 0.369 | 0.914 | 0.451 | 0.980 | 1.128 | 0.113 |
| 97-12-30-97 | 0.014 | 0.122 | 0.394 | 1.025 | 0.479 | 1.047 | 1.199 | 0.120 |
| 97-24-30-97 | 0.002 | 0.095 | 0.376 | 1.076 | 0.436 | 0.982 | 1.091 | 0.109 |
| 118-24-30-118 | 0.003 | 0.104 | 0.390 | 1.077 | 0.456 | 1.018 | 1.140 | 0.114 |
| 188-12-30 | 0.004 | 0.038 | 0.165 | 0.594 | 0.306 | 0.641 | 0.766 | 0.077 |
| 188-24-30 | 0.002 | 0.037 | 0.227 | 0.790 | 0.439 | 0.959 | 1.098 | 0.110 |
| 375-19-30 | 0.006 | 0.062 | 0.208 | 0.648 | 0.420 | 0.913 | 1.051 | 0.105 |

Table 14b. Test data characterization average values for all cyclic tests (mm; kN)

| Specimen Type | D ₁ (mm) | D ₂ (mm) | D ₃ (mm) | D ₄ (mm) | P ₁ (kN) | P ₂ (kN) | P ₃ (kN) | P ₄ (kN) |
|---------------|---------------------|---------------------|---------------------|---------------------|---------------------|---------------------|---------------------|---------------------|
| 54-10-13 | 0.08 | 0.13 | 1.07 | 13.65 | 0.54 | 1.13 | 1.34 | 0.13 |
| 54-10-19 | 0.07 | 0.13 | 3.36 | 11.53 | 0.75 | 1.57 | 1.88 | 0.19 |
| 54-10-30 | 0.14 | 2.98 | 10.23 | 18.85 | 1.63 | 3.52 | 4.08 | 0.41 |
| 54-8-13 | 0.06 | 0.11 | 1.04 | 13.13 | 0.45 | 0.97 | 1.14 | 0.11 |
| 54-8-19 | 0.07 | 0.53 | 3.39 | 11.50 | 0.67 | 1.44 | 1.67 | 0.17 |
| 54-8-30 | 0.31 | 4.80 | 12.55 | 19.66 | 1.66 | 3.58 | 4.14 | 0.41 |
| 97-10-13 | 0.04 | 0.07 | 0.10 | 12.11 | 0.60 | 1.20 | 1.51 | 0.15 |
| 97-10-19 | 0.05 | 0.10 | 2.88 | 14.61 | 0.70 | 1.47 | 1.75 | 0.18 |
| 97-10-30 | 0.08 | 1.66 | 5.70 | 13.88 | 1.36 | 2.93 | 3.41 | 0.34 |
| 97-12-30 | 0.05 | 0.75 | 5.45 | 14.02 | 1.40 | 2.88 | 3.51 | 0.35 |
| 97-8-30 | 0.07 | 1.58 | 5.32 | 13.68 | 1.42 | 3.01 | 3.56 | 0.36 |
| 97-10-13-97 | 0.12 | 1.48 | 3.80 | 17.69 | 1.04 | 2.17 | 2.58 | 0.26 |
| 97-10-19-97 | 0.30 | 2.53 | 8.53 | 19.04 | 1.38 | 3.02 | 3.46 | 0.35 |
| 97-10-30-97 | 0.34 | 3.00 | 9.38 | 23.21 | 2.01 | 4.36 | 5.02 | 0.50 |
| 97-12-30-97 | 0.35 | 3.09 | 10.01 | 26.04 | 2.13 | 4.66 | 5.33 | 0.53 |
| 97-24-30-97 | 0.06 | 2.40 | 9.56 | 27.32 | 1.94 | 4.37 | 4.85 | 0.49 |
| 118-24-30-118 | 0.06 | 2.65 | 9.89 | 27.36 | 2.03 | 4.53 | 5.07 | 0.51 |
| 188-12-30 | 0.10 | 0.97 | 4.19 | 15.10 | 1.36 | 2.85 | 3.41 | 0.34 |
| 188-24-30 | 0.05 | 0.95 | 5.77 | 20.08 | 1.95 | 4.27 | 4.89 | 0.49 |
| 375-19-30 | 0.15 | 1.58 | 5.29 | 16.47 | 1.87 | 4.06 | 4.67 | 0.47 |

9 Conclusions

This report presents the experimental efforts of fastener-level force-deformation response appropriate for steel sheet sheathed cold-formed steel (CFS) framed shear walls in cyclic and monotonic loading. Behavior of the fastener connection for CFS-framed steel sheet shear walls is unique as it not only resists shear demand but also resists out-of-plane forces that works on the screw head due to extensive buckling of the thin steel sheet during loading cycles. Cyclic lap shear tests with a small compression cycle to buckle the thin sheet followed by progressively larger tension cycles can reasonably capture the sensitivity and strength degradation inherent in fastened steel sheet shear walls.

For configurations where the framing and sheet thickness are relatively close (e.g. 54 mil framing and 30 mil sheet) the test strength is sensitive to whether the thin steel sheet ply is buckling away from or towards the fastener head. When the sheet buckles away from the fastener head it creates additional tension demand on the connection that can trigger a unique pull-through limit state that degrades the strength and post-peak shear behavior of the connection. The dominant limit states of these buckling away cases are bearing, tilting, and pull-through. For cases where buckling of the thin sheet is towards the fastener head the thin steel sheet ply tends to flatly align with the shear load path and the fastener head does not create additional tension demand on the connection. In this case the limit states are dominated by bearing and shear rupture which normally results in higher test strength.

For configurations where the framing and sheet thickness are far apart (e.g., 54 mil framing with 13 or 19 mil sheet, and 97 mil framing with 13 or 19 mil sheet) the test strength is not sensitive to whether the thin steel sheet ply is buckling away or towards the fastener head. Nonetheless, the buckling of the thin ply still influences the results as the additional shear-tension interaction demand on the fastener connection triggers a bearing and pull-through limit state degrading the strength and post-peak shear behavior in all test cases.

When a mid-ply or double shear connection configuration is adopted, as in the Phase II tests, the strength is consistently higher than the similarly configured Phase I tests.

For the thickest framing, as tested in Phase III, strength of the connection only increases when a PAF instead of a screw is used for the connection. Thicker framing is largely pursued in shear walls for providing increased axial capacity in the chord studs, not for increased shear capacity of the wall, but the PAF connections demonstrate that increased wall shear capacity (and ductility) is possible even with the same steel sheet sheathing.

All the connector configurations in this test program shows good ductility. #10 screw size cases generally demonstrate lower ductility for the same framing and sheet thickness than #8 screw size cases, but 97 mil framing generally provides higher ductility than 54 mil framing for sheet thickness between 13 and 30 mil and screw fasteners between #8 and #12.

The fastener test data characterization provides the force-deformation relationship and corresponding hysteretic response characteristics of fastener connections between steel framing and steel sheet commonly used or to be adopted in steel sheet sheathed CFS-framed shear wall construction. This fastener test program provides “fastener-level” force-deformation cyclic response incorporating steel sheet local buckling for steel sheet sheathed CFS-framed shear wall that can be adopted in future high fidelity shear wall simulations.

References

- Rizk, R., Rogers, C.A. (2018) "Higher Strength Cold-formed Steel Framed / Steel Shear Walls for Mid-rise Construction." Project Report, Dept. of Civil Engineering and Applied Mechanics, McGill University, Montreal, QC, Canada.
- Santos, V., Rogers, C.A. (2018) "Higher Capacity Cold-formed Steel Sheathed and Framed Shear Walls for Mid-rise Buildings: Part 1." Project Report, Dept. of Civil Engineering and Applied Mechanics, McGill University, Montreal, QC, Canada.
- Briere, V., Rogers, C.A. (2018) "Higher Capacity Cold-formed Steel Sheathed and Framed Shear Walls for Mid-rise Buildings: Part 2." Project Report, Dept. of Civil Engineering and Applied Mechanics, McGill University, Montreal, QC, Canada.
- DaBreo J, Rogers CA. (2012) "Steel sheathed shear walls subjected to combined lateral and gravity loads." research report., Department. of Civil Engineering & Applied Mechanics, McGill University, Montreal, Canada.
- Balh N, Rogers CA. (2010). "Development of seismic design provisions for steel sheathed shear walls." research report., Department of Civil Engineering & Applied Mechanics, McGill University, Montreal, Canada.
- Ong-Tone C, Rogers CA. (2009). "Tests and evaluation of cold-formed steel frame/steel sheathed shear walls." research report., Department of Civil Engineering & Applied Mechanics, McGill University, Montreal, Canada.
- Singh, A., Wang, X., Torabian, S., Hutchinson, T. C., Peterman, K. D., Schafer, B. W. (2020) "Seismic Performance of Symmetric Unfinished CFS In-Line Wall Systems." In Structures Congress 2020 (pp. 629-642). Reston, VA: American Society of Civil Engineers.
- Yu, C., Vora, H., Dainard, T., Tucker, J., & Veetvkuri, P. (2007). "Steel sheet sheathing options for CFS framed shear wall assemblies providing shear resistance. Report No. UNT-G76234, Department of Engineering Technology, University of North Texas, Denton, Texas, USA.
- Yu, C., Chen, Y. (2009) "Steel sheathing options for cold-formed steel framed shear walls assemblies providing shear resistance - Phase 2." Report No. UNT-G70752, Department of Engineering Technology, University of North Texas, Denton, Texas, USA.
- Serrette, R.L. (1997). "Additional Shear Wall Values for Light Weight Steel Framing." Report No. LGSRG-1-97, Santa Clara University, Santa Clara, CA, USA.
- Serrette, R.L. (2002). "Performance of Cold-Formed Steel-Framed Shear Walls: Alternative Configurations," Final Report:LGSRG-06-02, Santa Clara University, Santa Clara, CA, USA.
- Tao, F., Chatterjee, A., & Moen, C. D. (2016). "Monotonic and cyclic response of single shear cold-formed steel-to-steel and sheathing-to-steel connections. " Virginia Tech Research Report No. CE/VPI-ST-16/01, Blacksburg, VA, USA.
- Torabian, S., Schafer, B. W. (2017). "Cyclic performance and characterization of steel deck connections." Test report. (<https://jscholarship.library.jhu.edu/handle/1774.2/62849>)
- Torabian, S., Fratamico, D., Shannahan , K., Schafer, B.W. (2018). "Cyclic Performance and Behavior Characterization of Steel Deck Sidelap and Framing Connections." Proceedings of the International Specialty Conference on Cold-Formed Steel Structures. St. Louis, MO, USA.

- Shi, Y., Torabian, S., Schafer†, B.W., Easterling, W.S., Eatherton, M.R. (2018). “Sidelap and Structural Fastener Tests for Steel Deck Diaphragms.” Proceedings of the International Specialty Conference on Cold-Formed Steel Structures. St. Louis, MO, USA.
- Rogers, C. A., and Tremblay, R. (2003). “Inelastic seismic response of frame fasteners for steel roof deck diaphragms.” *Journal of Structural Engineering*, 129(12), 1647-1657.
10.1061/(ASCE)0733-9445(2003)129:12(1647)
- Rogers, C. A., and Tremblay, R. (2000). “Inelastic seismic response of frame and side lap fasteners for steel roof decks.” Research Report No. EPM/CGS-2000-09, Department of Civil, Geological and Mining Engineering, Ecole Polytechnique, Montreal QC, Canada.
- Zhang, Z., Schafer, B.W. (2019). “Simulation of steel sheet sheathed cold-formed steel framed shear walls.” SSRC Annual Stability Conference. St. Louis, MO, USA.
- American Iron and Steel Institute (AISI) (2013). “AISI S905-13, Test Standard for Cold-Formed Steel Connections.” Washington, D.C., USA.
- American Iron and Steel Institute (AISI) (2007). “AISI S213-07, North American Standard for Cold-Formed Steel Framing – Lateral Design.” Washington, D.C., USA.
- American Iron and Steel Institute (AISI) (2016). “AISI S100-16, North American Specification for the Design of Cold-Formed Steel Structural Members.” Washington, D.C., USA.
- American Iron and Steel Institute (AISI) (2015). “AISI S400-15, North American specification for seismic design of cold-formed steel structural systems.” Washington, D.C., USA.
- American Institute of Steel Construction (AISC) (2010). “AISC 341-10, Seismic provisions for structural steel buildings”., Chicago, IL, USA.
- American Society for Testing and Materials (ASTM) (2013). “ASTM-E8/E8M-13a, Standard Test Methods for Tension Testing of Metallic Materials.” West Conshohocken, PA, USA.
- Federal Emergency Management Agency (FEMA) (2007). “FEMA 461, Interim Protocols for Determining Seismic Performance Characteristics of Structural and Nonstructural Components Through Laboratory Testing.” Washington, D.C., USA.
- Applied Technology Council, Mid-America Earthquake Center, Multidisciplinary Center for Earthquake Engineering Research (US), Pacific Earthquake Engineering Research Center, United States. Federal Emergency Management Agency, & National Earthquake Hazards Reduction Program (US). (2007). “Interim Testing Protocols for Determining the Seismic Performance Characteristics of Structural and Nonstructural Components.” Washington, D.C., USA.
- Cold-Formed Steel Engineers Institute (CFSEI) (2012). “ TECHNICAL NOTE on Cold-Formed Steel Construction F102-11: SCREW FASTENER SELECTION FOR COLD-FORMED STEEL FRAME CONSTRUCTION.” Washington, D.C., USA.
- Torabian, S., Zheng, B., Shifferaw, Y., Schafer, B.W. (2016). “Direct Strength Prediction of Cold-Formed Steel Beam-Columns ” CFSRC Report R-2016-01.
(<http://jhir.library.jhu.edu/handle/1774.2/40593>)
- Fratamico, D. C. (2017). “Experiments, Analysis, and Design of Built-Up Cold-Formed Steel Columns” Doctoral dissertation, Johns Hopkins University. Baltimore, MD, USA.
(<http://jhir.library.jhu.edu/handle/1774.2/62379>)
- Peterman, K. D., Nakata, N., & Schafer, B. W. (2014). “Hysteretic characterization of cold-formed steel stud-to-sheathing connections.” *Journal of Constructional Steel Research*, 101, 254-264.

Appendix 1: Test Result Summary

Summaries for specimen information and fundamental test result of each test conducted are provided in this appendix.

Table 15. Test result summary

| Test ID | Phase | Test type | Fastener # | Thin ply (mil) | Thick ply (mil) | Peak Strength (kip) | Disp @ Peak Strength (in.) | Failure Mode |
|---------------|-------|-----------|------------|----------------|-----------------|---------------------|----------------------------|--------------|
| 1-54-10-13-A | I | A | 10 | 13 | 54 | 0.252 | 0.012 | B |
| 2-54-10-13-A | I | A | 10 | 13 | 54 | 0.292 | 0.005 | B |
| 3-54-10-13-A | I | A | 10 | 13 | 54 | 0.340 | 0.081 | B |
| 4-54-10-13-T | I | T | 10 | 13 | 54 | 0.326 | 0.003 | B |
| 5-54-10-13-T | I | T | 10 | 13 | 54 | 0.249 | 0.092 | B |
| 6-54-10-13-T | I | T | 10 | 13 | 54 | 0.349 | 0.059 | B |
| 7-54-10-13-M | I | M | 10 | 13 | 54 | 0.251 | 0.033 | B |
| 8-54-10-19-A | I | A | 10 | 19 | 54 | 0.425 | 0.133 | B |
| 9-54-10-19-A | I | A | 10 | 19 | 54 | 0.415 | 0.153 | B |
| 10-54-10-19-A | I | A | 10 | 19 | 54 | 0.420 | 0.132 | B |
| 11-54-10-19-T | I | T | 10 | 19 | 54 | 0.405 | 0.118 | B |
| 12-54-10-19-T | I | T | 10 | 19 | 54 | 0.431 | 0.139 | B |
| 13-54-10-19-T | I | T | 10 | 19 | 54 | 0.441 | 0.120 | B |
| 14-54-10-19-M | I | M | 10 | 19 | 54 | 0.388 | 0.113 | B |
| 15-54-10-30-A | I | A | 10 | 30 | 54 | 0.813 | 0.337 | TB+P |
| 16-54-10-30-A | I | A | 10 | 30 | 54 | 0.816 | 0.323 | TB+P |
| 17-54-10-30-A | I | A | 10 | 30 | 54 | 0.818 | 0.323 | TB+P |
| 18-54-10-30-T | I | T | 10 | 30 | 54 | 1.150 | 0.362 | TB+R |
| 19-54-10-30-T | I | T | 10 | 30 | 54 | 0.811 | 0.348 | TB+P |
| 20-54-10-30-T | I | T | 10 | 30 | 54 | 1.122 | 0.649 | TB+R |
| 21-54-10-30-T | I | T | 10 | 30 | 54 | 0.804 | 0.279 | TB+P |
| 22-54-10-30-T | I | T | 10 | 30 | 54 | 1.013 | 0.599 | TB+R |
| 23-54-10-30-M | I | M | 10 | 30 | 54 | 0.791 | 0.260 | TB+P |
| 24-54-10-30-M | I | M | 10 | 30 | 54 | 0.795 | 0.251 | TB+P |
| 25-54-10-30-M | I | M | 10 | 30 | 54 | 0.788 | 0.266 | TB+P |
| 26-54-8-13-A | I | A | 8 | 13 | 54 | 0.234 | 0.068 | B |
| 27-54-8-13-A | I | A | 8 | 13 | 54 | 0.274 | 0.084 | B |
| 28-54-8-13-A | I | A | 8 | 13 | 54 | 0.256 | 0.061 | B |
| 29-54-8-13-T | I | T | 8 | 13 | 54 | 0.286 | 0.005 | B |
| 30-54-8-13-T | I | T | 8 | 13 | 54 | 0.248 | 0.011 | B |
| 31-54-8-13-T | I | T | 8 | 13 | 54 | 0.234 | 0.016 | B |
| 32-54-8-13-M | I | M | 8 | 13 | 54 | 0.236 | 0.041 | B |
| 33-54-8-19-A | I | A | 8 | 19 | 54 | 0.375 | 0.142 | B |
| 34-54-8-19-A | I | A | 8 | 19 | 54 | 0.391 | 0.182 | B |
| 35-54-8-19-A | I | A | 8 | 19 | 54 | 0.404 | 0.185 | B |
| 36-54-8-19-T | I | T | 8 | 19 | 54 | 0.338 | 0.086 | B |
| 37-54-8-19-T | I | T | 8 | 19 | 54 | 0.384 | 0.115 | B |
| 38-54-8-19-T | I | T | 8 | 19 | 54 | 0.364 | 0.090 | B |
| 39-54-8-19-M | I | M | 8 | 19 | 54 | 0.401 | 0.150 | B |
| 40-54-8-30-A | I | A | 8 | 30 | 54 | 0.761 | 0.376 | TB+P |
| 41-54-8-30-A | I | A | 8 | 30 | 54 | 0.746 | 0.314 | TB+P |
| 42-54-8-30-A | I | A | 8 | 30 | 54 | 0.727 | 0.361 | TB+P |
| 43-54-8-30-T | I | T | 8 | 30 | 54 | 1.102 | 0.608 | TB+R |
| 44-54-8-30-T | I | T | 8 | 30 | 54 | 1.133 | 0.642 | TB+R |

| | | | | | | | | |
|------------------|----|-----|----|----|----|-------|-------|-------|
| 45-54-8-30-T | I | T | 8 | 30 | 54 | 1.115 | 0.664 | TB+R |
| 46-54-8-30-M | I | M | 8 | 30 | 54 | 1.077 | 0.437 | TB+R |
| 47-54-8-30-M | I | M | 8 | 30 | 54 | 1.095 | 0.521 | TB+R |
| 48-97-10-13-A | I | A | 10 | 13 | 97 | 0.308 | 0.003 | B |
| 49-97-10-13-A | I | A | 10 | 13 | 97 | 0.333 | 0.003 | B |
| 50-97-10-13-A | I | A | 10 | 13 | 97 | 0.354 | 0.003 | B |
| 51-97-10-13-T | I | T | 10 | 13 | 97 | 0.344 | 0.001 | B |
| 52-97-10-13-T | I | T | 10 | 13 | 97 | 0.295 | 0.007 | B |
| 53-97-10-13-T | I | T | 10 | 13 | 97 | 0.406 | 0.009 | B |
| 54-97-10-13-M | I | M | 10 | 13 | 97 | 0.380 | 0.001 | B |
| 55-97-10-19-A | I | A | 10 | 19 | 97 | 0.354 | 0.095 | B |
| 56-97-10-19-A | I | A | 10 | 19 | 97 | 0.418 | 0.121 | B |
| 57-97-10-19-A | I | A | 10 | 19 | 97 | 0.397 | 0.093 | B |
| 58-97-10-19-T | I | T | 10 | 19 | 97 | 0.387 | 0.112 | B |
| 59-97-10-19-T | I | T | 10 | 19 | 97 | 0.392 | 0.122 | B |
| 60-97-10-19-T | I | T | 10 | 19 | 97 | 0.414 | 0.137 | B |
| 61-97-10-19-M | I | M | 10 | 19 | 97 | 0.348 | 0.092 | B |
| 62-97-10-30-A | I | A | 10 | 30 | 97 | 0.725 | 0.199 | B+P |
| 63-97-10-30-A | I | A | 10 | 30 | 97 | 0.739 | 0.246 | B+P |
| 64-97-10-30-A | I | A | 10 | 30 | 97 | 0.680 | 0.188 | B+P |
| 65-97-10-30-A | I | A | 10 | 30 | 97 | 0.775 | 0.263 | B+P |
| 66-97-10-30-T | I | T | 10 | 30 | 97 | 1.064 | 0.266 | B+R |
| 67-97-10-30-T | I | T | 10 | 30 | 97 | 0.725 | 0.202 | B+P |
| 68-97-10-30-T | I | T | 10 | 30 | 97 | 0.734 | 0.209 | B+P |
| 69-97-10-30-T | I | T | 10 | 30 | 97 | 0.727 | 0.221 | B+P |
| 70-97-10-30-T | I | T | 10 | 30 | 97 | 0.727 | 0.228 | B+P |
| 71-97-10-30-M | I | M | 10 | 30 | 97 | 0.722 | 0.191 | B+P |
| 72-97-10-30-Ten | I | Ten | 10 | 30 | 97 | 0.792 | 0.242 | B+P |
| 73-97-10-30-Ten | I | Ten | 10 | 30 | 97 | 0.731 | 0.206 | B+P |
| 74-97-10-30-Ten | I | Ten | 10 | 30 | 97 | 0.693 | 0.189 | B+P |
| 75-97-10-30-Ten | I | Ten | 10 | 30 | 97 | 0.759 | 0.230 | B+P |
| 76-97-12-30-A | I | A | 12 | 30 | 97 | 0.675 | 0.187 | B+P |
| 77-97-12-30-A | I | A | 12 | 30 | 97 | 0.663 | 0.193 | B+P |
| 78-97-12-30-A | I | A | 12 | 30 | 97 | 0.733 | 0.220 | B+P |
| 79-97-12-30-A | I | A | 12 | 30 | 97 | 0.701 | 0.209 | B+P |
| 80-97-12-30-T | I | T | 12 | 30 | 97 | 0.713 | 0.213 | B+P |
| 81-97-12-30-T | I | T | 12 | 30 | 97 | 1.052 | 0.193 | B+R |
| 82-97-12-30-T | I | T | 12 | 30 | 97 | 1.081 | 0.313 | TB+R |
| 83-97-12-30-T | I | T | 12 | 30 | 97 | 0.692 | 0.190 | B+P |
| 84-97-12-30-M | I | M | 12 | 30 | 97 | 0.697 | 0.178 | B+P |
| 85-97-8-30-A | I | A | 8 | 30 | 97 | 0.662 | 0.209 | B+P |
| 86-97-8-30-A | I | A | 8 | 30 | 97 | 0.681 | 0.228 | B+P |
| 87-97-8-30-A | I | A | 8 | 30 | 97 | 0.657 | 0.209 | B+P |
| 88-97-8-30-T | I | T | 8 | 30 | 97 | 0.658 | 0.190 | B+P |
| 89-97-8-30-T | I | T | 8 | 30 | 97 | 1.093 | 0.282 | B+R |
| 90-97-8-30-T | I | T | 8 | 30 | 97 | 1.143 | 0.317 | B+R |
| 91-97-8-30-T | I | T | 8 | 30 | 97 | 0.835 | 0.055 | B+R+P |
| 92-97-8-30-T | I | T | 8 | 30 | 97 | 0.667 | 0.185 | B+P |
| 93-97-8-30-M | I | M | 8 | 30 | 97 | 0.697 | 0.180 | B+P |
| 94-97-10-13-97-A | II | A | 10 | 13 | 97 | 0.575 | 0.142 | B+R |
| 95-97-10-13-97-A | II | A | 10 | 13 | 97 | 0.584 | 0.131 | B+R |
| 96-97-10-13-97-A | II | A | 10 | 13 | 97 | 0.598 | 0.176 | B+R |

| | | | | | | | | |
|---------------------|-----|---|----|----|-----|-------|-------|-----|
| 97-97-10-13-97-T | II | T | 10 | 13 | 97 | 0.549 | 0.141 | B+R |
| 98-97-10-13-97-T | II | T | 10 | 13 | 97 | 0.598 | 0.136 | B+R |
| 99-97-10-13-97-T | II | T | 10 | 13 | 97 | 0.577 | 0.172 | B+R |
| 100-97-10-13-97-M | II | M | 10 | 13 | 97 | 0.625 | 0.134 | B+R |
| 101-97-10-19-97-A | II | A | 10 | 19 | 97 | 0.780 | 0.346 | B+R |
| 102-97-10-19-97-A | II | A | 10 | 19 | 97 | 0.773 | 0.352 | B+R |
| 103-97-10-19-97-A | II | A | 10 | 19 | 97 | 0.790 | 0.355 | B+R |
| 104-97-10-19-97-T | II | T | 10 | 19 | 97 | 0.791 | 0.286 | B+R |
| 105-97-10-19-97-T | II | T | 10 | 19 | 97 | 0.770 | 0.339 | B+R |
| 106-97-10-19-97-T | II | T | 10 | 19 | 97 | 0.766 | 0.337 | B+R |
| 107-97-10-19-97-M | II | M | 10 | 19 | 97 | 0.744 | 0.290 | B+R |
| 108-97-10-30-97-A | II | A | 10 | 30 | 97 | 1.162 | 0.387 | B+R |
| 109-97-10-30-97-A | II | A | 10 | 30 | 97 | 1.137 | 0.382 | B+R |
| 110-97-10-30-97-A | II | A | 10 | 30 | 97 | 1.095 | 0.356 | B+R |
| 111-97-10-30-97-T | II | T | 10 | 30 | 97 | 1.067 | 0.343 | B+R |
| 112-97-10-30-97-T | II | T | 10 | 30 | 97 | 1.137 | 0.374 | B+R |
| 113-97-10-30-97-T | II | T | 10 | 30 | 97 | 1.167 | 0.374 | B+R |
| 114-97-10-30-97-M | II | M | 10 | 30 | 97 | 1.076 | 0.381 | B+R |
| 115-97-12-30-97-A | II | A | 12 | 30 | 97 | 1.259 | 0.407 | B+R |
| 116-97-12-30-97-A | II | A | 12 | 30 | 97 | 1.231 | 0.391 | B+R |
| 117-97-12-30-97-A | II | A | 12 | 30 | 97 | 1.182 | 0.360 | B+R |
| 118-97-12-30-97-T | II | T | 12 | 30 | 97 | 1.191 | 0.396 | B+R |
| 119-97-12-30-97-T | II | T | 12 | 30 | 97 | 1.166 | 0.410 | B+R |
| 120-97-12-30-97-T | II | T | 12 | 30 | 97 | 1.161 | 0.401 | B+R |
| 121-97-12-30-97-M | II | M | 12 | 30 | 97 | 1.166 | 0.378 | B+R |
| 122-97-24-30-97-A | II | A | 24 | 30 | 97 | 1.083 | 0.364 | B+R |
| 123-97-24-30-97-A | II | A | 24 | 30 | 97 | 1.176 | 0.399 | B+R |
| 124-97-24-30-97-A | II | A | 24 | 30 | 97 | 1.159 | 0.406 | B+R |
| 125-97-24-30-97-T | II | T | 24 | 30 | 97 | 1.060 | 0.373 | B+R |
| 126-97-24-30-97-T | II | T | 24 | 30 | 97 | 1.005 | 0.356 | B+R |
| 127-97-24-30-97-T | II | T | 24 | 30 | 97 | 1.063 | 0.359 | B+R |
| 128-97-24-30-97-M | II | M | 24 | 30 | 97 | 1.173 | 0.391 | B+R |
| 129-118-24-30-118-A | II | A | 24 | 30 | 118 | 0.973 | 0.364 | B+R |
| 130-118-24-30-118-A | II | A | 24 | 30 | 118 | 1.119 | 0.373 | B+R |
| 131-118-24-30-118-A | II | A | 24 | 30 | 118 | 1.178 | 0.407 | B+R |
| 132-118-24-30-118-T | II | T | 24 | 30 | 118 | 1.227 | 0.412 | B+R |
| 133-118-24-30-118-T | II | T | 24 | 30 | 118 | 1.166 | 0.375 | B+R |
| 134-118-24-30-118-T | II | T | 24 | 30 | 118 | 1.177 | 0.406 | B+R |
| 135-118-24-30-118-M | II | M | 24 | 30 | 118 | 1.095 | 0.405 | B+R |
| 136-188-12-30-A | III | A | 12 | 30 | 188 | 0.635 | 0.139 | B |
| 137-188-12-30-A | III | A | 12 | 30 | 188 | 0.686 | 0.191 | B |
| 138-188-12-30-A | III | A | 12 | 30 | 188 | 0.646 | 0.143 | B |
| 139-188-12-30-T | III | T | 12 | 30 | 188 | 0.894 | 0.099 | B+R |
| 140-188-12-30-T | III | T | 12 | 30 | 188 | 1.066 | 0.228 | B+R |
| 141-188-12-30-T | III | T | 12 | 30 | 188 | 0.668 | 0.190 | B |
| 142-188-12-30-M | III | M | 12 | 30 | 188 | 0.820 | 0.057 | B |
| 143-188-24-30-A | III | A | 24 | 30 | 188 | 1.121 | 0.267 | B+R |
| 144-188-24-30-A | III | A | 24 | 30 | 188 | 1.146 | 0.193 | B+R |
| 145-188-24-30-A | III | A | 24 | 30 | 188 | 1.086 | 0.278 | B+R |
| 146-188-24-30-T | III | T | 24 | 30 | 188 | 1.113 | 0.305 | B+R |
| 147-188-24-30-T | III | T | 24 | 30 | 188 | 1.099 | 0.180 | B+R |
| 148-188-24-30-T | III | T | 24 | 30 | 188 | 1.024 | 0.139 | B+R |

| | | | | | | | | |
|-----------------|-----|---|----|----|-----|-------|-------|-----|
| 149-188-24-30-M | III | M | 24 | 30 | 188 | 1.052 | 0.154 | B+R |
| 150-375-19-30-A | III | A | 19 | 30 | 375 | 1.121 | 0.194 | B+R |
| 151-375-19-30-A | III | A | 19 | 30 | 375 | 0.997 | 0.240 | B+R |
| 152-375-19-30-A | III | A | 19 | 30 | 375 | 0.989 | 0.187 | B+R |
| 153-375-19-30-T | III | T | 19 | 30 | 375 | 1.069 | 0.241 | B+R |
| 154-375-19-30-T | III | T | 19 | 30 | 375 | 1.092 | 0.203 | B+R |
| 155-375-19-30-T | III | T | 19 | 30 | 375 | 1.035 | 0.183 | B+R |
| 156-375-19-30-M | III | M | 19 | 30 | 375 | 1.142 | 0.164 | B+R |

Notes:

- a. II* refers to test series with two outer thick steel framing plies sandwiching one inner thin steel sheet ply.
- b. In the fastener # column, 24 stands for X-HSN-24 PAF fastener while 19 represents X-ENP-19 PAF fastener, and 8, 10, 12 represents #8, #10, #12 screw respectively.
- c. In the failure mode column, “B”, “TB”, “P”, “R” represents “bearing”, “tilting and bearing”, “pull-through with tilting/bearing”, and “shear rupture” respectively.
- d. In the test type column, “M”, “A”, “T”, “Ten” stands for monotonic test, asymmetric cyclic test with thin steel sheet buckling away from the fastener head, asymmetric cyclic test with thin steel sheet buckling towards the fastener head, and tension only cyclic test respectively.

Appendix 2: Test Data Characterization Summary

Summaries for test data characterization result and ductility index of each test conducted are provided in this appendix. The average characterization result and ductility index values for different test type are also summarized in this appendix.

Table 16. Test data characterization summary

| Test ID | D ₁ (in.) | D ₂ (in.) | D ₃ (in.) | D ₄ (in.) | P ₁ (kip) | P ₂ (kip) | P ₃ (kip) | P ₄ (kip) |
|---------------|----------------------|----------------------|----------------------|----------------------|----------------------|----------------------|----------------------|----------------------|
| 1-54-10-13-A | 0.006 | 0.008 | 0.012 | 0.646 | 0.101 | 0.211 | 0.252 | 0.025 |
| 2-54-10-13-A | 0.002 | 0.004 | 0.005 | 0.618 | 0.117 | 0.235 | 0.292 | 0.029 |
| 3-54-10-13-A | 0.006 | 0.008 | 0.081 | 0.480 | 0.136 | 0.275 | 0.340 | 0.034 |
| 4-54-10-13-T | 0.001 | 0.002 | 0.003 | 0.438 | 0.130 | 0.262 | 0.326 | 0.033 |
| 5-54-10-13-T | 0.003 | 0.005 | 0.092 | 0.685 | 0.100 | 0.222 | 0.249 | 0.025 |
| 6-54-10-13-T | 0.001 | 0.002 | 0.059 | 0.355 | 0.140 | 0.319 | 0.349 | 0.035 |
| 7-54-10-13-M | 0.001 | 0.001 | 0.033 | 0.445 | 0.100 | 0.219 | 0.251 | 0.025 |
| 8-54-10-19-A | 0.003 | 0.005 | 0.133 | 0.364 | 0.170 | 0.352 | 0.425 | 0.043 |
| 9-54-10-19-A | 0.001 | 0.001 | 0.153 | 0.569 | 0.166 | 0.312 | 0.415 | 0.041 |
| 10-54-10-19-A | 0.002 | 0.004 | 0.132 | 0.452 | 0.168 | 0.363 | 0.420 | 0.042 |
| 11-54-10-19-T | 0.004 | 0.007 | 0.118 | 0.616 | 0.162 | 0.315 | 0.405 | 0.040 |
| 12-54-10-19-T | 0.004 | 0.009 | 0.139 | 0.371 | 0.172 | 0.369 | 0.431 | 0.043 |
| 13-54-10-19-T | 0.004 | 0.005 | 0.120 | 0.352 | 0.177 | 0.407 | 0.441 | 0.044 |
| 14-54-10-19-M | 0.008 | 0.011 | 0.113 | 0.620 | 0.155 | 0.322 | 0.388 | 0.039 |
| 15-54-10-30-A | 0.009 | 0.150 | 0.337 | 0.600 | 0.325 | 0.722 | 0.813 | 0.081 |
| 16-54-10-30-A | 0.003 | 0.119 | 0.323 | 0.470 | 0.326 | 0.707 | 0.816 | 0.082 |
| 17-54-10-30-A | 0.004 | 0.099 | 0.323 | 0.622 | 0.327 | 0.654 | 0.818 | 0.082 |
| 18-54-10-30-T | 0.009 | 0.166 | 0.362 | 1.132 | 0.460 | 0.971 | 1.150 | 0.115 |
| 19-54-10-30-T | 0.001 | 0.049 | 0.348 | 0.632 | 0.324 | 0.648 | 0.811 | 0.081 |
| 20-54-10-30-T | 0.007 | 0.159 | 0.649 | 0.954 | 0.449 | 1.020 | 1.122 | 0.112 |
| 21-54-10-30-T | 0.003 | 0.024 | 0.279 | 0.595 | 0.322 | 0.684 | 0.804 | 0.080 |
| 22-54-10-30-T | 0.010 | 0.175 | 0.599 | 0.931 | 0.405 | 0.931 | 1.013 | 0.101 |
| 23-54-10-30-M | 0.001 | 0.104 | 0.260 | 0.688 | 0.316 | 0.707 | 0.791 | 0.079 |
| 24-54-10-30-M | 0.001 | 0.029 | 0.251 | 0.715 | 0.318 | 0.648 | 0.795 | 0.080 |
| 25-54-10-30-M | 0.005 | 0.031 | 0.266 | 0.673 | 0.315 | 0.619 | 0.788 | 0.079 |
| 26-54-8-13-A | 0.002 | 0.004 | 0.068 | 0.550 | 0.094 | 0.188 | 0.234 | 0.023 |
| 27-54-8-13-A | 0.002 | 0.005 | 0.084 | 0.263 | 0.110 | 0.242 | 0.274 | 0.027 |
| 28-54-8-13-A | 0.003 | 0.006 | 0.061 | 0.538 | 0.102 | 0.235 | 0.256 | 0.026 |
| 29-54-8-13-T | 0.002 | 0.003 | 0.005 | 0.536 | 0.115 | 0.240 | 0.286 | 0.029 |
| 30-54-8-13-T | 0.003 | 0.005 | 0.011 | 0.623 | 0.099 | 0.208 | 0.248 | 0.025 |
| 31-54-8-13-T | 0.001 | 0.003 | 0.016 | 0.592 | 0.094 | 0.201 | 0.234 | 0.023 |
| 32-54-8-13-M | 0.001 | 0.001 | 0.041 | 0.595 | 0.095 | 0.219 | 0.236 | 0.024 |
| 33-54-8-19-A | 0.004 | 0.012 | 0.142 | 0.346 | 0.150 | 0.309 | 0.375 | 0.037 |
| 34-54-8-19-A | 0.004 | 0.033 | 0.182 | 0.367 | 0.156 | 0.310 | 0.391 | 0.039 |
| 35-54-8-19-A | 0.005 | 0.068 | 0.185 | 0.415 | 0.162 | 0.355 | 0.404 | 0.040 |
| 36-54-8-19-T | 0.001 | 0.003 | 0.086 | 0.514 | 0.135 | 0.318 | 0.338 | 0.034 |
| 37-54-8-19-T | 0.002 | 0.008 | 0.115 | 0.381 | 0.153 | 0.327 | 0.384 | 0.038 |
| 38-54-8-19-T | 0.001 | 0.002 | 0.090 | 0.692 | 0.145 | 0.328 | 0.364 | 0.036 |
| 39-54-8-19-M | 0.003 | 0.021 | 0.150 | 0.557 | 0.160 | 0.311 | 0.401 | 0.040 |
| 40-54-8-30-A | 0.002 | 0.158 | 0.376 | 0.500 | 0.305 | 0.673 | 0.761 | 0.076 |
| 41-54-8-30-A | 0.005 | 0.145 | 0.314 | 0.533 | 0.298 | 0.643 | 0.746 | 0.075 |
| 42-54-8-30-A | 0.008 | 0.167 | 0.361 | 0.761 | 0.291 | 0.632 | 0.727 | 0.073 |
| 43-54-8-30-T | 0.036 | 0.192 | 0.608 | 0.961 | 0.441 | 0.967 | 1.102 | 0.110 |
| 44-54-8-30-T | 0.008 | 0.259 | 0.642 | 0.921 | 0.453 | 0.963 | 1.133 | 0.113 |

| | | | | | | | | |
|------------------|-------|-------|-------|-------|-------|-------|-------|-------|
| 45-54-8-30-T | 0.014 | 0.213 | 0.664 | 0.969 | 0.446 | 0.952 | 1.115 | 0.112 |
| 46-54-8-30-M | 0.001 | 0.159 | 0.437 | 0.932 | 0.431 | 0.954 | 1.077 | 0.108 |
| 47-54-8-30-M | 0.007 | 0.170 | 0.521 | 0.896 | 0.438 | 0.932 | 1.095 | 0.109 |
| 48-97-10-13-A | 0.001 | 0.002 | 0.003 | 0.528 | 0.123 | 0.260 | 0.308 | 0.031 |
| 49-97-10-13-A | 0.001 | 0.002 | 0.003 | 0.518 | 0.133 | 0.269 | 0.333 | 0.033 |
| 50-97-10-13-A | 0.002 | 0.002 | 0.003 | 0.447 | 0.142 | 0.246 | 0.354 | 0.035 |
| 51-97-10-13-T | 0.001 | 0.001 | 0.001 | 0.458 | 0.138 | 0.275 | 0.344 | 0.034 |
| 52-97-10-13-T | 0.002 | 0.005 | 0.007 | 0.480 | 0.118 | 0.237 | 0.295 | 0.029 |
| 53-97-10-13-T | 0.002 | 0.005 | 0.009 | 0.429 | 0.162 | 0.335 | 0.406 | 0.041 |
| 54-97-10-13-M | 0.001 | 0.001 | 0.001 | 0.344 | 0.152 | 0.304 | 0.380 | 0.038 |
| 55-97-10-19-A | 0.001 | 0.001 | 0.095 | 0.540 | 0.142 | 0.312 | 0.354 | 0.035 |
| 56-97-10-19-A | 0.003 | 0.005 | 0.121 | 0.517 | 0.167 | 0.328 | 0.418 | 0.042 |
| 57-97-10-19-A | 0.002 | 0.002 | 0.093 | 0.376 | 0.159 | 0.326 | 0.397 | 0.040 |
| 58-97-10-19-T | 0.001 | 0.002 | 0.112 | 0.676 | 0.155 | 0.319 | 0.387 | 0.039 |
| 59-97-10-19-T | 0.002 | 0.003 | 0.122 | 0.681 | 0.157 | 0.344 | 0.392 | 0.039 |
| 60-97-10-19-T | 0.005 | 0.009 | 0.137 | 0.662 | 0.165 | 0.355 | 0.414 | 0.041 |
| 61-97-10-19-M | 0.002 | 0.002 | 0.092 | 0.622 | 0.139 | 0.314 | 0.348 | 0.035 |
| 62-97-10-30-A | 0.002 | 0.056 | 0.199 | 0.442 | 0.290 | 0.642 | 0.725 | 0.072 |
| 63-97-10-30-A | 0.004 | 0.108 | 0.246 | 0.507 | 0.296 | 0.651 | 0.739 | 0.074 |
| 64-97-10-30-A | 0.003 | 0.062 | 0.188 | 0.580 | 0.272 | 0.596 | 0.680 | 0.068 |
| 65-97-10-30-A | 0.006 | 0.118 | 0.263 | 0.543 | 0.310 | 0.686 | 0.775 | 0.078 |
| 66-97-10-30-T | 0.001 | 0.102 | 0.266 | 0.698 | 0.425 | 0.902 | 1.064 | 0.106 |
| 67-97-10-30-T | 0.003 | 0.019 | 0.202 | 0.559 | 0.290 | 0.600 | 0.725 | 0.072 |
| 68-97-10-30-T | 0.001 | 0.039 | 0.209 | 0.526 | 0.294 | 0.631 | 0.734 | 0.073 |
| 69-97-10-30-T | 0.001 | 0.027 | 0.221 | 0.544 | 0.291 | 0.606 | 0.727 | 0.073 |
| 70-97-10-30-T | 0.008 | 0.058 | 0.228 | 0.520 | 0.291 | 0.622 | 0.727 | 0.073 |
| 71-97-10-30-M | 0.003 | 0.017 | 0.191 | 0.685 | 0.289 | 0.586 | 0.722 | 0.072 |
| 72-97-10-30-Ten | 0.005 | 0.019 | 0.242 | 0.595 | 0.317 | 0.656 | 0.792 | 0.079 |
| 73-97-10-30-Ten | 0.005 | 0.032 | 0.206 | 0.619 | 0.292 | 0.588 | 0.731 | 0.073 |
| 74-97-10-30-Ten | 0.003 | 0.013 | 0.189 | 0.645 | 0.277 | 0.593 | 0.693 | 0.069 |
| 75-97-10-30-Ten | 0.001 | 0.013 | 0.230 | 0.565 | 0.304 | 0.644 | 0.759 | 0.076 |
| 76-97-12-30-A | 0.001 | 0.007 | 0.187 | 0.533 | 0.270 | 0.531 | 0.675 | 0.067 |
| 77-97-12-30-A | 0.003 | 0.014 | 0.193 | 0.570 | 0.265 | 0.525 | 0.663 | 0.066 |
| 78-97-12-30-A | 0.001 | 0.009 | 0.220 | 0.429 | 0.293 | 0.574 | 0.733 | 0.073 |
| 79-97-12-30-A | 0.002 | 0.011 | 0.209 | 0.413 | 0.281 | 0.559 | 0.701 | 0.070 |
| 80-97-12-30-T | 0.001 | 0.011 | 0.213 | 0.409 | 0.285 | 0.575 | 0.713 | 0.071 |
| 81-97-12-30-T | 0.001 | 0.078 | 0.193 | 0.742 | 0.421 | 0.906 | 1.052 | 0.105 |
| 82-97-12-30-T | 0.004 | 0.097 | 0.313 | 0.747 | 0.433 | 0.952 | 1.081 | 0.108 |
| 83-97-12-30-T | 0.002 | 0.011 | 0.190 | 0.574 | 0.277 | 0.563 | 0.692 | 0.069 |
| 84-97-12-30-M | 0.001 | 0.001 | 0.178 | 0.630 | 0.279 | 0.582 | 0.697 | 0.070 |
| 85-97-8-30-A | 0.001 | 0.063 | 0.209 | 0.446 | 0.265 | 0.574 | 0.662 | 0.066 |
| 86-97-8-30-A | 0.002 | 0.043 | 0.228 | 0.422 | 0.272 | 0.563 | 0.681 | 0.068 |
| 87-97-8-30-A | 0.001 | 0.050 | 0.209 | 0.469 | 0.263 | 0.571 | 0.657 | 0.066 |
| 88-97-8-30-T | 0.001 | 0.032 | 0.190 | 0.550 | 0.263 | 0.530 | 0.658 | 0.066 |
| 89-97-8-30-T | 0.005 | 0.137 | 0.282 | 0.741 | 0.437 | 0.924 | 1.093 | 0.109 |
| 90-97-8-30-T | 0.008 | 0.151 | 0.317 | 0.801 | 0.457 | 0.967 | 1.143 | 0.114 |
| 91-97-8-30-T | 0.001 | 0.006 | 0.055 | 0.374 | 0.334 | 0.710 | 0.835 | 0.083 |
| 92-97-8-30-T | 0.001 | 0.014 | 0.185 | 0.507 | 0.267 | 0.570 | 0.667 | 0.067 |
| 93-97-8-30-M | 0.001 | 0.001 | 0.180 | 0.608 | 0.279 | 0.545 | 0.697 | 0.070 |
| 94-97-10-13-97-A | 0.004 | 0.055 | 0.142 | 0.762 | 0.240 | 0.459 | 0.575 | 0.058 |
| 95-97-10-13-97-A | 0.002 | 0.046 | 0.131 | 0.656 | 0.234 | 0.513 | 0.584 | 0.058 |
| 96-97-10-13-97-A | 0.001 | 0.066 | 0.176 | 0.659 | 0.239 | 0.505 | 0.598 | 0.060 |

| | | | | | | | | |
|---------------------|-------|-------|-------|-------|-------|-------|-------|-------|
| 97-97-10-13-97-T | 0.001 | 0.052 | 0.141 | 0.700 | 0.220 | 0.483 | 0.549 | 0.055 |
| 98-97-10-13-97-T | 0.004 | 0.050 | 0.136 | 0.681 | 0.239 | 0.478 | 0.598 | 0.060 |
| 99-97-10-13-97-T | 0.016 | 0.080 | 0.172 | 0.723 | 0.231 | 0.488 | 0.577 | 0.058 |
| 100-97-10-13-97-M | 0.001 | 0.047 | 0.134 | 0.648 | 0.250 | 0.537 | 0.625 | 0.062 |
| 101-97-10-19-97-A | 0.017 | 0.112 | 0.346 | 0.758 | 0.312 | 0.677 | 0.780 | 0.078 |
| 102-97-10-19-97-A | 0.003 | 0.088 | 0.352 | 0.770 | 0.309 | 0.679 | 0.773 | 0.077 |
| 103-97-10-19-97-A | 0.026 | 0.110 | 0.355 | 0.707 | 0.316 | 0.694 | 0.790 | 0.079 |
| 104-97-10-19-97-T | 0.010 | 0.093 | 0.286 | 0.875 | 0.317 | 0.676 | 0.791 | 0.079 |
| 105-97-10-19-97-T | 0.010 | 0.105 | 0.339 | 0.595 | 0.308 | 0.667 | 0.770 | 0.077 |
| 106-97-10-19-97-T | 0.006 | 0.089 | 0.337 | 0.791 | 0.306 | 0.687 | 0.766 | 0.077 |
| 107-97-10-19-97-M | 0.014 | 0.107 | 0.290 | 0.622 | 0.298 | 0.630 | 0.744 | 0.074 |
| 108-97-10-30-97-A | 0.011 | 0.121 | 0.387 | 0.908 | 0.465 | 1.012 | 1.162 | 0.116 |
| 109-97-10-30-97-A | 0.011 | 0.122 | 0.382 | 0.940 | 0.455 | 0.990 | 1.137 | 0.114 |
| 110-97-10-30-97-A | 0.013 | 0.112 | 0.356 | 0.736 | 0.438 | 0.951 | 1.095 | 0.109 |
| 111-97-10-30-97-T | 0.023 | 0.106 | 0.343 | 1.068 | 0.427 | 0.937 | 1.067 | 0.107 |
| 112-97-10-30-97-T | 0.012 | 0.119 | 0.374 | 0.890 | 0.455 | 0.997 | 1.137 | 0.114 |
| 113-97-10-30-97-T | 0.011 | 0.128 | 0.374 | 0.941 | 0.467 | 0.995 | 1.167 | 0.117 |
| 114-97-10-30-97-M | 0.020 | 0.119 | 0.381 | 0.791 | 0.430 | 0.940 | 1.076 | 0.108 |
| 115-97-12-30-97-A | 0.016 | 0.134 | 0.407 | 1.032 | 0.504 | 1.081 | 1.259 | 0.126 |
| 116-97-12-30-97-A | 0.012 | 0.128 | 0.391 | 1.063 | 0.493 | 1.078 | 1.231 | 0.123 |
| 117-97-12-30-97-A | 0.008 | 0.108 | 0.360 | 0.995 | 0.473 | 1.036 | 1.182 | 0.118 |
| 118-97-12-30-97-T | 0.013 | 0.122 | 0.396 | 0.990 | 0.476 | 1.042 | 1.191 | 0.119 |
| 119-97-12-30-97-T | 0.017 | 0.121 | 0.410 | 1.043 | 0.466 | 1.029 | 1.166 | 0.117 |
| 120-97-12-30-97-T | 0.016 | 0.117 | 0.401 | 1.029 | 0.465 | 1.015 | 1.161 | 0.116 |
| 121-97-12-30-97-M | 0.014 | 0.108 | 0.378 | 0.899 | 0.466 | 1.020 | 1.166 | 0.117 |
| 122-97-24-30-97-A | 0.002 | 0.091 | 0.364 | 1.105 | 0.433 | 0.977 | 1.083 | 0.108 |
| 123-97-24-30-97-A | 0.003 | 0.121 | 0.399 | 1.106 | 0.470 | 1.043 | 1.176 | 0.118 |
| 124-97-24-30-97-A | 0.002 | 0.109 | 0.406 | 1.041 | 0.464 | 1.048 | 1.159 | 0.116 |
| 125-97-24-30-97-T | 0.002 | 0.094 | 0.373 | 1.064 | 0.424 | 0.961 | 1.060 | 0.106 |
| 126-97-24-30-97-T | 0.003 | 0.075 | 0.356 | 1.062 | 0.402 | 0.913 | 1.005 | 0.100 |
| 127-97-24-30-97-T | 0.002 | 0.077 | 0.359 | 1.077 | 0.425 | 0.949 | 1.063 | 0.106 |
| 128-97-24-30-97-M | 0.002 | 0.111 | 0.391 | 1.000 | 0.469 | 1.058 | 1.173 | 0.117 |
| 129-118-24-30-118-A | 0.004 | 0.087 | 0.364 | 1.010 | 0.389 | 0.876 | 0.973 | 0.097 |
| 130-118-24-30-118-A | 0.002 | 0.093 | 0.373 | 1.077 | 0.448 | 1.008 | 1.119 | 0.112 |
| 131-118-24-30-118-A | 0.002 | 0.110 | 0.407 | 1.090 | 0.471 | 1.052 | 1.178 | 0.118 |
| 132-118-24-30-118-T | 0.003 | 0.122 | 0.412 | 1.097 | 0.491 | 1.082 | 1.227 | 0.123 |
| 133-118-24-30-118-T | 0.002 | 0.103 | 0.375 | 1.098 | 0.466 | 1.036 | 1.166 | 0.117 |
| 134-118-24-30-118-T | 0.002 | 0.111 | 0.406 | 1.092 | 0.471 | 1.053 | 1.177 | 0.118 |
| 135-118-24-30-118-M | 0.003 | 0.103 | 0.405 | 1.113 | 0.438 | 0.968 | 1.095 | 0.110 |
| 136-188-12-30-A | 0.001 | 0.004 | 0.139 | 0.575 | 0.254 | 0.536 | 0.635 | 0.063 |
| 137-188-12-30-A | 0.005 | 0.073 | 0.191 | 0.450 | 0.274 | 0.626 | 0.686 | 0.069 |
| 138-188-12-30-A | 0.001 | 0.010 | 0.143 | 0.579 | 0.258 | 0.502 | 0.646 | 0.065 |
| 139-188-12-30-T | 0.003 | 0.029 | 0.099 | 0.673 | 0.358 | 0.751 | 0.894 | 0.089 |
| 140-188-12-30-T | 0.007 | 0.082 | 0.228 | 0.657 | 0.426 | 0.908 | 1.066 | 0.107 |
| 141-188-12-30-T | 0.006 | 0.030 | 0.190 | 0.633 | 0.267 | 0.523 | 0.668 | 0.067 |
| 142-188-12-30-M | 0.001 | 0.022 | 0.057 | 0.710 | 0.328 | 0.704 | 0.820 | 0.082 |
| 143-188-24-30-A | 0.001 | 0.024 | 0.267 | 0.854 | 0.448 | 0.965 | 1.121 | 0.112 |
| 144-188-24-30-A | 0.002 | 0.030 | 0.193 | 0.895 | 0.458 | 0.994 | 1.146 | 0.115 |
| 145-188-24-30-A | 0.002 | 0.062 | 0.278 | 0.814 | 0.434 | 0.980 | 1.086 | 0.109 |
| 146-188-24-30-T | 0.001 | 0.060 | 0.305 | 0.728 | 0.445 | 1.008 | 1.113 | 0.111 |
| 147-188-24-30-T | 0.003 | 0.026 | 0.180 | 0.683 | 0.440 | 0.948 | 1.099 | 0.110 |
| 148-188-24-30-T | 0.002 | 0.021 | 0.139 | 0.769 | 0.410 | 0.861 | 1.024 | 0.102 |

| | | | | | | | | |
|-----------------|-------|-------|-------|-------|-------|-------|-------|-------|
| 149-188-24-30-M | 0.002 | 0.023 | 0.154 | 0.699 | 0.421 | 0.904 | 1.052 | 0.105 |
| 150-375-19-30-A | 0.005 | 0.048 | 0.194 | 0.683 | 0.449 | 0.999 | 1.121 | 0.112 |
| 151-375-19-30-A | 0.005 | 0.062 | 0.240 | 0.783 | 0.399 | 0.853 | 0.997 | 0.100 |
| 152-375-19-30-A | 0.008 | 0.069 | 0.187 | 0.595 | 0.396 | 0.847 | 0.989 | 0.099 |
| 153-375-19-30-T | 0.007 | 0.058 | 0.241 | 0.722 | 0.427 | 0.927 | 1.069 | 0.107 |
| 154-375-19-30-T | 0.005 | 0.063 | 0.203 | 0.513 | 0.437 | 0.957 | 1.092 | 0.109 |
| 155-375-19-30-T | 0.008 | 0.073 | 0.183 | 0.594 | 0.414 | 0.897 | 1.035 | 0.104 |
| 156-375-19-30-M | 0.004 | 0.036 | 0.164 | 0.651 | 0.457 | 1.015 | 1.142 | 0.114 |

Table 17. Test data characterization average values for monotonic tests

| Specimen Type | D ₁ (in.) | D ₂ (in.) | D ₃ (in.) | D ₄ (in.) | P ₁ (kip) | P ₂ (kip) | P ₃ (kip) | P ₄ (kip) |
|---------------|----------------------|----------------------|----------------------|----------------------|----------------------|----------------------|----------------------|----------------------|
| 54-10-13 | 0.001 | 0.001 | 0.033 | 0.445 | 0.100 | 0.219 | 0.251 | 0.025 |
| 54-10-19 | 0.008 | 0.011 | 0.113 | 0.620 | 0.155 | 0.322 | 0.388 | 0.039 |
| 54-10-30 | 0.002 | 0.055 | 0.259 | 0.692 | 0.317 | 0.658 | 0.791 | 0.079 |
| 54-8-13 | 0.001 | 0.001 | 0.041 | 0.595 | 0.095 | 0.219 | 0.236 | 0.024 |
| 54-8-19 | 0.003 | 0.021 | 0.150 | 0.557 | 0.160 | 0.311 | 0.401 | 0.040 |
| 54-8-30 | 0.004 | 0.164 | 0.479 | 0.914 | 0.434 | 0.943 | 1.086 | 0.109 |
| 97-10-13 | 0.001 | 0.001 | 0.001 | 0.344 | 0.152 | 0.304 | 0.380 | 0.038 |
| 97-10-19 | 0.002 | 0.002 | 0.092 | 0.622 | 0.139 | 0.314 | 0.348 | 0.035 |
| 97-10-30 | 0.003 | 0.017 | 0.191 | 0.685 | 0.289 | 0.586 | 0.722 | 0.072 |
| 97-12-30 | 0.001 | 0.001 | 0.178 | 0.630 | 0.279 | 0.582 | 0.697 | 0.070 |
| 97-8-30 | 0.001 | 0.001 | 0.180 | 0.608 | 0.279 | 0.545 | 0.697 | 0.070 |
| 97-10-13-97 | 0.001 | 0.047 | 0.134 | 0.648 | 0.250 | 0.537 | 0.625 | 0.062 |
| 97-10-19-97 | 0.014 | 0.107 | 0.290 | 0.622 | 0.298 | 0.630 | 0.744 | 0.074 |
| 97-10-30-97 | 0.020 | 0.119 | 0.381 | 0.791 | 0.430 | 0.940 | 1.076 | 0.108 |
| 97-12-30-97 | 0.014 | 0.108 | 0.378 | 0.899 | 0.466 | 1.020 | 1.166 | 0.117 |
| 97-24-30-97 | 0.002 | 0.111 | 0.391 | 1.000 | 0.469 | 1.058 | 1.173 | 0.117 |
| 118-24-30-118 | 0.003 | 0.103 | 0.405 | 1.113 | 0.438 | 0.968 | 1.095 | 0.110 |
| 188-12-30 | 0.001 | 0.022 | 0.057 | 0.710 | 0.328 | 0.704 | 0.820 | 0.082 |
| 188-24-30 | 0.002 | 0.023 | 0.154 | 0.699 | 0.421 | 0.904 | 1.052 | 0.105 |
| 375-19-30 | 0.004 | 0.036 | 0.164 | 0.651 | 0.457 | 1.015 | 1.142 | 0.114 |

Table 18. Test data characterization average values for buckling away cyclic tests

| Specimen Type | D ₁ (in.) | D ₂ (in.) | D ₃ (in.) | D ₄ (in.) | P ₁ (kip) | P ₂ (kip) | P ₃ (kip) | P ₄ (kip) |
|---------------|----------------------|----------------------|----------------------|----------------------|----------------------|----------------------|----------------------|----------------------|
| 54-10-13 | 0.005 | 0.007 | 0.033 | 0.582 | 0.118 | 0.240 | 0.294 | 0.029 |
| 54-10-19 | 0.002 | 0.003 | 0.139 | 0.462 | 0.168 | 0.342 | 0.420 | 0.042 |
| 54-10-30 | 0.005 | 0.123 | 0.328 | 0.564 | 0.326 | 0.694 | 0.816 | 0.082 |
| 54-8-13 | 0.003 | 0.005 | 0.071 | 0.451 | 0.102 | 0.222 | 0.255 | 0.025 |
| 54-8-19 | 0.004 | 0.038 | 0.170 | 0.376 | 0.156 | 0.325 | 0.390 | 0.039 |
| 54-8-30 | 0.005 | 0.157 | 0.350 | 0.598 | 0.298 | 0.649 | 0.745 | 0.074 |
| 97-10-13 | 0.002 | 0.002 | 0.003 | 0.498 | 0.133 | 0.258 | 0.331 | 0.033 |
| 97-10-19 | 0.002 | 0.003 | 0.103 | 0.478 | 0.156 | 0.322 | 0.390 | 0.039 |
| 97-10-30 | 0.004 | 0.086 | 0.224 | 0.518 | 0.292 | 0.644 | 0.730 | 0.073 |
| 97-12-30 | 0.002 | 0.010 | 0.202 | 0.486 | 0.277 | 0.547 | 0.693 | 0.069 |
| 97-8-30 | 0.001 | 0.052 | 0.215 | 0.446 | 0.267 | 0.569 | 0.667 | 0.067 |
| 97-10-13-97 | 0.002 | 0.056 | 0.150 | 0.692 | 0.238 | 0.493 | 0.586 | 0.059 |
| 97-10-19-97 | 0.015 | 0.103 | 0.351 | 0.745 | 0.312 | 0.683 | 0.781 | 0.078 |
| 97-10-30-97 | 0.012 | 0.118 | 0.375 | 0.861 | 0.453 | 0.984 | 1.131 | 0.113 |
| 97-12-30-97 | 0.012 | 0.123 | 0.386 | 1.030 | 0.490 | 1.065 | 1.224 | 0.122 |
| 97-24-30-97 | 0.002 | 0.107 | 0.390 | 1.084 | 0.456 | 1.023 | 1.139 | 0.114 |
| 118-24-30-118 | 0.003 | 0.097 | 0.381 | 1.059 | 0.436 | 0.979 | 1.090 | 0.109 |
| 188-12-30 | 0.002 | 0.029 | 0.158 | 0.535 | 0.262 | 0.555 | 0.656 | 0.066 |
| 188-24-30 | 0.002 | 0.039 | 0.246 | 0.854 | 0.447 | 0.979 | 1.118 | 0.112 |
| 375-19-30 | 0.006 | 0.060 | 0.207 | 0.687 | 0.414 | 0.900 | 1.036 | 0.104 |

Table 19. Test data characterization average values for buckling towards cyclic tests

| Specimen Type | D ₁ (in.) | D ₂ (in.) | D ₃ (in.) | D ₄ (in.) | P ₁ (kip) | P ₂ (kip) | P ₃ (kip) | P ₄ (kip) |
|---------------|----------------------|----------------------|----------------------|----------------------|----------------------|----------------------|----------------------|----------------------|
| 54-10-13 | 0.002 | 0.003 | 0.052 | 0.493 | 0.123 | 0.268 | 0.308 | 0.031 |
| 54-10-19 | 0.004 | 0.007 | 0.126 | 0.446 | 0.170 | 0.364 | 0.426 | 0.043 |
| 54-10-30 | 0.006 | 0.114 | 0.447 | 0.849 | 0.392 | 0.851 | 0.980 | 0.098 |
| 54-8-13 | 0.002 | 0.004 | 0.011 | 0.584 | 0.102 | 0.216 | 0.256 | 0.026 |
| 54-8-19 | 0.001 | 0.004 | 0.097 | 0.529 | 0.145 | 0.324 | 0.362 | 0.036 |
| 54-8-30 | 0.019 | 0.221 | 0.638 | 0.950 | 0.447 | 0.961 | 1.117 | 0.112 |
| 97-10-13 | 0.002 | 0.004 | 0.005 | 0.456 | 0.139 | 0.282 | 0.348 | 0.035 |
| 97-10-19 | 0.002 | 0.005 | 0.124 | 0.673 | 0.159 | 0.340 | 0.398 | 0.040 |
| 97-10-30 | 0.003 | 0.049 | 0.225 | 0.569 | 0.318 | 0.672 | 0.795 | 0.080 |
| 97-12-30 | 0.002 | 0.049 | 0.227 | 0.618 | 0.354 | 0.749 | 0.885 | 0.088 |
| 97-8-30 | 0.003 | 0.068 | 0.206 | 0.595 | 0.352 | 0.740 | 0.879 | 0.088 |
| 97-10-13-97 | 0.007 | 0.061 | 0.150 | 0.701 | 0.230 | 0.483 | 0.575 | 0.057 |
| 97-10-19-97 | 0.009 | 0.096 | 0.320 | 0.754 | 0.310 | 0.677 | 0.776 | 0.078 |
| 97-10-30-97 | 0.015 | 0.118 | 0.364 | 0.966 | 0.450 | 0.976 | 1.124 | 0.112 |
| 97-12-30-97 | 0.015 | 0.120 | 0.402 | 1.021 | 0.469 | 1.029 | 1.173 | 0.117 |
| 97-24-30-97 | 0.002 | 0.082 | 0.363 | 1.068 | 0.417 | 0.941 | 1.043 | 0.104 |
| 118-24-30-118 | 0.002 | 0.112 | 0.398 | 1.096 | 0.476 | 1.057 | 1.190 | 0.119 |
| 188-12-30 | 0.005 | 0.047 | 0.172 | 0.654 | 0.350 | 0.727 | 0.876 | 0.088 |
| 188-24-30 | 0.002 | 0.036 | 0.208 | 0.727 | 0.432 | 0.939 | 1.079 | 0.108 |
| 375-19-30 | 0.006 | 0.065 | 0.209 | 0.610 | 0.426 | 0.927 | 1.065 | 0.107 |

Table 20. Test data characterization average values for tension only cyclic tests

| Specimen Type | D ₁ (in.) | D ₂ (in.) | D ₃ (in.) | D ₄ (in.) | P ₁ (kip) | P ₂ (kip) | P ₃ (kip) | P ₄ (kip) |
|---------------|----------------------|----------------------|----------------------|----------------------|----------------------|----------------------|----------------------|----------------------|
| 97-10-30 | 0.003 | 0.019 | 0.217 | 0.606 | 0.298 | 0.620 | 0.744 | 0.074 |

Table 21. Test ductility index summary

| Test ID | D_y (in.) | $D_{\text{postpeak80\%}}$ (in.) | D_u (in.) | $D_{\text{postpeak80\%}}/D_y$ | D_u/D_y |
|---------------|-------------|---------------------------------|-------------|-------------------------------|-----------|
| 1-54-10-13-A | 0.015 | 0.153 | 0.646 | 9.959 | 42.091 |
| 2-54-10-13-A | 0.005 | 0.142 | 0.618 | 27.088 | 118.395 |
| 3-54-10-13-A | 0.014 | 0.170 | 0.480 | 12.239 | 34.630 |
| 4-54-10-13-T | 0.003 | 0.100 | 0.438 | 32.571 | 143.071 |
| 5-54-10-13-T | 0.007 | 0.224 | 0.685 | 31.189 | 95.344 |
| 6-54-10-13-T | 0.004 | 0.125 | 0.355 | 34.845 | 98.882 |
| 7-54-10-13-M | 0.001 | 0.124 | 0.445 | 89.809 | 321.034 |
| 8-54-10-19-A | 0.007 | 0.184 | 0.364 | 26.682 | 52.778 |
| 9-54-10-19-A | 0.001 | 0.245 | 0.569 | 183.614 | 425.924 |
| 10-54-10-19-A | 0.006 | 0.203 | 0.452 | 35.610 | 79.299 |
| 11-54-10-19-T | 0.009 | 0.228 | 0.616 | 25.421 | 68.521 |
| 12-54-10-19-T | 0.011 | 0.191 | 0.371 | 17.191 | 33.456 |
| 13-54-10-19-T | 0.010 | 0.171 | 0.352 | 17.425 | 35.751 |
| 14-54-10-19-M | 0.021 | 0.225 | 0.620 | 10.617 | 29.221 |
| 15-54-10-30-A | 0.021 | 0.395 | 0.600 | 18.416 | 27.953 |
| 16-54-10-30-A | 0.007 | 0.356 | 0.470 | 49.392 | 65.321 |
| 17-54-10-30-A | 0.009 | 0.390 | 0.622 | 41.464 | 66.146 |
| 18-54-10-30-T | 0.022 | 0.534 | 1.132 | 24.332 | 51.640 |
| 19-54-10-30-T | 0.002 | 0.412 | 0.632 | 197.095 | 302.940 |
| 20-54-10-30-T | 0.017 | 0.717 | 0.954 | 41.675 | 55.473 |
| 21-54-10-30-T | 0.006 | 0.349 | 0.595 | 53.919 | 91.948 |
| 22-54-10-30-T | 0.025 | 0.673 | 0.931 | 27.206 | 37.649 |
| 23-54-10-30-M | 0.002 | 0.355 | 0.688 | 174.232 | 337.922 |
| 24-54-10-30-M | 0.003 | 0.354 | 0.715 | 102.713 | 207.415 |
| 25-54-10-30-M | 0.013 | 0.357 | 0.673 | 27.853 | 52.567 |
| 26-54-8-13-A | 0.006 | 0.175 | 0.550 | 28.671 | 90.189 |
| 27-54-8-13-A | 0.006 | 0.124 | 0.263 | 21.341 | 45.244 |
| 28-54-8-13-A | 0.009 | 0.167 | 0.538 | 19.620 | 63.189 |
| 29-54-8-13-T | 0.005 | 0.123 | 0.536 | 25.707 | 111.935 |
| 30-54-8-13-T | 0.007 | 0.147 | 0.623 | 22.274 | 94.419 |
| 31-54-8-13-T | 0.001 | 0.144 | 0.592 | 111.307 | 457.328 |
| 32-54-8-13-M | 0.001 | 0.164 | 0.595 | 125.495 | 455.330 |
| 33-54-8-19-A | 0.011 | 0.188 | 0.346 | 16.928 | 31.231 |
| 34-54-8-19-A | 0.010 | 0.223 | 0.367 | 22.000 | 36.138 |
| 35-54-8-19-A | 0.011 | 0.236 | 0.415 | 20.759 | 36.469 |
| 36-54-8-19-T | 0.002 | 0.181 | 0.514 | 84.732 | 240.297 |
| 37-54-8-19-T | 0.004 | 0.174 | 0.381 | 40.232 | 87.871 |
| 38-54-8-19-T | 0.001 | 0.224 | 0.692 | 158.392 | 490.472 |
| 39-54-8-19-M | 0.008 | 0.241 | 0.557 | 31.782 | 73.535 |
| 40-54-8-30-A | 0.005 | 0.404 | 0.500 | 80.260 | 99.436 |
| 41-54-8-30-A | 0.014 | 0.363 | 0.533 | 26.877 | 39.474 |
| 42-54-8-30-A | 0.020 | 0.450 | 0.761 | 22.941 | 38.801 |
| 43-54-8-30-T | 0.090 | 0.687 | 0.961 | 7.630 | 10.677 |
| 44-54-8-30-T | 0.020 | 0.704 | 0.921 | 34.555 | 45.236 |
| 45-54-8-30-T | 0.035 | 0.732 | 0.969 | 20.982 | 27.782 |
| 46-54-8-30-M | 0.003 | 0.547 | 0.932 | 197.371 | 336.214 |
| 47-54-8-30-M | 0.017 | 0.604 | 0.896 | 34.691 | 51.434 |
| 48-97-10-13-A | 0.003 | 0.120 | 0.528 | 41.212 | 181.973 |
| 49-97-10-13-A | 0.003 | 0.117 | 0.518 | 43.845 | 193.800 |

| | | | | | |
|-------------------|-------|-------|-------|---------|---------|
| 50-97-10-13-A | 0.006 | 0.101 | 0.447 | 17.640 | 77.721 |
| 51-97-10-13-T | 0.002 | 0.102 | 0.458 | 55.229 | 246.797 |
| 52-97-10-13-T | 0.005 | 0.112 | 0.480 | 21.745 | 93.301 |
| 53-97-10-13-T | 0.006 | 0.102 | 0.429 | 17.029 | 71.512 |
| 54-97-10-13-M | 0.002 | 0.077 | 0.344 | 37.654 | 168.042 |
| 55-97-10-19-A | 0.001 | 0.194 | 0.540 | 146.282 | 406.902 |
| 56-97-10-19-A | 0.008 | 0.209 | 0.517 | 27.823 | 68.724 |
| 57-97-10-19-A | 0.006 | 0.155 | 0.376 | 26.465 | 63.939 |
| 58-97-10-19-T | 0.003 | 0.237 | 0.676 | 93.273 | 265.864 |
| 59-97-10-19-T | 0.004 | 0.246 | 0.681 | 65.113 | 180.021 |
| 60-97-10-19-T | 0.011 | 0.254 | 0.662 | 22.547 | 58.800 |
| 61-97-10-19-M | 0.005 | 0.210 | 0.622 | 45.793 | 135.626 |
| 62-97-10-30-A | 0.004 | 0.253 | 0.442 | 59.658 | 104.135 |
| 63-97-10-30-A | 0.011 | 0.304 | 0.507 | 27.902 | 46.549 |
| 64-97-10-30-A | 0.007 | 0.275 | 0.580 | 40.990 | 86.448 |
| 65-97-10-30-A | 0.014 | 0.325 | 0.543 | 22.574 | 37.671 |
| 66-97-10-30-T | 0.003 | 0.362 | 0.698 | 111.308 | 214.861 |
| 67-97-10-30-T | 0.006 | 0.281 | 0.559 | 43.253 | 86.026 |
| 68-97-10-30-T | 0.003 | 0.279 | 0.526 | 91.756 | 172.853 |
| 69-97-10-30-T | 0.004 | 0.293 | 0.544 | 82.157 | 152.607 |
| 70-97-10-30-T | 0.019 | 0.293 | 0.520 | 15.198 | 26.968 |
| 71-97-10-30-M | 0.007 | 0.301 | 0.685 | 45.111 | 102.853 |
| 72-97-10-30-Ten | 0.011 | 0.320 | 0.595 | 28.384 | 52.740 |
| 73-97-10-30-Ten | 0.011 | 0.298 | 0.619 | 26.046 | 54.167 |
| 74-97-10-30-Ten | 0.008 | 0.290 | 0.645 | 37.124 | 82.452 |
| 75-97-10-30-Ten | 0.004 | 0.304 | 0.565 | 81.694 | 151.701 |
| 76-97-12-30-A | 0.002 | 0.263 | 0.533 | 160.416 | 324.334 |
| 77-97-12-30-A | 0.008 | 0.277 | 0.570 | 36.558 | 75.394 |
| 78-97-12-30-A | 0.003 | 0.266 | 0.429 | 83.417 | 134.438 |
| 79-97-12-30-A | 0.005 | 0.254 | 0.413 | 48.311 | 78.476 |
| 80-97-12-30-T | 0.003 | 0.256 | 0.409 | 83.380 | 133.007 |
| 81-97-12-30-T | 0.004 | 0.315 | 0.742 | 86.400 | 203.427 |
| 82-97-12-30-T | 0.011 | 0.410 | 0.747 | 36.628 | 66.841 |
| 83-97-12-30-T | 0.005 | 0.275 | 0.574 | 59.817 | 124.642 |
| 84-97-12-30-M | 0.002 | 0.278 | 0.630 | 164.018 | 371.362 |
| 85-97-8-30-A | 0.003 | 0.261 | 0.446 | 92.364 | 157.489 |
| 86-97-8-30-A | 0.006 | 0.271 | 0.422 | 45.945 | 71.578 |
| 87-97-8-30-A | 0.002 | 0.267 | 0.469 | 166.837 | 293.181 |
| 88-97-8-30-T | 0.004 | 0.270 | 0.550 | 74.550 | 151.830 |
| 89-97-8-30-T | 0.013 | 0.384 | 0.741 | 28.956 | 55.911 |
| 90-97-8-30-T | 0.019 | 0.424 | 0.801 | 22.534 | 42.503 |
| 91-97-8-30-T | 0.002 | 0.126 | 0.374 | 69.483 | 206.105 |
| 92-97-8-30-T | 0.004 | 0.257 | 0.507 | 70.246 | 138.808 |
| 93-97-8-30-M | 0.002 | 0.275 | 0.608 | 162.177 | 358.353 |
| 94-97-10-13-97-A | 0.009 | 0.279 | 0.762 | 31.157 | 84.963 |
| 95-97-10-13-97-A | 0.004 | 0.248 | 0.656 | 56.682 | 149.914 |
| 96-97-10-13-97-A | 0.004 | 0.283 | 0.659 | 79.596 | 184.931 |
| 97-97-10-13-97-T | 0.003 | 0.265 | 0.700 | 86.285 | 227.495 |
| 98-97-10-13-97-T | 0.009 | 0.257 | 0.681 | 27.299 | 72.389 |
| 99-97-10-13-97-T | 0.041 | 0.294 | 0.723 | 7.154 | 17.582 |
| 100-97-10-13-97-M | 0.003 | 0.248 | 0.648 | 73.758 | 192.285 |
| 101-97-10-19-97-A | 0.042 | 0.438 | 0.758 | 10.476 | 18.141 |

| | | | | | |
|---------------------|-------|-------|-------|---------|---------|
| 102-97-10-19-97-A | 0.007 | 0.445 | 0.770 | 65.411 | 113.179 |
| 103-97-10-19-97-A | 0.064 | 0.433 | 0.707 | 6.768 | 11.047 |
| 104-97-10-19-97-T | 0.025 | 0.417 | 0.875 | 16.693 | 35.077 |
| 105-97-10-19-97-T | 0.026 | 0.396 | 0.595 | 15.121 | 22.740 |
| 106-97-10-19-97-T | 0.014 | 0.438 | 0.791 | 30.233 | 54.579 |
| 107-97-10-19-97-M | 0.035 | 0.364 | 0.622 | 10.393 | 17.771 |
| 108-97-10-30-97-A | 0.027 | 0.503 | 0.908 | 18.292 | 33.052 |
| 109-97-10-30-97-A | 0.027 | 0.506 | 0.940 | 18.688 | 34.720 |
| 110-97-10-30-97-A | 0.032 | 0.441 | 0.736 | 13.796 | 23.057 |
| 111-97-10-30-97-T | 0.057 | 0.504 | 1.068 | 8.766 | 18.584 |
| 112-97-10-30-97-T | 0.030 | 0.489 | 0.890 | 16.563 | 30.158 |
| 113-97-10-30-97-T | 0.028 | 0.500 | 0.941 | 17.991 | 33.861 |
| 114-97-10-30-97-M | 0.051 | 0.472 | 0.791 | 9.337 | 15.639 |
| 115-97-12-30-97-A | 0.041 | 0.546 | 1.032 | 13.400 | 25.321 |
| 116-97-12-30-97-A | 0.030 | 0.540 | 1.063 | 18.117 | 35.649 |
| 117-97-12-30-97-A | 0.021 | 0.501 | 0.995 | 23.849 | 47.357 |
| 118-97-12-30-97-T | 0.033 | 0.528 | 0.990 | 16.015 | 30.025 |
| 119-97-12-30-97-T | 0.042 | 0.550 | 1.043 | 13.060 | 24.746 |
| 120-97-12-30-97-T | 0.039 | 0.541 | 1.029 | 13.816 | 26.291 |
| 121-97-12-30-97-M | 0.035 | 0.494 | 0.899 | 14.280 | 26.014 |
| 122-97-24-30-97-A | 0.005 | 0.529 | 1.105 | 106.740 | 223.110 |
| 123-97-24-30-97-A | 0.007 | 0.556 | 1.106 | 84.384 | 167.677 |
| 124-97-24-30-97-A | 0.005 | 0.547 | 1.041 | 118.748 | 226.135 |
| 125-97-24-30-97-T | 0.006 | 0.527 | 1.064 | 89.761 | 181.338 |
| 126-97-24-30-97-T | 0.007 | 0.513 | 1.062 | 73.351 | 151.820 |
| 127-97-24-30-97-T | 0.004 | 0.518 | 1.077 | 115.287 | 239.432 |
| 128-97-24-30-97-M | 0.005 | 0.526 | 1.000 | 98.085 | 186.313 |
| 129-118-24-30-118-A | 0.009 | 0.507 | 1.010 | 55.588 | 110.660 |
| 130-118-24-30-118-A | 0.005 | 0.530 | 1.077 | 109.038 | 221.718 |
| 131-118-24-30-118-A | 0.006 | 0.559 | 1.090 | 93.478 | 182.399 |
| 132-118-24-30-118-T | 0.008 | 0.564 | 1.097 | 72.241 | 140.535 |
| 133-118-24-30-118-T | 0.005 | 0.536 | 1.098 | 112.897 | 231.275 |
| 134-118-24-30-118-T | 0.006 | 0.559 | 1.092 | 101.588 | 198.504 |
| 135-118-24-30-118-M | 0.007 | 0.562 | 1.113 | 74.955 | 148.466 |
| 136-188-12-30-A | 0.002 | 0.236 | 0.575 | 99.336 | 241.938 |
| 137-188-12-30-A | 0.012 | 0.249 | 0.450 | 20.337 | 36.761 |
| 138-188-12-30-A | 0.003 | 0.240 | 0.579 | 74.206 | 179.245 |
| 139-188-12-30-T | 0.007 | 0.227 | 0.673 | 33.036 | 98.020 |
| 140-188-12-30-T | 0.018 | 0.323 | 0.657 | 18.124 | 36.839 |
| 141-188-12-30-T | 0.015 | 0.289 | 0.633 | 18.825 | 41.281 |
| 142-188-12-30-M | 0.003 | 0.202 | 0.710 | 57.949 | 203.243 |
| 143-188-24-30-A | 0.004 | 0.398 | 0.854 | 106.223 | 228.182 |
| 144-188-24-30-A | 0.004 | 0.349 | 0.895 | 82.053 | 210.427 |
| 145-188-24-30-A | 0.004 | 0.397 | 0.814 | 90.074 | 184.734 |
| 146-188-24-30-T | 0.002 | 0.399 | 0.728 | 160.499 | 292.685 |
| 147-188-24-30-T | 0.009 | 0.292 | 0.683 | 33.931 | 79.344 |
| 148-188-24-30-T | 0.005 | 0.279 | 0.769 | 56.049 | 154.430 |
| 149-188-24-30-M | 0.005 | 0.275 | 0.699 | 50.348 | 127.855 |
| 150-375-19-30-A | 0.011 | 0.303 | 0.683 | 26.600 | 59.961 |
| 151-375-19-30-A | 0.012 | 0.361 | 0.783 | 28.887 | 62.713 |
| 152-375-19-30-A | 0.019 | 0.278 | 0.595 | 14.681 | 31.435 |
| 153-375-19-30-T | 0.017 | 0.348 | 0.722 | 20.650 | 42.805 |

| | | | | | |
|-----------------|-------|-------|-------|--------|--------|
| 154-375-19-30-T | 0.012 | 0.272 | 0.513 | 22.887 | 43.242 |
| 155-375-19-30-T | 0.020 | 0.275 | 0.594 | 14.000 | 30.292 |
| 156-375-19-30-M | 0.009 | 0.272 | 0.651 | 28.965 | 69.317 |

Table 22. Test ductility index values for monotonic tests

| Specimen Type | D_y (in.) | $D_{\text{postpeak80\%}}$ (in.) | D_u (in.) | $D_{\text{postpeak80\%}} / D_y$ | D_u / D_y |
|---------------|-------------|---------------------------------|-------------|---------------------------------|-------------|
| 54-10-13 | 0.001 | 0.124 | 0.445 | 89.809 | 321.034 |
| 54-10-19 | 0.021 | 0.225 | 0.620 | 10.617 | 29.221 |
| 54-10-30 | 0.006 | 0.355 | 0.692 | 58.258 | 113.520 |
| 54-8-13 | 0.001 | 0.164 | 0.595 | 125.495 | 455.330 |
| 54-8-19 | 0.008 | 0.241 | 0.557 | 31.782 | 73.535 |
| 54-8-30 | 0.010 | 0.576 | 0.914 | 57.025 | 90.530 |
| 97-10-13 | 0.002 | 0.077 | 0.344 | 37.654 | 168.042 |
| 97-10-19 | 0.005 | 0.210 | 0.622 | 45.793 | 135.626 |
| 97-10-30 | 0.007 | 0.301 | 0.685 | 45.111 | 102.853 |
| 97-12-30 | 0.002 | 0.278 | 0.630 | 164.018 | 371.362 |
| 97-8-30 | 0.002 | 0.275 | 0.608 | 162.177 | 358.353 |
| 97-10-13-97 | 0.003 | 0.248 | 0.648 | 73.758 | 192.285 |
| 97-10-19-97 | 0.035 | 0.364 | 0.622 | 10.393 | 17.771 |
| 97-10-30-97 | 0.051 | 0.472 | 0.791 | 9.337 | 15.639 |
| 97-12-30-97 | 0.035 | 0.494 | 0.899 | 14.280 | 26.014 |
| 97-24-30-97 | 0.005 | 0.526 | 1.000 | 98.085 | 186.313 |
| 118-24-30-118 | 0.007 | 0.562 | 1.113 | 74.955 | 148.466 |
| 188-12-30 | 0.003 | 0.202 | 0.710 | 57.949 | 203.243 |
| 188-24-30 | 0.005 | 0.275 | 0.699 | 50.348 | 127.855 |
| 375-19-30 | 0.009 | 0.272 | 0.651 | 28.965 | 69.317 |

Table 23. Test ductility index values for buckling away cyclic tests

| Specimen Type | D_y (in.) | $D_{\text{postpeak80\%}}$ (in.) | D_u (in.) | $D_{\text{postpeak80\%}}/D_y$ | D_u/D_y |
|---------------|-------------|---------------------------------|-------------|-------------------------------|-----------|
| 54-10-13 | 0.011 | 0.155 | 0.582 | 13.475 | 50.659 |
| 54-10-19 | 0.005 | 0.211 | 0.462 | 45.361 | 99.357 |
| 54-10-30 | 0.013 | 0.380 | 0.564 | 29.966 | 44.451 |
| 54-8-13 | 0.007 | 0.155 | 0.451 | 22.812 | 66.136 |
| 54-8-19 | 0.011 | 0.216 | 0.376 | 19.842 | 34.585 |
| 54-8-30 | 0.013 | 0.405 | 0.598 | 31.892 | 47.034 |
| 97-10-13 | 0.004 | 0.113 | 0.498 | 29.866 | 131.837 |
| 97-10-19 | 0.005 | 0.186 | 0.478 | 37.955 | 97.286 |
| 97-10-30 | 0.009 | 0.289 | 0.518 | 31.928 | 57.154 |
| 97-12-30 | 0.004 | 0.265 | 0.486 | 60.039 | 110.118 |
| 97-8-30 | 0.003 | 0.266 | 0.446 | 77.393 | 129.451 |
| 97-10-13-97 | 0.006 | 0.270 | 0.692 | 47.540 | 121.738 |
| 97-10-19-97 | 0.038 | 0.439 | 0.745 | 11.687 | 19.850 |
| 97-10-30-97 | 0.029 | 0.483 | 0.861 | 16.756 | 29.884 |
| 97-12-30-97 | 0.031 | 0.529 | 1.030 | 17.333 | 33.738 |
| 97-24-30-97 | 0.005 | 0.544 | 1.084 | 101.037 | 201.343 |
| 118-24-30-118 | 0.007 | 0.532 | 1.059 | 79.936 | 159.159 |
| 188-12-30 | 0.006 | 0.242 | 0.535 | 40.611 | 89.882 |
| 188-24-30 | 0.004 | 0.381 | 0.854 | 92.198 | 206.656 |
| 375-19-30 | 0.014 | 0.314 | 0.687 | 21.997 | 48.150 |

Table 24. Test ductility index values for buckling towards cyclic tests

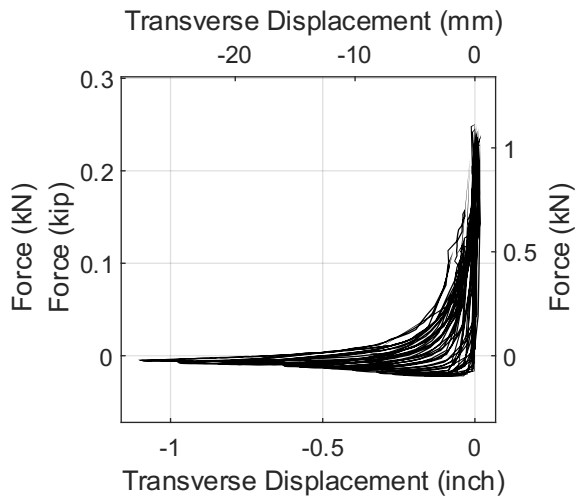
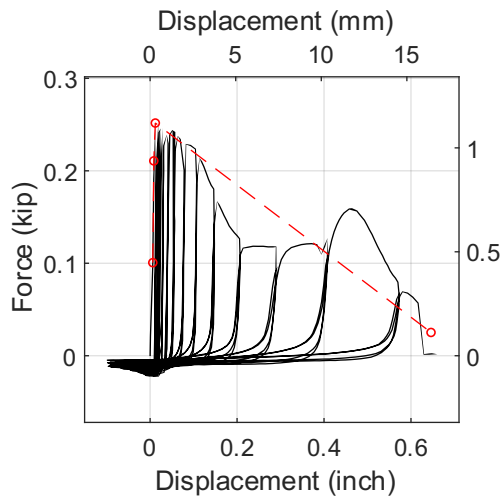
| Specimen Type | D_y (in.) | $D_{\text{postpeak80\%}}$ (in.) | D_u (in.) | $D_{\text{postpeak80\%}}/D_y$ | D_u/D_y |
|---------------|-------------|---------------------------------|-------------|-------------------------------|-----------|
| 54-10-13 | 0.005 | 0.150 | 0.493 | 32.444 | 106.815 |
| 54-10-19 | 0.010 | 0.197 | 0.446 | 19.740 | 44.744 |
| 54-10-30 | 0.014 | 0.537 | 0.849 | 37.058 | 58.622 |
| 54-8-13 | 0.004 | 0.138 | 0.584 | 32.669 | 138.119 |
| 54-8-19 | 0.003 | 0.193 | 0.529 | 73.444 | 201.251 |
| 54-8-30 | 0.048 | 0.707 | 0.950 | 14.611 | 19.629 |
| 97-10-13 | 0.004 | 0.106 | 0.456 | 24.342 | 105.129 |
| 97-10-19 | 0.006 | 0.246 | 0.673 | 41.928 | 114.811 |
| 97-10-30 | 0.007 | 0.301 | 0.569 | 42.323 | 79.915 |
| 97-12-30 | 0.006 | 0.314 | 0.618 | 55.818 | 109.830 |
| 97-8-30 | 0.008 | 0.292 | 0.595 | 35.481 | 72.198 |
| 97-10-13-97 | 0.018 | 0.272 | 0.701 | 15.231 | 39.248 |
| 97-10-19-97 | 0.022 | 0.417 | 0.754 | 19.056 | 34.462 |
| 97-10-30-97 | 0.038 | 0.498 | 0.966 | 13.004 | 25.258 |
| 97-12-30-97 | 0.038 | 0.540 | 1.021 | 14.171 | 26.798 |
| 97-24-30-97 | 0.006 | 0.519 | 1.068 | 89.761 | 184.493 |
| 118-24-30-118 | 0.006 | 0.553 | 1.096 | 91.871 | 182.053 |
| 188-12-30 | 0.013 | 0.280 | 0.654 | 20.949 | 49.032 |
| 188-24-30 | 0.005 | 0.323 | 0.727 | 60.381 | 135.638 |
| 375-19-30 | 0.016 | 0.298 | 0.610 | 18.500 | 37.834 |

Table 25. Test ductility index values for tension only cyclic tests

| Specimen Type | D_y (in.) | $D_{\text{postpeak80\%}}$ (in.) | D_u (in.) | $D_{\text{postpeak80\%}}/D_y$ | D_u/D_y |
|---------------|-------------|---------------------------------|-------------|-------------------------------|-----------|
| 97-10-30 | 0.009 | 0.303 | 0.606 | 35.392 | 70.750 |

Appendix 3: Test Detail Report

Summaries of test details including force-displacement curve, test data characterization result plot, and deformation and failure development at different force levels for each conducted test in the order of test ID are provided in this appendix. Note that the deformation and failure development images are the ones most close to the corresponding force levels.



Test 1-@Peak Force-Front View



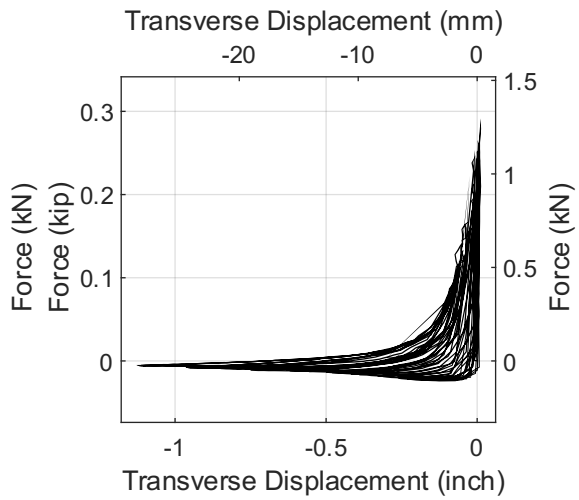
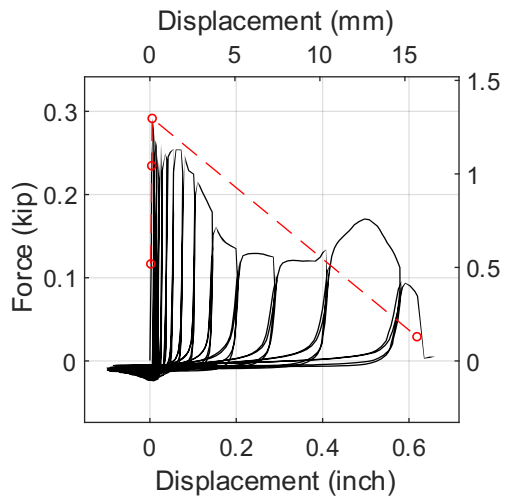
Test 1-@Peak Force-Side View



Test 1-Post Peak @80% Peak Force



Test 1-After Test



Test 2-@Peak Force-Front View



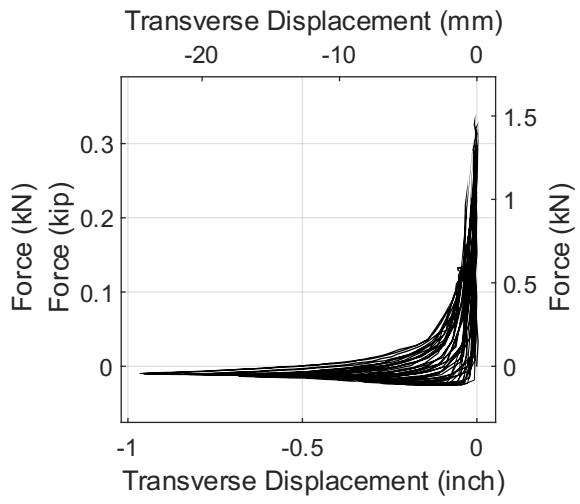
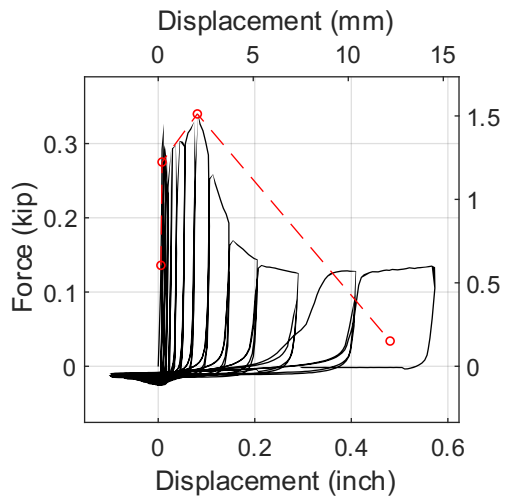
Test 2-@Peak Force-Side View



Test 2-Post Peak @80% Peak Force



Test 2-After Test



Test 3-@Peak Force-Front View



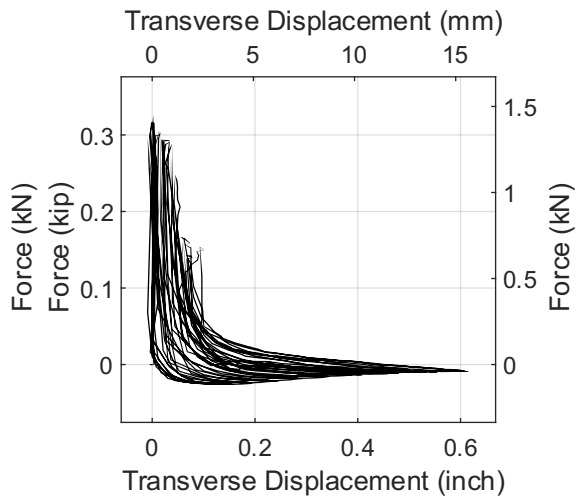
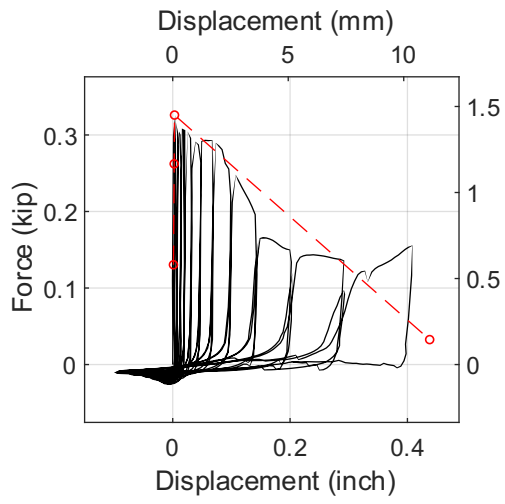
Test 3-@Peak Force-Side View



Test 3-Post Peak @80% Peak Force



Test 3-After Test



Test 4-@Peak Force-Front View



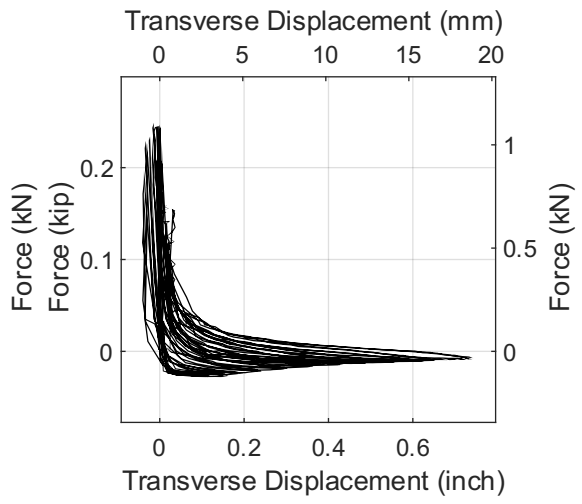
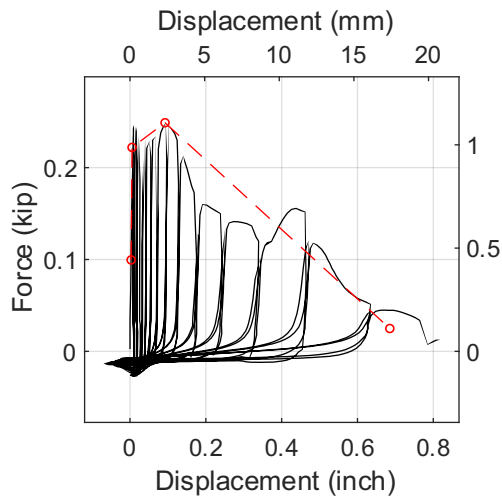
Test 4-@Peak Force-Side View



Test 4-Post Peak @80% Peak Force



Test 4-After Test



Test 5-@Peak Force-Front View



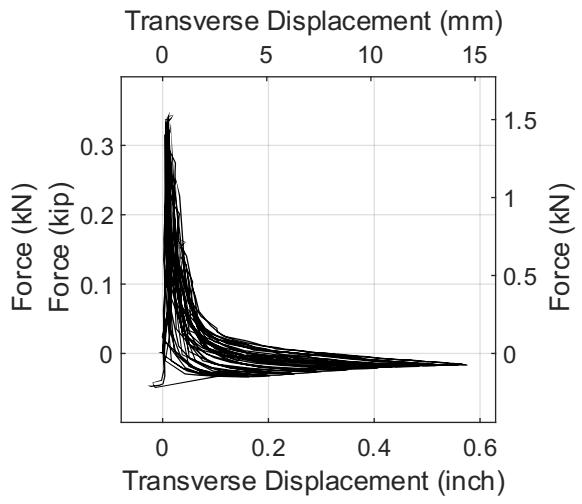
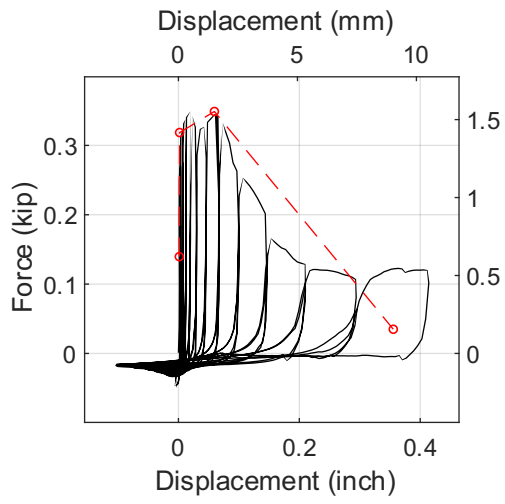
Test 5-@Peak Force-Side View



Test 5-Post Peak @80% Peak Force



Test 5-After Test



Test 6-@Peak Force-Front View



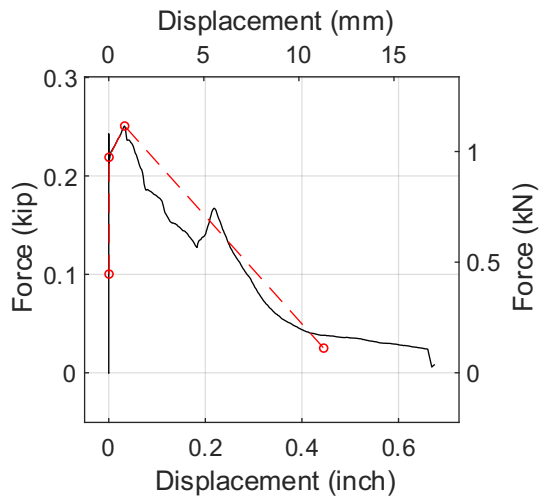
Test 6-@Peak Force-Side View



Test 6-Post Peak @80% Peak Force



Test 6-After Test



Test 7-@Peak Force-Front View



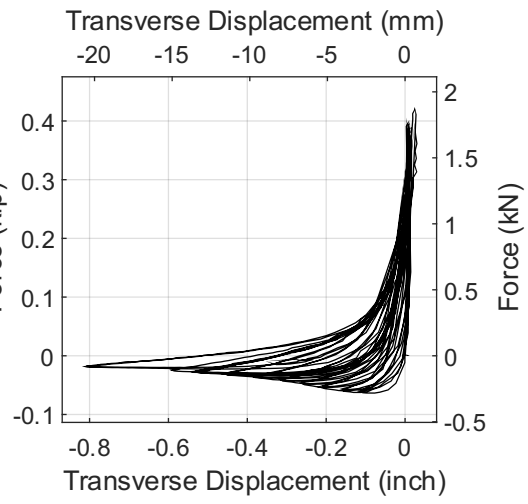
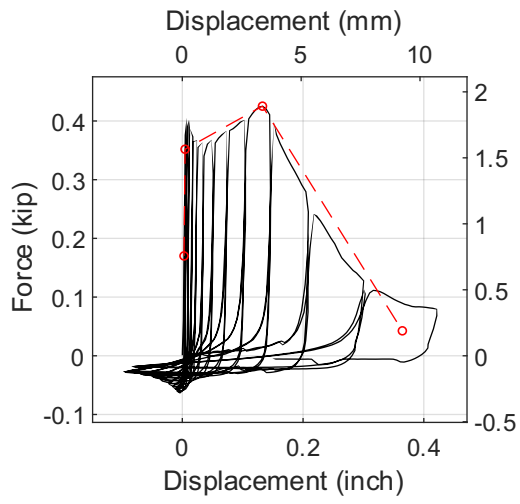
Test 7-@Peak Force-Side View



Test 7-Post Peak @80% Peak Force



Test 7-After Test



Test 8-@Peak Force-Front View



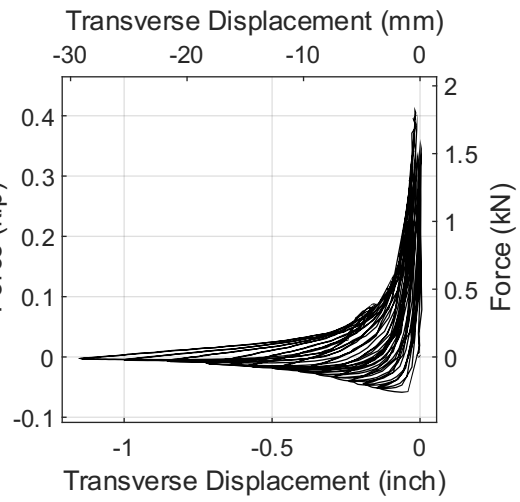
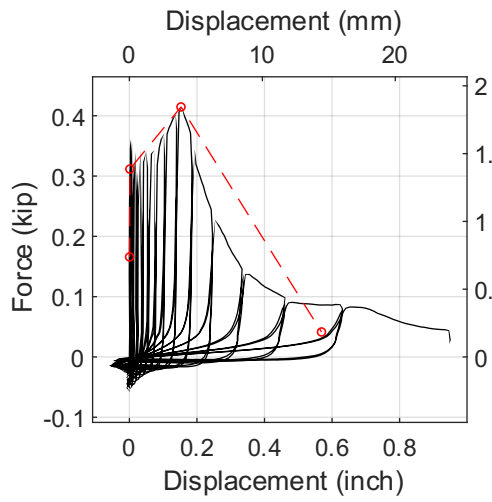
Test 8-@Peak Force-Side View



Test 8-Post Peak @80% Peak Force



Test 8-After Test



Test 9-@Peak Force-Front View



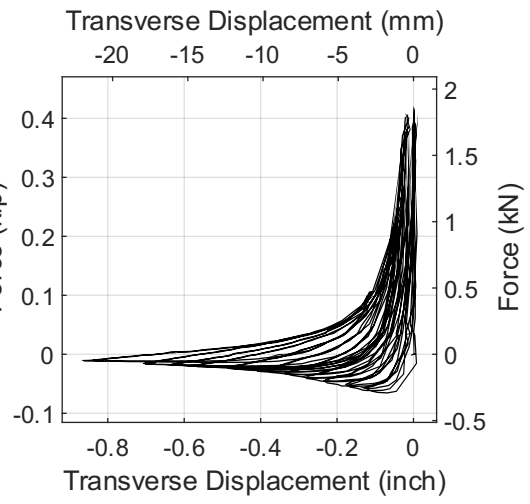
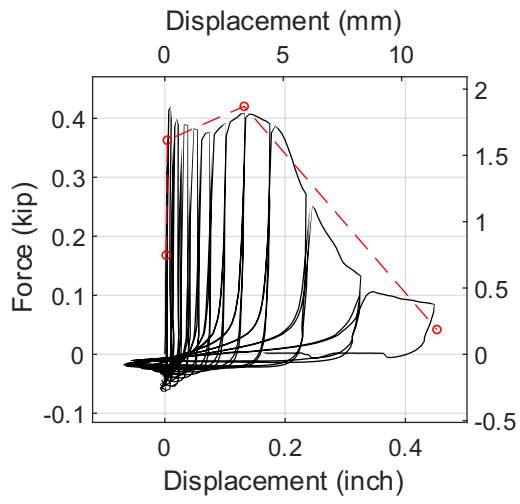
Test 9-@Peak Force-Side View



Test 9-Post Peak @80% Peak Force



Test 9-After Test



Test 10-@Peak Force-Front View



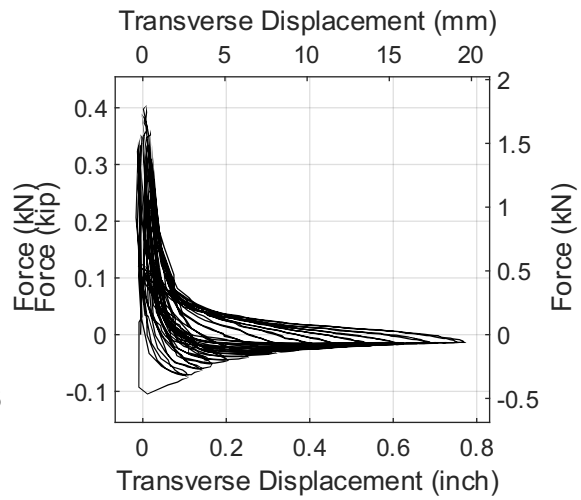
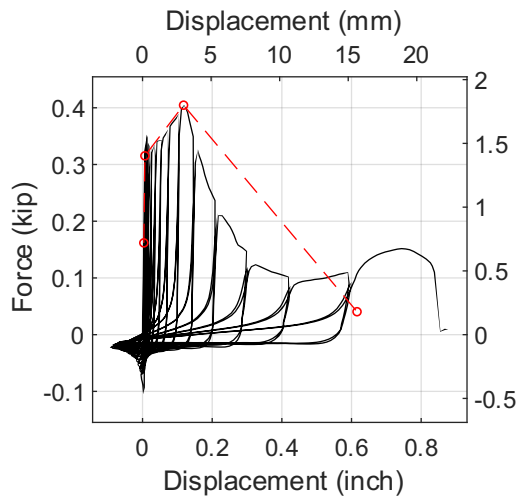
Test 10-@Peak Force-Side View



Test 10-Post Peak @80% Peak Force



Test 10-After Test



Test 11-@Peak Force-Front View



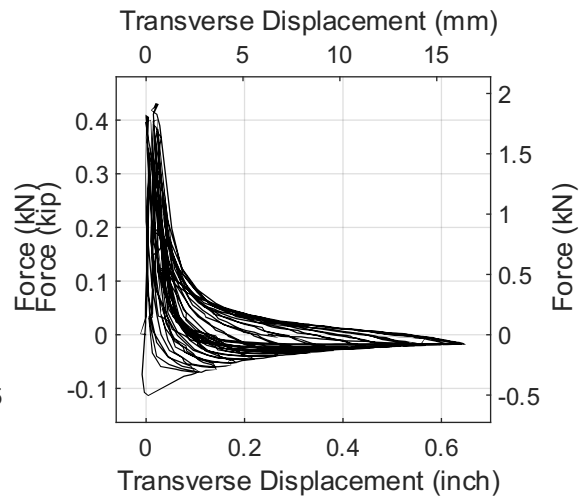
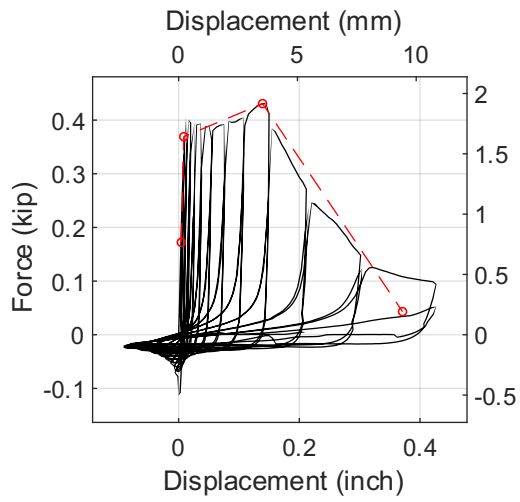
Test 11-@Peak Force-Side View



Test 11-Post Peak @80% Peak Force



Test 11-After Test



Test 12-@Peak Force-Front View



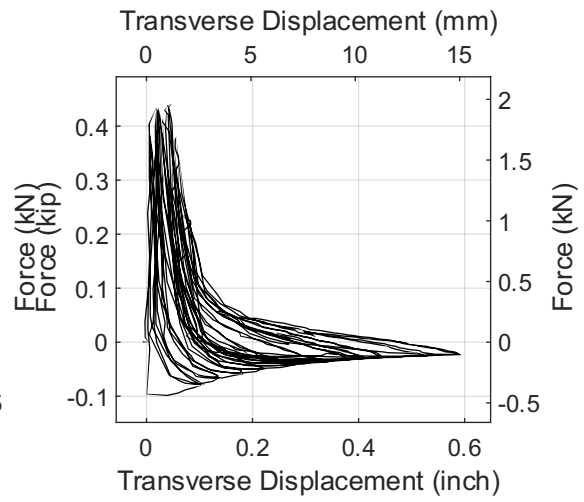
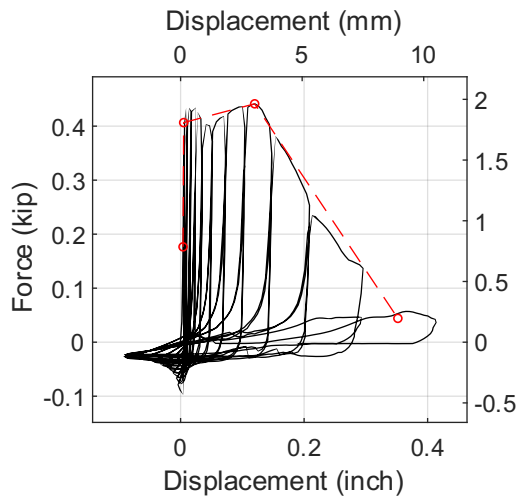
Test 12-@Peak Force-Side View



Test 12-Post Peak @80% Peak Force



Test 12-After Test



Test 13-@Peak Force-Front View



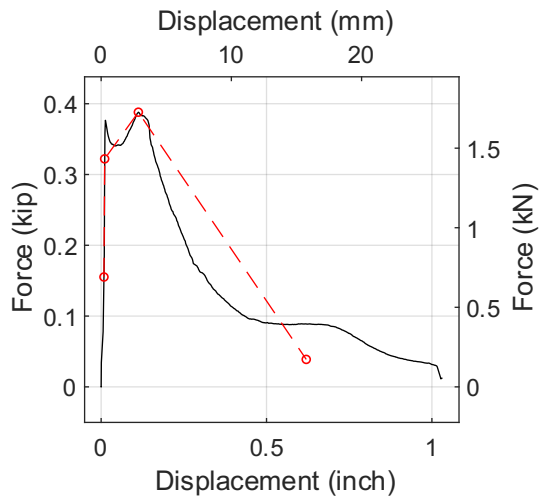
Test 13-@Peak Force-Side View



Test 13-Post Peak @80% Peak Force



Test 13-After Test



Test 14-@Peak Force-Front View



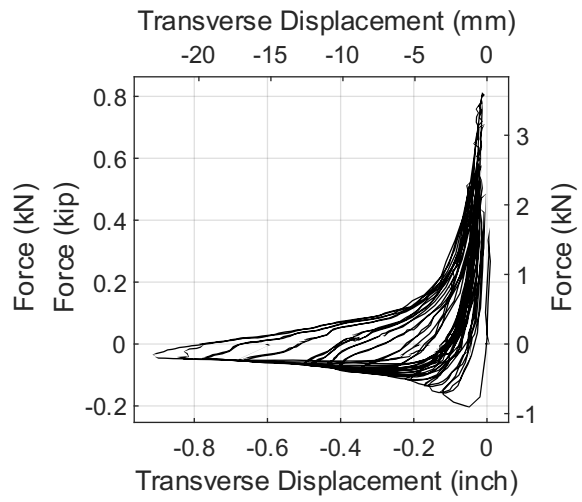
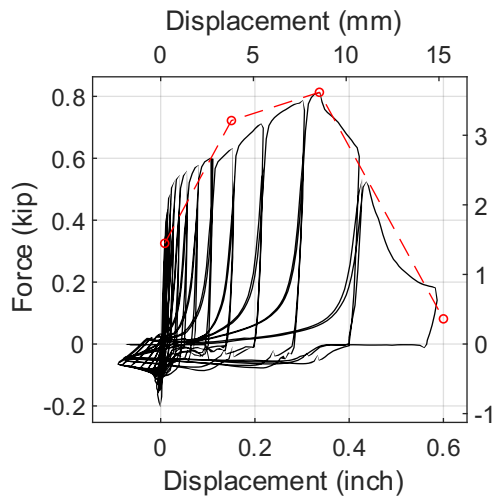
Test 14-@Peak Force-Side View



Test 14-Post Peak @80% Peak Force



Test 14-After Test



Test 15-@Peak Force-Front View



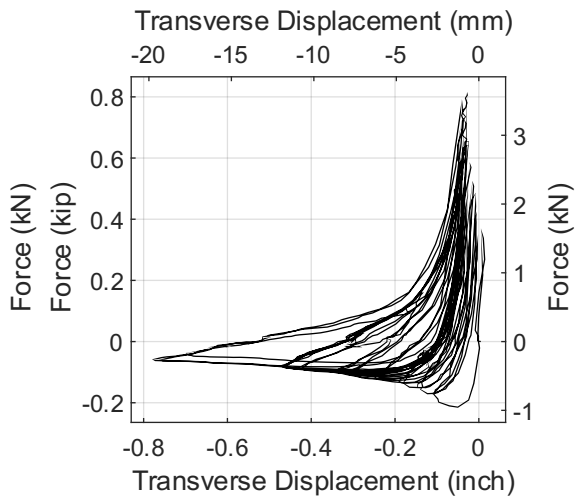
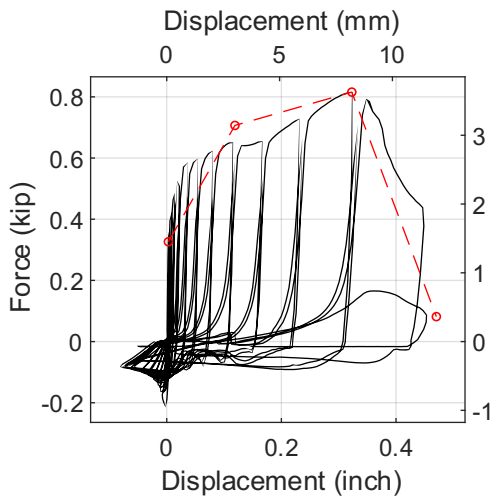
Test 15-@Peak Force-Side View



Test 15-Post Peak @80% Peak Force



Test 15-After Test



Test 16-@Peak Force-Front View



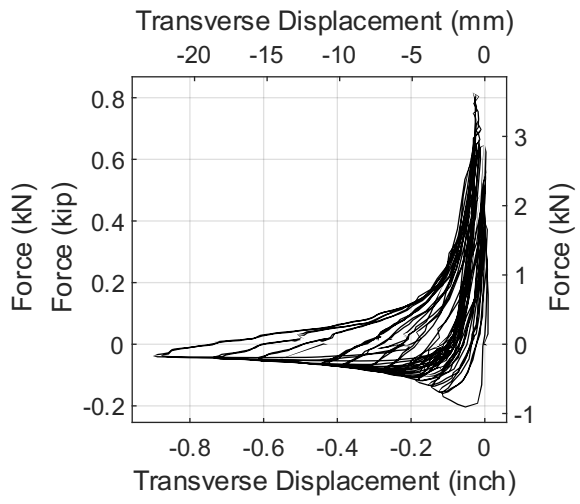
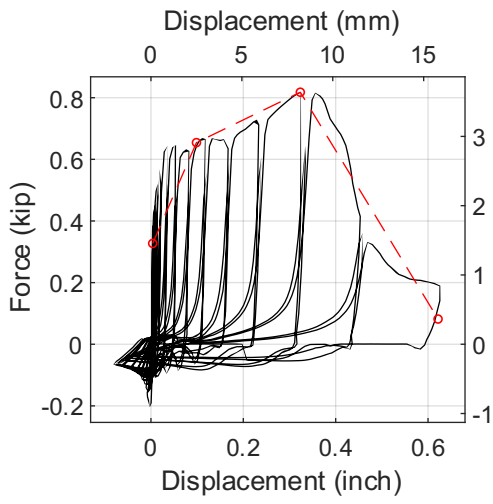
Test 16-@Peak Force-Side View



Test 16-Post Peak @80% Peak Force



Test 16-After Test



Test 17-@Peak Force-Front View



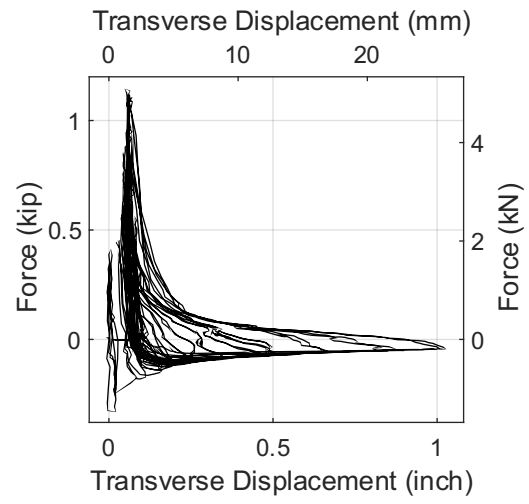
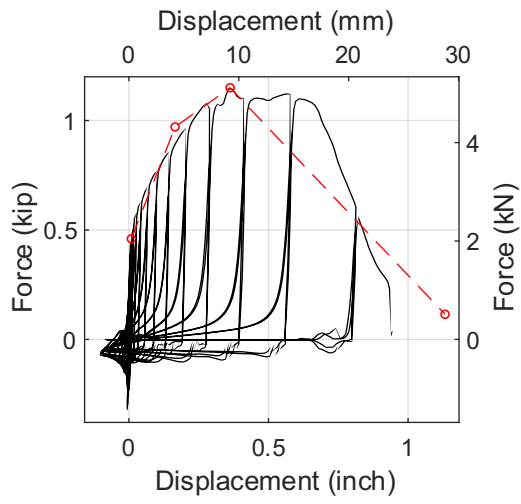
Test 17-@Peak Force-Side View



Test 17-Post Peak @80% Peak Force



Test 17-After Test



Test 18-@Peak Force-Front View



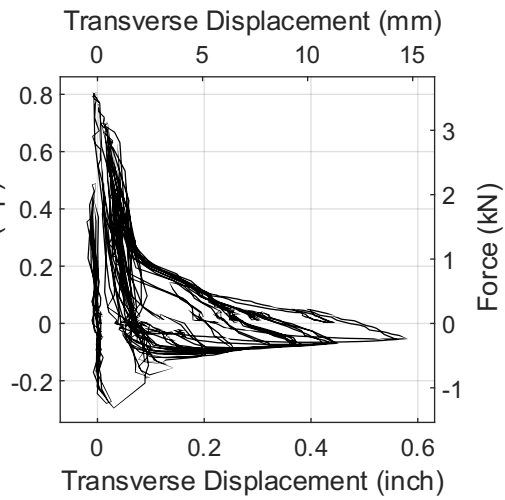
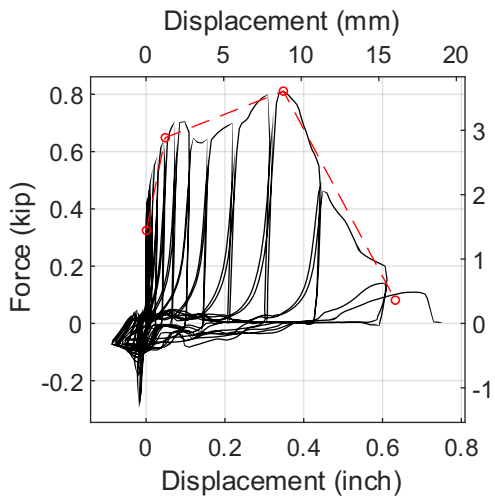
Test 18-@Peak Force-Side View



Test 18-Post Peak @80% Peak Force



Test 18-After Test



Test 19-@Peak Force-Front View



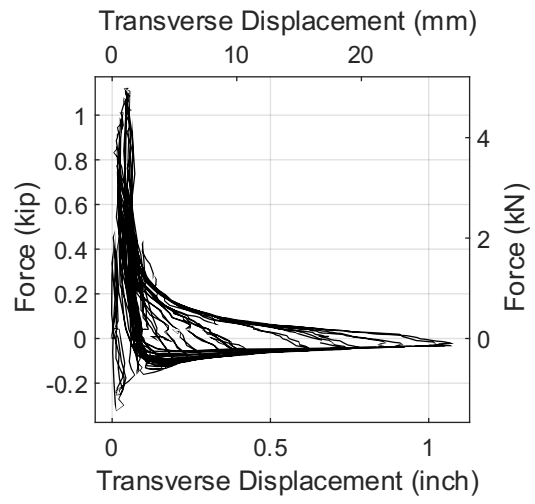
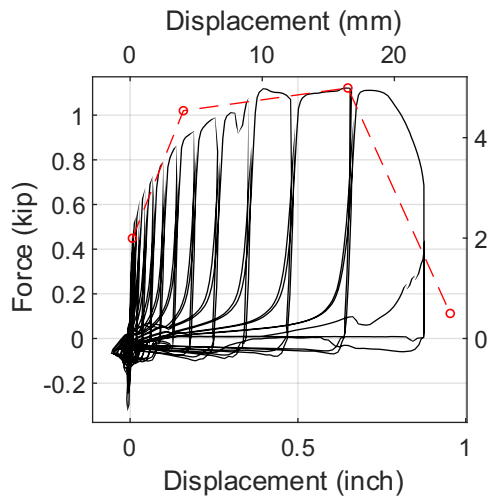
Test 19-@Peak Force-Side View



Test 19-Post Peak @80% Peak Force



Test 19-After Test



Test 20-@Peak Force-Front View



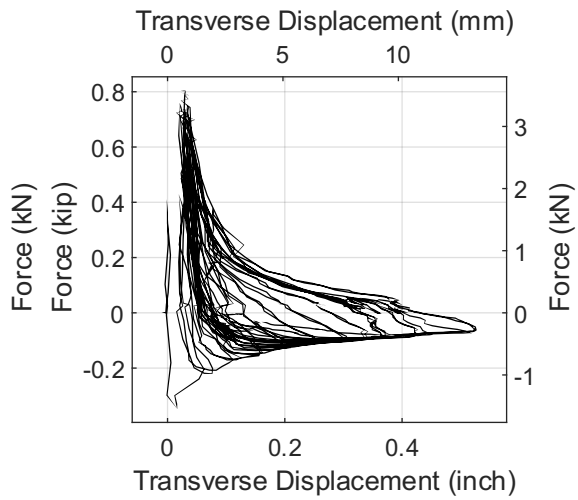
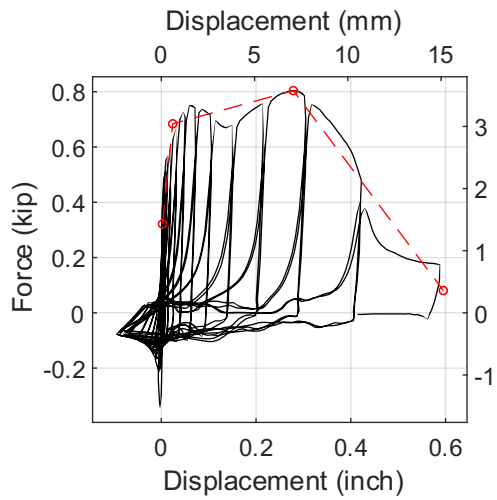
Test 20-@Peak Force-Side View



Test 20-Post Peak @80% Peak Force



Test 20-After Test



Test 21-@Peak Force-Front View



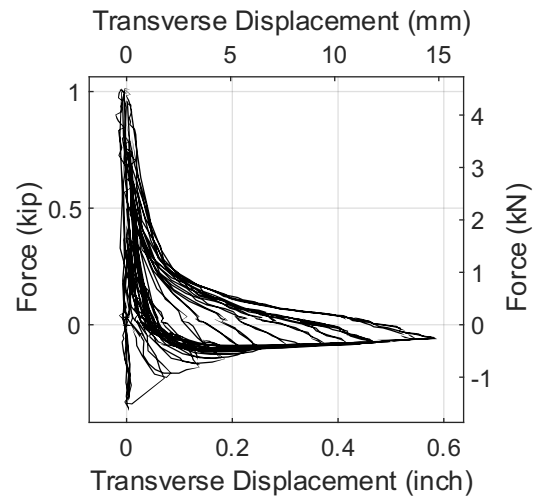
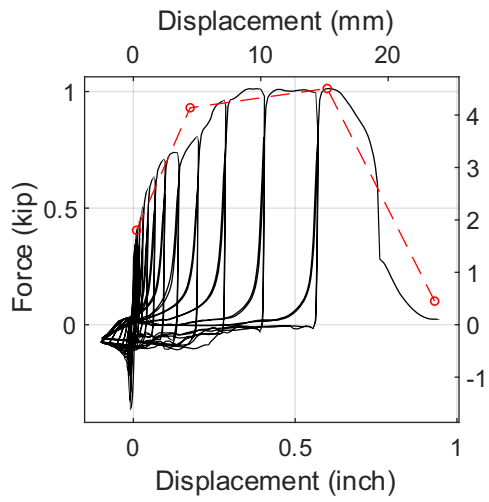
Test 21-@Peak Force-Side View



Test 21-Post Peak @80% Peak Force



Test 21-After Test



Test 22-@Peak Force-Front View



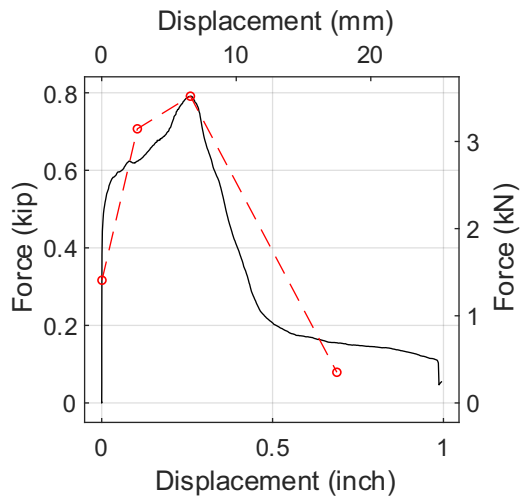
Test 22-@Peak Force-Side View



Test 22-Post Peak @80% Peak Force



Test 22-After Test



Test 23-@Peak Force-Front View



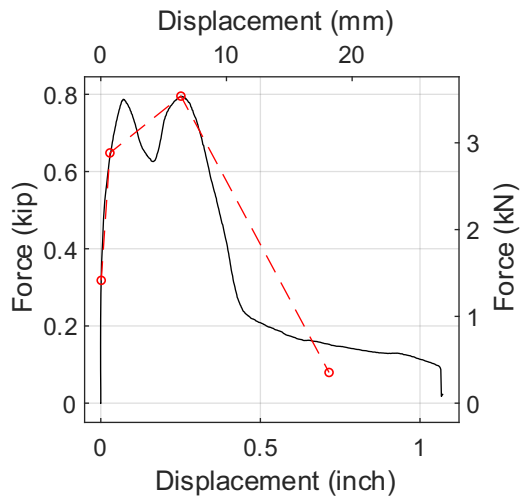
Test 23-@Peak Force-Side View



Test 23-Post Peak @80% Peak Force



Test 23-After Test



Test 24-@Peak Force-Front View



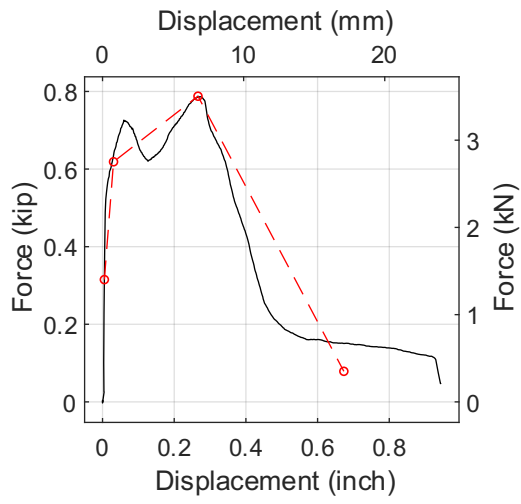
Test 24-@Peak Force-Side View



Test 24-Post Peak @80% Peak Force



Test 24-After Test



Test 25-@Peak Force-Front View



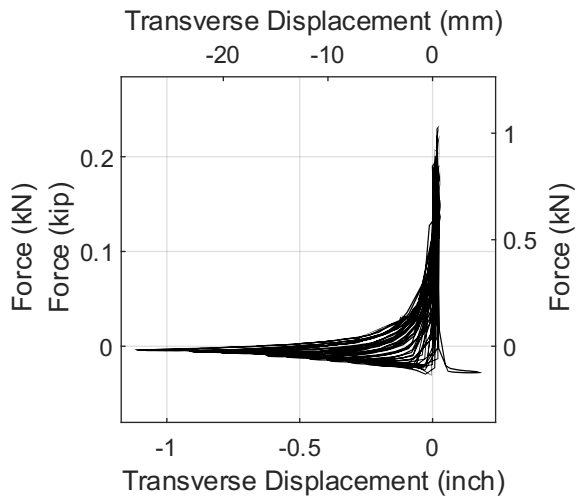
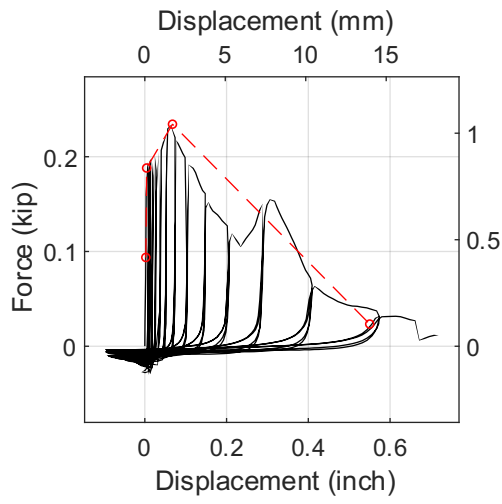
Test 25-@Peak Force-Side View



Test 25-Post Peak @80% Peak Force



Test 25-After Test



Test 26-@Peak Force-Front View



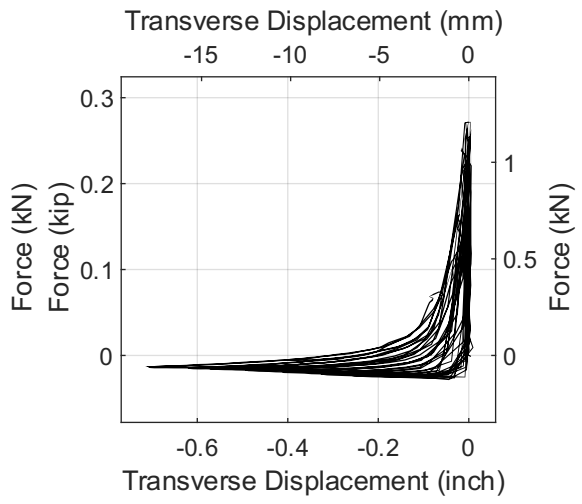
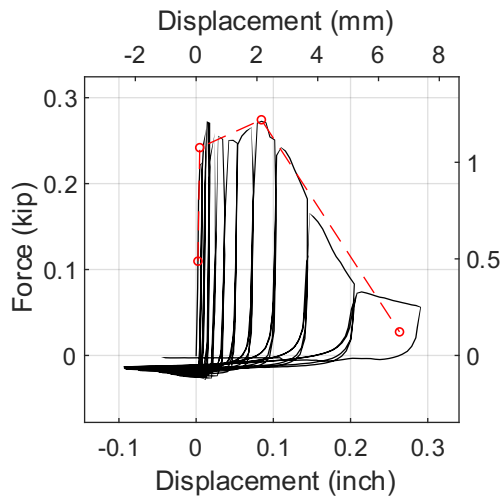
Test 26-@Peak Force-Side View



Test 26-Post Peak @80% Peak Force



Test 26-After Test



Test 27-@Peak Force-Front View



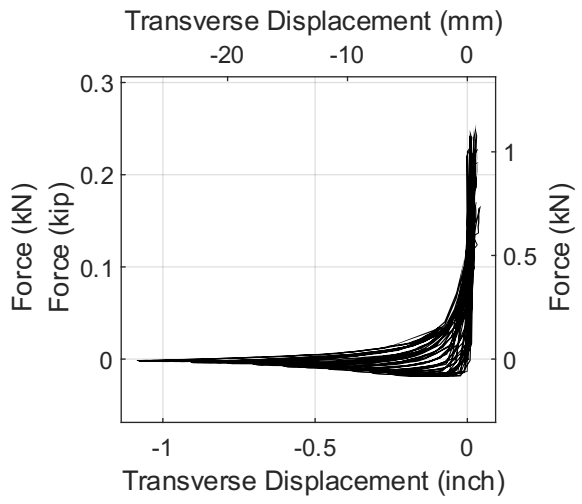
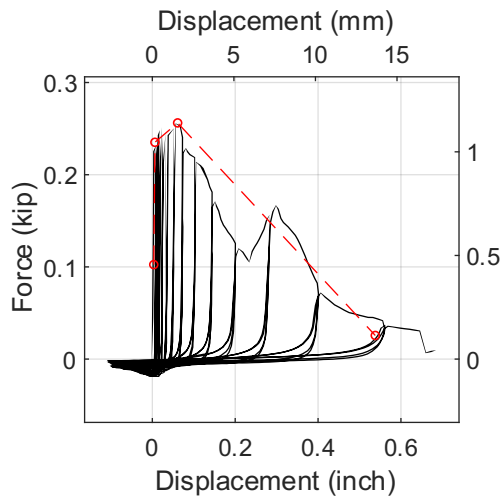
Test 27-@Peak Force-Side View



Test 27-Post Peak @80% Peak Force



Test 27-After Test



Test 28-@Peak Force-Front View



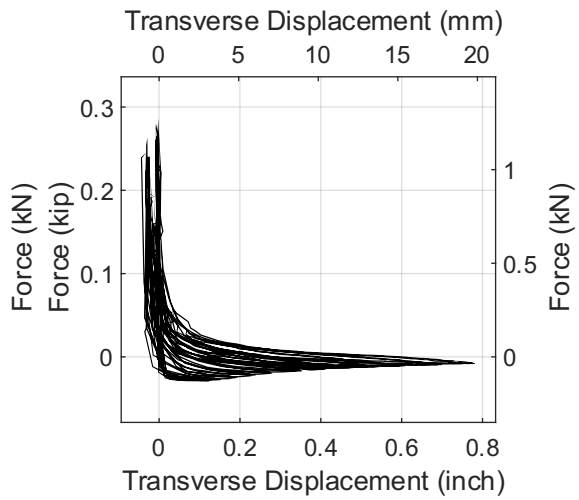
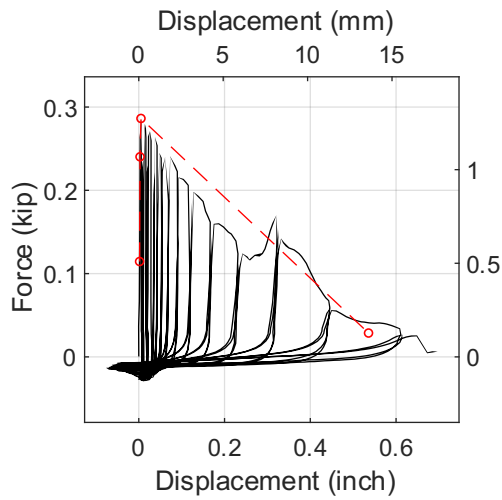
Test 28-@Peak Force-Side View



Test 28-Post Peak @80% Peak Force



Test 28-After Test



Test 29-@Peak Force-Front View



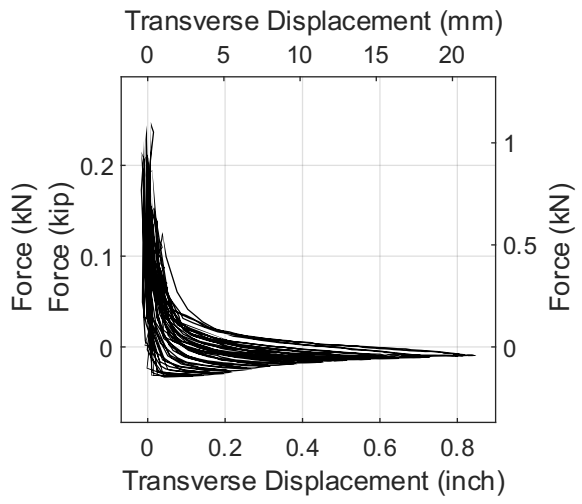
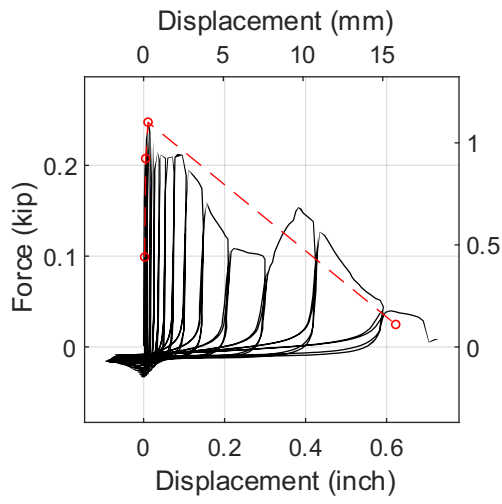
Test 29-@Peak Force-Side View



Test 29-Post Peak @80% Peak Force



Test 29-After Test



Test 30-@Peak Force-Front View



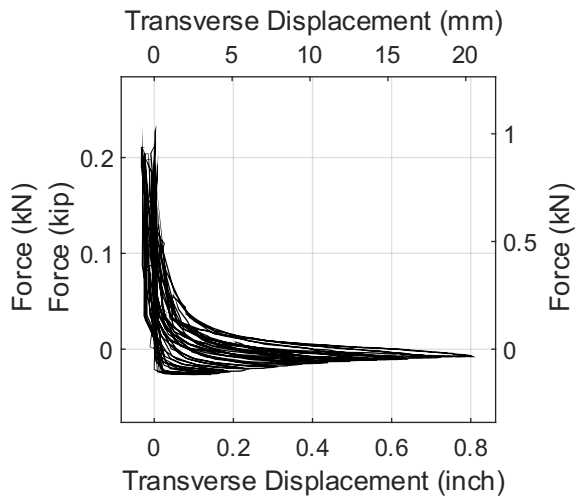
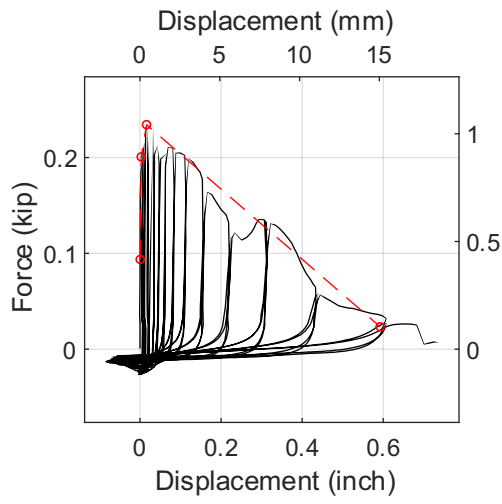
Test 30-@Peak Force-Side View



Test 30-Post Peak @80% Peak Force



Test 30-After Test



Test 31-@Peak Force-Front View



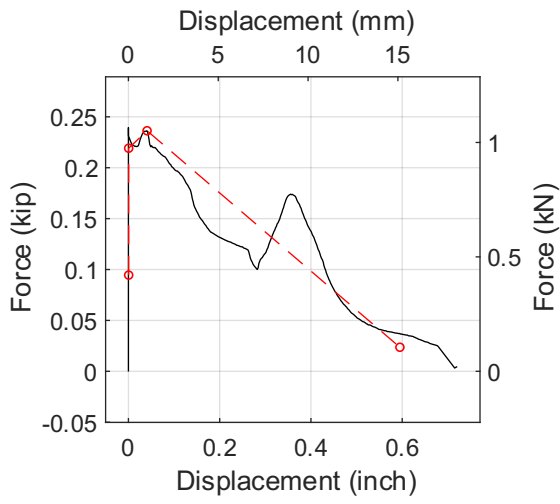
Test 31-@Peak Force-Side View



Test 31-Post Peak @80% Peak Force



Test 31-After Test



Test 32-@Peak Force-Front View



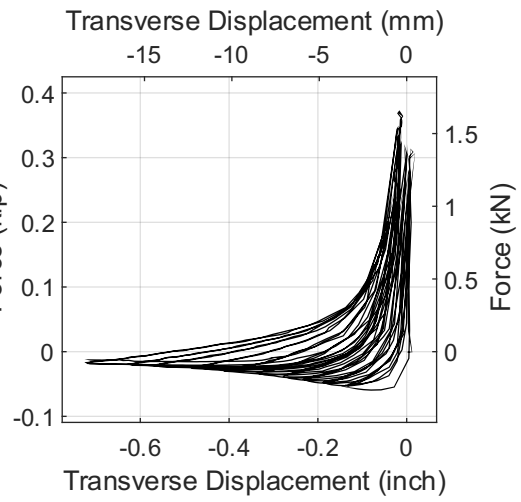
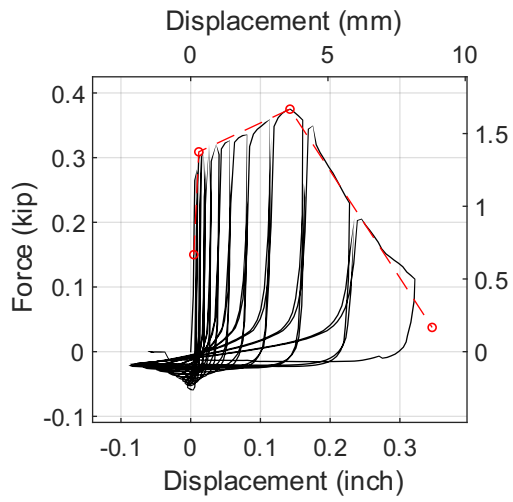
Test 32-@Peak Force-Side View



Test 32-Post Peak @80% Peak Force



Test 32-After Test



Test 33-@Peak Force-Front View



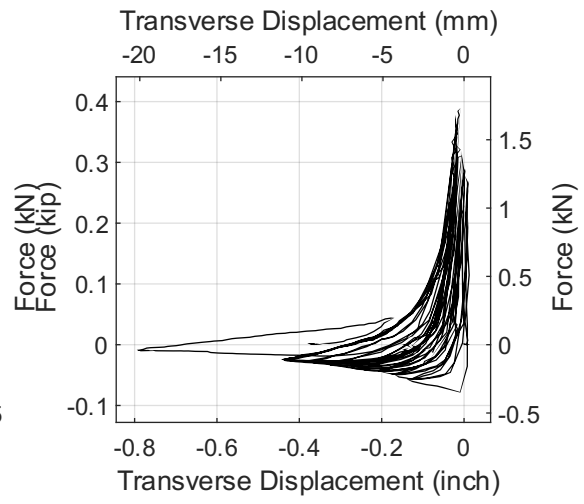
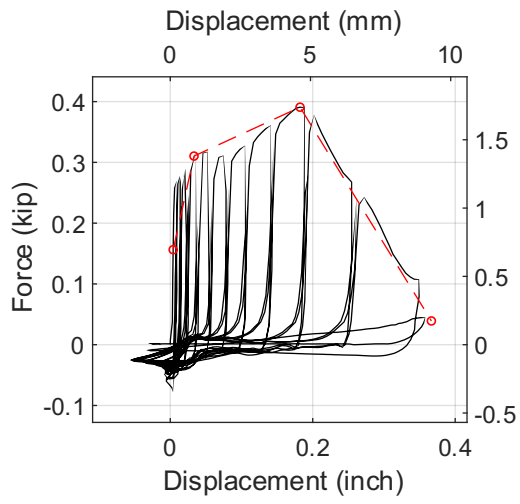
Test 33-@Peak Force-Side View



Test 33-Post Peak @80% Peak Force



Test 33-After Test



Test 34-@Peak Force-Front View



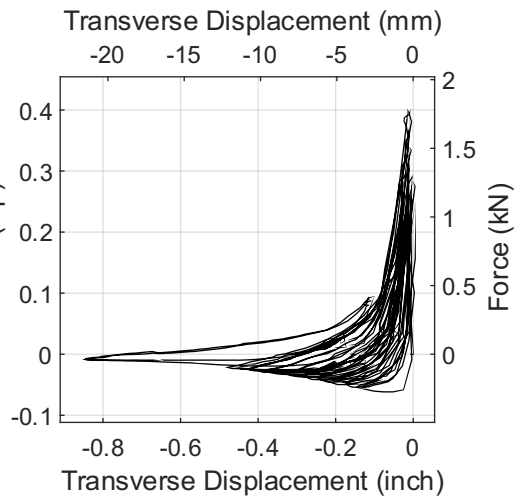
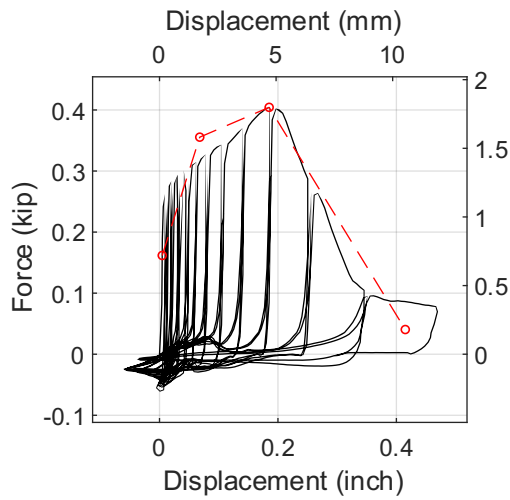
Test 34-@Peak Force-Side View



Test 34-Post Peak @80% Peak Force



Test 34-After Test



Test 35-@Peak Force-Front View



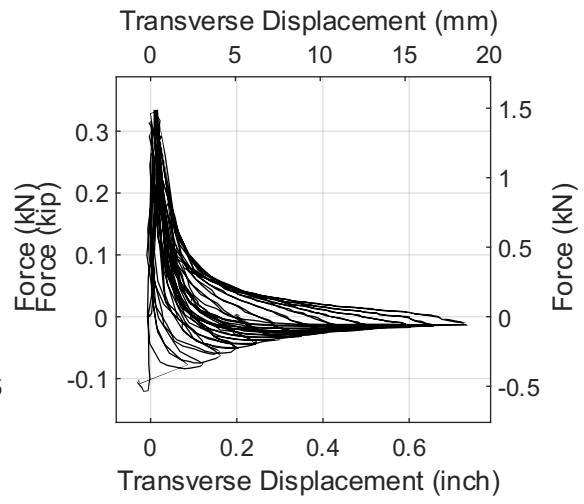
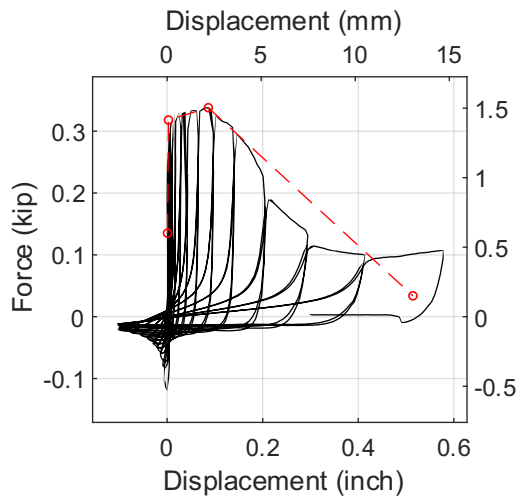
Test 35-@Peak Force-Side View



Test 35-Post Peak @80% Peak Force



Test 35-After Test



Test 36-@Peak Force-Front View



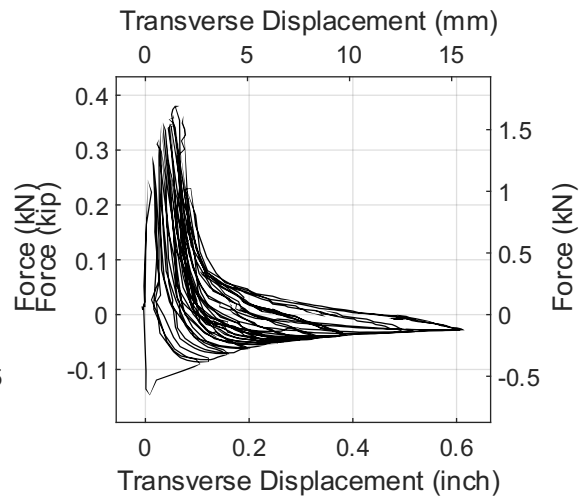
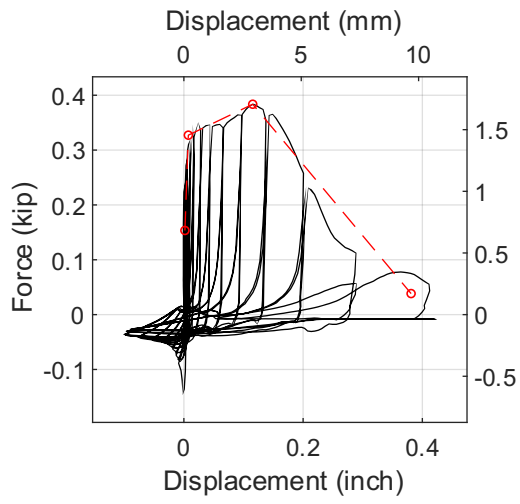
Test 36-@Peak Force-Side View



Test 36-Post Peak @80% Peak Force



Test 36-After Test



Test 37-@Peak Force-Front View



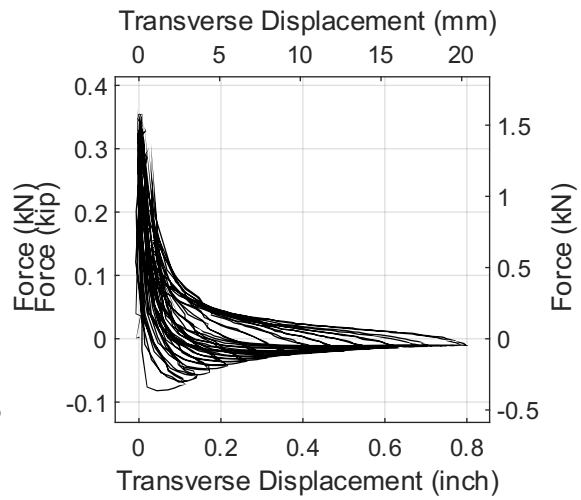
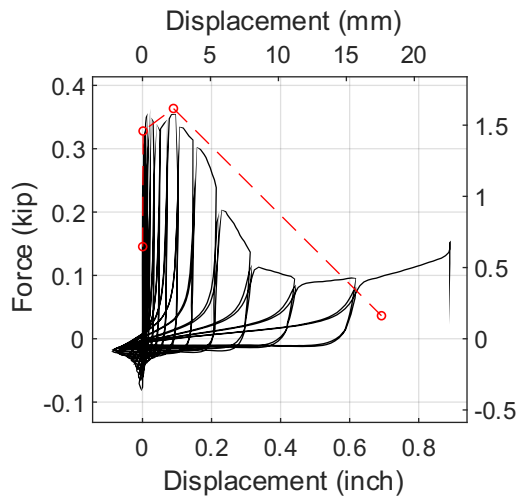
Test 37-@Peak Force-Side View



Test 37-Post Peak @80% Peak Force



Test 37-After Test



Test 38-@Peak Force-Front View



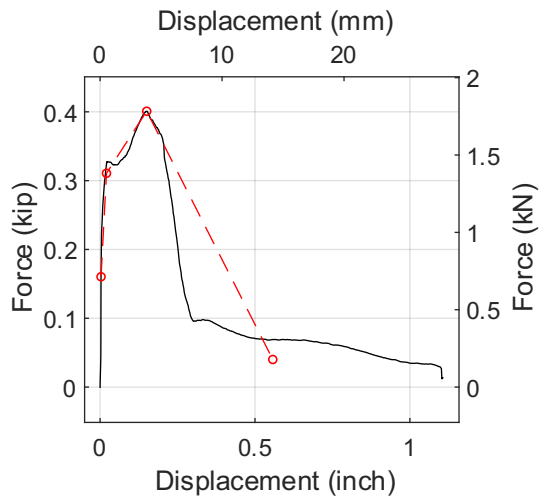
Test 38-@Peak Force-Side View



Test 38-Post Peak @80% Peak Force



Test 38-After Test



Test 39-@Peak Force-Front View



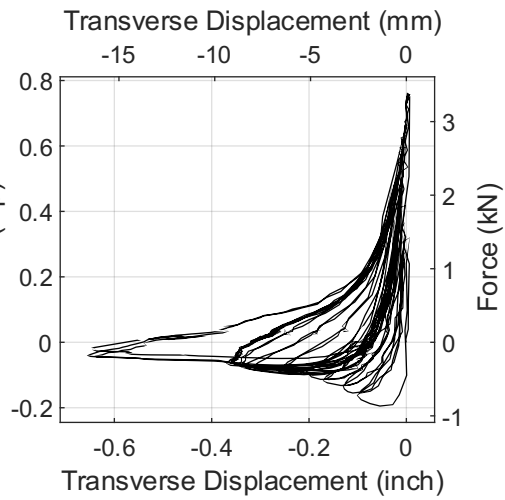
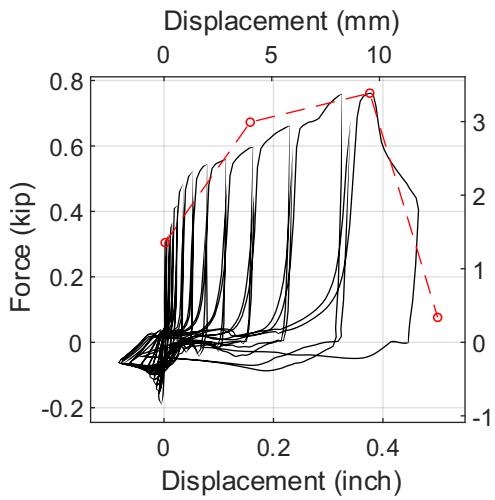
Test 39-@Peak Force-Side View



Test 39-Post Peak @80% Peak Force



Test 39-After Test



Test 40-@Peak Force-Front View



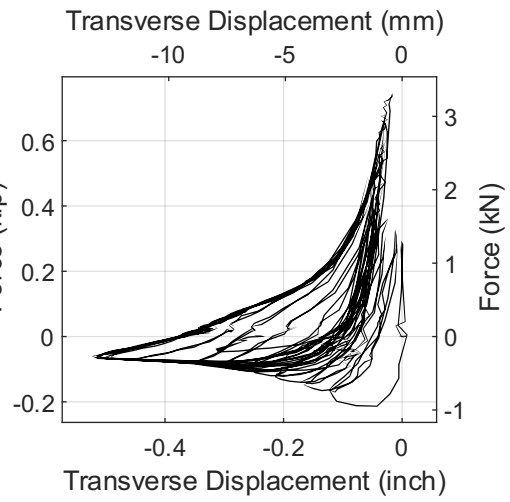
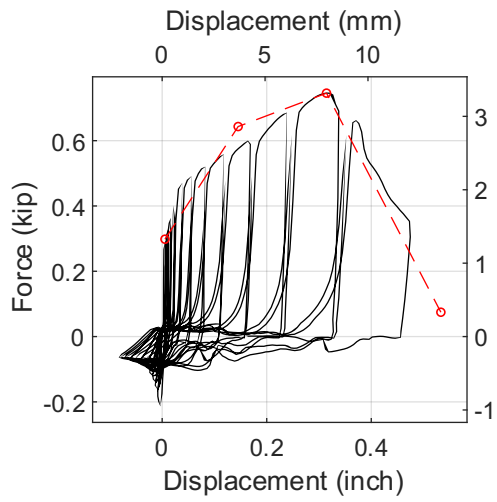
Test 40-@Peak Force-Side View



Test 40-Post Peak @80% Peak Force



Test 40-After Test



Test 41-@Peak Force-Front View



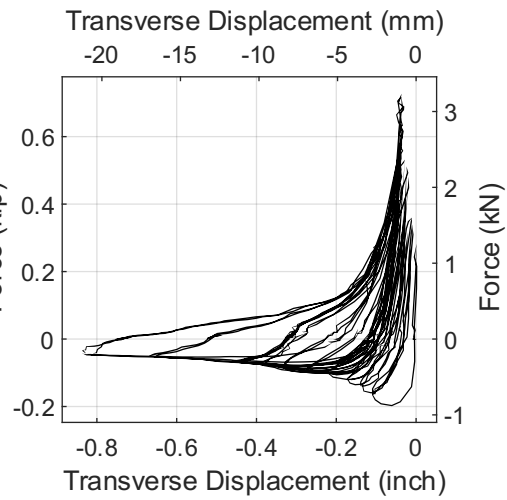
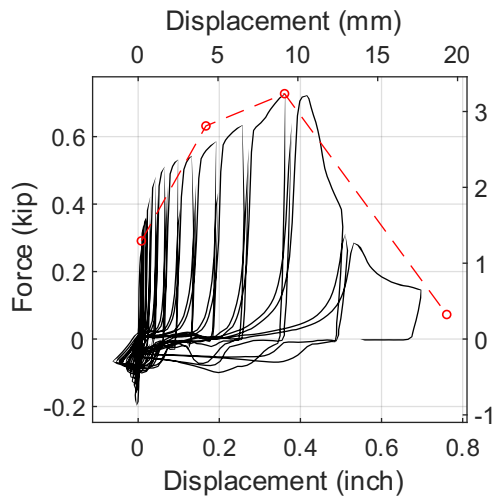
Test 41-@Peak Force-Side View



Test 41-Post Peak @80% Peak Force



Test 41-After Test



Test 42-@Peak Force-Front View



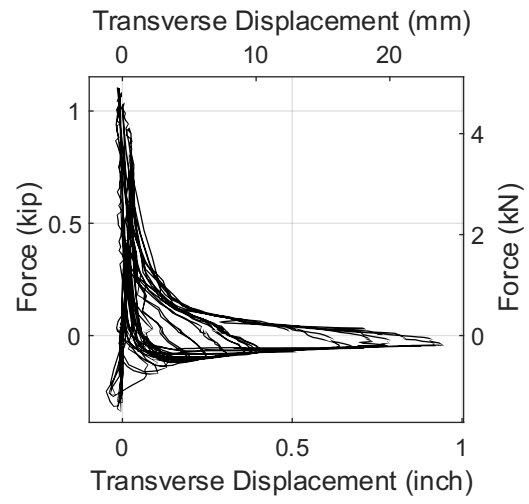
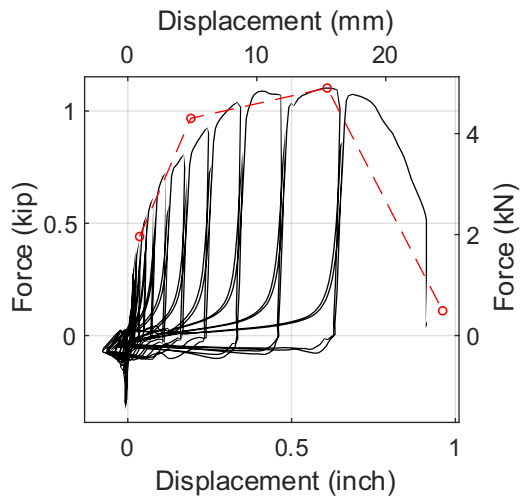
Test 42-@Peak Force-Side View



Test 42-Post Peak @80% Peak Force



Test 42-After Test



Test 43-@Peak Force-Front View



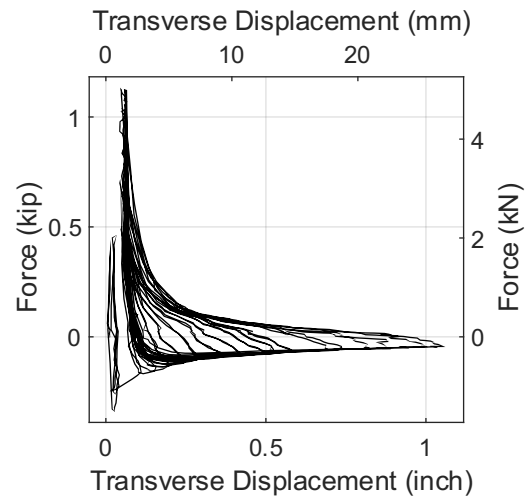
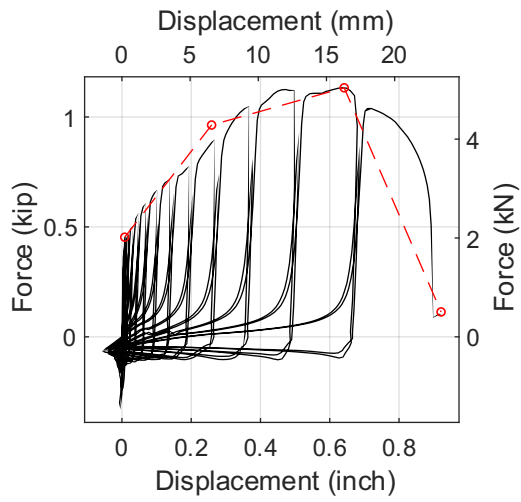
Test 43-@Peak Force-Side View



Test 43-Post Peak @80% Peak Force



Test 43-After Test



Test 44-@Peak Force-Front View



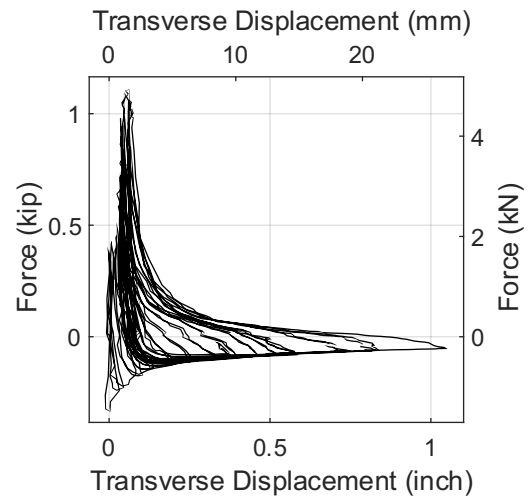
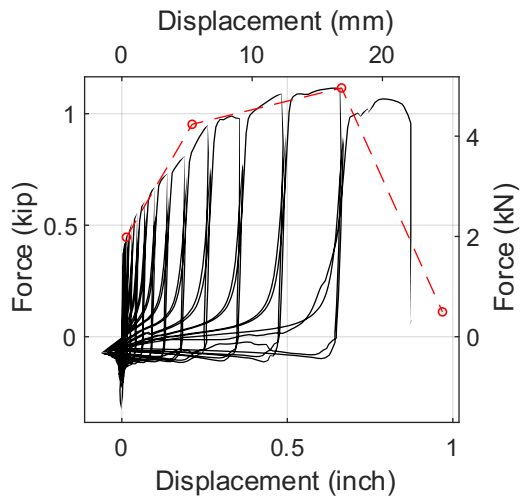
Test 44-@Peak Force-Side View



Test 44-Post Peak @80% Peak Force



Test 44-After Test



Test 45-@Peak Force-Front View



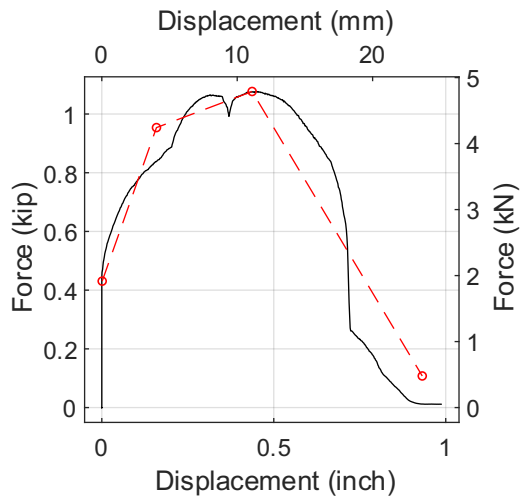
Test 45-@Peak Force-Side View



Test 45-Post Peak @80% Peak Force



Test 45-After Test



Test 46-@Peak Force-Front View



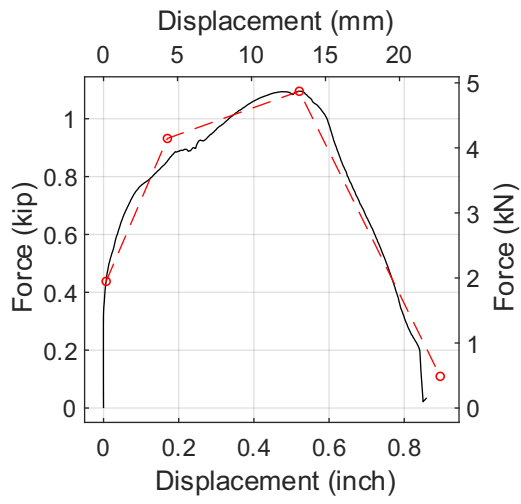
Test 46-@Peak Force-Side View



Test 46-Post Peak @80% Peak Force



Test 46-After Test



Test 47-@Peak Force-Front View



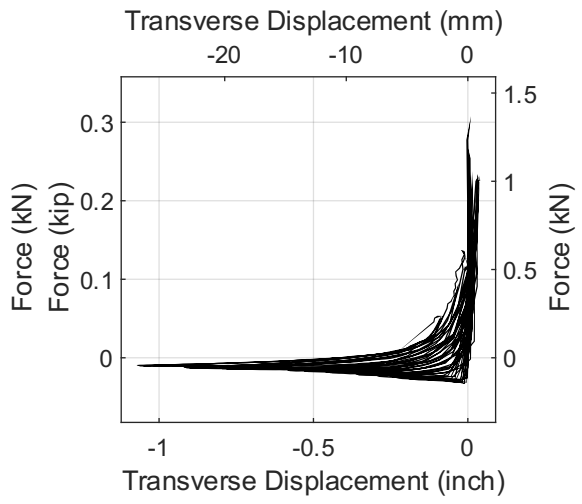
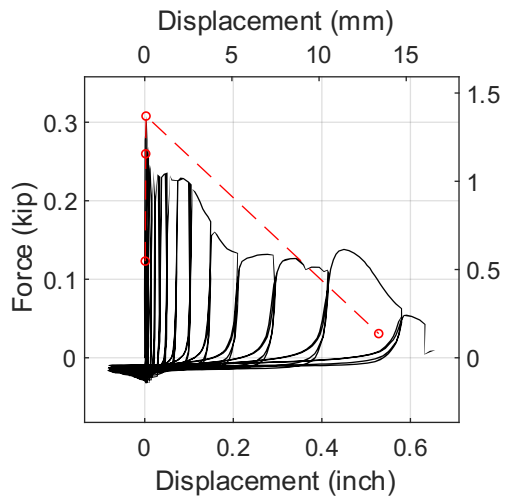
Test 47-@Peak Force-Side View



Test 47-Post Peak @80% Peak Force



Test 47-After Test



Test 48-@Peak Force-Front View



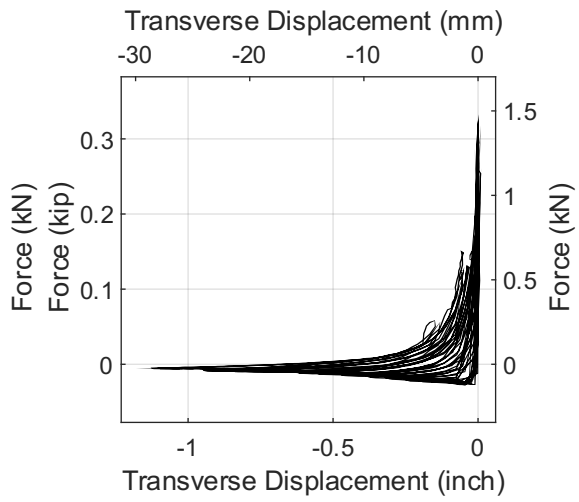
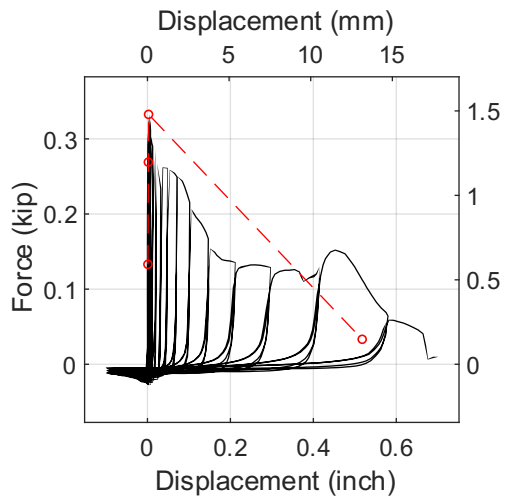
Test 48-@Peak Force-Side View



Test 48-Post Peak @80% Peak Force



Test 48-After Test



Test 49-@Peak Force-Front View



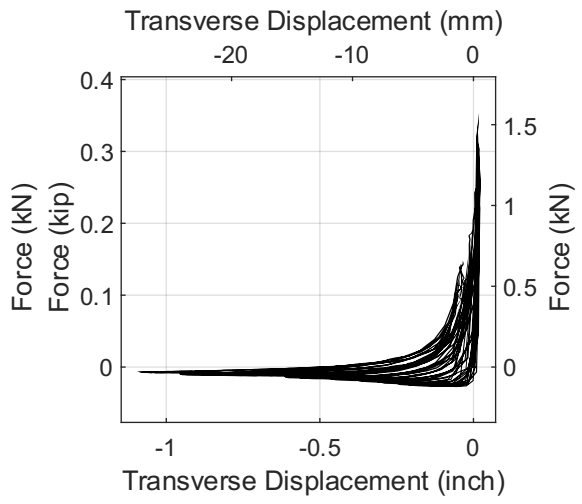
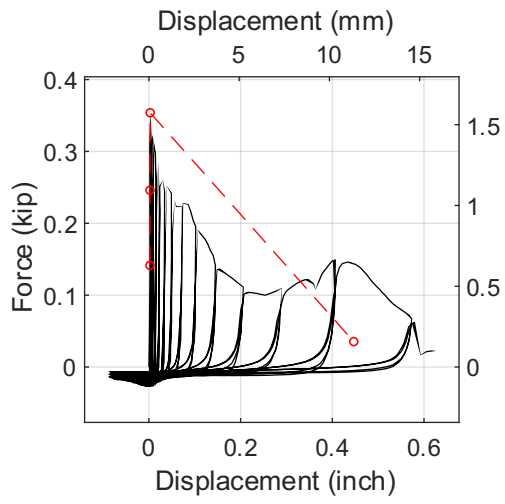
Test 49-@Peak Force-Side View



Test 49-Post Peak @80% Peak Force



Test 49-After Test



Test 50-@Peak Force-Front View



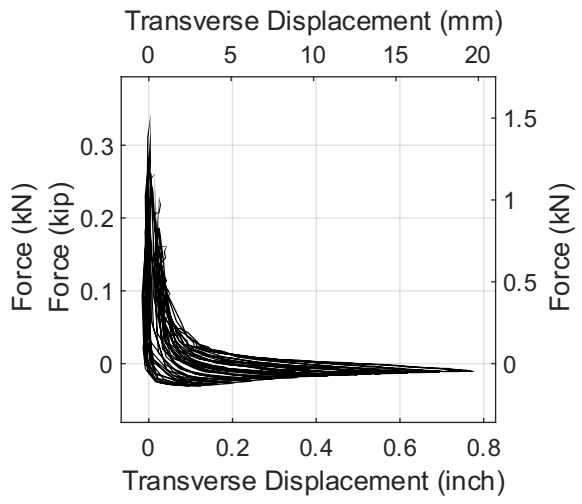
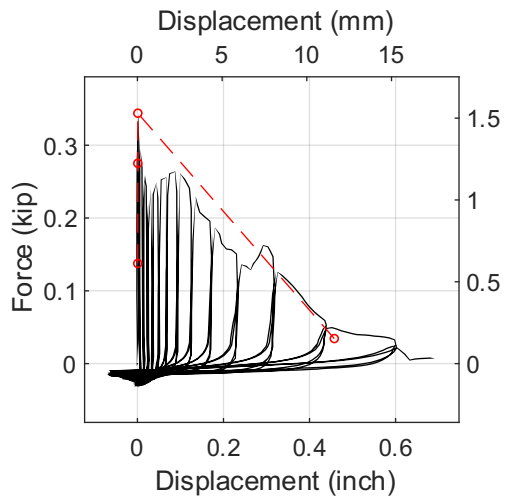
Test 50-@Peak Force-Side View



Test 50-Post Peak @80% Peak Force



Test 50-After Test



Test 51-@Peak Force-Front View



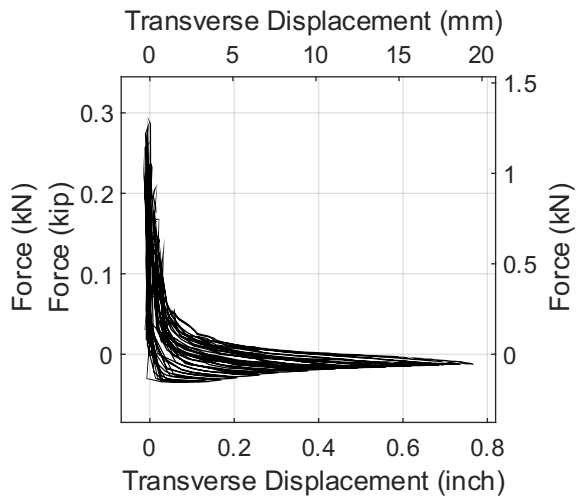
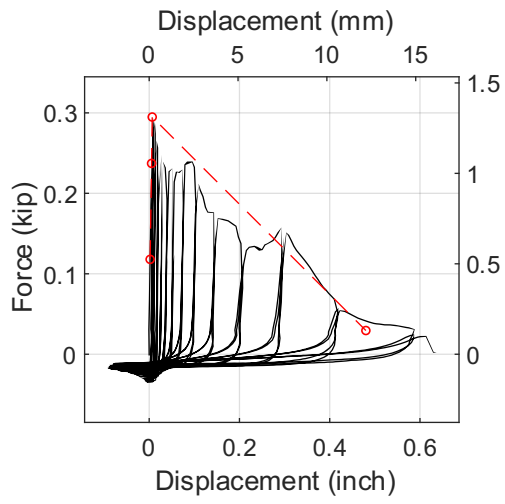
Test 51-@Peak Force-Side View



Test 51-Post Peak @80% Peak Force



Test 51-After Test



Test 52-@Peak Force-Front View



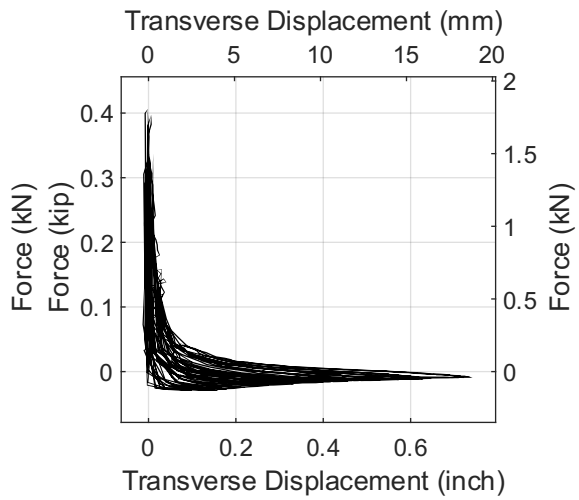
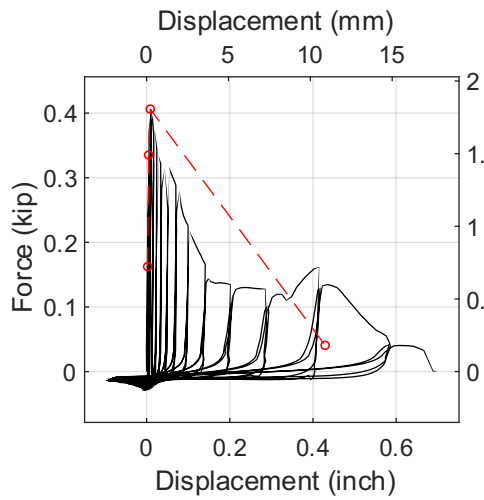
Test 52-@Peak Force-Side View



Test 52-Post Peak @80% Peak Force



Test 52-After Test



Test 53-@Peak Force-Front View



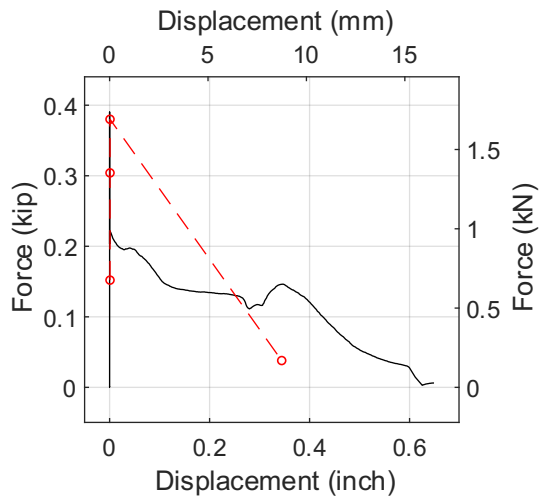
Test 53-@Peak Force-Side View



Test 53-Post Peak @80% Peak Force



Test 53-After Test



Test 54-@Peak Force-Front View



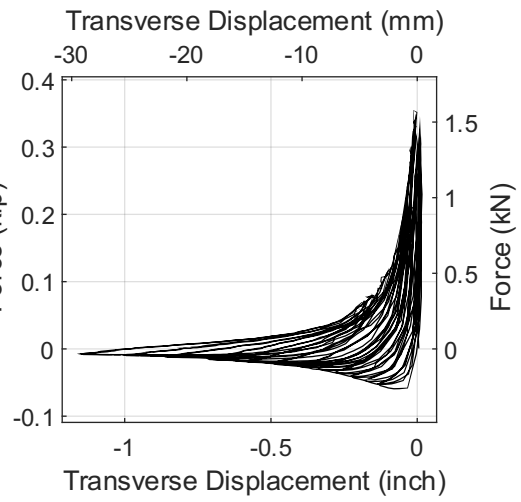
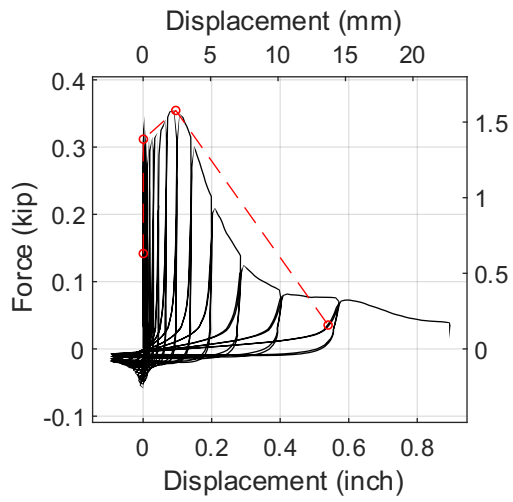
Test 54-@Peak Force-Side View



Test 54-Post Peak @80% Peak Force



Test 54-After Test



Test 55-@Peak Force-Front View



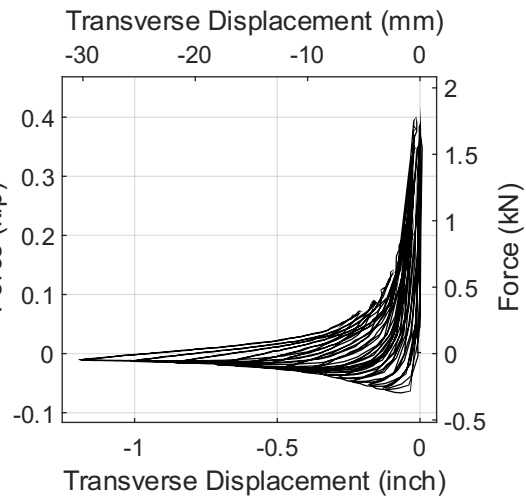
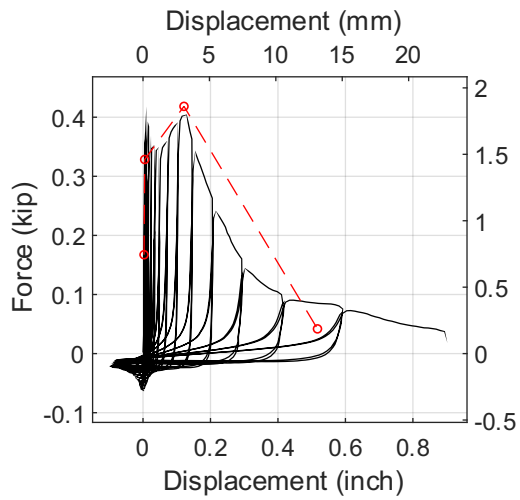
Test 55-@Peak Force-Side View



Test 55-Post Peak @80% Peak Force



Test 55-After Test



Test 56-@Peak Force-Front View



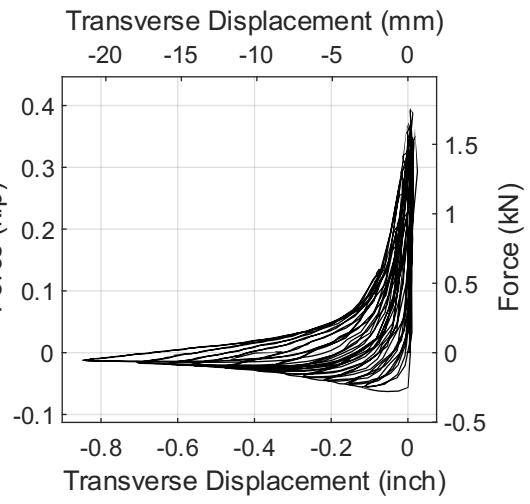
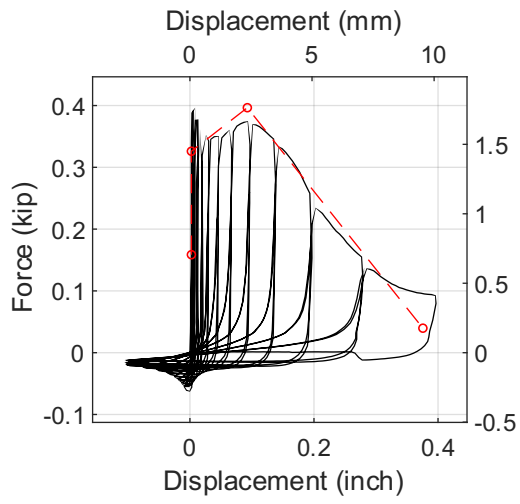
Test 56-@Peak Force-Side View



Test 56-Post Peak @80% Peak Force



Test 56-After Test



Test 57-@Peak Force-Front View



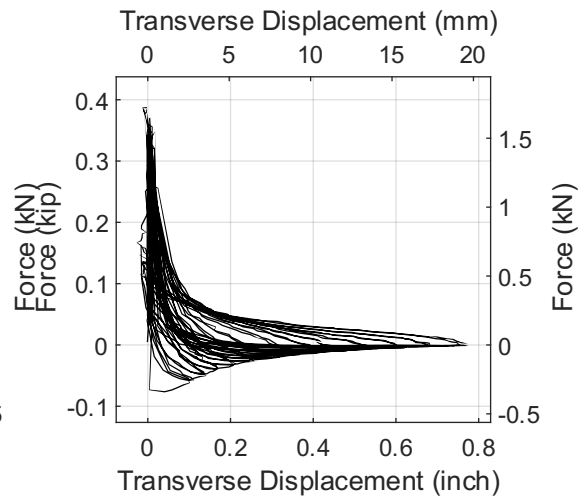
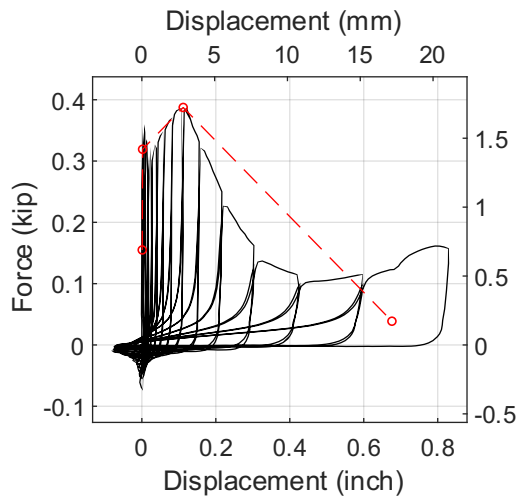
Test 57-@Peak Force-Side View



Test 57-Post Peak @80% Peak Force



Test 57-After Test



Test 58-@Peak Force-Front View



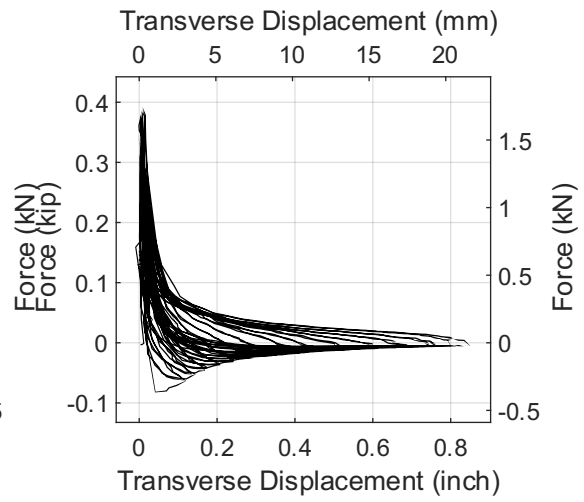
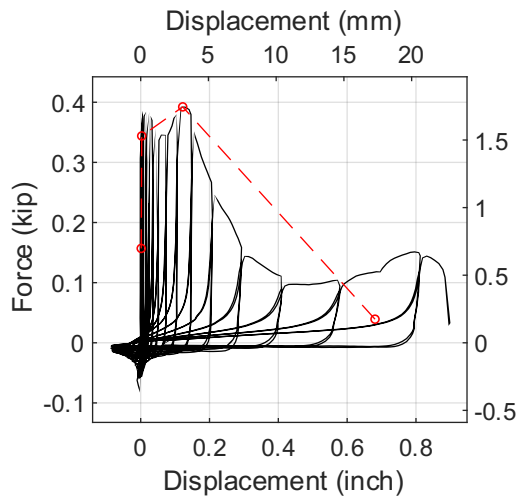
Test 58-@Peak Force-Side View



Test 58-Post Peak @80% Peak Force



Test 58-After Test



Test 59-@Peak Force-Front View



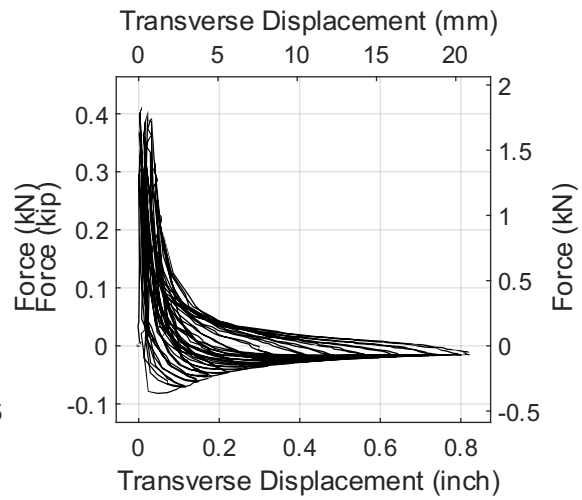
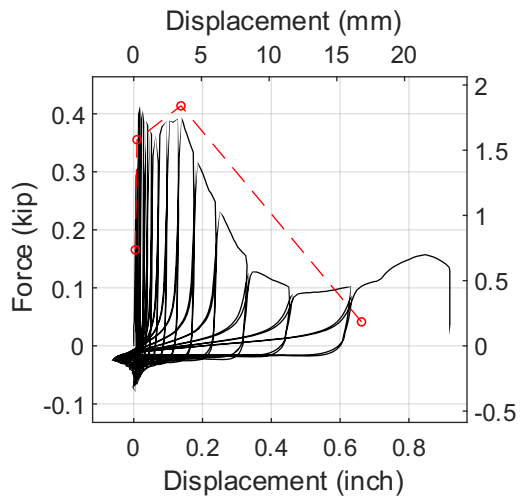
Test 59-@Peak Force-Side View



Test 59-Post Peak @80% Peak Force



Test 59-After Test



Test 60-@Peak Force-Front View



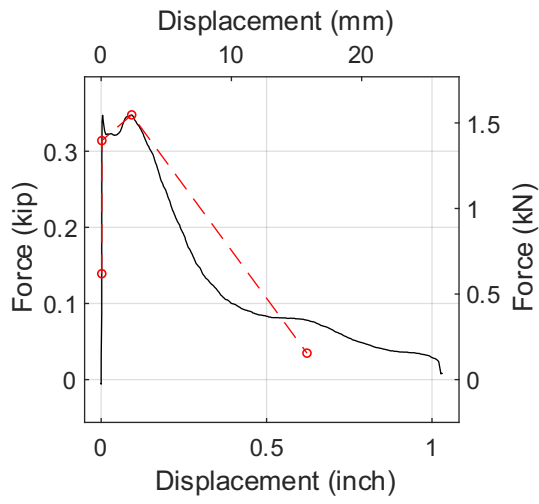
Test 60-@Peak Force-Side View



Test 60-Post Peak @80% Peak Force



Test 60-After Test



Test 61-@Peak Force-Front View



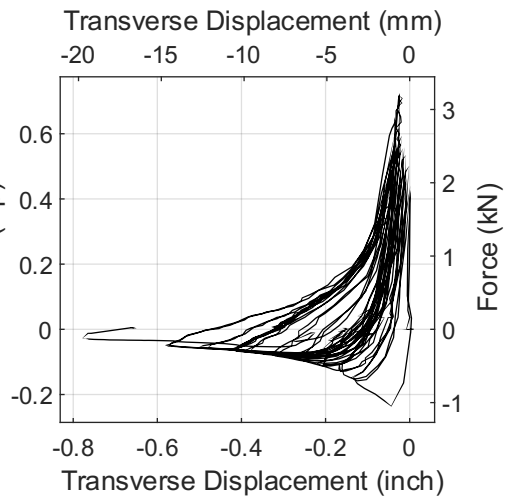
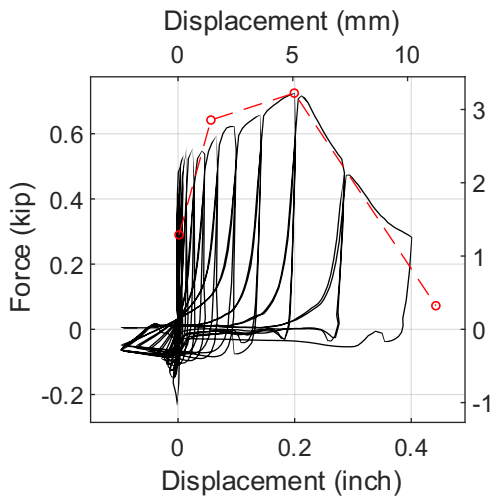
Test 61-@Peak Force-Side View



Test 61-Post Peak @80% Peak Force



Test 61-After Test



Test 62-@Peak Force-Front View



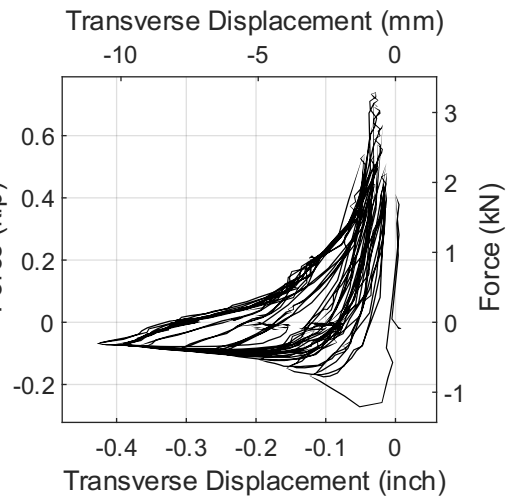
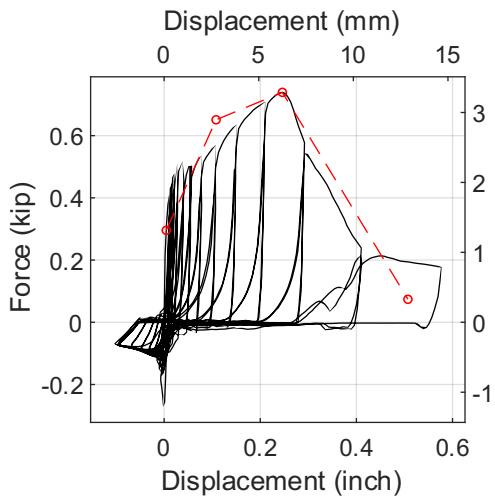
Test 62-@Peak Force-Side View



Test 62-Post Peak @80% Peak Force



Test 62-After Test



Test 63-@Peak Force-Front View



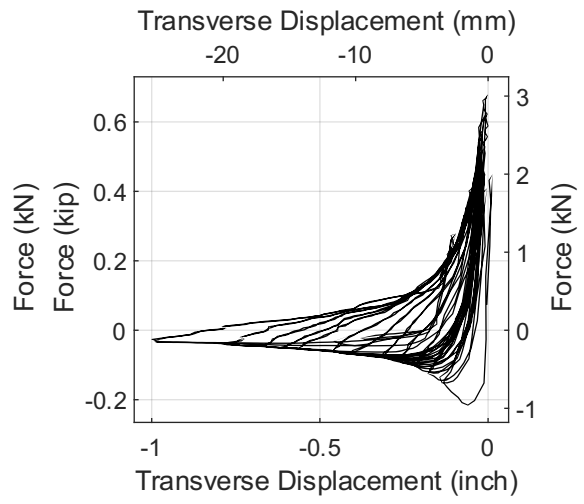
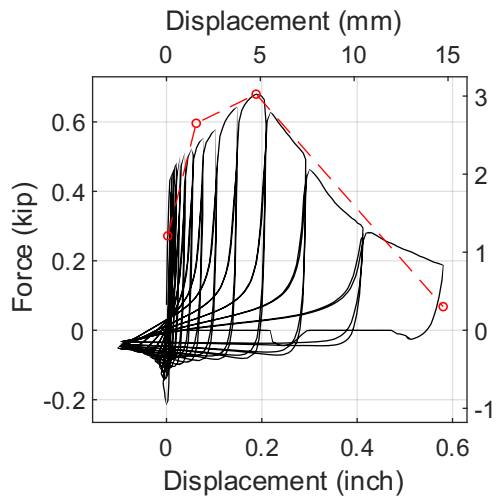
Test 63-@Peak Force-Side View



Test 63-Post Peak @80% Peak Force



Test 63-After Test



Test 64-@Peak Force-Front View



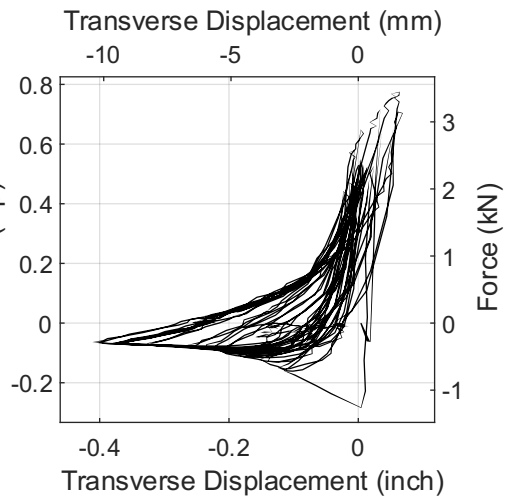
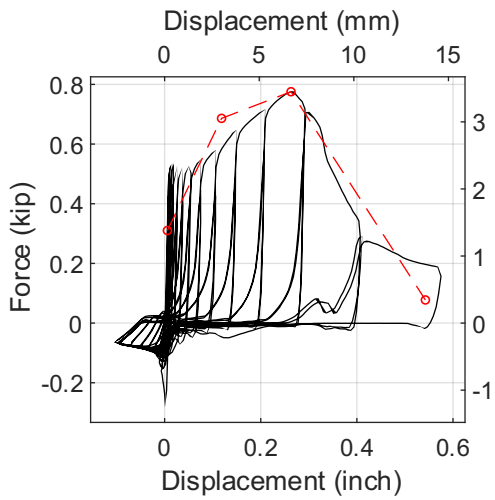
Test 64-@Peak Force-Side View



Test 64-Post Peak @80% Peak Force



Test 64-After Test



Test 65-@Peak Force-Front View



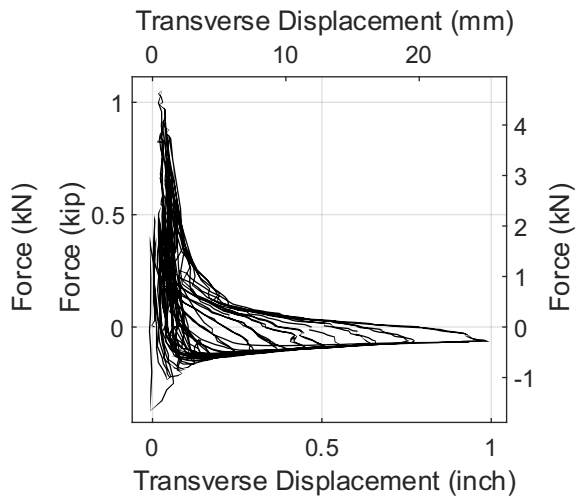
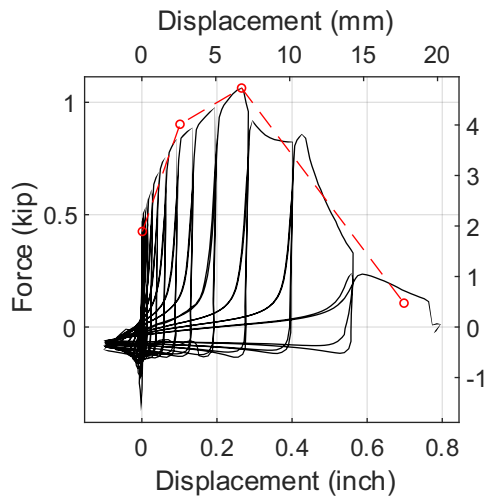
Test 65-@Peak Force-Side View



Test 65-Post Peak @80% Peak Force



Test 65-After Test



Test 66-@Peak Force-Front View



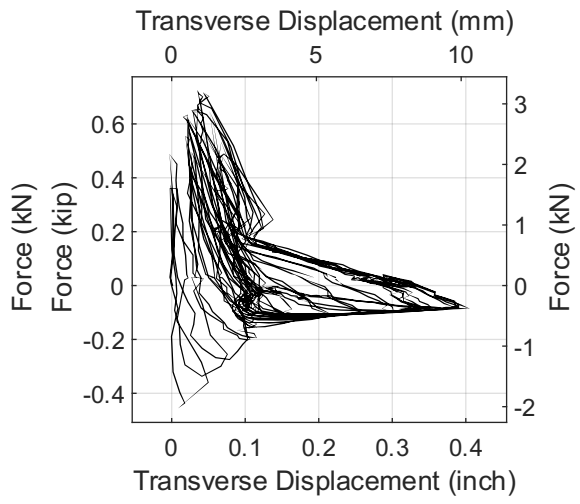
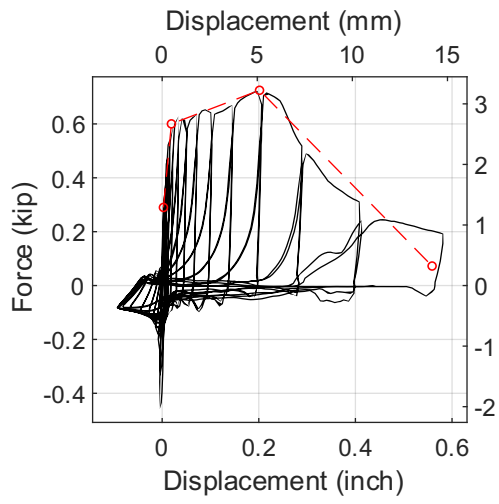
Test 66-@Peak Force-Side View



Test 66-Post Peak @80% Peak Force



Test 66-After Test



Test 67-@Peak Force-Front View



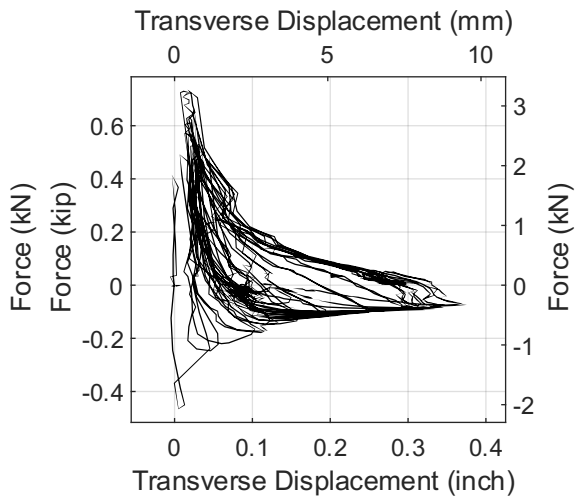
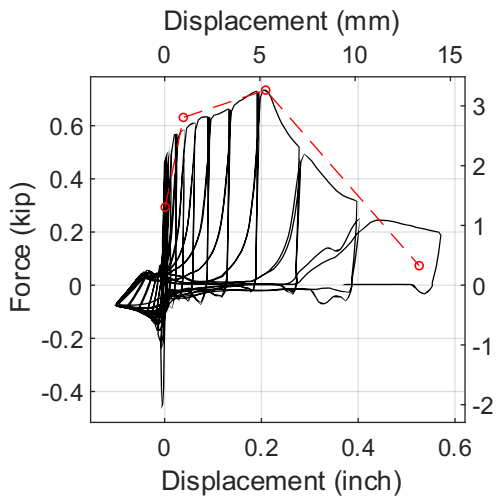
Test 67-@Peak Force-Side View



Test 67-Post Peak @80% Peak Force



Test 67-After Test



Test 68-@Peak Force-Front View



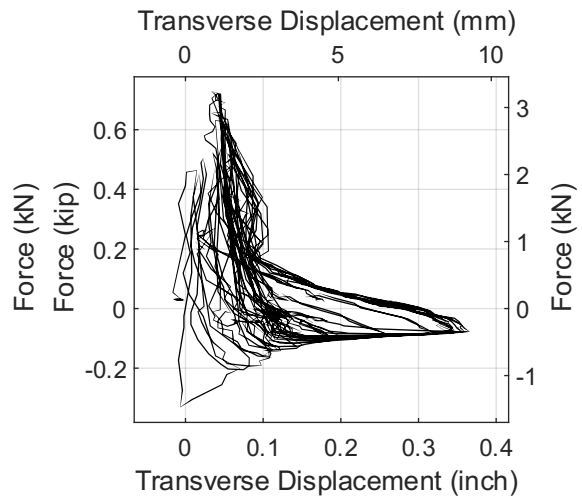
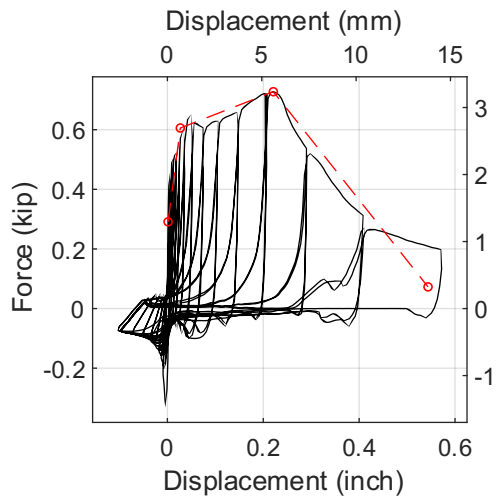
Test 68-@Peak Force-Side View



Test 68-Post Peak @80% Peak Force



Test 68-After Test



Test 69-@Peak Force-Front View



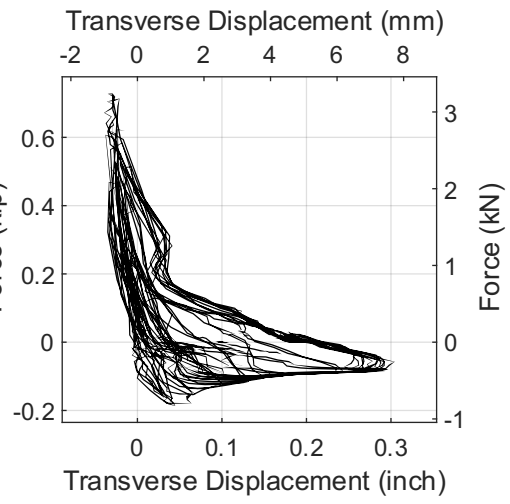
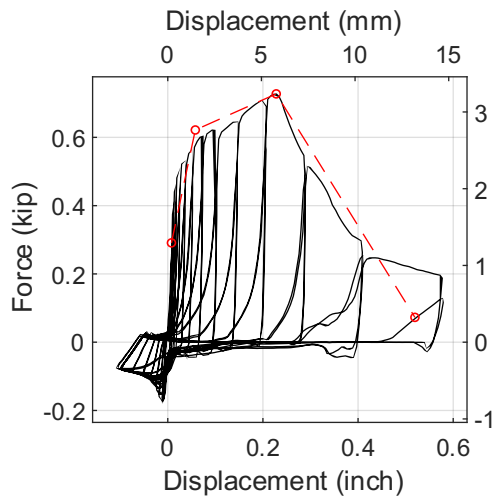
Test 69-@Peak Force-Side View



Test 69-Post Peak @80% Peak Force



Test 69-After Test



Test 70-@Peak Force-Front View



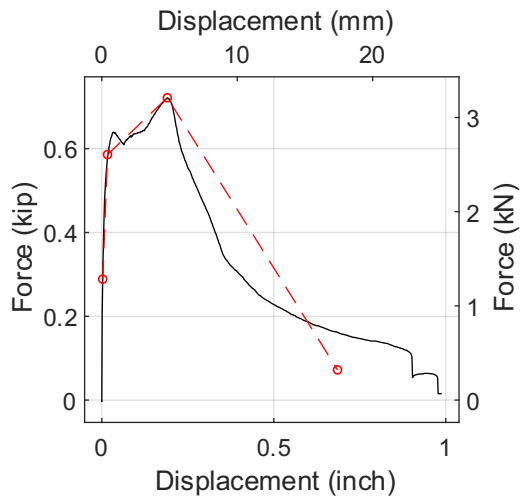
Test 70-@Peak Force-Side View



Test 70-Post Peak @80% Peak Force



Test 70-After Test



Test 71-@Peak Force-Front View



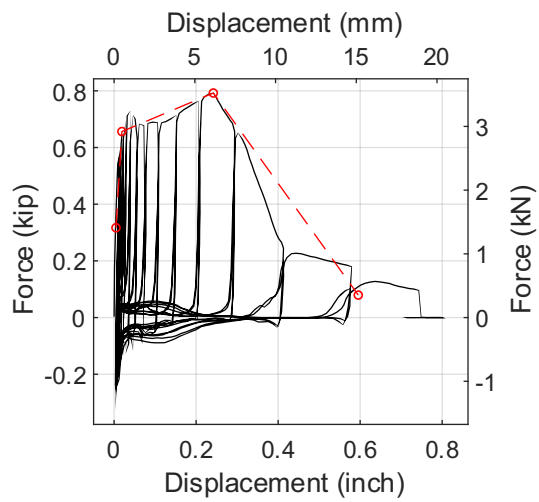
Test 71-@Peak Force-Side View



Test 71-Post Peak @80% Peak Force



Test 71-After Test



Test 72-@Peak Force-Front View



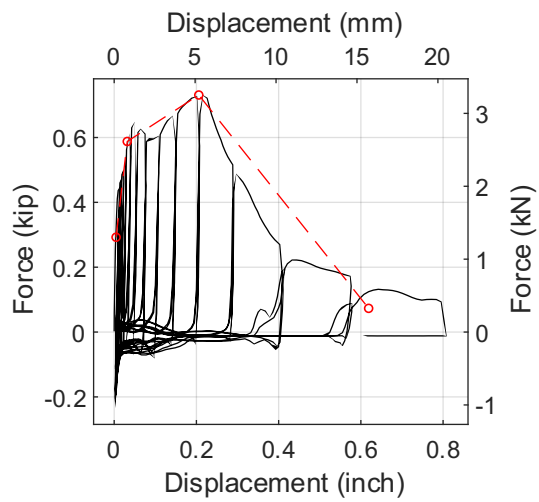
Test 72-@Peak Force-Side View



Test 72-Post Peak @80% Peak Force



Test 72-After Test



Test 73-@Peak Force-Front View



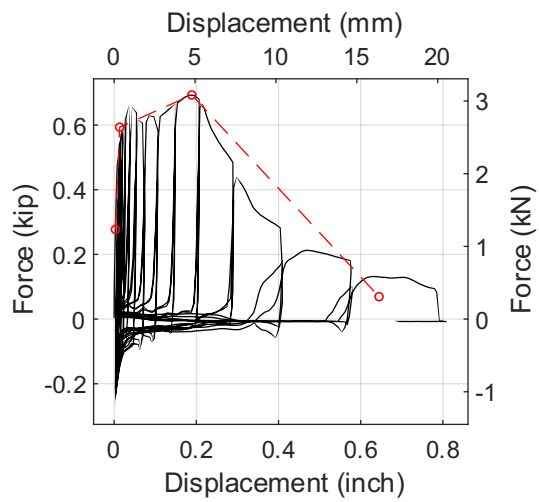
Test 73-@Peak Force-Side View



Test 73-Post Peak @80% Peak Force



Test 73-After Test



Test 74-@Peak Force-Front View



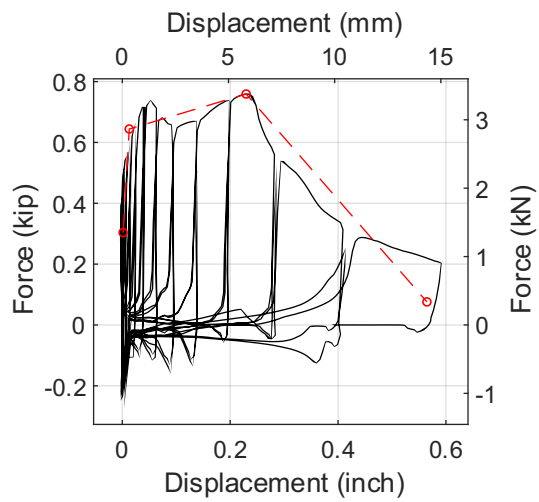
Test 74-@Peak Force-Side View



Test 74-Post Peak @80% Peak Force



Test 74-After Test



Test 75-@Peak Force-Front View



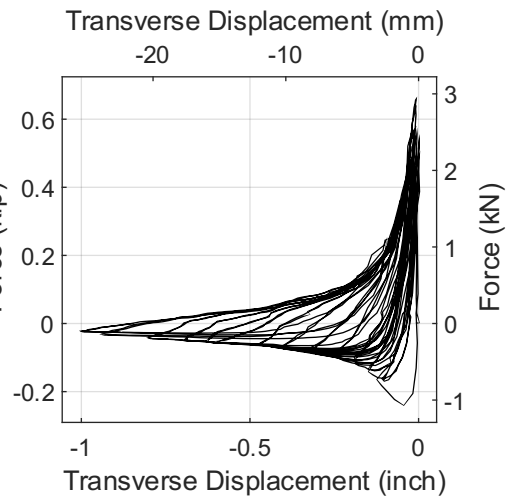
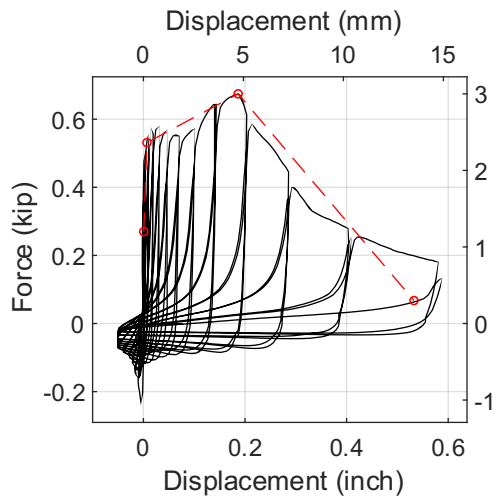
Test 75-@Peak Force-Side View



Test 75-Post Peak @80% Peak Force



Test 75-After Test



Test 76-@Peak Force-Front View



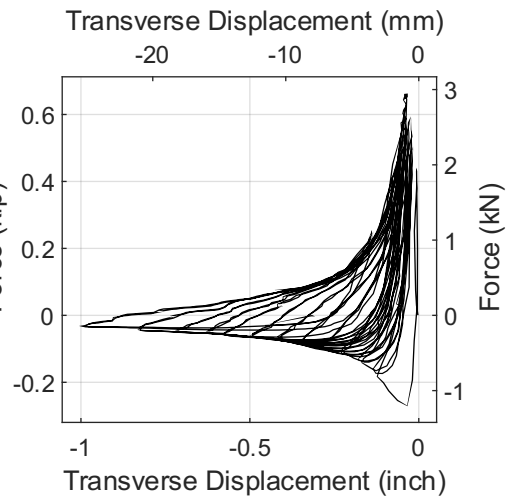
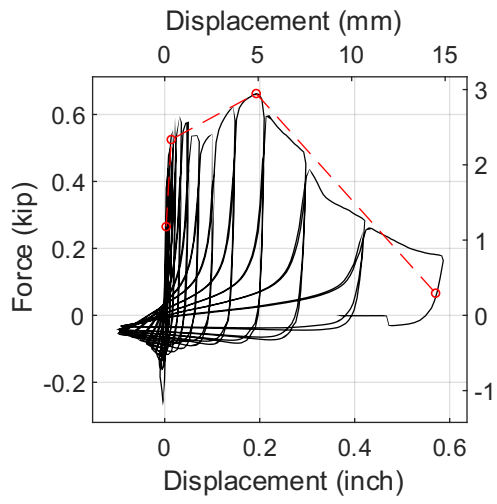
Test 76-@Peak Force-Side View



Test 76-Post Peak @80% Peak Force



Test 76-After Test



Test 77-@Peak Force-Front View



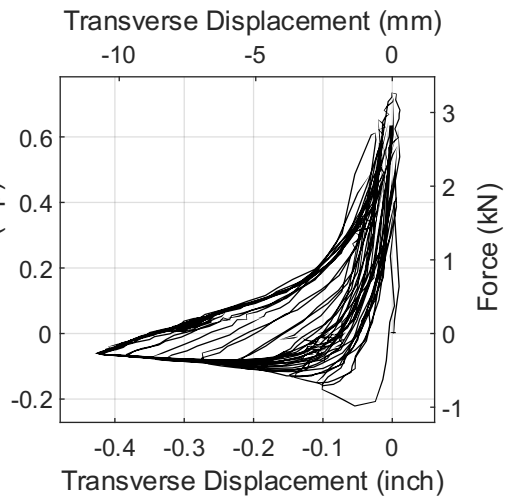
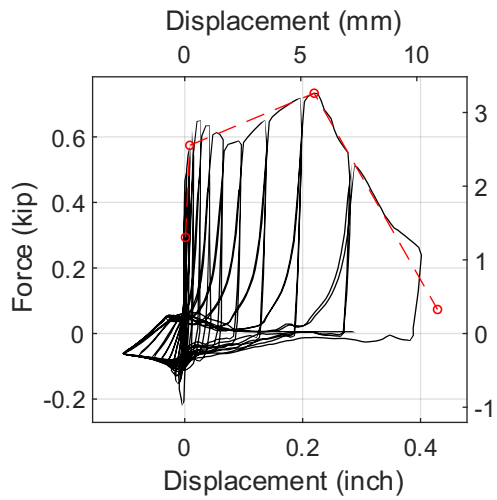
Test 77-@Peak Force-Side View



Test 77-Post Peak @80% Peak Force



Test 77-After Test



Test 78-@Peak Force-Front View



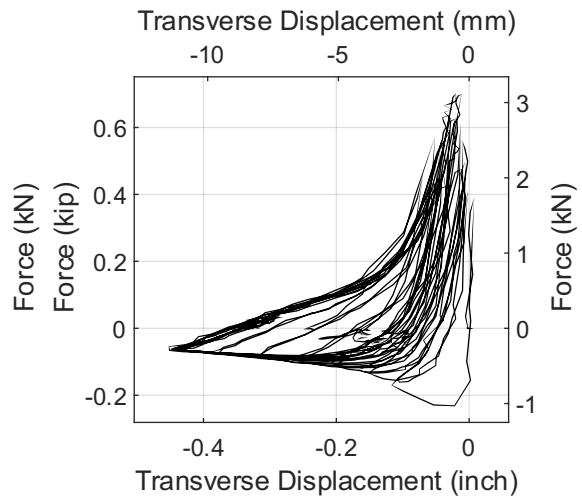
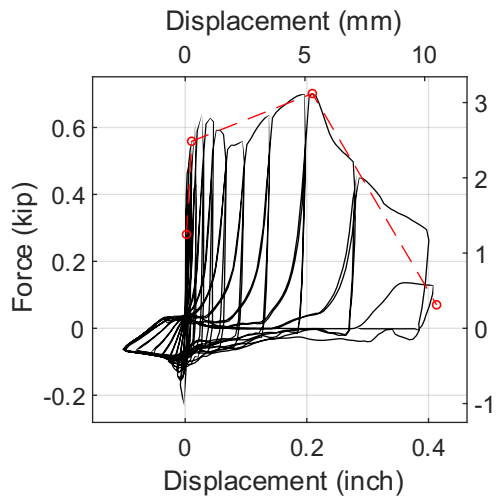
Test 78-@Peak Force-Side View



Test 78-Post Peak @80% Peak Force



Test 78-After Test



Test 79-@Peak Force-Front View



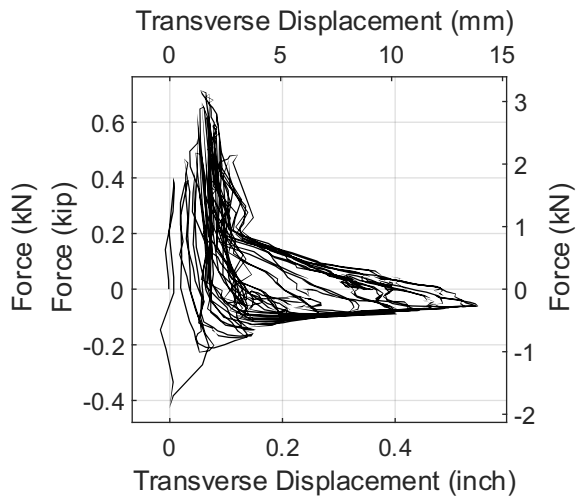
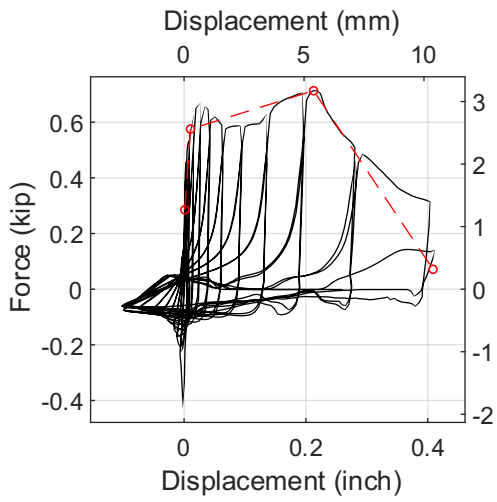
Test 79-@Peak Force-Side View



Test 79-Post Peak @80% Peak Force



Test 79-After Test



Test 80-@Peak Force-Front View



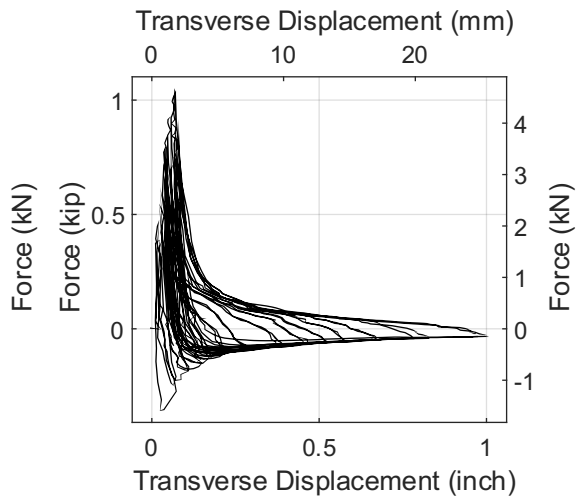
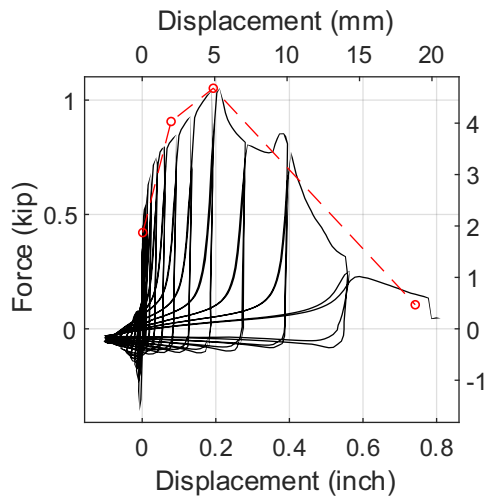
Test 80-@Peak Force-Side View



Test 80-Post Peak @80% Peak Force



Test 80-After Test



Test 81-@Peak Force-Front View



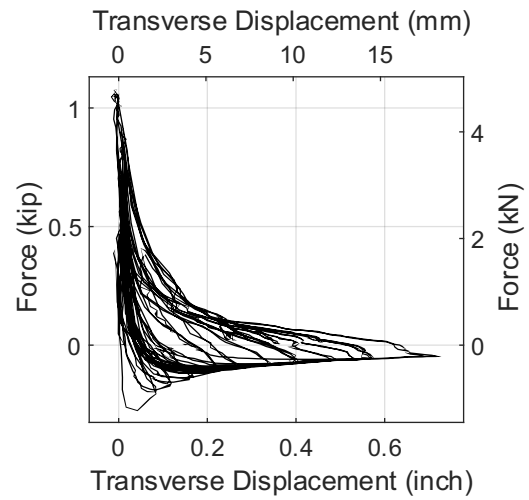
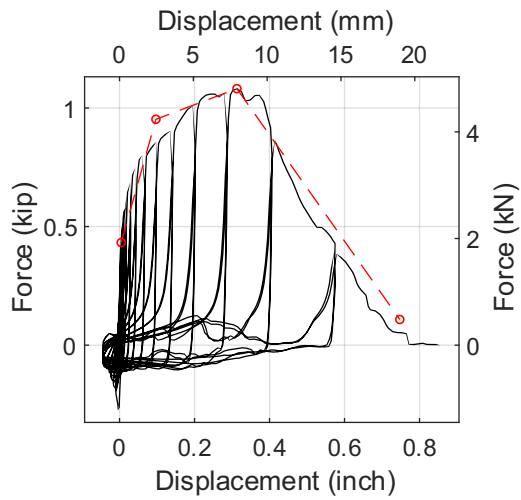
Test 81-@Peak Force-Side View



Test 81-Post Peak @80% Peak Force



Test 81-After Test



Test 82-@Peak Force-Front View



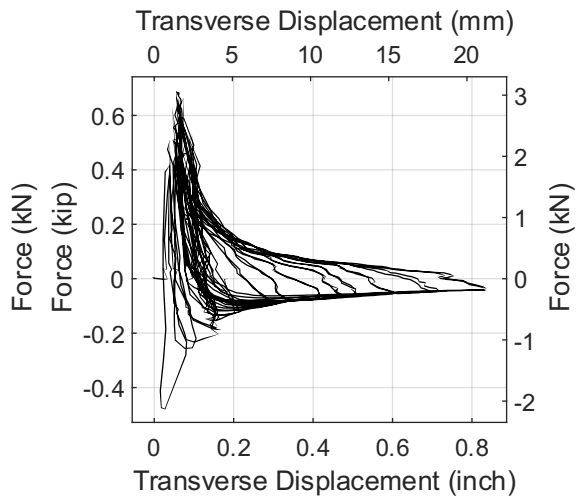
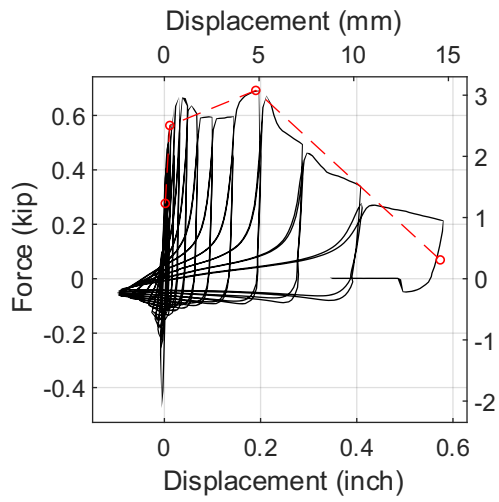
Test 82-@Peak Force-Side View



Test 82-Post Peak @80% Peak Force



Test 82-After Test



Test 83-@Peak Force-Front View



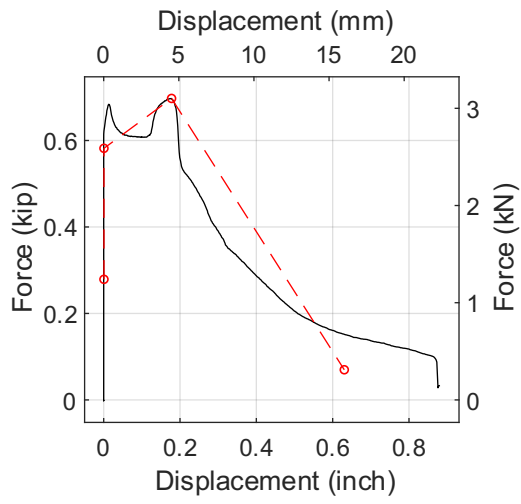
Test 83-@Peak Force-Side View



Test 83-Post Peak @80% Peak Force



Test 83-After Test



Test 84-@Peak Force-Front View



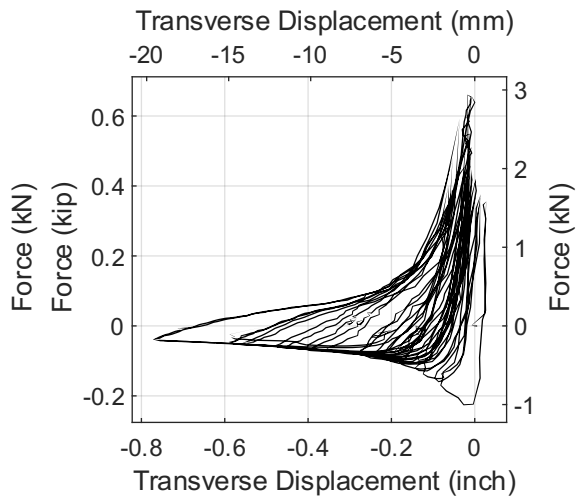
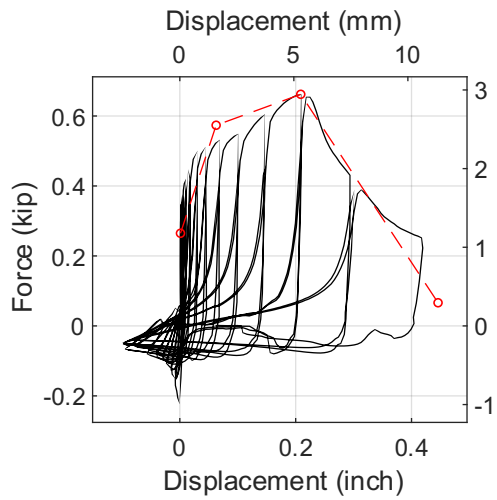
Test 84-@Peak Force-Side View



Test 84-Post Peak @80% Peak Force



Test 84-After Test



Test 85-@Peak Force-Front View



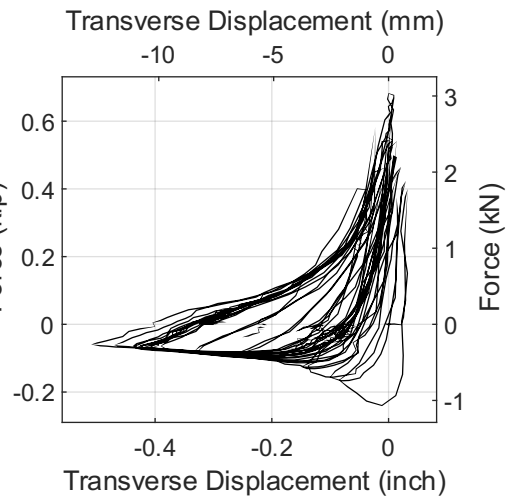
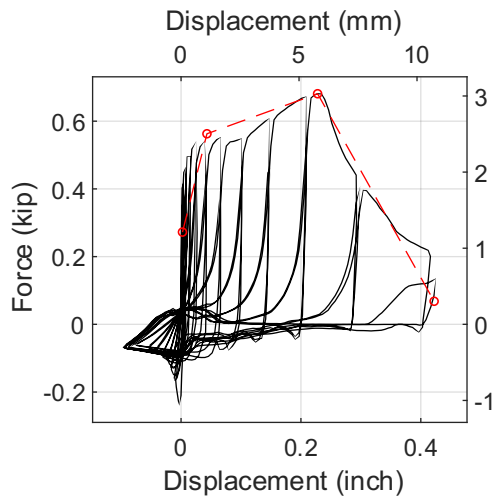
Test 85-@Peak Force-Side View



Test 85-Post Peak @80% Peak Force



Test 85-After Test



Test 86-@Peak Force-Front View



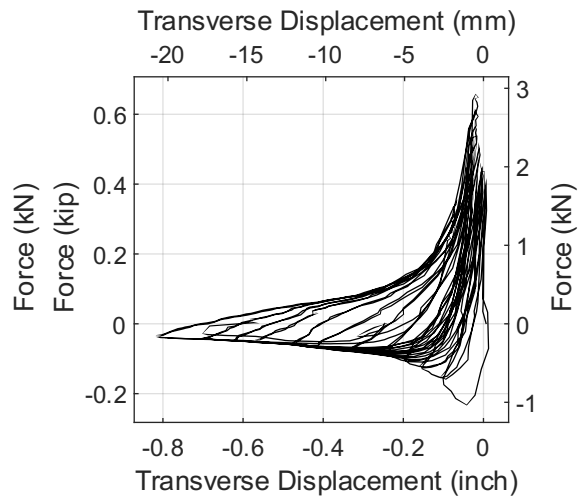
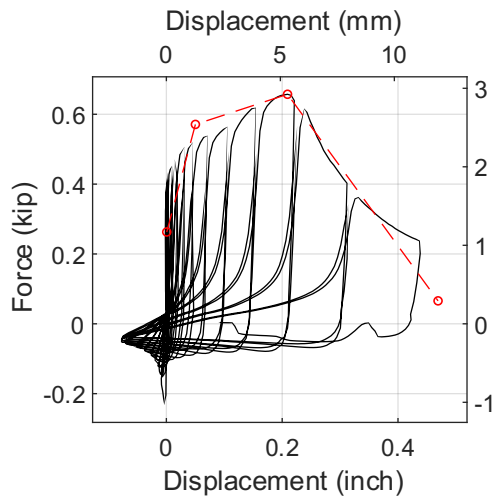
Test 86-@Peak Force-Side View



Test 86-Post Peak @80% Peak Force



Test 86-After Test



Test 87-@Peak Force-Front View



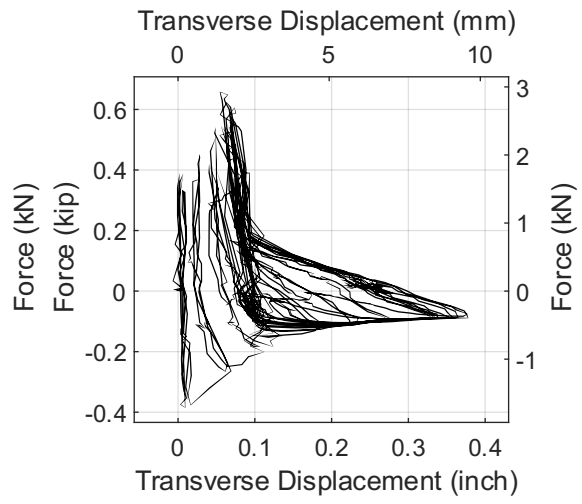
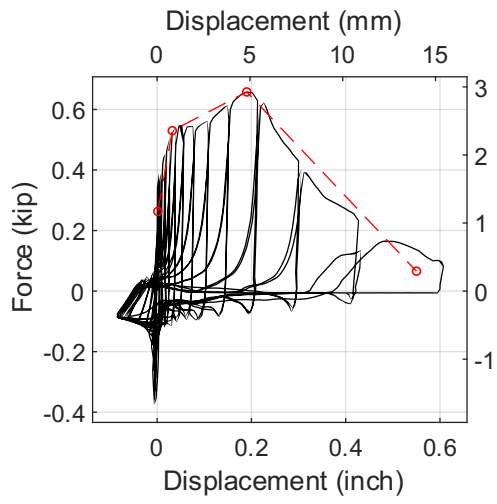
Test 87-@Peak Force-Side View



Test 87-Post Peak @80% Peak Force



Test 87-After Test



Test 88-@Peak Force-Front View



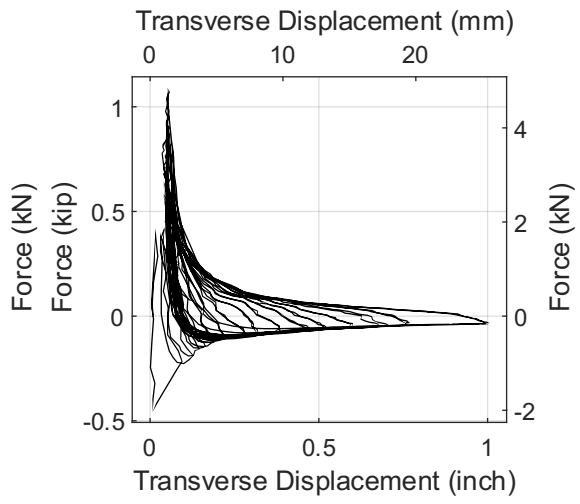
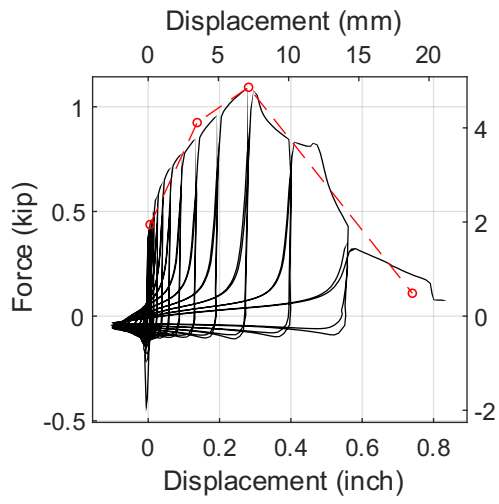
Test 88-@Peak Force-Side View



Test 88-Post Peak @80% Peak Force



Test 88-After Test



Test 89-@Peak Force-Front View



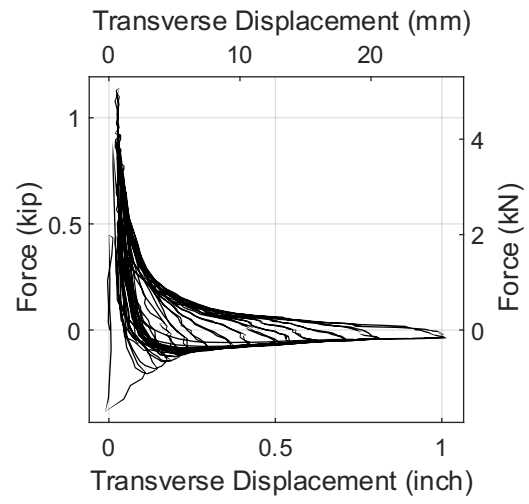
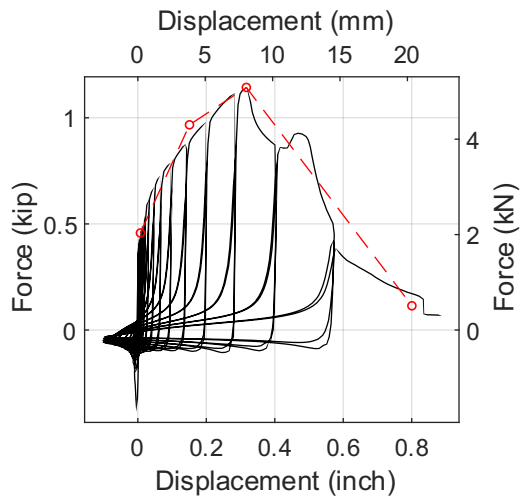
Test 89-@Peak Force-Side View



Test 89-Post Peak @80% Peak Force



Test 89-After Test



Test 90-@Peak Force-Front View



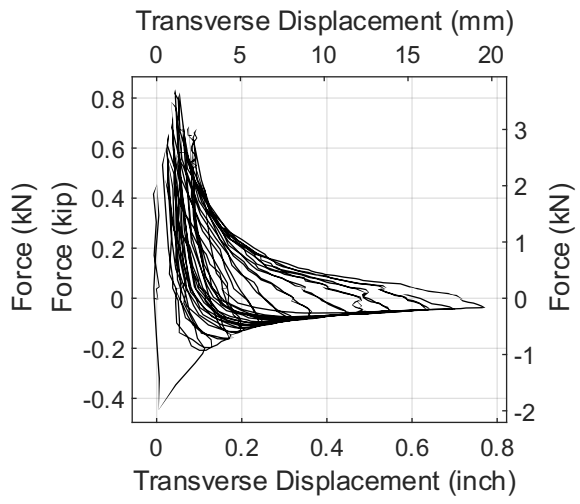
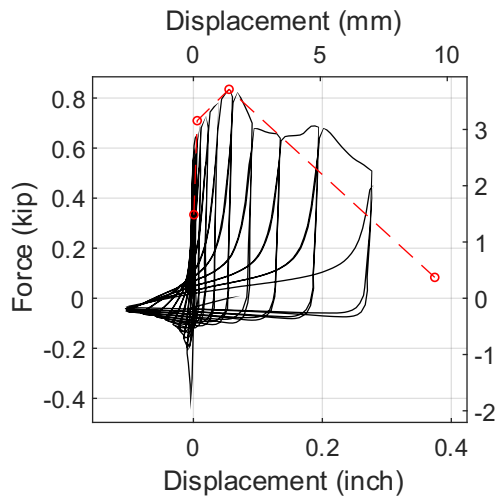
Test 90-@Peak Force-Side View



Test 90-Post Peak @80% Peak Force



Test 90-After Test



Test 91-@Peak Force-Front View



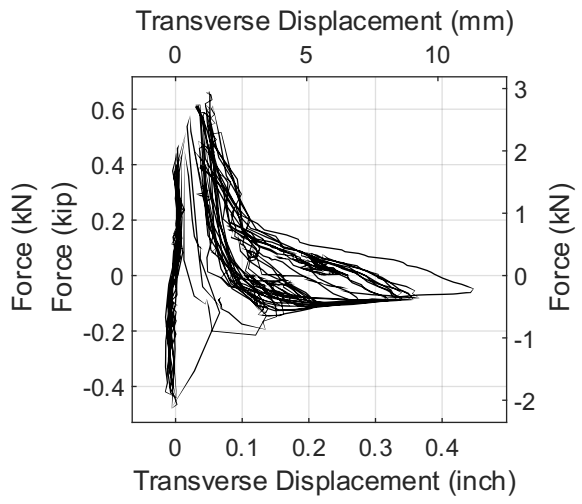
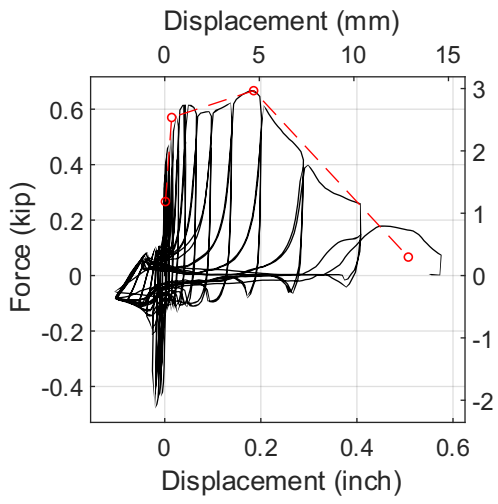
Test 91-@Peak Force-Side View



Test 91-Post Peak @80% Peak Force



Test 91-After Test



Test 92-@Peak Force-Front View



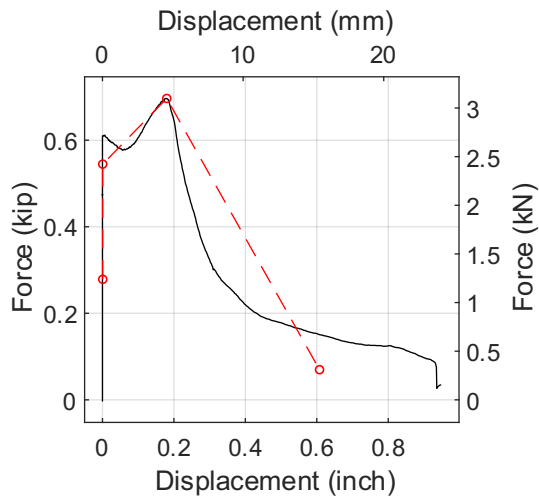
Test 92-@Peak Force-Side View



Test 92-Post Peak @80% Peak Force



Test 92-After Test



Test 93-@Peak Force-Front View



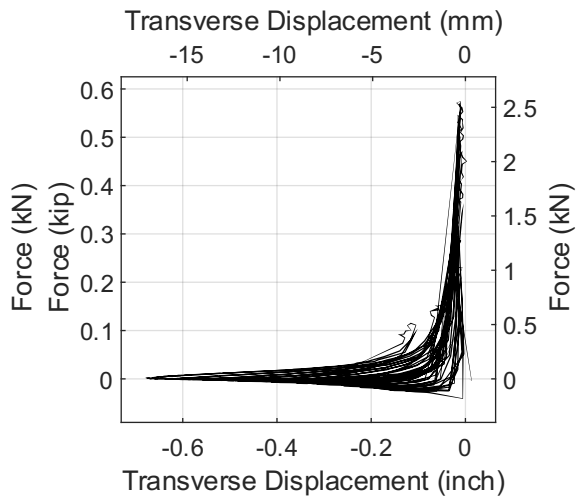
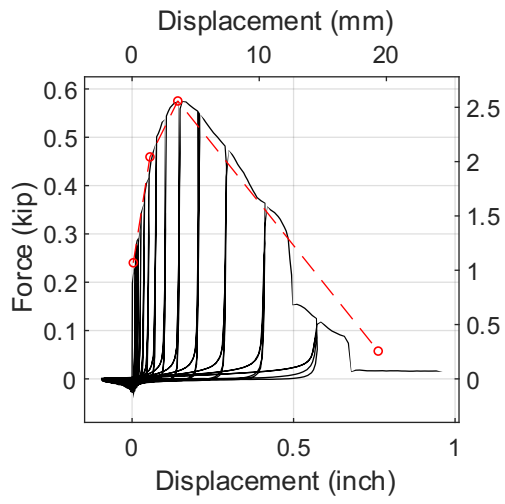
Test 93-@Peak Force-Side View



Test 93-Post Peak @80% Peak Force



Test 93-After Test



Test 94-@Peak-Front View



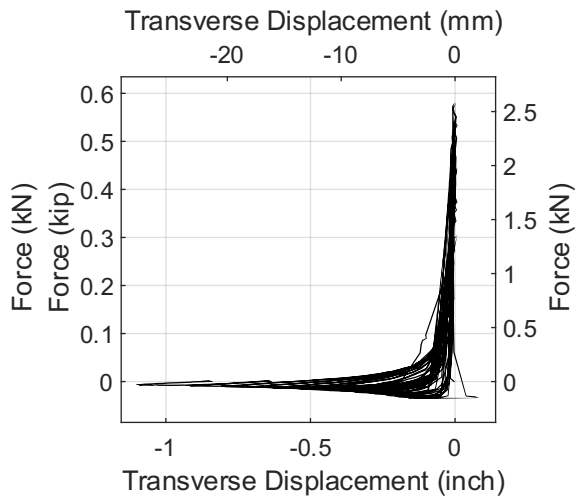
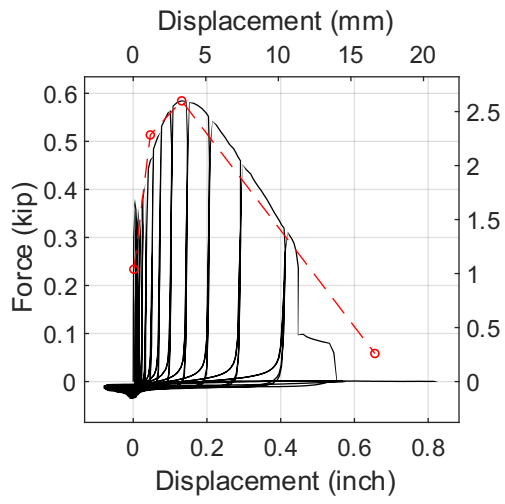
Test 94-@Peak-Side View



Test 94-@80% Post Peak



Test 94-After Test



Test 95-@Peak-Front View



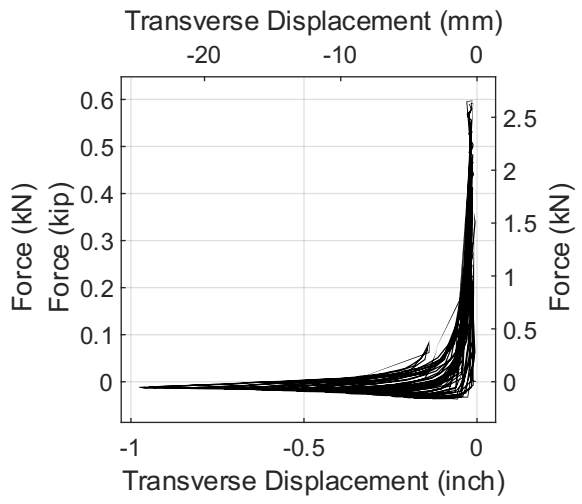
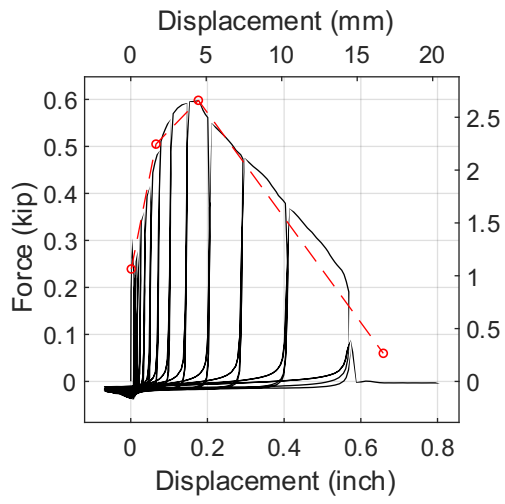
Test 95-@Peak-Side View



Test 95-@80% Post Peak



Test 95-After Test



Test 96-@Peak-Front View



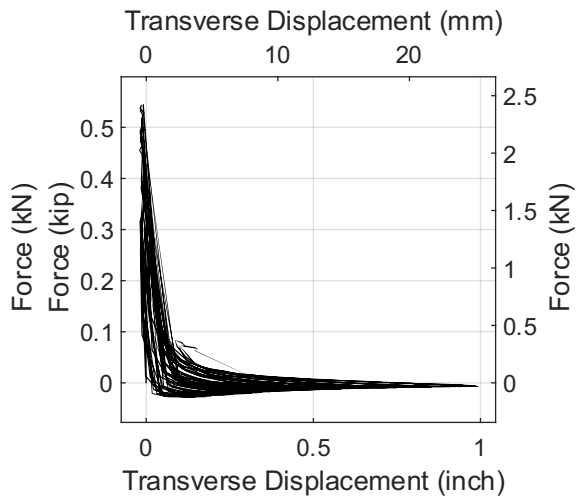
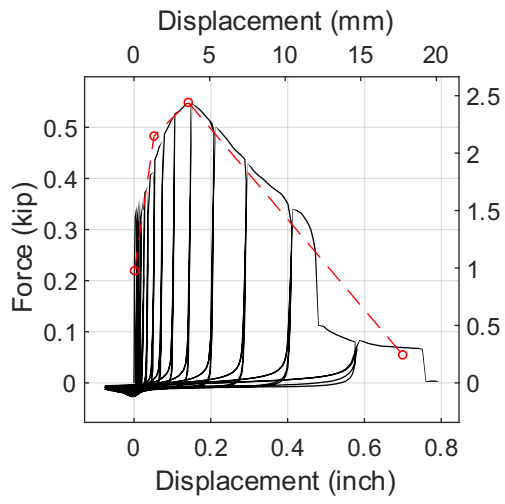
Test 96-@Peak-Side View



Test 96-@80% Post Peak



Test 96-After Test



Test 97-@Peak-Front View



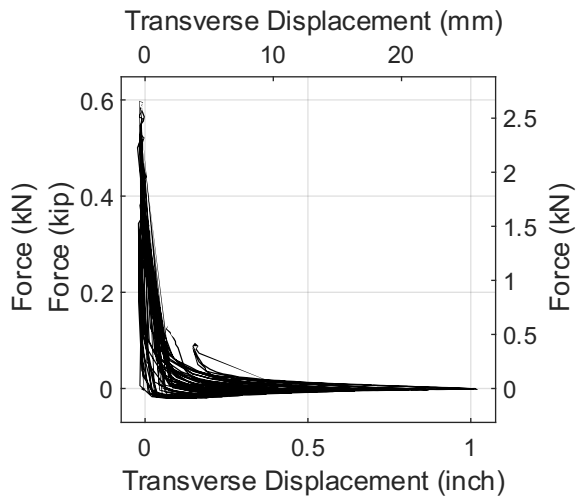
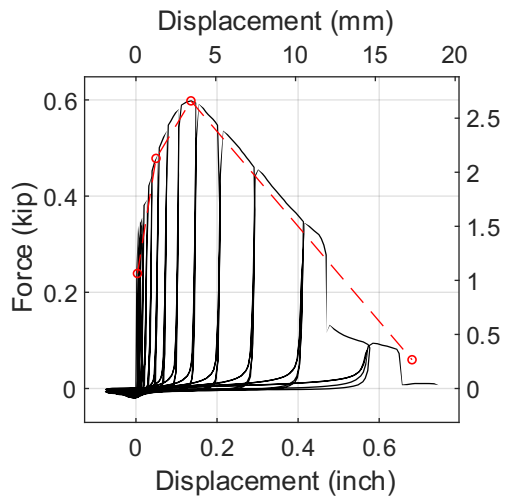
Test 97-@Peak-Side View



Test 97-@80% Post Peak



Test 97-After Test



Test 98-@Peak-Front View



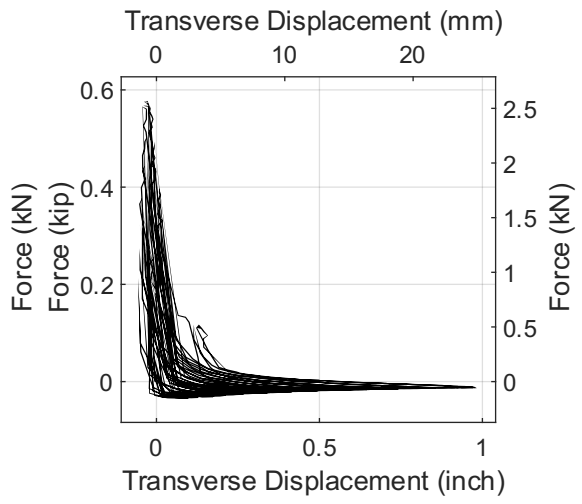
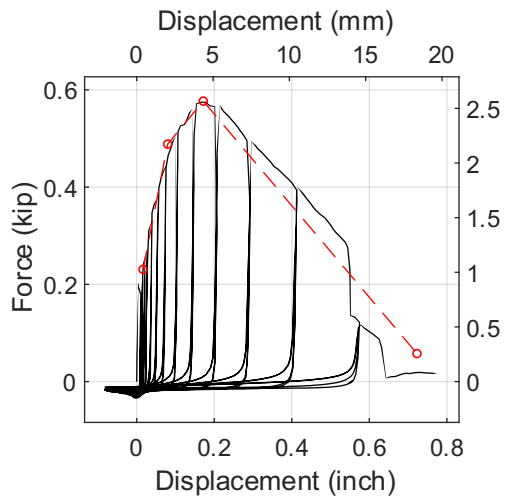
Test 98-@Peak-Side View



Test 98-@80% Post Peak



Test 98-After Test



Test 99-@Peak-Front View



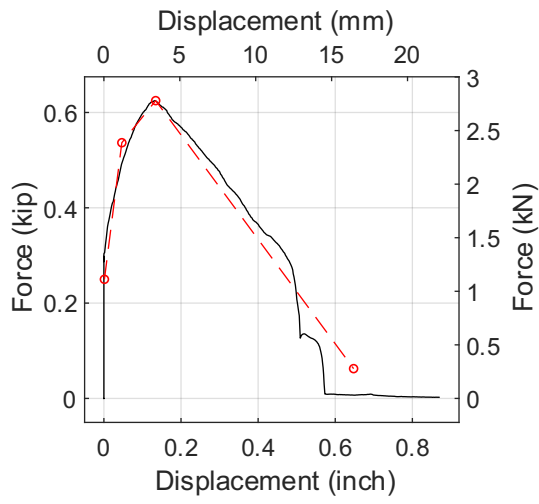
Test 99-@Peak-Side View



Test 99-@80% Post Peak



Test 99-After Test



Test 100-@Peak-Front View



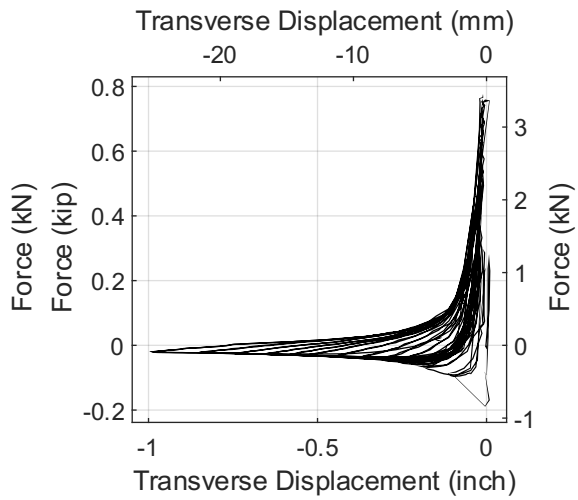
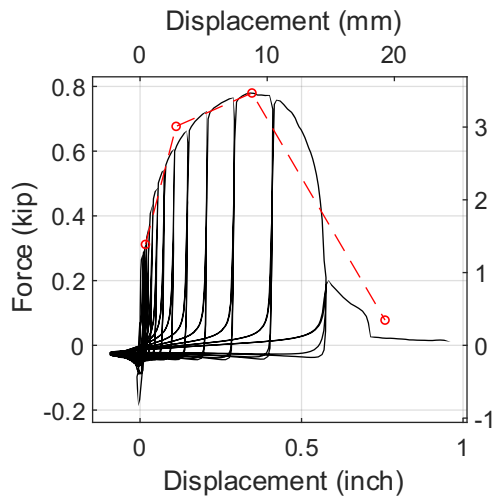
Test 100-@Peak-Side View



Test 100-@80% Post Peak



Test 100-After Test



Test 101-@Peak-Front View



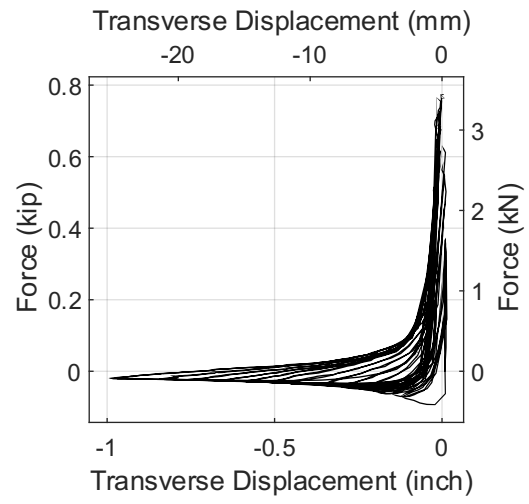
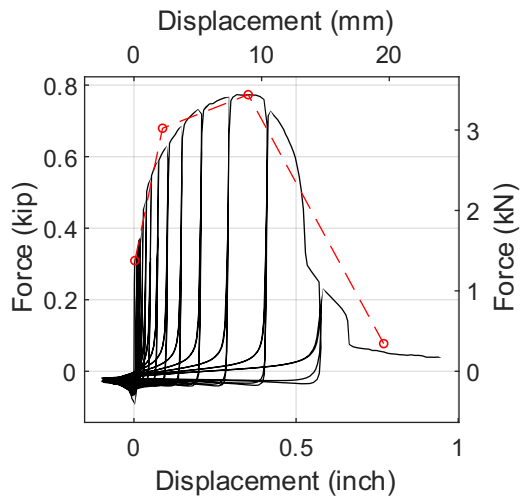
Test 101-@Peak-Side View



Test 101-@80% Post Peak



Test 101-After Test



Test 102-@Peak-Front View



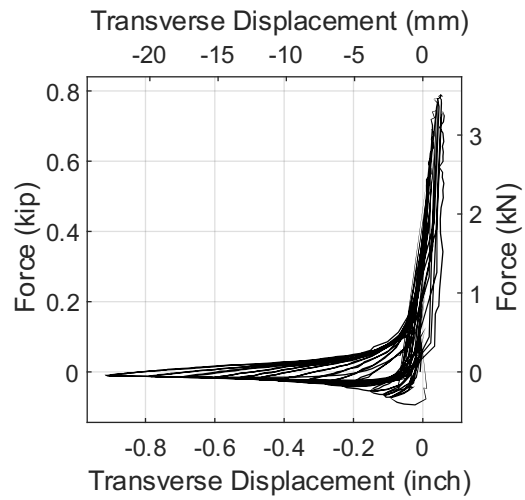
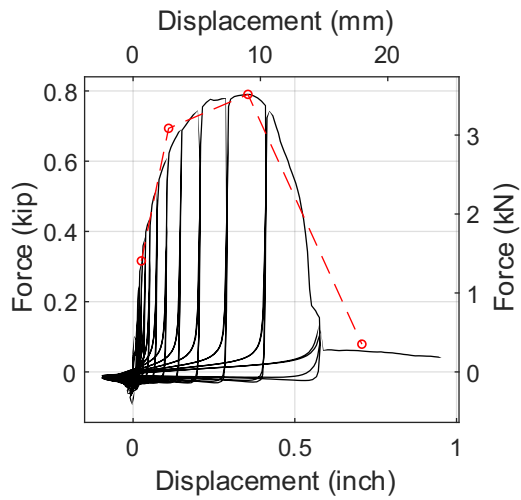
Test 102-@Peak-Side View



Test 102-@80% Post Peak



Test 102-After Test



Test 103-@Peak-Front View



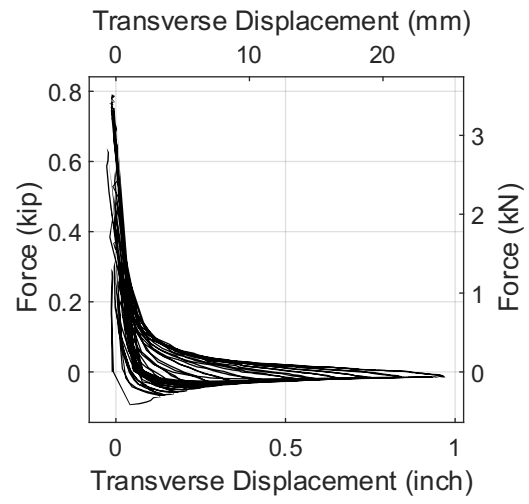
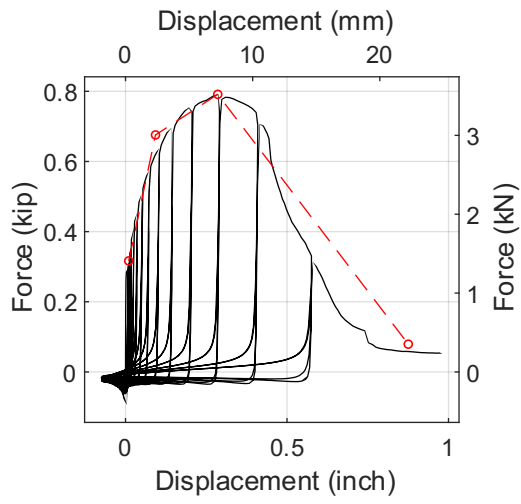
Test 103-@Peak-Side View



Test 103-@80% Post Peak



Test 103-After Test



Test 104-@Peak-Front View



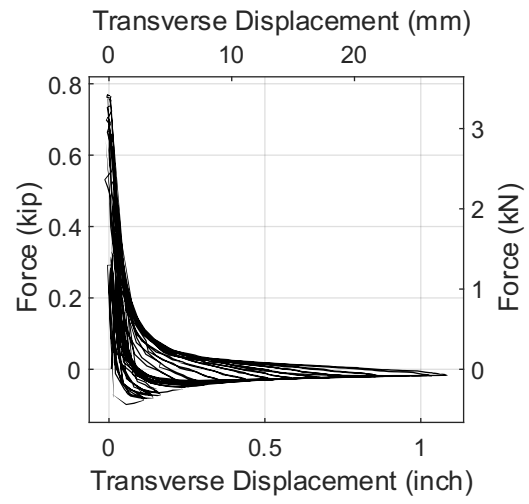
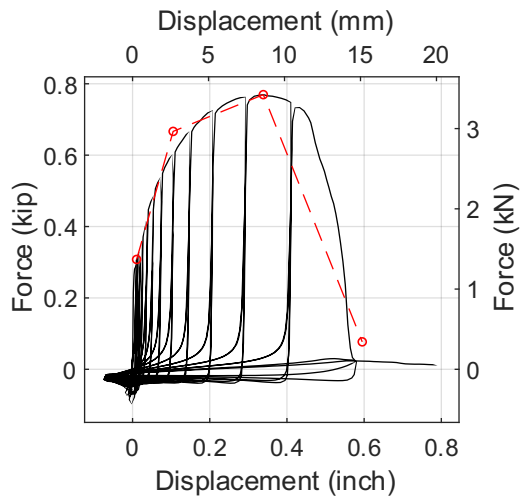
Test 104-@Peak-Side View



Test 104-@80% Post Peak



Test 104-After Test



Test 105-@Peak-Front View



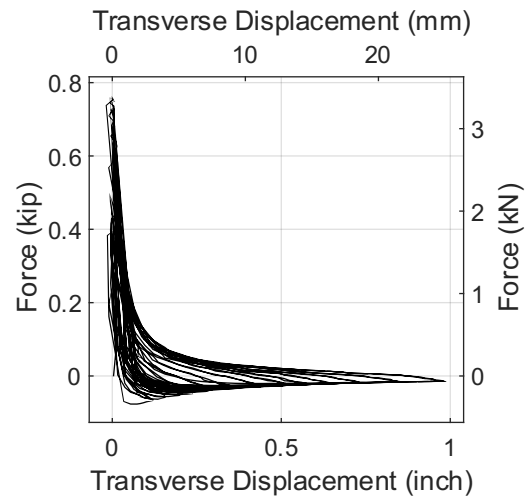
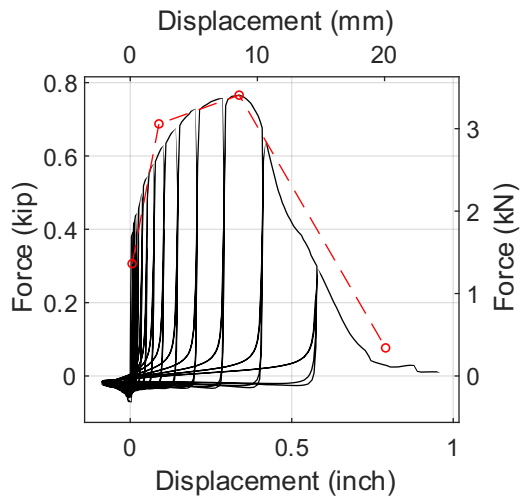
Test 105-@Peak-Side View



Test 105-@80% Post Peak



Test 105-After Test



Test 106-@Peak-Front View



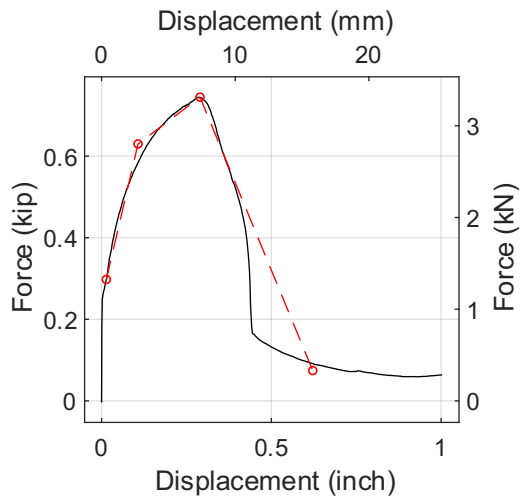
Test 106-@Peak-Side View



Test 106-@80% Post Peak



Test 106-After Test



Test 107-@Peak-Front View



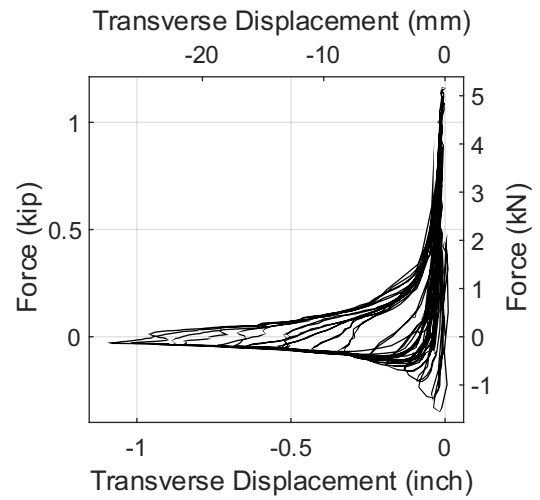
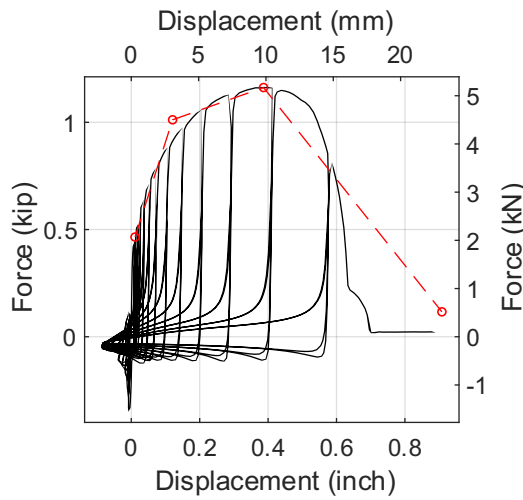
Test 107-@Peak-Side View



Test 107-@80% Post Peak



Test 107-After Test



Test 108-@Peak-Front View



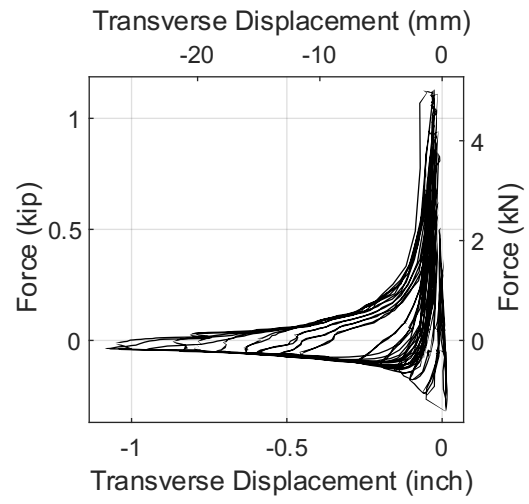
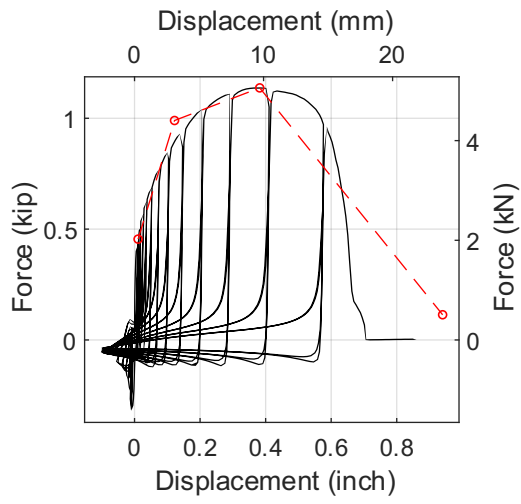
Test 108-@Peak-Side View



Test 108-@80% Post Peak



Test 108-After Test



Test 109-@Peak-Front View



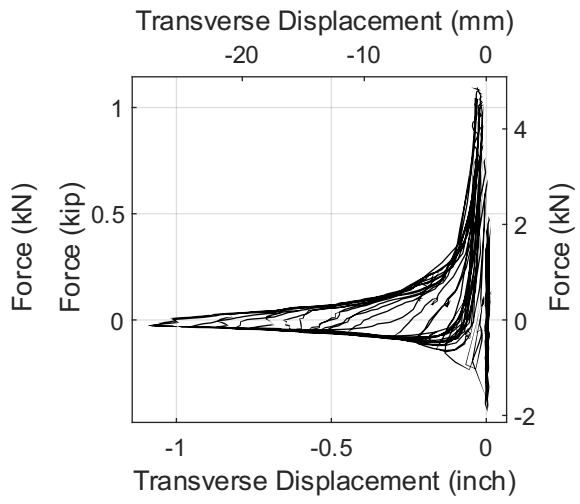
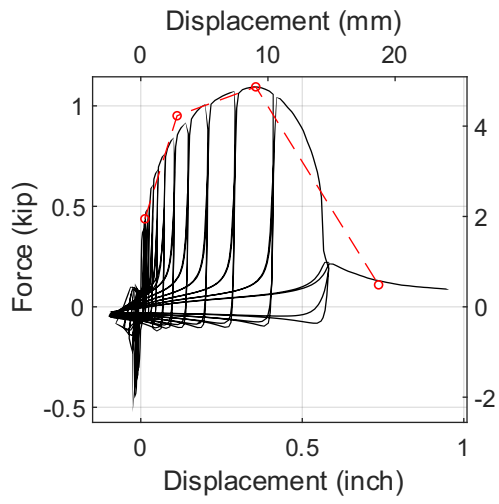
Test 109-@Peak-Side View



Test 109-@80% Post Peak



Test 109-After Test



Test 110-@Peak-Front View



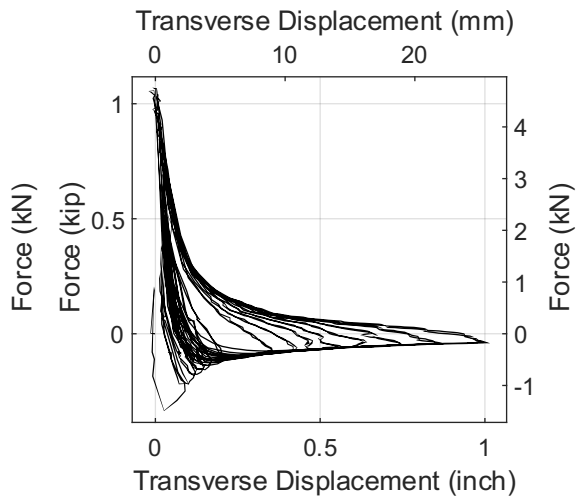
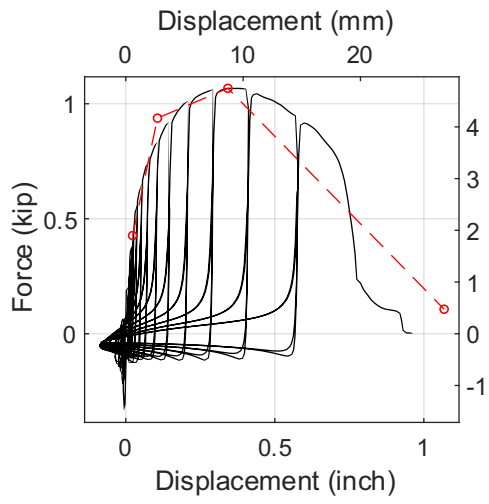
Test 110-@Peak-Side View



Test 110-@80% Post Peak



Test 110-After Test



Test 111-@Peak-Front View



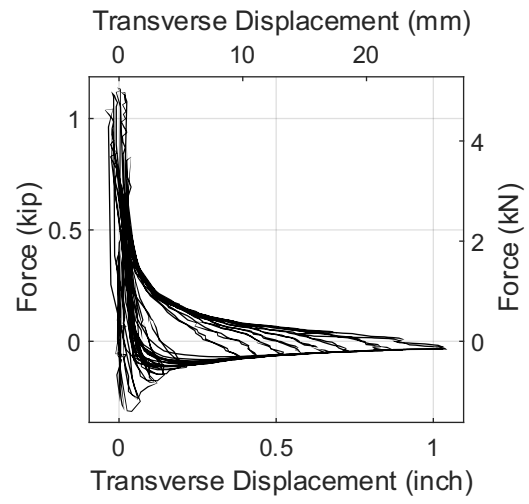
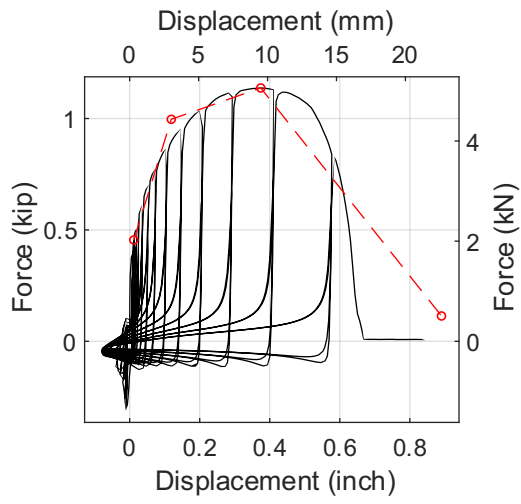
Test 111-@Peak-Side View



Test 111-@80% Post Peak



Test 111-After Test



Test 112-@Peak-Front View



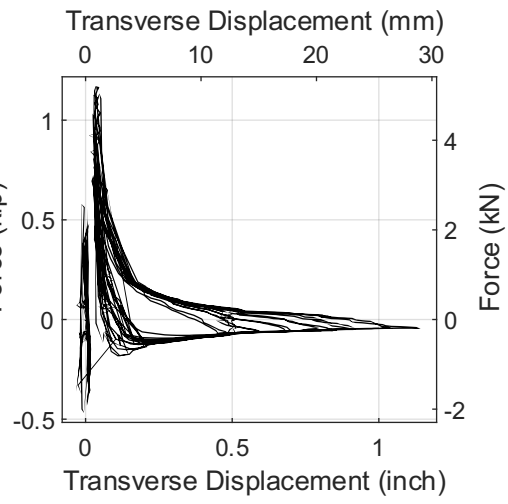
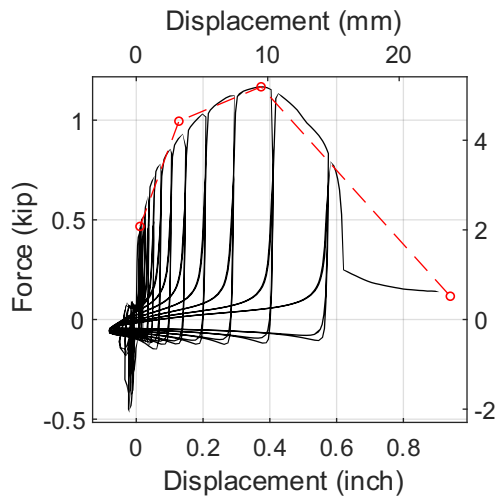
Test 112-@Peak-Side View



Test 112-@80% Post Peak



Test 112-After Test



Test 113-@Peak-Front View



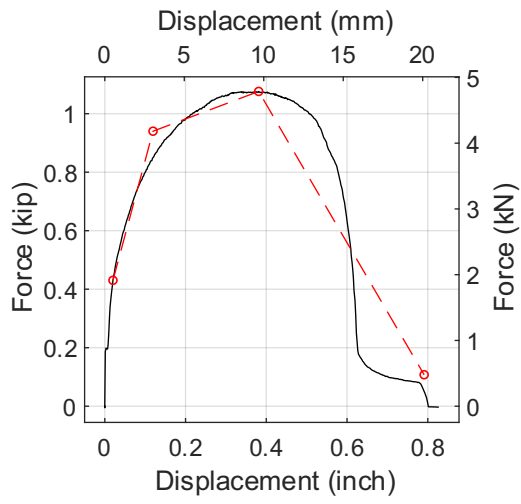
Test 113-@Peak-Side View



Test 113-@80% Post Peak



Test 113-After Test



Test 114-@Peak-Front View



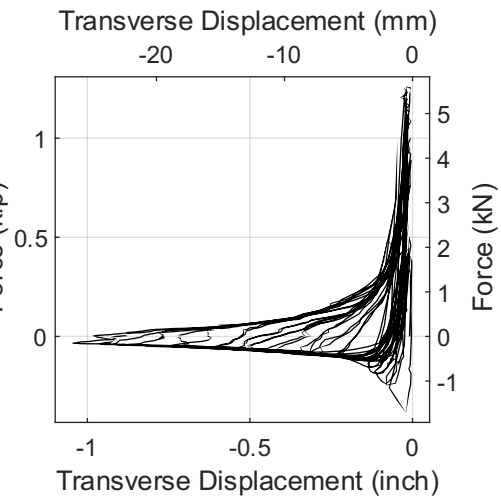
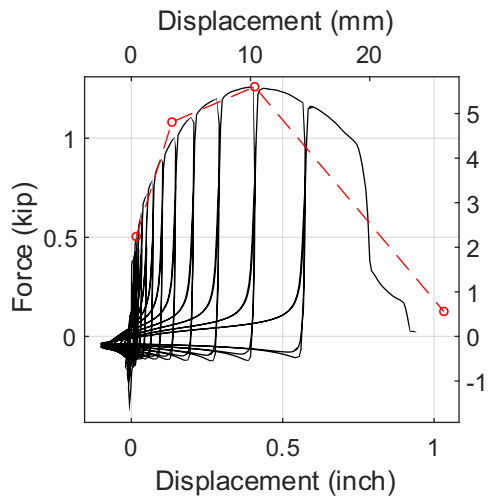
Test 114-@Peak-Side View



Test 114-@80% Post Peak



Test 114-After Test



Test 115-@Peak-Front View



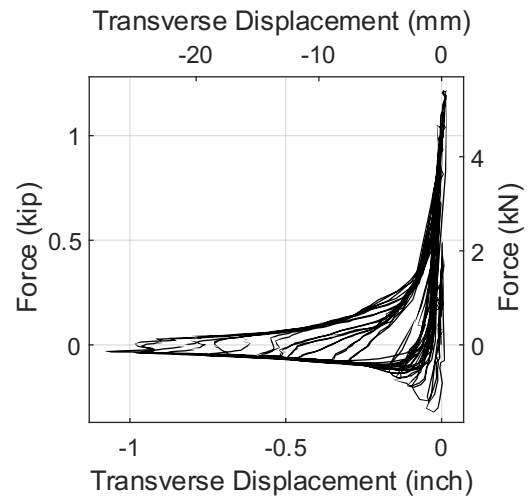
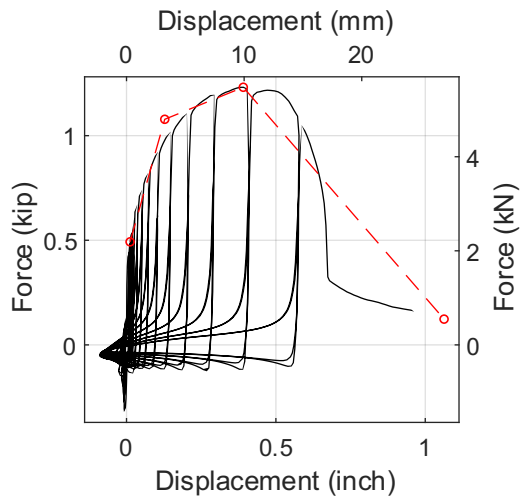
Test 115-@Peak-Side View



Test 115-@80% Post Peak



Test 115-After Test



Test 116-@Peak-Front View



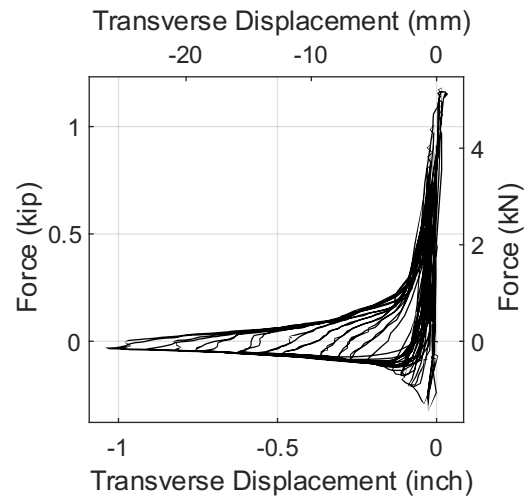
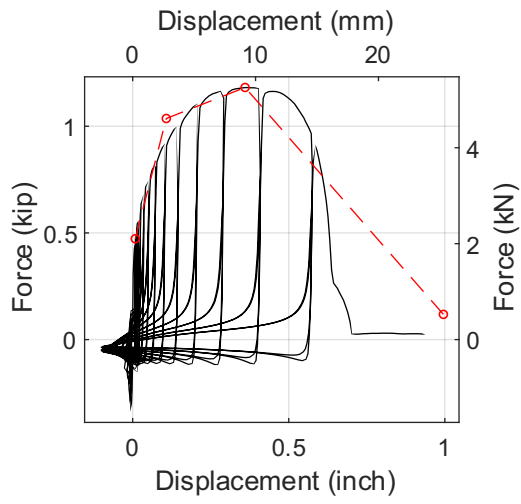
Test 116-@Peak-Side View



Test 116-@80% Post Peak



Test 116-After Test



Test 117-@Peak-Front View



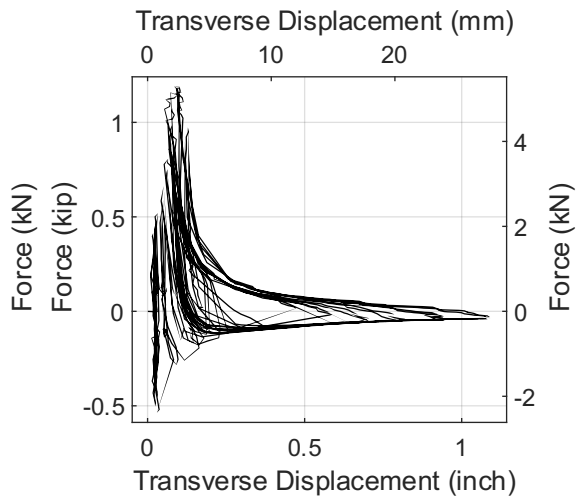
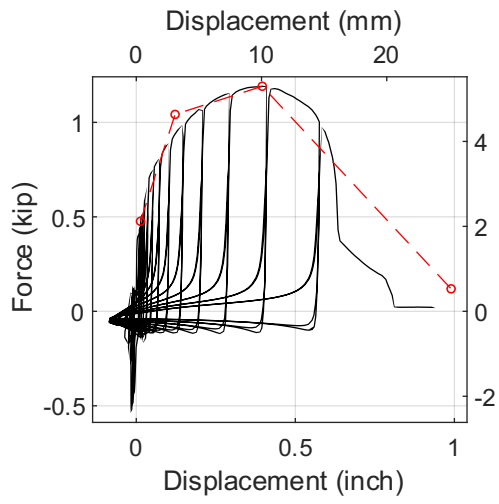
Test 117-@Peak-Side View



Test 117-@80% Post Peak



Test 117-After Test



Test 118-@Peak-Front View



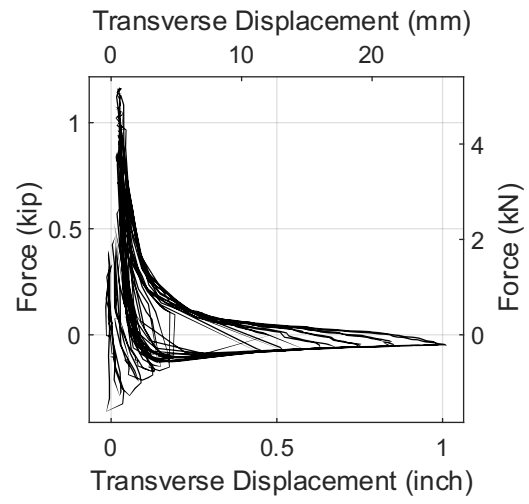
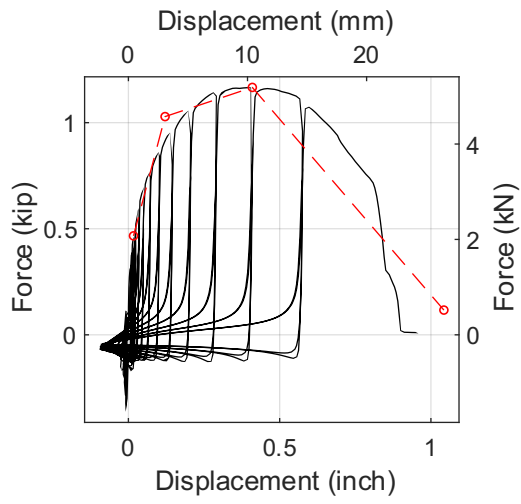
Test 118-@Peak-Side View



Test 118-@80% Post Peak



Test 118-After Test



Test 119-@Peak-Front View



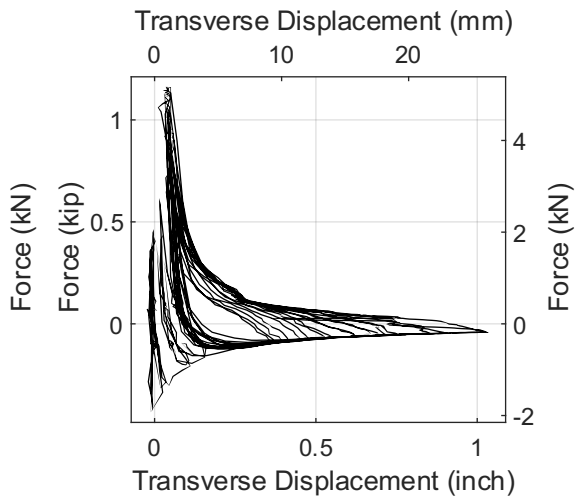
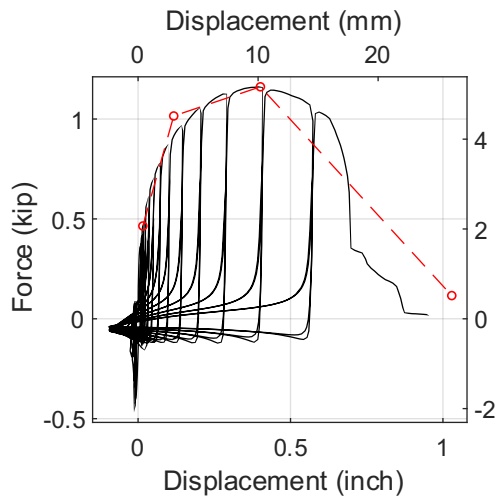
Test 119-@Peak-Side View



Test 119-@80% Post Peak



Test 119-After Test



Test 120-@Peak-Front View



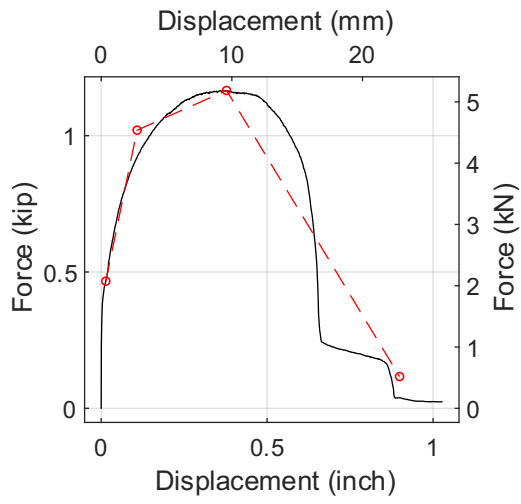
Test 120-@Peak-Side View



Test 120-@80% Post Peak



Test 120-After Test



Test 121-@Peak-Front View



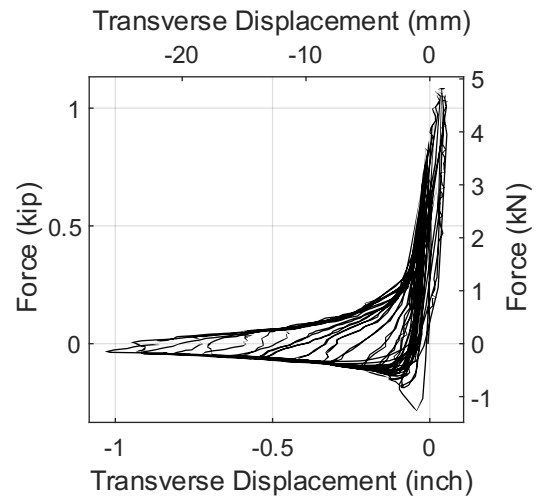
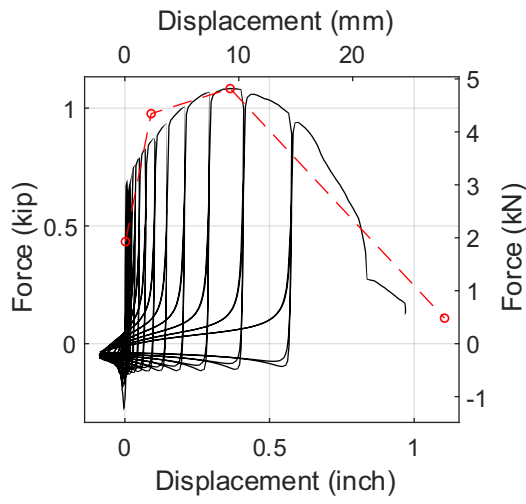
Test 121-@Peak-Side View



Test 121-@80% Post Peak



Test 121-After Test



Test 122-@Peak-Front View



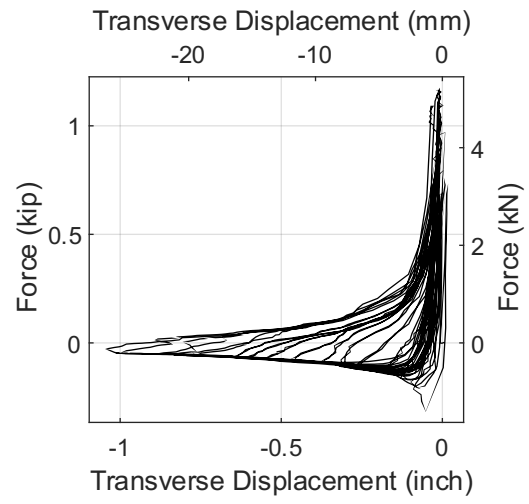
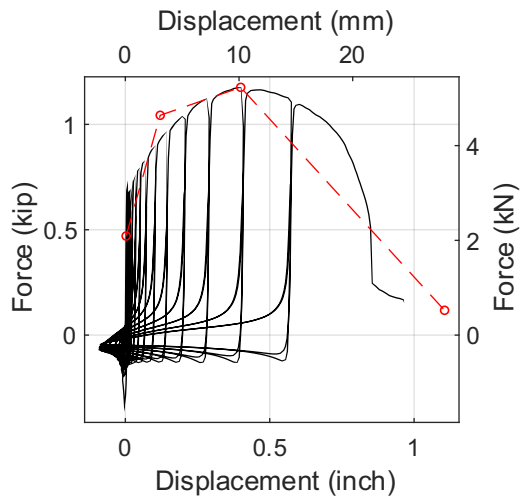
Test 122-@Peak-Side View



Test 122-@80% Post Peak



Test 122-After Test



Test 123-@Peak-Front View



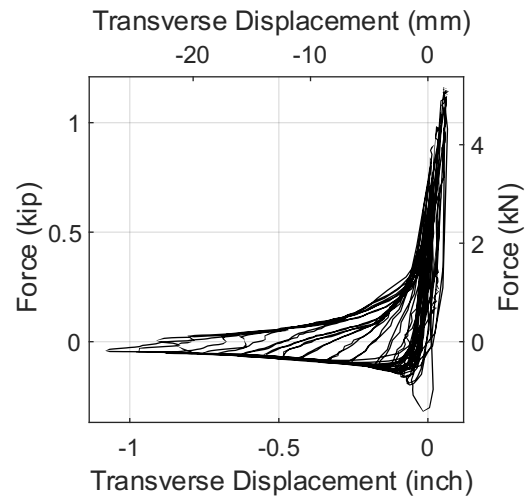
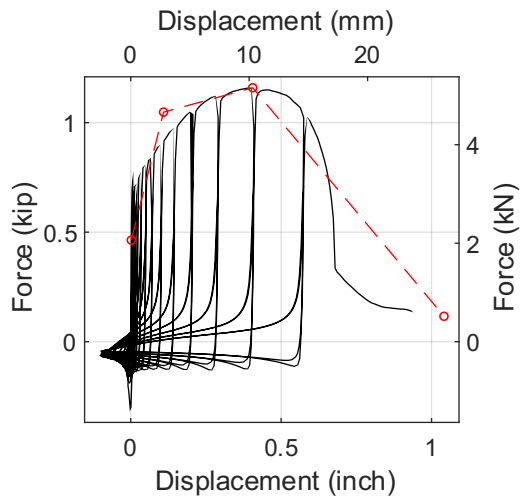
Test 123-@Peak-Side View



Test 123-@80% Post Peak



Test 123-After Test



Test 124-@Peak-Front View



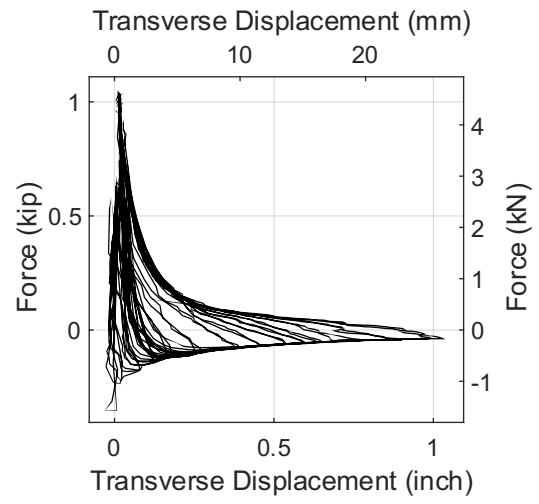
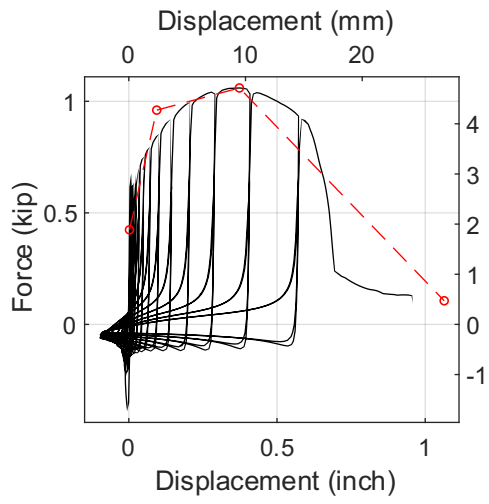
Test 124-@Peak-Side View



Test 124-@80% Post Peak



Test 124-After Test



Test 125-@Peak-Front View



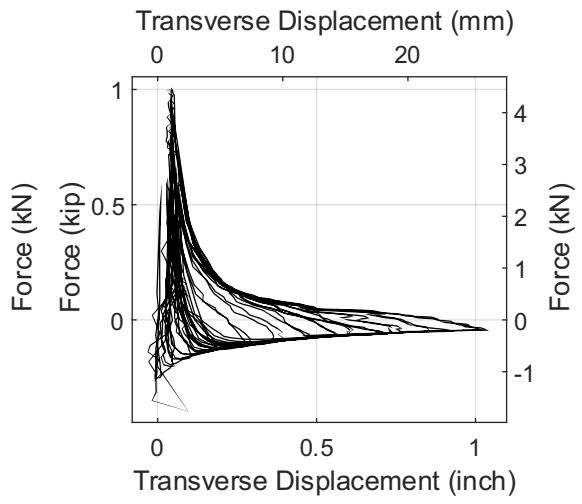
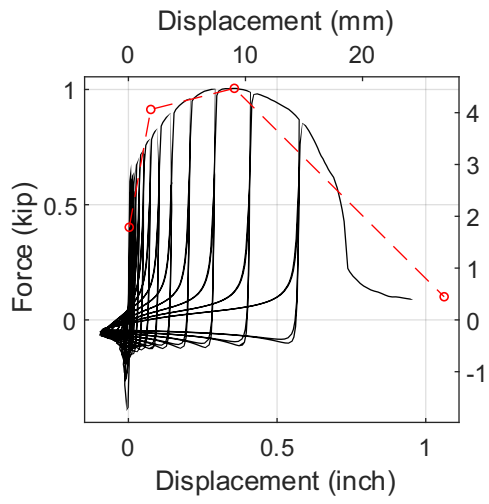
Test 125-@Peak-Side View



Test 125-@80% Post Peak



Test 125-After Test



Test 126-@Peak-Front View



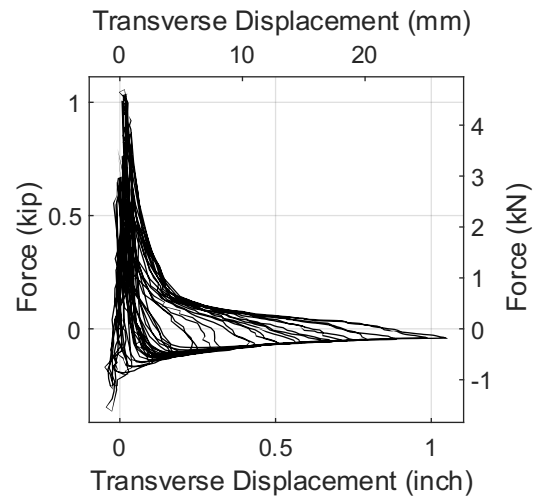
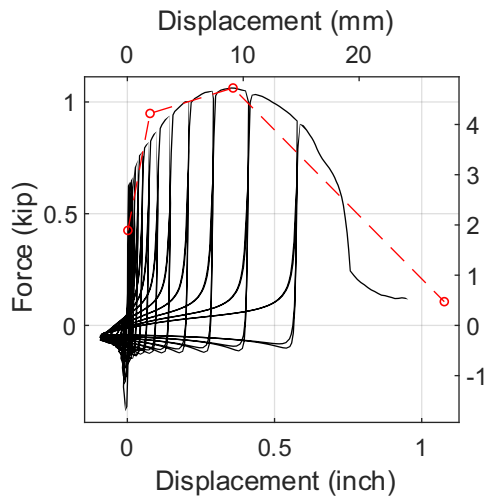
Test 126-@Peak-Side View



Test 126-@80% Post Peak



Test 126-After Test



Test 127-@Peak-Front View



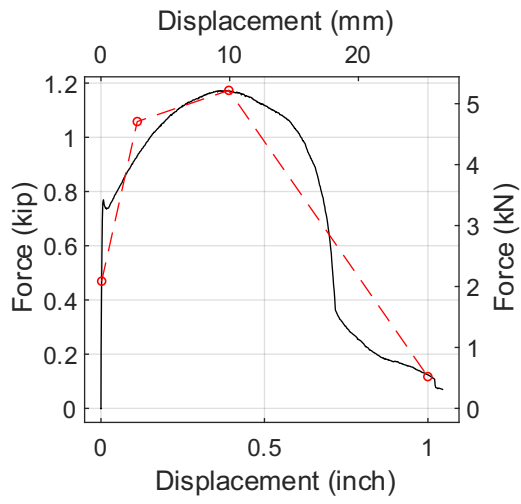
Test 127-@Peak-Side View



Test 127-@80% Post Peak



Test 127-After Test



Test 128-@Peak-Front View



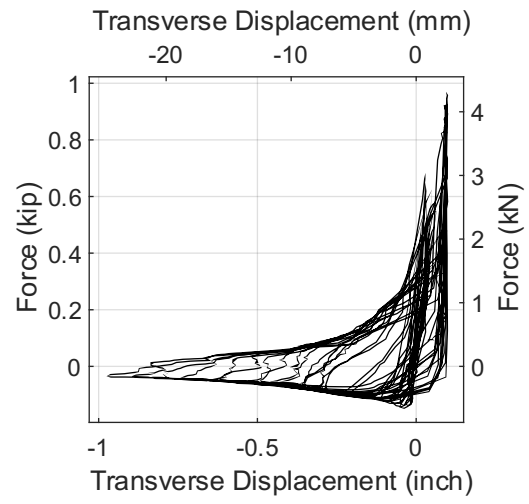
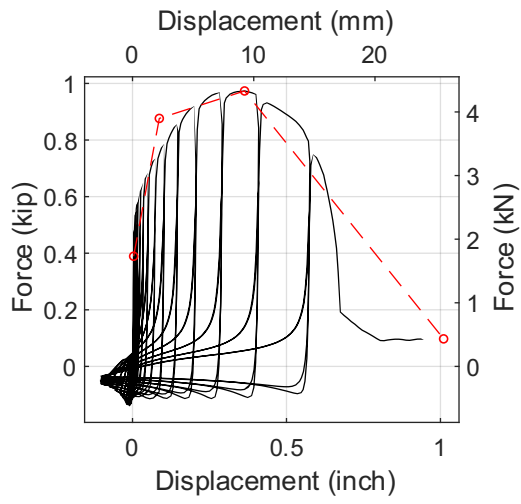
Test 128-@Peak-Side View



Test 128-@80% Post Peak



Test 128-After Test



Test 129-@Peak-Front View



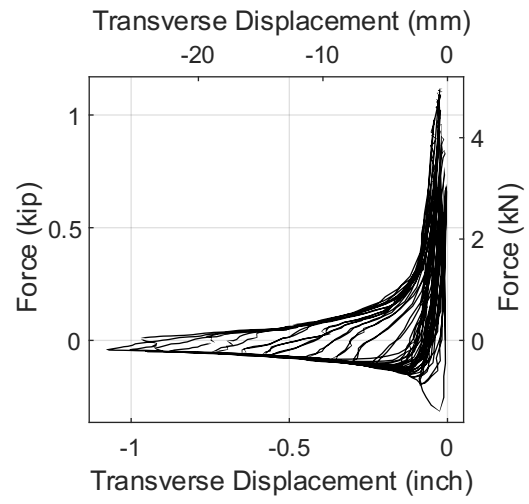
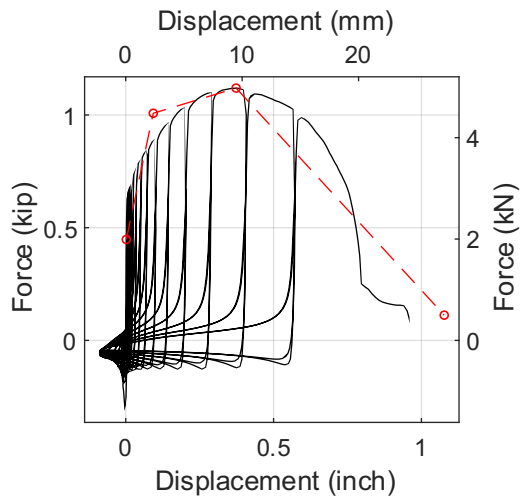
Test 129-@Peak-Side View



Test 129-@80% Post Peak



Test 129-After Test



Test 130-@Peak-Front View



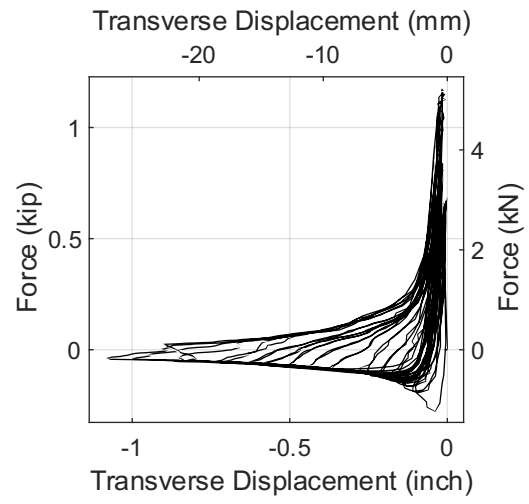
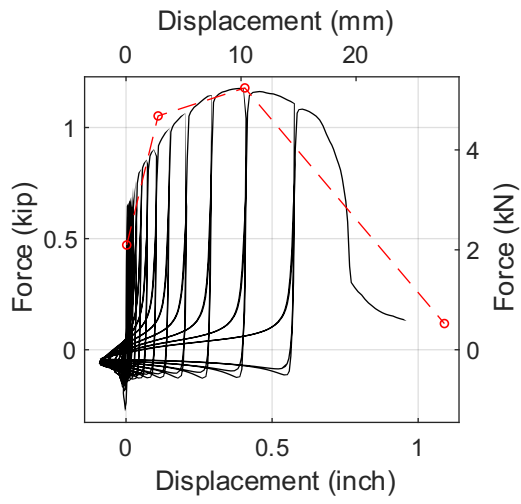
Test 130-@Peak-Side View



Test 130-@80% Post Peak



Test 130-After Test



Test 131-@Peak-Front View



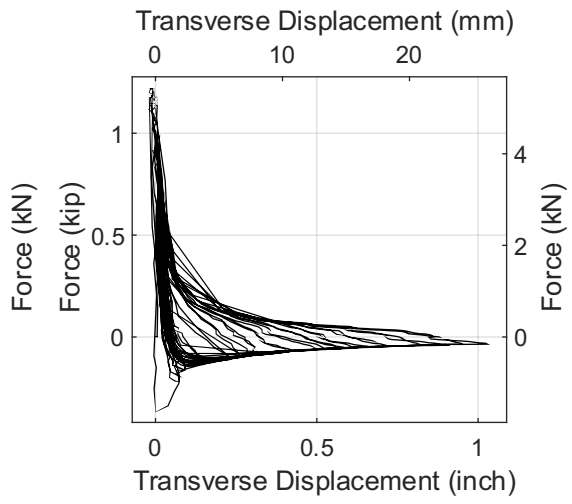
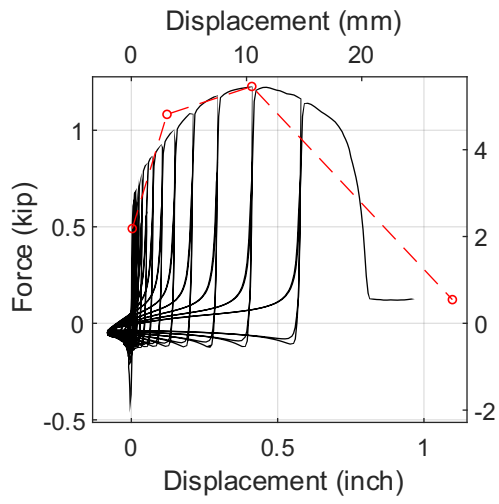
Test 131-@Peak-Side View



Test 131-@80% Post Peak



Test 131-After Test



Test 132-@Peak-Front View



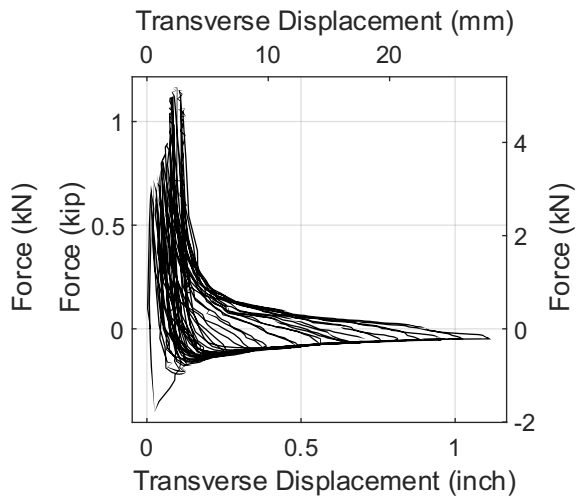
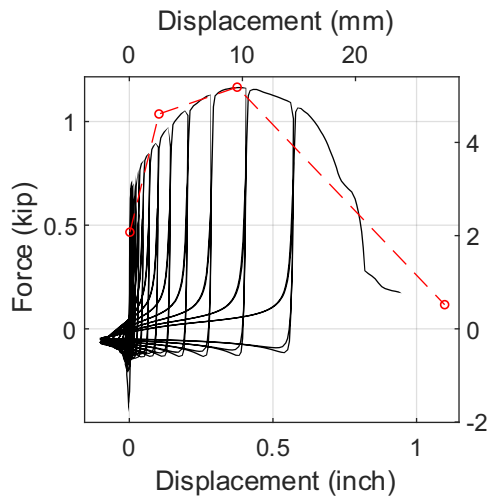
Test 132-@Peak-Side View



Test 132-@80% Post Peak



Test 132-After Test



Test 133-@Peak-Front View



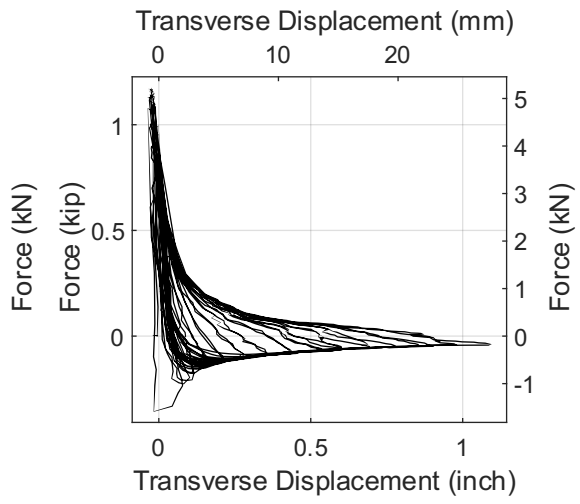
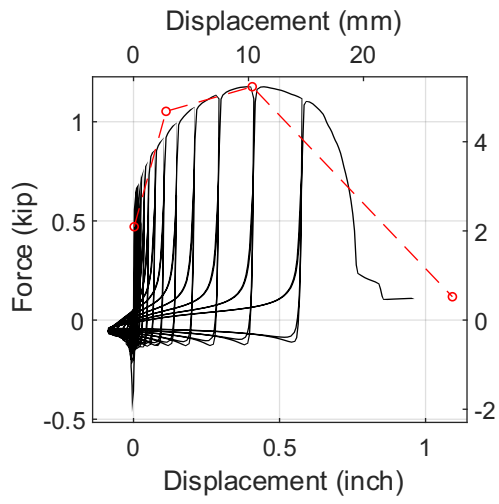
Test 133-@Peak-Side View



Test 133-@80% Post Peak



Test 133-After Test



Test 134-@Peak-Front View



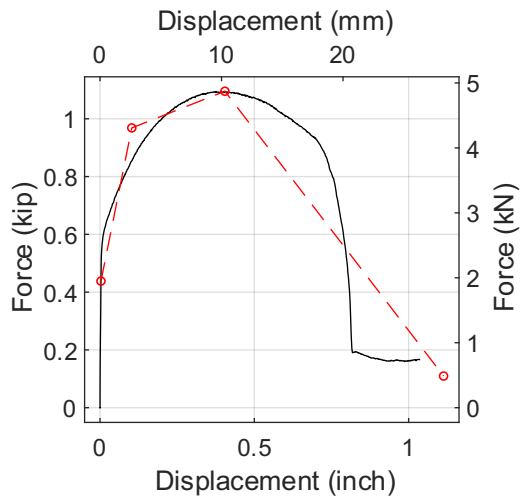
Test 134-@Peak-Side View



Test 134-@80% Post Peak



Test 134-After Test



Test 135-@Peak-Front View



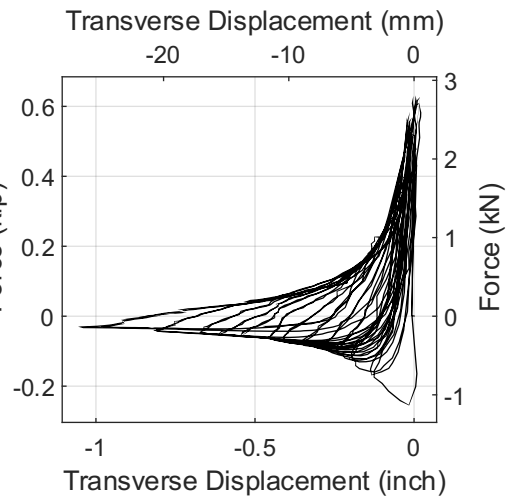
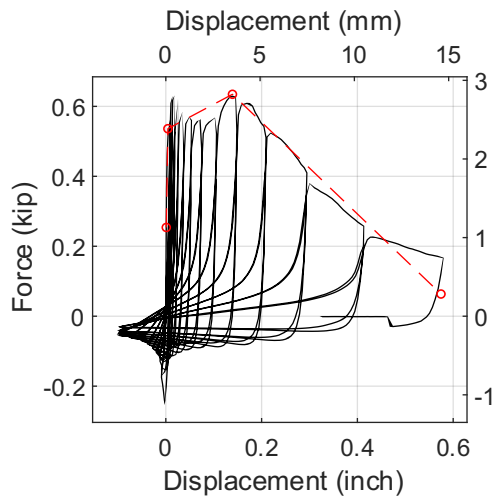
Test 135-@Peak-Side View



Test 135-@80% Post Peak



Test 135-After Test



Test 136-@Peak-Front View



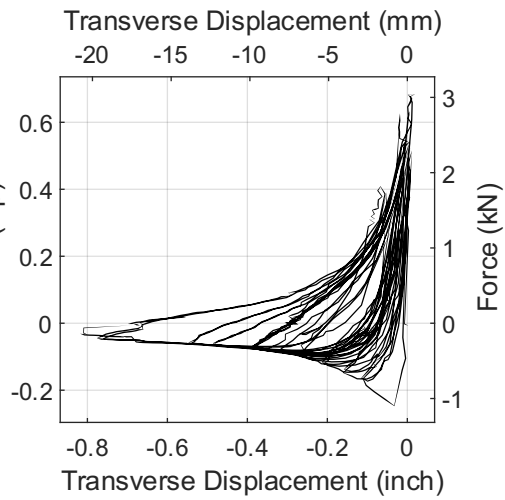
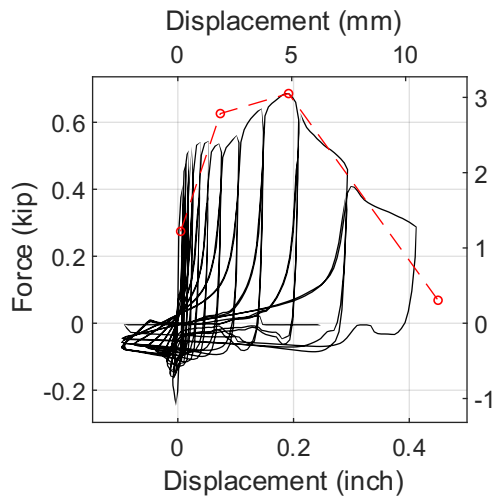
Test 136-@Peak-Side View



Test 136-@80% Post Peak



Test 136-After Test



Test 137-@Peak-Front View



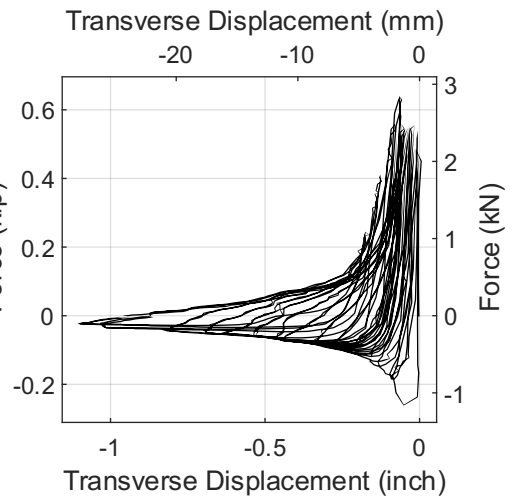
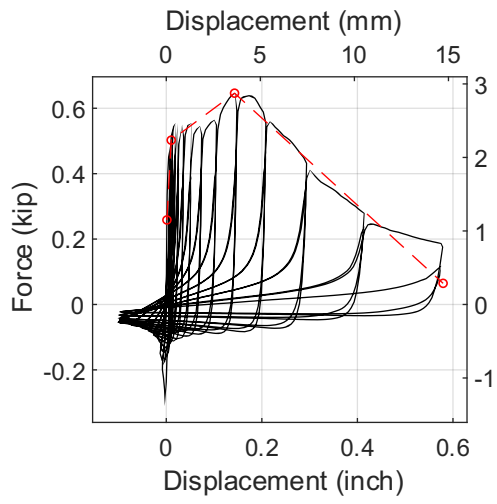
Test 137-@Peak-Side View



Test 137-@80% Post Peak



Test 137-After Test



Test 138-@Peak-Front View



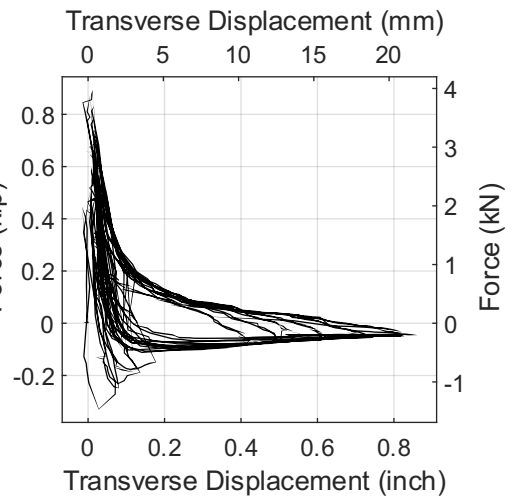
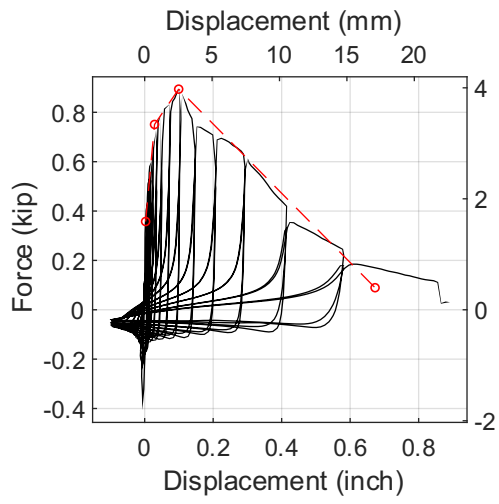
Test 138-@Peak-Side View



Test 138-@80% Post Peak



Test 138-After Test



Test 139-@Peak-Front View



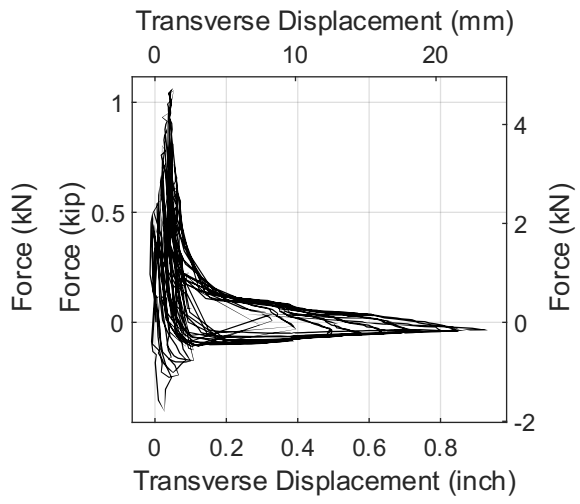
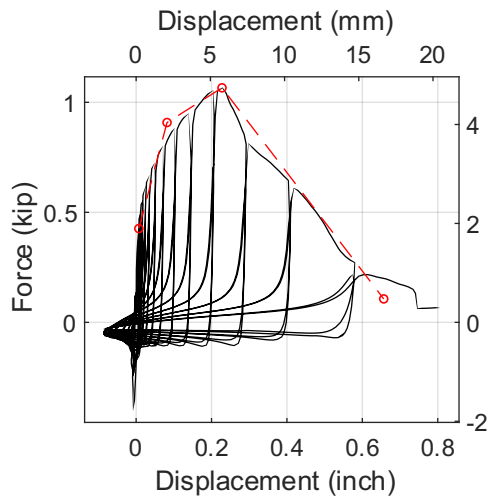
Test 139-@Peak-Side View



Test 139-@80% Post Peak



Test 139-After Test



Test 140-@Peak-Front View



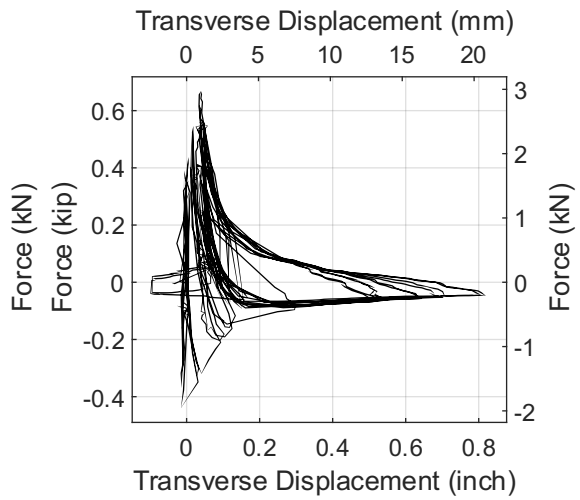
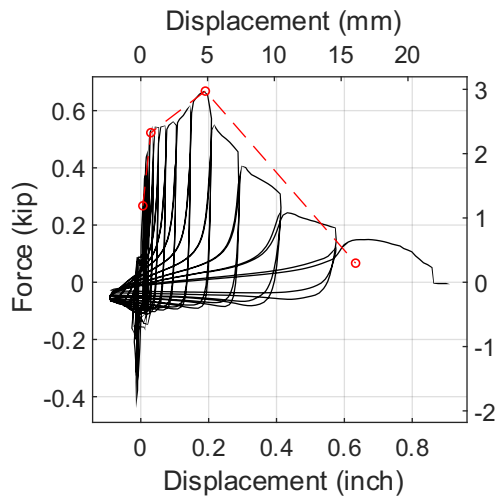
Test 140-@Peak-Side View



Test 140-@80% Post Peak



Test 140-After Test



Test 141-@Peak-Front View



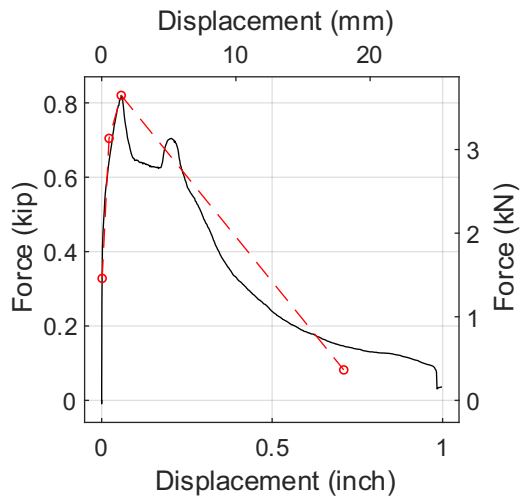
Test 141-@Peak-Side View



Test 141-@80% Post Peak



Test 141-After Test



Test 142-@Peak-Front View



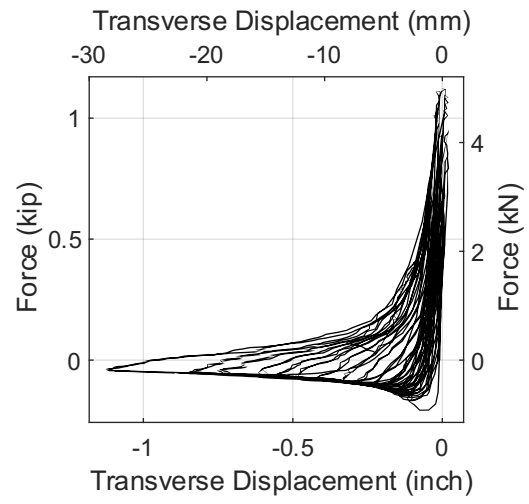
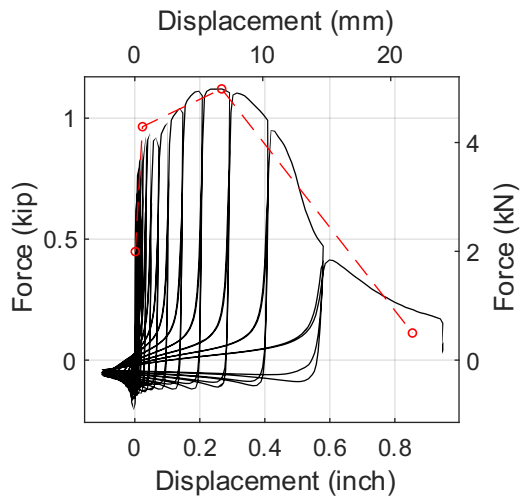
Test 142-@Peak-Side View



Test 142-@80% Post Peak



Test 142-After Test



Test 143-@Peak-Front View



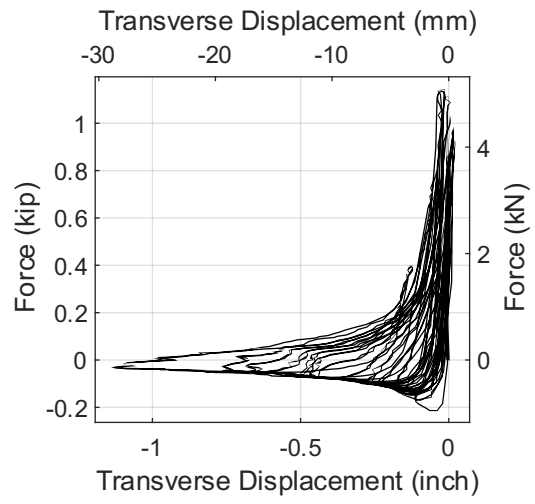
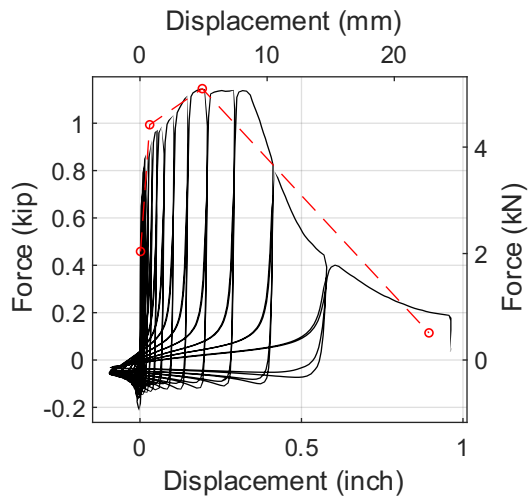
Test 143-@Peak-Side View



Test 143-@80% Post Peak



Test 143-After Test



Test 144-@Peak-Front View



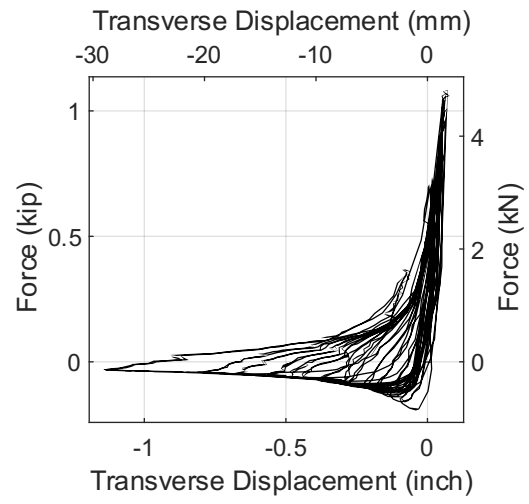
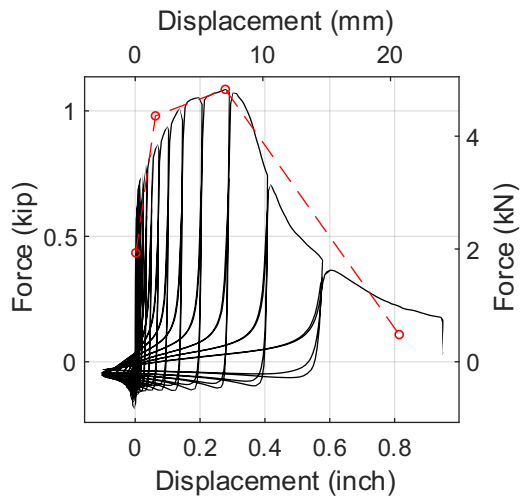
Test 144-@Peak-Side View



Test 144-@80% Post Peak



Test 144-After Test



Test 145-@Peak-Front View



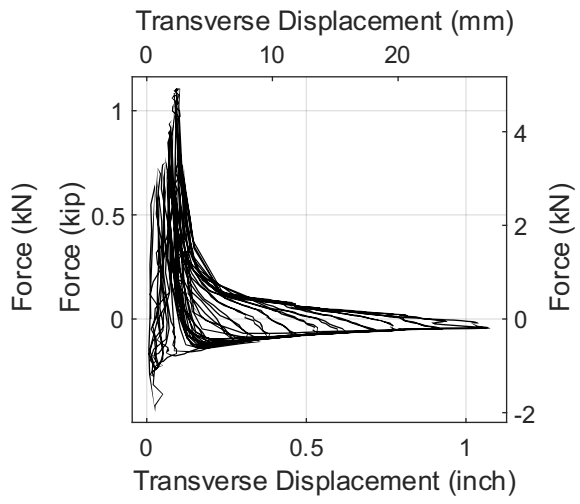
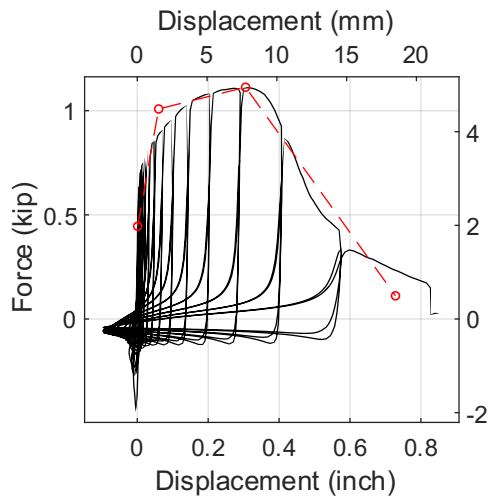
Test 145-@Peak-Side View



Test 145-@80% Post Peak



Test 145-After Test



Test 146-@Peak-Front View



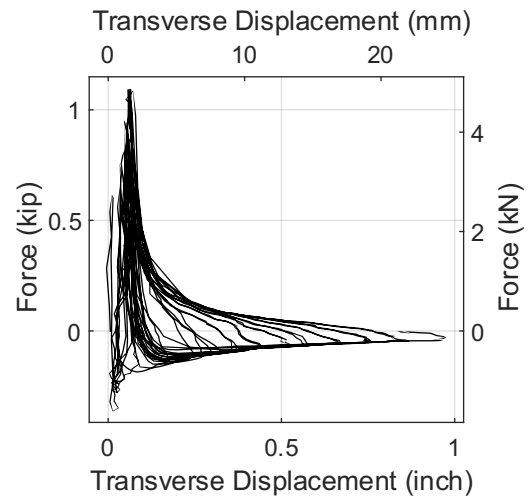
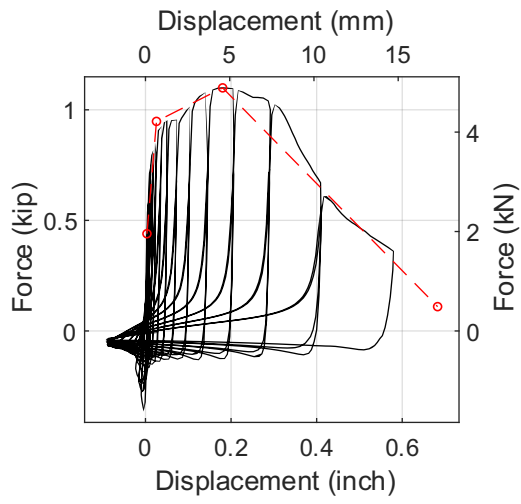
Test 146-@Peak-Side View



Test 146-@80% Post Peak



Test 146-After Test



Test 147-@Peak-Front View



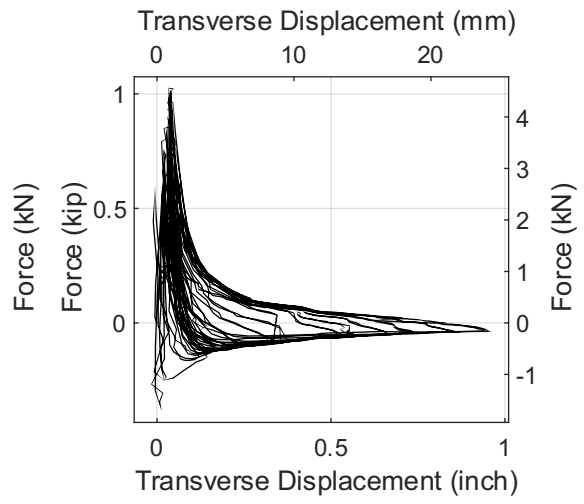
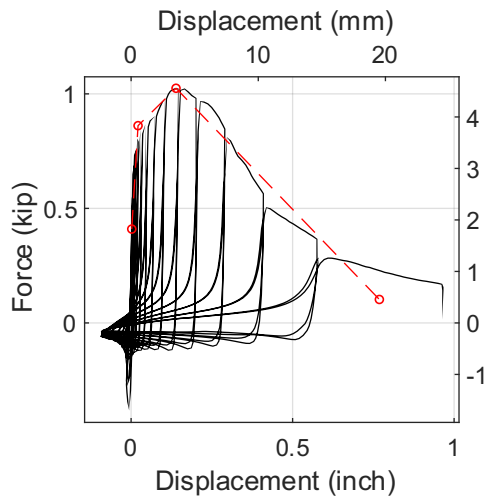
Test 147-@Peak-Side View



Test 147-@80% Post Peak



Test 147-After Test



Test 148-@Peak-Front View



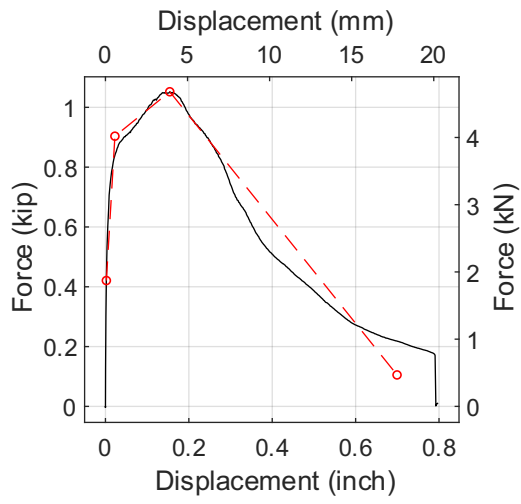
Test 148-@Peak-Side View



Test 148-@80% Post Peak



Test 148-After Test



Test 149-@Peak-Front View



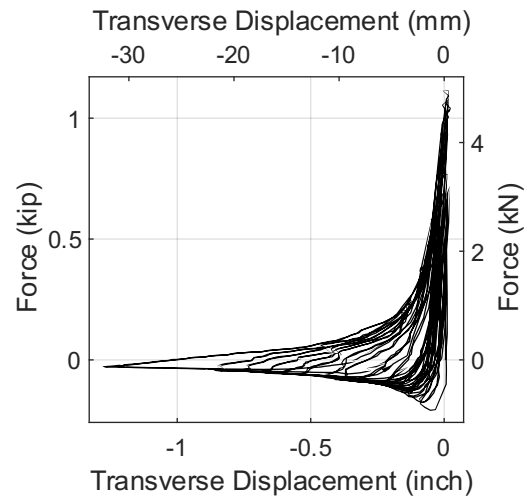
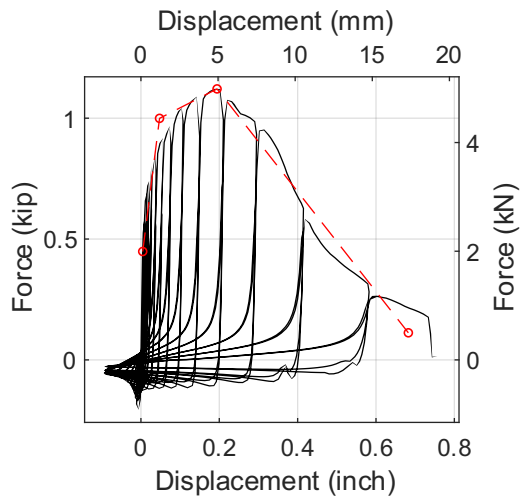
Test 149-@Peak-Side View



Test 149-@80% Post Peak



Test 149-After Test



Test 150-@Peak-Front View



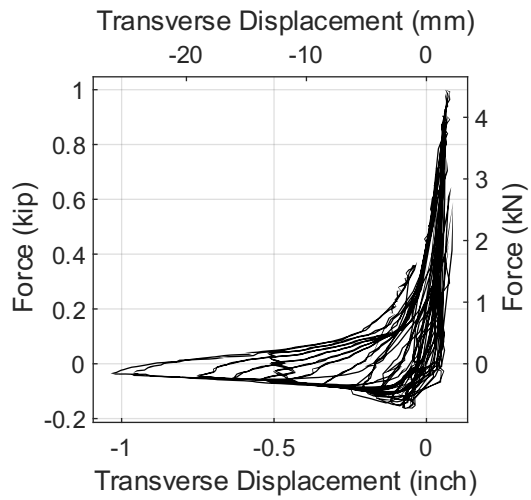
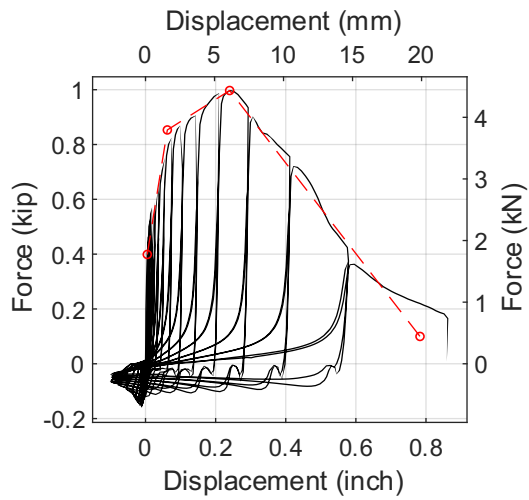
Test 150-@Peak-Side View



Test 150-@80% Post Peak



Test 150-After Test



Test 151-@Peak-Front View



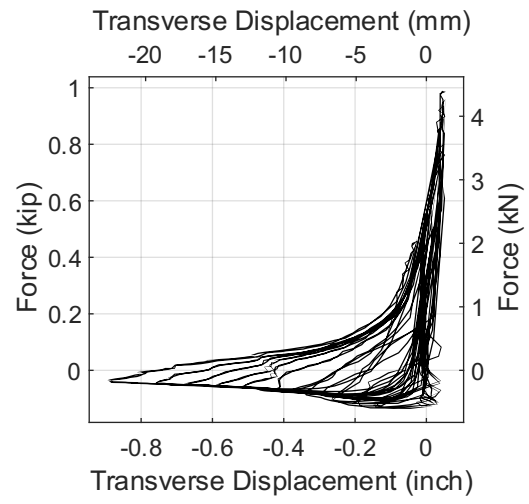
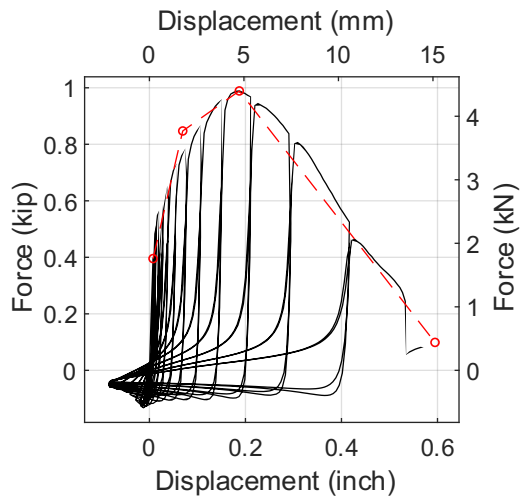
Test 151-@Peak-Side View



Test 151-@80% Post Peak



Test 151-After Test



Test 152-@Peak-Front View



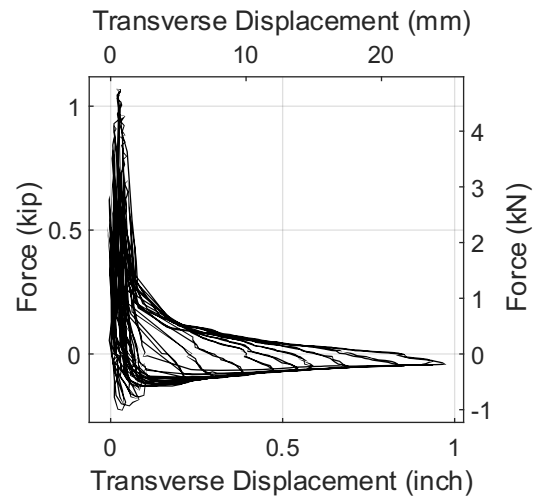
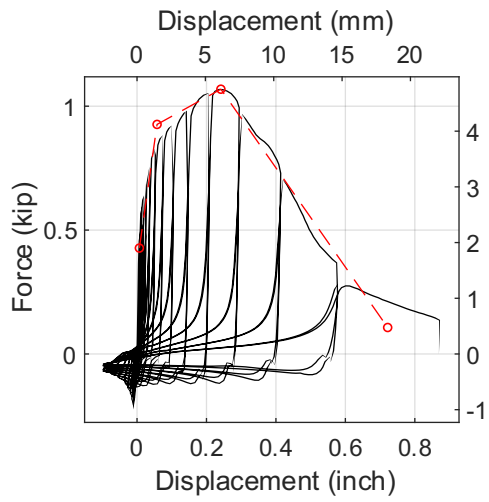
Test 152-@Peak-Side View



Test 152-@80% Post Peak



Test 152-After Test



Test 153-@Peak-Front View



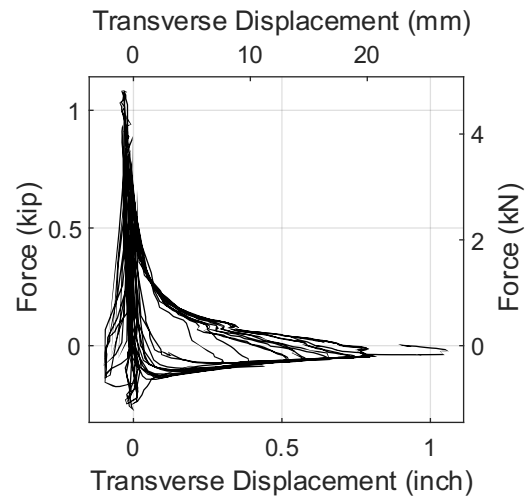
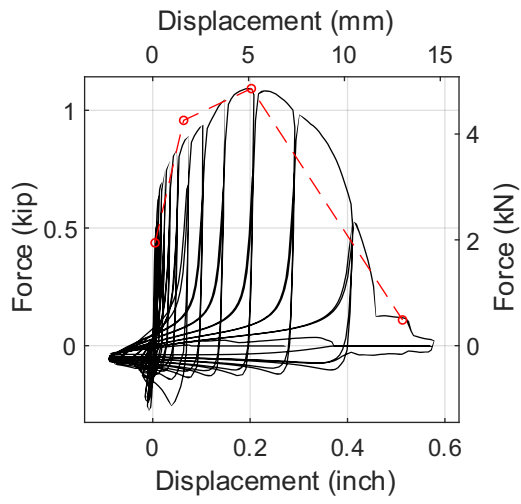
Test 153-@Peak-Side View



Test 153-@80% Post Peak



Test 153-After Test



Test 154-@Peak-Front View



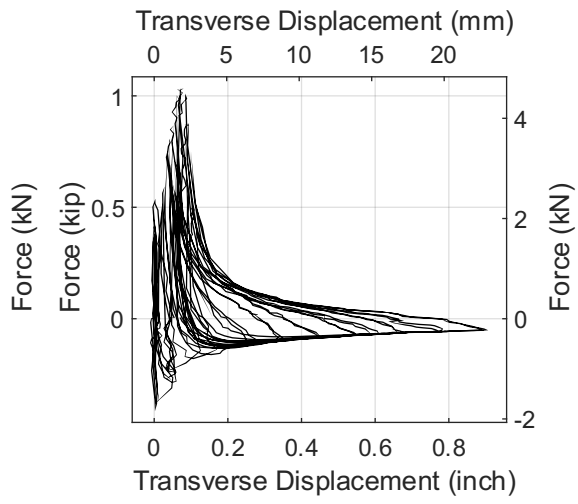
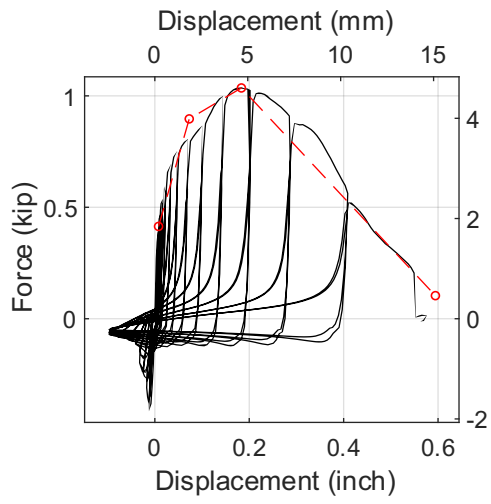
Test 154-@Peak-Side View



Test 154-@80% Post Peak



Test 154-After Test



Test 155-@Peak-Front View



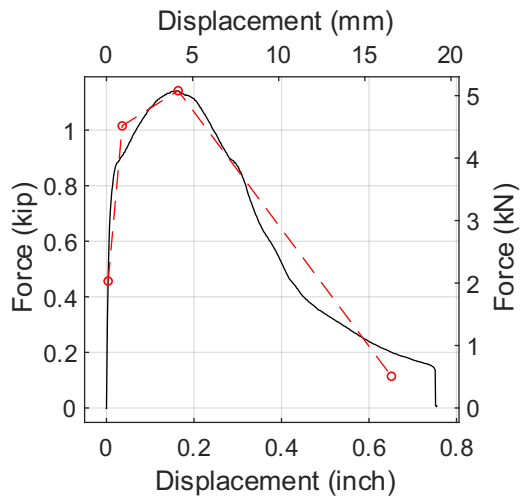
Test 155-@Peak-Side View



Test 155-@80% Post Peak



Test 155-After Test



Test 156-@Peak-Front View



Test 156-@Peak-Side View



Test 156-@80% Post Peak



Test 156-After Test